Isolated sulfite oxidase deficiency in mice: potential treatment strategies and discovery of a novel dermal phenotype

Inaugural-Dissertation

zur

Erlangung des Doktorgrades

der Mathematisch-Naturwissenschaftlichen Fakultät

der Universität zu Köln

vorgelegt von

Lena Johannes

aus Leverkusen

Juli 2023

Content

List of Abbreviations

AMP	Adenosine monophosphate
AOAA	Aminooxyacetic acid
AOX	Aldehyde oxidase
AST	Aspartate:2-oxoglutarate aminotransferase
ATP	Adenosine triphosphate
bis-MGD	Bis-molybdopterin-guanine dinucleotide
CBS	Cystathionine β-synthase
CDO	Cysteine dioxygenase
cPMP	Cyclic pyranopterin monophosphate
CSA	Cysteine sulfinic acid
CSAD	CSA decarboxylase
CSE	Cystathionine γ-lyase
CV	Column volume
Da	Dalton
DISC	Death-inducing signaling complex
DMSO	Dimethyl sulfoxide
DTNB	5,5′-dithiobis-(2-nitrobenzoic acid, Ellman’s reagent
E. coli	*Escherichia coli*
EEG	Electroencephalogram
ETHE1	Ethylmalonic encephalopathy protein 1
FAD	Flavin adenine dinucleotide
Fe	Iron
FeCN	Ferricyanide
FeMoco	Iron-sulfur cluster bound molybdenum cofactor
GABA	γ-aminobutyric acid
$GABA_AR$	$GABA_A$ receptor
GCL	Glutamate cysteine ligase
GlyR	Glycine receptor

GOT	Glutamate oxaloacetate transaminase
GPHN-E	Gephyrin E-domain
GPHN-G	Gephyrin G-domain
GPX4	Glutathione peroxidase
GSH	Reduced glutathione
GSR	Glutathione reductase
GSS	GSH synthetase
GSSG	Oxidized glutathione
GSSH	Persulfidated glutathione
$GSSO_3$	S-sulfonated glutathione
GTP	Guanosine triphosphate
H_2O_2	Hydrogen peroxide
H_2S	Hydrogen sulfide
HEK	Human embryonic kidney
IET	Intramolecular electron transfer
IMS	Intermembrane space
LANUV	Landesamt für Natur, Umwelt und Verbraucherschutz
LB medium	Lysogeny broth medium
M	Molar
m	meter
mARC	Mitochondrial amidoxime-reducing component
min	Minute
MoCD	Molybdenum cofactor deficiency
Moco	Molybdenum cofactor
MOSC domain	Molybdenum cofactor sulfurase C-terminal domain
MPST	3-mercaptopyruvate sulfurtransferase
MPT	Molybdopterin
mSOX-Mo	Heme-deficient murine sulfite oxidase
MTS	Mitochondrial targeting signal
MTT	3-(4,5-dimethylthiazol-2-yl)-2,5-diphenyltetrazolium bromide

n.d.	Not detectable
NAD+	Oxidized nicotinamide adenine dinucleotide
NADH	Reduced nicotinamide adenine dinucleotide
NB medium	Neurobasal medium
NGS	Normal goat serum
Ni-NTA	Nickel nitrilotriacetic acid
NMDA	N-methyl-D-aspartic acid
NMDAR	NMDA receptor
NO	Nitric oxide
NR	Nitrate reductase
P6C	Δ^1-piperideine-6-carboxylate
PAGE	Polyacrylamide gel electrophoresis
PC	Phosphatidylcholine
PDO	Persulfide dioxygenase
PE	Phosphatidylethanolamine
PEG	Polyethylene glycol
PLP	Pyridoxal-5’-phosphate
pSOX	Plant sulfite oxidase
ROS	Reactive oxygen species
s	Second
S	Sulfur
SB	Stratum basale
SC	Stratum corneum
SDS	Sodium dodecyl sulfate
SG	Stratum granulosum
SOX	Sulfite oxidase
SOXD	Isolated sulfite oxidase deficiency
SQR	sulfide:quinone oxidoreductase
SS	Stratum spinosum
SSC	S-sulfocysteine

Tau	Taurine
TEWL	Transepidermal water loss
TST	Thiosulfate sulfurtransferase
XOR	Xanthine oxidoreductase

Abstract

Isolated sulfite oxidase deficiency (SOXD) is a rare autosomal recessively inherited disease presenting with severe seizures, neurological damage and altered facial and head morphology, which collectively lead to infant death if left untreated. It can be caused by a loss of function of the mitochondrial molybdoenzyme sulfite oxidase (SOX) due to mutation in the *SUOX* gene (named SOXD) or by defects in the biogenesis of its molybdenum cofactor (named MoCD), forming the active site of the enzyme.

The disease is characterized by a vast increase of sulfite and related sulfur-containing metabolites, including S-sulfocysteine, in urine accompanied by a decrease of plasma cystine and homocysteine levels. Sulfite is a molecule with strong nucleophilic properties that has the ability to cleave disulfide bonds and thus globally affect protein stability and function. In contrast to the versatile mechanism of sulfite-mediated toxicity, SSC functions as a structural analogue of glutamate triggering N-methyl D-aspartate receptor (NMDAR)-mediated excitotoxicity resulting in elevated neurodegeneration.

Up to date, effective long-term treatment strategies are still lacking for SOXD. So far, therapy is restricted to symptomatic treatment including anti-epileptic medication aiming for a reduction in seizures and spasticity. Deceleration of the disease progression was attempted via dietary restriction of sulfur-containing amino acids to reduce cysteine catabolism and thus sulfite formation, but has only proven successful in mild, late onset cases of SOXD.

The generation of a *Suox*$^{-/-}$ mouse line provided a new model system to investigate the effects of non-functional SOX on the symptom progression of SOXD and thus new possibilities in the search for an effective long-term treatment. Hence, the current study investigated several therapeutic approaches aiming to treat SOXD in mice by (i) blockage of NMDAR-mediated excitotoxicity, (ii) dietary restriction of proteins and sulfur-containing amino acids, (iii) chemical sulfite scavenging, (iv) inhibition of ferroptosis and (v) an enzyme replacement therapy using a modified SOX variant.

The results indicate an absence of beneficial effects of NMDAR blockage on the survival time of *Suox*$^{-/-}$ mice, which is in line with their cerebral phenotype being significantly milder than reported in patients, thus suggesting a different underlying cause of death, which is in strong contrast to the disease progression in human patients.

Therapeutic prevention of major sulfite accumulation was attempted by dietary restriction of sulfur-containing amino acids to reduce cysteine catabolism. However, dietary restriction proved difficult in mice, as manipulation of the mother's chow to alter the diet of pups complicated the right dosage finding, thus resulting in no improvement of the phenotype.

An attempt to reduce sulfite accumulation via usage of different thiol-reactive compounds (D-cysteine/cystine, cystamine) did also not improve the symptomatology or life span of *Suox*$^{-/-}$ mice. As it nevertheless presents an easy, straightforward treatment approach, chemical sulfite scavenging still holds great potential for future studies on the treatment of SOXD.

Based on the fact that SOXD causes cystine depletion, we hypothesized a pathomechanism that involves the regulated cell death pathway ferroptosis, which is characterized by increased levels of intracellular lipid peroxidation caused by a depletion of cysteine and glutathione. However, the current study excluded the contribution of ferroptosis to the phenotype of *Suox*$^{-/-}$ mice. In contrast, absence of SOX activity resulted in an inhibition of ferroptosis, which is hypothesized to be caused by a faster recovery of reduced glutathione due to sulfite-mediated cleavage of disulfide bonds in intracellular glutathione disulfide and was also confirmed by reduced lipid peroxidation in kidneys of *Suox*$^{-/-}$ mice.

Enzyme replacement therapy presented an alternative treatment approach aiming for the reconstitution of SOX activity. Murine SOX lacking the heme domain was utilized to allow usage of blood-dissolved oxygen as a final electron acceptor for sulfite oxidation *in vivo*. The treatment resulted in a small, but significant increase in the average survival time of *Suox*$^{-/-}$ mice and upon further advancement presents a promising treatment strategy for SOXD in mice, which in the long term might lead to the discovery of a potent therapy usable for SOXD in humans as well.

In the course of the current study, a difference in the cause of death between human SOXD patients and *Suox*$^{-/-}$ mice became apparent. In line with this, a dermal phenotype was discovered and investigated in *Suox*$^{-/-}$ mice, which is characterized by epidermal hyperproliferation and defective terminal differentiation presumably caused by the sulfite-mediated cleavage of disulfide bonds in keratins and other structural proteins, which are crucial for structural integrity of the epidermis. The data strongly suggest the development of an epidermal barrier defect in the progression of the disease, but future studies will be required to unravel the contribution of the observed phenotype to the overall lethality in those mice.

Zusammenfassung

Isolierte Sulfitoxidasedefizienz (SOXD) ist eine seltene, autosomal-rezessive Erbkrankheit, die mit schweren Krämpfen, neurologischen Schäden und Veränderungen der Gesichts- und Schädelmorphologie, einhergeht und unbehandelt zu einem frühen Tod führt. Sie wird durch einen Funktionsverlust des mitochondrialen Molybdoenzyms Sulfitoxidase (SOX) entweder aufgrund von Mutationen des *SUOX*-Gens (SOXD) oder durch Defekte in der Biogenese des Molybdäncofaktors (MoCD), der das aktive Zentrum des Enzyms bildet, verursacht.

Die Krankheit ist durch einen starken Anstieg der Konzentrationen von Sulfit und schwefelhaltigen Metaboliten wie beispielsweise S-sulfocystein im Urin gekennzeichnet, der mit einem Rückgang der Cystin- und Homocysteinwerte im Plasma einhergeht. Sulfit ist ein Molekül mit stark nukleophilen Eigenschaften, das Disulfidbrücken spalten und so die Stabilität und Funktion von Proteinen global beeinflussen kann. Im Gegensatz zu dem vielseitigen Mechanismus der Sulfit-vermittelten Toxizität löst SSC als strukturelles Analogon von Glutamat hauptsächlich N-Methyl-D-Aspartat (NMDA) Rezeptor-vermittelte Exzitotoxizität aus, die zu Neurodegeneration führt.

Bis heute gibt es keine wirksamen langfristigen Behandlungsstrategien für SOXD. Bisher beschränkt sich die Therapie hauptsächlich auf die symptomatische Behandlung mit Antiepileptika, die auf eine Verringerung der Anfälle und Spastik abzielen. Eine Verlangsamung des Krankheitsverlaufs wird durch eine verringerte Aufnahme von schwefelhaltigen Aminosäuren über die Nahrung angestrebt, um den Cysteinkatabolismus und somit die Bildung von Sulfit zu reduzieren, hat sich jedoch nur bei milden, spät auftretenden Fällen von SOXD als erfolgreich erwiesen.

Die Generierung einer *Suox*$^{-/-}$ Mauslinie lieferte ein neues Modellsystem zur Untersuchung der Auswirkungen von nicht-funktioneller SOX auf den Krankheitsverlauf von SOXD und bot damit neue Möglichkeiten für die Suche nach einer wirksamen Langzeitbehandlung. Daher untersuchte die vorliegende Studie mehrere Therapieansätze zur Behandlung von SOXD in Mäusen durch (i) Blockierung NMDA-Rezeptor-vermittelter Exzitotoxizität, (ii) Einschränkung der Aufnahme von Proteinen und schwefelhaltigen Aminosäuren über die Nahrung, (iii) chemisches Abfangen von Sulfit, (iv) Inhibition von Ferroptose und (v) eine Enzymersatztherapie unter Verwendung einer modifizierten SOX-Variante.

Die Ergebnisse zeigen keine positiven Auswirkungen der Blockierung von NMDA-Rezeptoren auf die Überlebenszeit von *Suox*$^{-/-}$ Mäusen. Dies stimmt überein mit der Tatsache, dass der zerebrale Phänotyp deutlich milder ausgeprägt ist als bei humanen Patienten, was auf eine andere zugrunde liegende Todesursache schließen lässt, und in starkem Kontrast zum Krankheitsverlauf bei menschlichen Patienten steht.

Eine therapeutische Verhinderung übermäßiger Sulfitakkumulation wurde durch eine Einschränkung der Aufnahme schwefelhaltiger Aminosäuren in der Nahrung zur Reduzierung des Cysteinkatabolismus angestrebt. Die Einschränkung der Ernährung bei Mäusen erwies sich jedoch als schwierig, da eine Manipulation des Futters der Mutter zur Veränderung der Ernährung der neugeborenen Mäuse die richtige Dosierung erschwerte, sodass keine Verbesserung des Phänotyps erzielt werden konnte.

Ein direkter Versuch, die Sulfitakkumulation durch die Verwendung verschiedener Thiol-reaktiver Verbindungen (D-Cystein/Cystin, Cystamin) zu reduzieren, führte ebenfalls nicht zu einer Verbesserung der Symptomatik oder Lebensdauer von *Suox*$^{-/-}$ Mäusen. Da es sich dennoch um einen einfachen und unkomplizierten Behandlungsansatz handelt, birgt chemisches Abfangen von Sulfit großes Potenzial für zukünftige Studien zur Behandlung von SOXD.

Da SOXD eine Depletion von Cystin verursacht, stellten wir die Hypothese auf, dass der regulierte Zelltodweg Ferroptose für einen Pathomechanismus der SOXD verantwortlich ist. Ferroptose ist durch eine erhöhte intrazelluläre Lipidperoxidation gekennzeichnet, die durch einen Cystein- und Glutathionmangel verursacht wird. Die aktuelle Studie schloss jedoch einen Beitrag der Ferroptose zum Phänotyp von *Suox*$^{-/-}$ Mäusen aus. Im Gegenteil führte der Funktionsverlust der SOX zu einer Inhibition der Ferroptose, was vermutlich auf eine schnellere Wiederherstellung von reduziertem Glutathion aufgrund der Sulfit-vermittelten Spaltung von Disulfidbindungen im intrazellulären Glutathiondisulfid zurückzuführen ist und durch eine verringerte Lipidperoxidation in den Nieren von *Suox*$^{-/-}$ Mäusen bestätigt wurde.

Die Enzymersatztherapie stellt einen alternativen Behandlungsansatz dar, der eine Wiederherstellung der SOX-Aktivität anstrebt. Durch die Verwendung von muriner SOX ohne Häm-Domäne ist es möglich, den im Blut gelösten Sauerstoff als finalen Elektronenakzeptor für die Sulfitoxidation *in vivo* zu nutzen. Die Behandlung führte zu einer begrenzten, aber signifikanten Verlängerung der durchschnittlichen Überlebenszeit von *Suox*$^{-/-}$ Mäusen und stellt in weiterentwickelter Form eine vielversprechende Behandlungsstrategie für SOXD in Mäusen dar, die langfristig auch zur Entdeckung einer wirksamen Therapie für SOXD im Menschen führen könnte.

Im Verlauf der aktuellen Studie zeigten sich Unterschiede in den Todesursachen von menschlichen SOXD-Patienten und *Suox*$^{-/-}$ Mäusen. Damit übereinstimmend wurde bei *Suox*$^{-/-}$ Mäusen ein dermaler Phänotyp entdeckt und untersucht. Dieser zeichnet sich aus durch epidermale Hyperproliferation und fehlerhafte terminale Differenzierung, die vermutlich durch die Sulfit-vermittelte Spaltung von Disulfidbindungen in Keratinen und anderen Strukturproteinen verursacht werden, die für die strukturelle Integrität der Epidermis essentiell sind. Die Daten deuten stark auf die Ausbildung eines epidermalen Barrieredefekts im weiteren Krankheitsverlauf hin, aber weitere Studien sind erforderlich, um den Beitrag des beobachteten Phänotyps zur Letalität der Mäuse aufzuklären.

I Introduction

Part A Molybdenum in health and disease

1.1 The Molybdenum Cofactor

The transition element molybdenum is a powerful catalyst for redox reactions and as such it can be found in a variety of different species throughout all kingdoms of life as part of the catalytic center of enzymes. These so-called molybdoenzymes overtake crucial functions in sulfur, nitrogen and carbon metabolism, thus rendering them essential for survival (Kisker, Schindelin, & Rees, 1997). Molybdenum enters the cell as molybdate (MoO_4^{2-}). While its exact route of import has not been fully understood yet in humans, in bacteria and some plants it has been found to be transported into the cell via high-affinity ABC transporters (Grunden & Shanmugam, 1997; Tejada-Jiménez et al., 2007; Tomatsu et al., 2007). These transporters consist of three different proteins: a periplasmic binding protein, an intrinsic membrane protein and an ATPase.

In the cell, in order to fulfill its vital functions and gain catalytic activity, molybdenum needs to be incorporated into a cofactor. So far, two different forms of molybdenum-containing cofactors have been found: iron-sulfur cluster bound molybdenum is exclusively found in the cofactor (FeMoco) of nitrogenase, an enzyme produced by a number of bacteria including cyanobacteria and rhizobacteria (Burgess & Lowe, 1996; Koirala & Brözel, 2021). The cofactor contains one [4Fe-3S] and one [Mo-3Fe-3S] cluster, which are bridged by three sulfides and one central carbon atom (J. Kim & Rees, 1992; Lancaster et al., 2011; Spatzal et al., 2011). All other organisms harbor a pterin-based form of the molybdenum cofactor (Moco). This form consists of a tricyclic pterin named molybdopterin, which contains a C6-substituted pyran ring, a terminal phosphate and a dithiolate group that binds the molybdenum (K. v. Rajagopalan & Johnson, 1992).

Moco-containing enzymes can be further subdivided into three different classes depending on the coordination of the molybdenum within their cofactors. Members of the sulfite oxidase family show covalent binding of the molybdenum to a cysteine residue of the apoprotein, while in the xanthine oxidoreductase family molybdenum is bound to a third, terminal sulfido ligand, which gets added in a final maturation step (Schwarz & Mendel, 2006). Those two families can be found throughout all kingdoms of life, while the third and last DMSO reductase family only exists in bacteria and archaea. In this family of enzymes, Moco is bound to a bis-molybdopterin-guanine dinucleotide (bis-MGD) consisting of two

pyranopterin molecules, which are further modified via nucleosides such as cytosine or guanosine (Miralles-Robledillo et al., 2019).

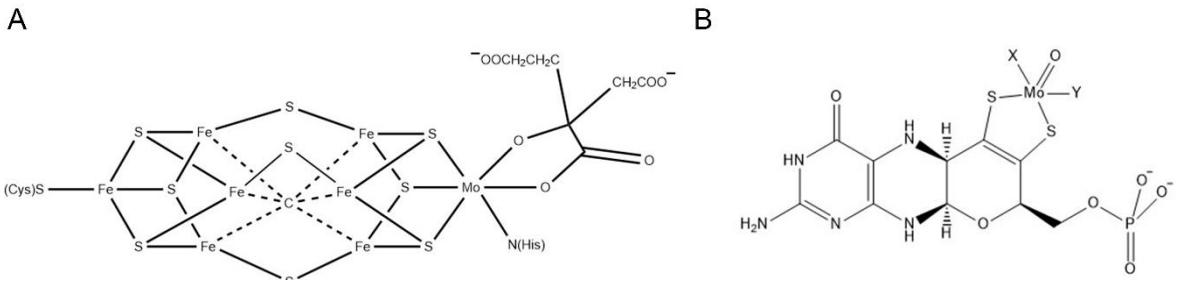

Figure 1: Molecular structures of FeMoco and pterin-bound Moco.
(A) Bacterial FeMoco harbors one [4Fe-3S] and one [Mo-3Fe-3S] cluster bridged by three sulfides and one central carbon atom. (B) The pterin-bound Moco consists of a tricyclic pterin that contains a C6-substituted pyran ring, a terminal phosphate and a dithiolate group binding the molybdenum. In members of the SOX family, X represents the single-bonded sulfur atom of a cysteine residue and Y a double-bonded oxygen. Enzymes of the XOR family contain a double-bonded inorganic sulfur and a hydroxyl group at the X and Y position, respectively. Figure modified from (Demtröder et al., 2019; Mendel, 2013).

1.2 Moco biosynthesis in bacteria

Moco biosynthesis can be divided into three main steps. In the first step, GTP is converted into cyclic pyranopterin monophosphate (cPMP). In bacteria, this step involves two proteins named MoaA and MoaC. The S-adenosylmethionine- and [4Fe4S] cluster-dependent enzyme MoaA catalyzes the formation of the intermediate 3′,8-cH_2GTP, which is further converted into cPMP by diphosphate cleavage and pterin ring formation via MoaC (Hover et al., 2013). In a second step, molybdopterin (MPT) is formed by insertion of two sulfur atoms at the C1' and C2' positions of cPMP (Daniels et al., 2008). The reaction is catalyzed by MPT synthase, a heterotetrameric complex consisting of two small and two large subunits named MoaD and MoaE (Pitterle & Rajagopalan, 1989). The two MoaE subunits form the center of the complex and are capable of binding one molecule of cPMP each, while the MoaD subunits are attached one on each end, respectively, and allow sulfur transfer from their C-terminal thiocarboxylate group to the pterin (Rudolph et al., 2001). Antecedently, MoaD gets primed by MoeB via the formation of a MoeB-MoaD adenylate complex at a C-terminal double glycine motif in MoaD, which in a second step is activated by a sulfur transferase utilizing L-cysteine as sulfur donor (Leimkühler & Rajagopalan, 2001). While *in vitro* any of the three bacterial NifS-like L-cysteine desulfurases CsdA, SufS and IscS can act as a sulfur donor, IscS has been proven to show the only specific interaction with MoeB and MoaD (Leimkühler & Rajagopalan, 2001; W. Zhang et al., 2010).

The last step of Moco biosynthesis can be divided into two reactions. In the first part, the homotrimeric protein MogA mediates ATP-dependent MPT adenylation, which yields the intermediate MPT-AMP (Kuper et al., 2004; Liu et al., 2000). Subsequently, MoeA in its

active dimeric form hydrolyzes the phosphodiester bond in a molybdenum-dependent manner leading to the ligation of the molybdenum to the pterin dithiolene, resulting in the formation of the basic, tri-oxo form of Moco, which can directly be inserted into members of the sulfite oxidase family (Leimkühler, 2020; Xiang et al., 2001). For enzymes of the xanthine oxidoreductase family, additional sulfuration is needed which requires Moco-binding chaperones of the XdhC family prior to insertion (Leimkühler & Neumann, 2011). Alternative modification by nucleotide addition is a two-step reaction essential for cofactor formation in the DMSO reductase family. In a first step, MobA catalyzes the conversion of Mo-MPT into a bis-Mo-MPT intermediate. This intermediate can be inserted directly into the cofactor of the YdhV protein in *E. coli* (Reschke et al., 2019), but for the majority of enzymes is further modified by the addition of two GMP molecules resulting in the bis-MGD cofactor (Lake et al., 2000; Palmer et al., 1996). Moreover, in a third group of enzymes from the DMSO reductase family the cofactor contains an additional sulfido ligand, which is transferred from the L-cysteine desulfurase IscS to the molybdenum cofactor by the enzyme FdhD (Arnoux et al., 2015; Thomé et al., 2012).

1.3 The enzymes of Moco biosynthesis in humans

1.3.1 MOCS1A + MOCS1B

Human Moco biosynthesis shows a high resemblance to the bacterial pathway. In the first step, cPMP is formed from GTP via the intermediate 3′,8-cH_2GTP (Hover et al., 2013). As in bacteria, the reactions are catalyzed by two distinct proteins MOCS1A and MOCS1B, which are homologous to MoaA and MoaC. In humans, however, those proteins are derived from the same unique bicistronic *MOCS1* gene (Gray & Nicholls, 2000; Reiss, Christensen, et al., 1998).

Alternative splicing of exons 1 and 9 results in four different N-terminal and three different C-terminal variants (I-III), respectively (Arenas et al., 2009). Splice type I produces bicistronic transcripts with two non-overlapping open reading frames, however only the first nine exons containing MOCS1A are translated (Mayr et al., 2020). In splice types II and III, alternative splicing of exon 9 leads to the production of MOCS1AB fusion proteins, in which exon 9 is either partially or entirely skipped. This results in the loss of the contained stop codon and a catalytically essential C-terminal double-glycine motif located just prior to the stop codon, which is thus skipped as well. Therefore, the fusion protein contains fully functional MOCS1B, but catalytically inactive MOCS1A. Proteolytic cleavage results in the liberation of active MOCS1B and the presentation of an internal mitochondrial targeting signal (MTS), which leads to its import into the mitochondrial matrix (Mayr et al., 2020).

Splice types I and III predominate *in vivo*, making up 41% and 55% of all *MOCS1* transcripts, while splice type II is only found in 4% of *MOCS1* expression (Arenas et al., 2009).

Moreover, N-terminal splicing of exon 1 results in four additional variations of *MOCS1* only affecting MOCS1A, which use mutually exclusive start codons and affect catalytic activity (Mayr et al., 2020). Similar to bacterial MoaA, MOCS1A belongs to the superfamily of radical S-adenosylmethionine proteins and requires two [4Fe-4S] clusters to be active, whose binding sites are found in exon 1d and at the C-terminus of MOCS1A (Hänzelmann et al., 2004). Two splice variants start on exon 1a: the Larin variant contains exon 1ad and is fully active, while in the Arenas variant exon 1a is directly followed by exon 2, thus lacking one Fe-S binding site and rendering the resulting protein inactive (Arenas et al., 2009; Gross-Hardt & Reiss, 2002). The other two variants start on exon 1b, with the Reiss variant containing exons 1bcd and the Gross-Hardt variant skipping exon 1c resulting in a truncated exon 1bd (Gross-Hardt & Reiss, 2002; Reiss, Cohen, et al., 1998). Exon 1c is believed to support protein stability, as its absence was shown to result in aggregate formation (Mayr et al., 2020). Furthermore, exon 1a was predicted to contain an MTS, which is absent in exon 1b (Mayr et al., 2020).

The question of a necessity for distinct mitochondrial and cytosolic MOCS1A proteins and their role in Moco biosynthesis, however, remains to be elucidated. Following conversion of GTP into the intermediate 3,8′cH2-GTP, MOCS1B catalyzes its conversion into cPMP. Due to its strong MTS MOCS1B is located in mitochondria, thus locating the entire second step of cPMP formation to mitochondria (Mayr et al., 2020). How the unstable intermediate 3,8′cH2-GTP formed by MOCS1A could be transported from cytosol to mitochondria has not been discovered yet, so further studies will be crucial to fully understand the exact process and the contribution of both mitochondrial and cytosolic MOCS1A to cPMP biosynthesis.

1.3.2 MPT synthase and MOCS3

The second step of Moco biosynthesis is the conversion of cPMP into MPT mediated by MPT synthase. Similar to bacteria, in humans MPT synthase consists of two distinct proteins forming a heterotetrameric complex (Rudolph et al., 2001). MOCS2A and MOCS2B are both derived from a bicistronic transcript of the *MOCS2* gene containing overlapping and shifted open reading frames (Stallmeyer et al., 1999). Splicing of exon 1 results in two distinct splice forms (I and III) with alternate start codons. Splice form I uses a start codon in exon 1a and a stop codon in exon 3, which results in translation of a MOCS2A protein containing the catalytically essential C-terminal double-glycine motif, which as described above can also be found in bacterial MoaD (Rudolph et al., 2001; Stallmeyer et al., 1999).

In contrast, splice form III contains exon 1b instead of exon 1a, which causes a shift of the open reading frame and results in the usage of a start codon in exon 3 and a stop codon in exon 7, thus translating into the protein MOCS2B (Hahnewald et al., 2006). Splice form II cannot be found in the databases anymore and is believed to have been an artifact (Reiss & Hahnewald, 2011).

The mode of action of human MPT synthase is identical to the pathway found in bacteria (Leimkühler, 2017). MOCS2A and MOCS2B show high sequence homology to bacterial MoaD and MoaE and chimeric studies have proven them interchangeable (Leimkühler et al., 2003). However, human MPT synthase has a significantly slower reaction rate than MPT synthase from *E. coli* (Leimkühler et al., 2003). Moreover, bacterial MoeB is not sufficient for the activation of MOCS2B, which is exclusively carried out by its human homologue MOCS3. Sequence homology can be observed between MoeB and the N-terminal part of MOCS3, with the latter harboring an additional C-terminal rhodanese-like domain absent in MoeB (Leimkühler et al., 2003). Similar to bacteria, humans use L-cysteine as sulfur donor. The sulfur is bound by the L-cysteine desulfurase NFS1 in form of a persulfide group, which in a second step is further transferred onto a cysteine residue in the rhodanese-like domain of MOCS3 (Marelja et al., 2008, 2013; Matthies et al., 2005). Hence, MOCS3 is a multifunctional protein, which in contrast to MoeB catalyzes the adenylation of MOCS2 as well as the subsequent sulfur transfer reaction, while in bacteria the latter is performed by an L-cysteine desulfurase (Leimkühler, 2017; Leimkühler & Rajagopalan, 2001; Matthies et al., 2004).

1.3.3 Gephyrin

The third and final step of Moco biosynthesis comprises the adenylation of MPT and the subsequent insertion of molybdate to form the mature eukaryotic form of Moco. While in bacteria these reactions are catalyzed by MogA and MoeA, respectively, in humans both steps are combined by a single protein called gephyrin, which is encoded by the *GPHN* gene (G. Feng et al., 1998; Leimkühler, 2020).

Gephyrin is a cytosolic three-domain protein comprising an N-terminal G-domain and a C-terminal E-domain, which are homologues of MogA and MoeA, respectively, as well as a central C-domain (Sola et al., 2001). Similar to their bacterial homologues, gephyrin G-domain forms trimers and gephyrin E-domain is present in dimers (Sola et al., 2001, 2004). First, the G-domain catalyzes the adenylation to form MPT-AMP upon ATP consumption. In a second step, the MPT-AMP is transferred to the nucleotide-binding pocket of the E-domain, which includes an adenine-binding region, a loop for the recognition of the nucleotide and a catalytic site for MPT-AMP hydrolysis. The metal binding site is

located in close spatial proximity to the predicted position of the dithiolene group of MPT to allow Mo-dependent MPT-AMP hydrolysis upon the formation of Moco (Kasaragod & Schindelin, 2016; Llamas et al., 2006).

In addition to its function in Moco biosynthesis, gephyrin plays an essential role in the formation of inhibitory synapses by serving as an anchor protein for glycine receptors (GlyRs) and $GABA_A$ receptors ($GABA_ARs$) at the postsynaptic membrane in neurons. Posttranslational modifications such as palmitoylation, S-nitrosylation and proteolytic cleavage by calpain, as well as alternative splicing serve as regulatory mechanisms, thus providing additional structural and functional complexity to the protein in different organs (Dejanovic et al., 2014; Dejanovic & Schwarz, 2014; Dos Reis et al., 2022; B. T. Kawasaki et al., 1997). The majority of alternatively spliced cassettes are found in the C-domain and have no impact on the metabolic function of gephyrin. However, insertion of the G2 splice cassette abolishes the last step of Moco biosynthesis by changing the oligomerization state of gephyrin G-domain from trimer to dimer (Smolinsky et al., 2008).

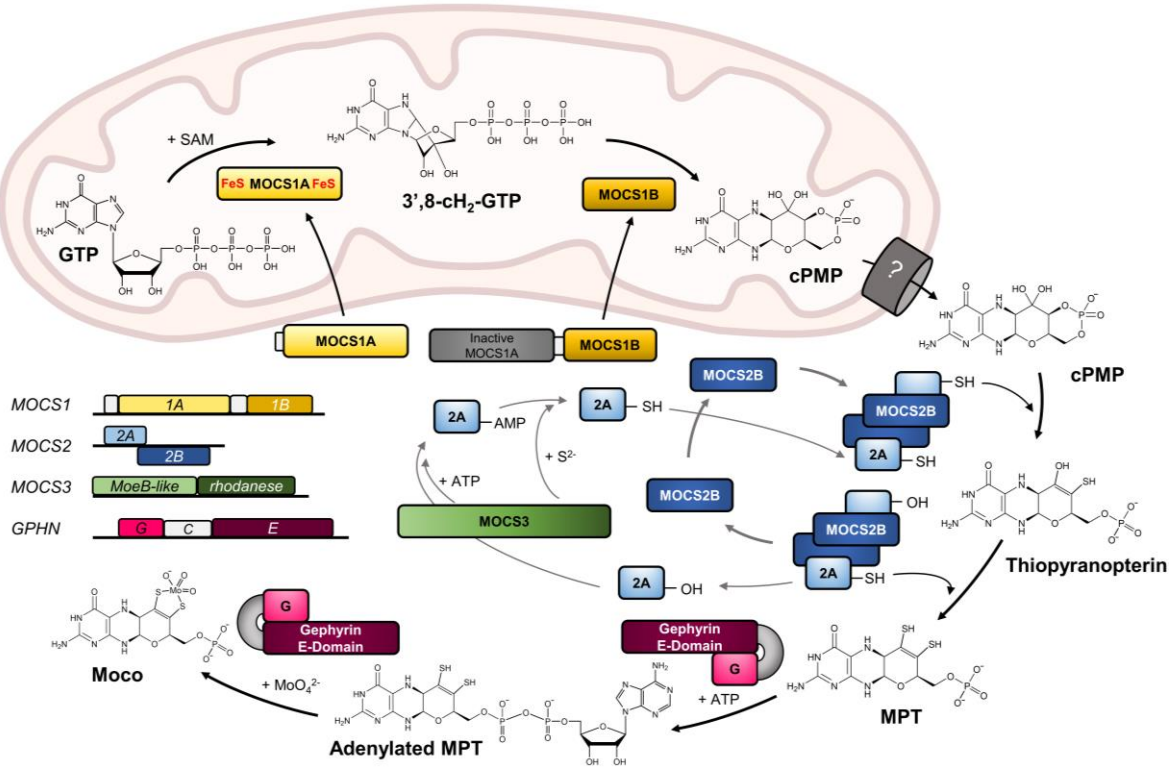

Figure 2: Human Moco biosynthesis.
Human Moco biosynthesis is a three-step reaction catalyzed by different enzymes depicted as colored boxes. Schematic representations of the genes encoding for those enzymes are depicted on the left in the same color code. The transporter involved in cPMP translocation to the cytosol is not known yet and thus depicted with a question mark. Figure modified from (Mayr et al., 2021).

1.4 Human molybdoenzymes

Up to date, in total more than 100 molybdoenzymes have been identified and classified, but only five of them have been found in eukaryotes (Hille et al., 2011). These include aldehyde oxidase (AOX), xanthine oxidoreductase (XOR), sulfite oxidase (SOX) and the mitochondrial amidoxime-reducing component (mARC) in mammals, as well as nitrate reductase (NR) in plants. According to the coordination of their Moco, XOR and AOX belong to the XOR family, while SOX and NR form the SOX family (Hille et al., 2011). In mARC, the Moco is coordinated by covalent attachment to a highly conserved cysteine residue as seen in the SOX family, while simultaneously displaying a pyranopterin conformation, which is typical for the XOR family, and harboring a fold being distinct from any of the two families. Hence, mARC represents an own class of molybdoenzymes and rather portrays the first evolutionary link between both known families (Kubitza et al., 2018).

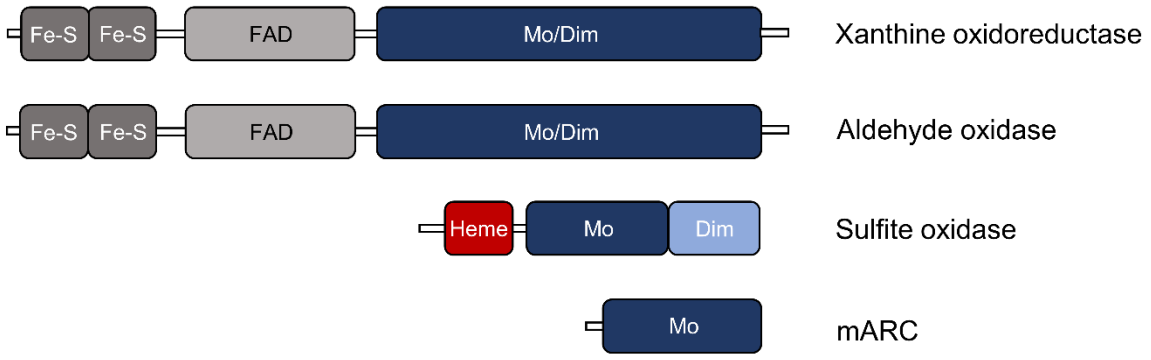

Figure 3: Domain structures of human molybdoenzymes.
Comparison of the domain structures of all known human molybdoenzymes.

1.4.1 Xanthine oxidoreductase

The cytosolic protein XOR is the first member of the highly conserved XOR family of molybdoenzymes, which can be found among prokaryotic and eukaryotic organisms, presumably sharing a common biological ancestor (Terao et al., 2016). Both subunits of the homodimeric protein XOR comprise an N-terminal Fe-S domain harboring two [2Fe-2S] clusters and a C-terminal Moco and dimerization domain, which are linked to a central FAD domain via two flexible hinge regions (Nishino et al., 2020). XOR preferably acts on low substituted purines and *in vivo* mainly catalyzes the hydroxylation of hypoxanthine and xanthine to yield urate, thus functioning as the terminal enzyme in purine catabolism (Harrison, 2002; Hille & Nishino, 1995). Moreover, it can act on a broad number of other substrates including pteridines, pyrimidines, N-heterocyclic compounds, aldehydes, as well as several xenobiotics, which attributes it an additional role in liver detoxification reactions (Krenitsky et al., 1972). XOR by default functions as an NAD^+ dependent dehydrogenase, however reversible oxidation of two essential cysteine residues, as well as irreversible

partial proteolysis of the region containing the two cysteines, converts it into an oxidase using oxygen instead of NAD^+ as its electron acceptor (Corte & Stirpe, 1972; Nishino et al., 2008; Stirpe & Della Corte, 1969). An intermediate product showing modification of only one of the sulfhydryl groups is capable of performing both dehydrogenase and oxidase function (Nishino et al., 2015). *In vivo*, the conversion from dehydrogenase to oxidase form is involved in numerous processes including lactation and the development of the innate immune system (Vorbach et al., 2002, 2003). Further posttranslational modifications, mainly including demolybdo and desulfo forms, render the enzyme inactive and are found in 98% of human enzyme in studies from milk (Abadeh et al., 1992).

1.4.2 Aldehyde oxidase

Besides XOR, in eukaryotes AOX is the second human member of the XOR family of molybdoenzymes. Both enzymes display a high structural similarity attributable to their high sequence identity of about 50% (Mahro et al., 2013). As XOR, AOX is located in the cytosol and forms homodimers. Each subunit contains an N-terminal Fe-S domain harboring two [2Fe-2S] clusters, which is linked to a central FAD domain via a flexible hinge region and a C-terminal Moco and dimerization domain, again bridged to the FAD domain via a flexible tether (Coelho et al., 2012). Despite their huge structural similarities, XOR and AOX display major differences in their substrate specificity. While XOR favorizes hypoxanthine and xanthine, AOX generally catalyzes the hydroxylation of higher substituted aromatic ring structures and the oxidation of aldehydes to their respective carboxylic acids utilizing water and oxygen (Garattini et al., 2008). It has an overall broader range of substrates *in vivo*, but its precise physiological function has not been identified yet, although it is known to be involved in drug metabolism (Garattini et al., 2008).

The first crystal structure of a mammalian AOX protein was AOX3 from murine liver and gave further insights into the difference in substrate specificity between AOX and XOR (Coelho et al., 2012). While the overall structure is highly similar to bovine XOR, AOX lacks a flexible loop around the FAD site, which enables XOR in its reduced form to utilize NAD^+ as the final electron acceptor, thus rendering AOX a pure oxidase. Moreover, some conserved residues within the active sites of both proteins differ and presumably are the main reason for the differences in substrate specificity (Coelho et al., 2012). While in rodents, including mice and rats, four distinct genes on the same chromosome encode for four isoforms of the enzyme, the only isoform of AOX in humans is encoded by the *AOX1* gene. Human AOX shows a high sequence identity of 85% towards its rodent orthologue AOX1, while it only shares about 60% of its sequence with the other three isoforms (Garattini & Terao, 2011). However, two of the latter can be found as pseudogenes in close proximity to the human *AOX1* gene (Garattini et al., 2008).

1.4.3 Mitochondrial amidoxime-reducing component

MARC is the smallest and simplest of the human molybdoenzymes, as it does not only form monomers, but also lacks any additional prosthetic groups despite the Moco (Ott et al., 2015). Therefore, it requires the activity of the two electron transport proteins cytochrome *b5* type B and NADH cytochrome *b5* reductase (Ott et al., 2015). The electrons provided by this system are utilized for the reduction of N-hydroxylated substrates, which among others plays a role in the activation of amidoxime prodrugs and in the general reduction of N-oxygenated metabolites formed by P450 enzymes (Gruenewald et al., 2008; Ott et al., 2015). Moreover, studies suggest its involvement in the protection of cellular DNA by detoxification of N-hydroxylated base analogues (Krompholz et al., 2012).

In mammalians, the two genes *MARC1* and *MARC2* encode for two paralogue enzymes mARC1 and mARC2, but to date the knowledge on gene regulation and potentially differing tissue expression is still limited (Neve et al., 2015). However, one recent finding suggested mARC2 as a predictive factor for hepatocellular carcinoma, as mARC2, but not mARC1 shows strong downregulation proportional to the severity of the disease, thus pointing towards different physiological functions of both enzymes (Wu et al., 2020). In line with this, mARC2-deficient mice showed a distinct phenotype including decreased body weight, increased body temperature, lower levels of total cholesterol, and higher glucose levels (Dickinson et al., 2016; Rixen et al., 2019). These mice also harbor significantly reduced reductase activity towards a number of N-oxygenated substrates, which could not be rescued by the unaltered expression of mARC1, thus again verifying a difference in the function of the two isoforms *in vivo*, which will need to be further elucidated in the future (Rixen et al., 2019).

In the past, computational studies on mARC1 and mARC2 predicted similar protein structures including an N-terminal MTS, a domain containing a β-barrel and a molybdenum cofactor sulfurase C-terminal (MOSC) domain for both of them (Anantharaman & Aravind, 2002). A few years later, the crystal structure of human mARC1 indeed revealed the existence of two distinct domains within the protein (Kubitza et al., 2018). However, they do not resemble the predictions, as tertiary-structure elements found were not clearly separated but rather comprised parts of both predicted domains. The study also found two highly conserved key residues in close proximity to the active site, which differ between mARC1 and mARC2 proteins and influence their catalytic activity and substrate specificity (Kubitza et al., 2018). Moreover, the crystal structure showed an unexpected conformation of the bound Moco, as it is typically found in the XOR family, while biochemical and biophysical features of mARC resemble more to the SOX family (Kubitza et al., 2018).

Therefore, mARC seems to represent an evolutionary link between the SOX and XOR family of molybdoenzymes.

1.4.5 Sulfite oxidase

SOX is the fourth and due to its pivotal role in human health also described as the most crucial human molybdoenzyme (Schwarz, 2005). It is the only human member of the SOX protein family, in which the molybdenum of the cofactor is covalently bound to an invariant cysteine residue of the apoprotein (Hille, 2002). The enzyme is highly conserved among various kingdoms of life, as alternative forms can also be found in plants (plant SOX) as well as in bacteria (sulfite dehydrogenase) (Eilers et al., 2001; C. Feng et al., 2007). Mammalian SOX consists of three domains: a central Mo domain harboring the pterin-bound Moco, the N-terminal b_5-type-like heme domain, which is linked to the Mo domain via a flexible tether region and a C-terminal dimerization domain allowing the formation of homodimers (Kisker, Schindelin, Pacheco, et al., 1997).

SOX is localized in the intermembrane space of mitochondria (IMS), where it catalyzes the detoxification of sulfite to sulfate as the terminal step of cysteine catabolism (Johnson & Rajagopalan, 1979; Ono & Ito, 1984). The reaction mechanism of SOX can be subdivided into a reductive and an oxidative half. In the reductive half reaction, a nucleophilic attack of the sulfite lone pair on the oxo-ligand of the Moco initiates the reduction of molybdenum from Mo^{VI} to Mo^{IV} (Hille, 1994). Following the dissociation of sulfate, in the oxidative part the electrons accepted by the molybdenum are transferred onto the heme domain in two independent intramolecular electron transfer (IET) reactions. Transfer of the first electron leads to a paramagnetic Mo^{V} as well as a diamagnetic Fe^{II}, which are detectable via electron paramagnetic resonance (EPR) spectroscopy (Astashkin et al., 2002). Oxidation from Fe^{II} to Fe^{III} is achieved by transfer of the electron onto the final electron acceptor cytochrome *c* (Johnson-Winters et al., 2010). A second IET followed by reduction of a second molecule of cytochrome *c* regenerates the initial Fe^{III}/Mo^{VI} state (K. V. Rajagopalan, 1980).

The crystal structure of chicken SOX, which to date is the only fully resolved crystal structure of mammalian SOX, revealed a huge distance of 32 Å between Mo and heme domain, which was contrastive to the high velocity observed for the IETs (Kisker, Schindelin, & Rees, 1997; Sullivan et al., 1993). This led to the hypothesis that a conformational change might be essential for the reduction of the spatial distance and facilitation of the IETs (Kisker, Schindelin, & Rees, 1997). Previous studies showed a decrease in SOX activity upon increase of the viscosity of the reaction buffer and truncation of the linker region between Mo and heme domain (Bender, 2017; C. Feng et al., 2002). Combined, these findings

emphasize the significance of the flexibility of the tether region for the fast accomplishment of the IET.

A recent study also investigated the aspect whether IET occurs within or between the two subunits of SO by measuring activities of differently modified heterodimeric complexes. Their data suggest that one fully functional subunit of SO is sufficient for steady-state sulfite oxidation, leading to the hypothesis that homodimerization is more crucial for protein stability especially during maturation than for catalytic activity (Eh et al., 2022).

Besides sulfite oxidation, a novel function of SOX in nitric oxide (NO) production has been described in the literature. Similar to the molybdoenzymes XOR and AOX, which have been shown to exhibit nitrite reductase activity, SOX can catalyze a single-electron transfer exclusively from the fully reduced Mo^{IV} center to nitrite yielding NO under hypoxic conditions (Maia et al., 2015; Maia & Moura, 2018; Wang et al., 2015). As nitrite and the iron of the heme domain compete for the first sulfite-derived electron, full-length SOX exhibits a lower reaction rate of NO production as recombinant, isolated Mo domain (Wang et al., 2015). Nevertheless, knockdown of all molybdoenzymes compared to single knockdown of full-length SOX in fibroblasts resulted in almost equally reduced levels of nitrite-dependent cGMP formation and thus ascribed the highest contribution to NO production *in vivo* to SOX (Wang et al., 2015).

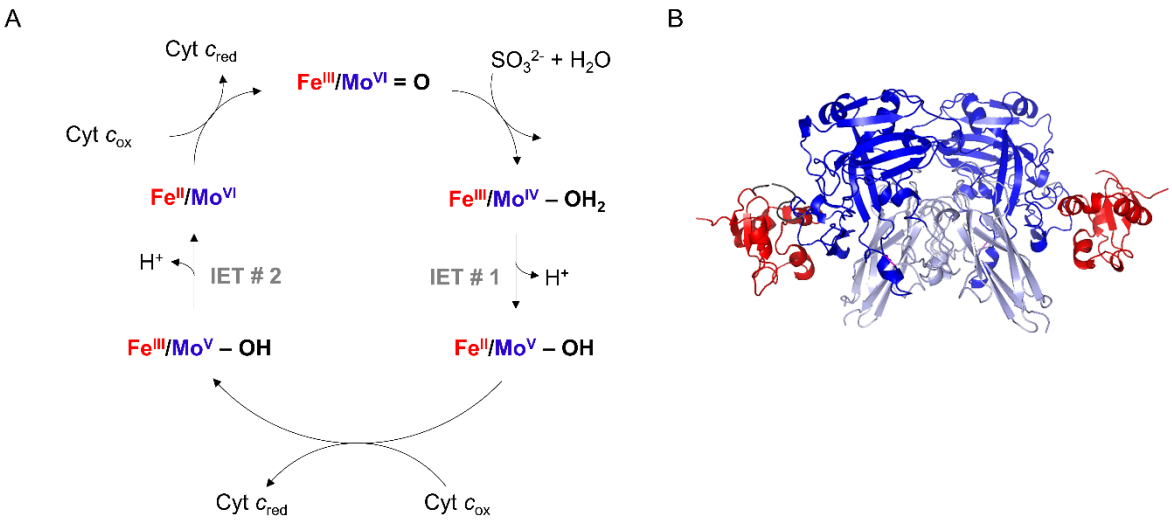

Figure 4: Reaction cycle and crystal structure of SOX.
(A) Reaction cycle of SOX-catalyzed sulfite oxidation. In the reductive half of the reaction, two electrons are transferred onto the molybdenum of the Mo domain. In the oxidative second half, two IETs from molybdenum to the iron of the heme domain and subsequent transfer onto two cytochrome *c* molecules regenerates the initial oxidation state. Figure modified from (C. Feng et al., 2007). (B) Crystal structure of chicken SOX dimer modified from (Kisker, Schindelin, & Rees, 1997). Mo domain is depicted in dark blue, dimerization domain in light blue and heme domain in red.

1.5 Molybdenum cofactor and isolated sulfite oxidase deficiency

Molybdenum cofactor deficiency (MoCD) and isolated sulfite oxidase deficiency (SOXD) are rare autosomal recessively inherited diseases, which are characterized by severe seizures, neurological damage and altered facial and head morphology, which collectively lead to infant death if left untreated (Johnson & Duran, 2001). MoCD involves a loss of function of all the above described molybdoenzymes and can be caused by defects in one of the three steps of Moco biosynthesis, as they were described in more than 200 cases so far (Spiegel et al., 2022). Depending on which step of Moco biosynthesis is affected, the disease can be further divided into three different subtypes (Reiss & Hahnewald, 2011).

In MoCD type A, which is the most frequent form of MoCD comprising 50-60% of MoCD patients worldwide, the first step of Moco biosynthesis is disturbed by mutations in the *MOCS1* gene (Reiss, Cohen, et al., 1998; Reiss & Hahnewald, 2011). One third of reported MoCD cases are classified as type B patients, which carry mutations in the *MOCS2* or *MOCS3* gene encoding for the proteins that are involved in the second step of Moco biosynthesis (Huijmans et al., 2017; Stallmeyer et al., 1999). MoCD type C is the rarest form, as so far only two patients have been diagnosed, and affects the *GPHN* gene (Reiss et al., 2001; Reiss & Hahnewald, 2011). Mutations in this gene abolish the last step of Moco biosynthesis, but can also affect the crucial neuronal function of gephyrin, thus causing an extremely severe phenotype in MoCD type C patients (Reiss et al., 2001).

SOX can be described as the most important member of the family of molybdoenzymes (Schwarz, 2005), given that loss of SOX activity results in a similar phenotype as seen in MoCD. SOXD is caused by a loss of SOX function due to mutation of the *SUOX* gene, which is located on chromosome 12 and encodes for SOX itself (Aghanoori et al., 2016; Johnson et al., 2002). Up to date, more than 50 cases of SOXD have been described in the literature (Claerhout et al., 2018; Sharawat et al., 2020; Tian et al., 2019). Loss of function of SOX, the final enzyme of cysteine catabolism, leads to a fatal accumulation of toxic sulfite in the body, as well as an increase in the levels of other sulfur metabolites including thiosulfate, taurine and S-sulfocysteine (SSC), which is formed in the reaction of sulfite and the disulfide cystine (Rupar et al., 1996).

1.5.1 Cysteine catabolism

MoCD and SOXD present with highly elevated levels of various sulfur metabolites due to the loss of function of SOX, the final enzyme of cysteine catabolism. Cysteine is a semi-essential amino acid, which promotes protein structure and stability by the formation of disulfide bridges and plays a crucial role in cellular redox regulation, as it is one of three

amino acids required for synthesis of the intracellular antioxidant glutathione (GSH). GSH biosynthesis is a two-step reaction catalyzed by glutamate cysteine ligase (GCL) and GSH synthetase (GSS). In a first, rate-limiting step, GCL forms the intermediate γ-glutamyl-cysteine from glutamate and cysteine. In a second step, attachment of a glycine molecule yields the final product GSH (Lu, 2013).

Cysteine can enter the cell as its oxidized form cystine via the x_c^- antiporter, which transports cystine into and glutamate out of the cell (Bannai, 1986). Alternatively, cysteine can be produced from methionine intracellularly via the transsulfuration pathway (Sbodio et al., 2019). In the form of S-adenosylmethione, methionine acts as an important methyl group donor in the cell, which results in its conversion into S-adenosylhomocysteine followed by hydrolysis to adenosine and homocysteine. The latter can be converted to cystathionine via condensation with serine catalyzed by the enzyme cystathionine β-synthase (CBS), which is followed by cleavage into cysteine and α-ketobutyrate by cystathionine γ-lyase (CSE). In the oxidative part of cysteine catabolism, cysteine is oxidized to cysteine sulfinic acid (CSA) by the enzyme cysteine dioxygenase (CDO). A part of CSA is then decarboxylated by CSA decarboxylase (CSAD) to yield hypotaurine, which further converts into taurine in a non-enzymatic reaction. The other part of CSA is deaminated to β-sulfinylpyruvate, which spontaneously decomposes to pyruvate and sulfite, by cytosolic and mitochondrial glutamate oxaloacetate transaminase (GOT1 and GOT2, respectively). In a last step, sulfite is immediately detoxified by oxidation to sulfate catalyzed by SOX (Kohl et al., 2019).

In the hydrogen sulfide (H_2S) pathway, several reactions lead to the formation of H_2S. On the one hand, CBS and CSE both independently can catalyze the reaction of cysteine with water producing serine and H_2S. Additionally, in an alternative reaction catalyzed by the enzymes GOT1 and GOT2, cysteine and α-ketoglutarate are converted into glutamate and 3-mercaptopyruvate. Subsequently, reductive desulfuration of the latter is catalyzed by the enzyme 3-mercaptopyruvate sulfurtransferase (MPST), yielding pyruvate and H_2S. H_2S clearance is performed in a multistep reaction starting with its oxidation to a zero-valent sulfur by generating a protein-bound persulfide followed by transfer onto an acceptor, which is mediated by the membrane-bound mitochondrial enzyme sulfide:quinone oxidoreductase (SQR). So far, GSH has been discussed as the primary acceptor, which would result in the formation of glutathione persulfide (GSSH). Regeneration of glutathione is catalyzed by thiosulfate sulfurtransferase (TST) and persulfide dioxygenase (PDO) under formation of thiosulfate and sulfite, respectively. Hence, in both parts of cysteine catabolism, SOX is the key enzyme required for clearance of sulfite and its loss of function impacts a complex, highly regulated pathway resulting in the elevation of several different and potentially toxic metabolites (Kohl et al., 2019).

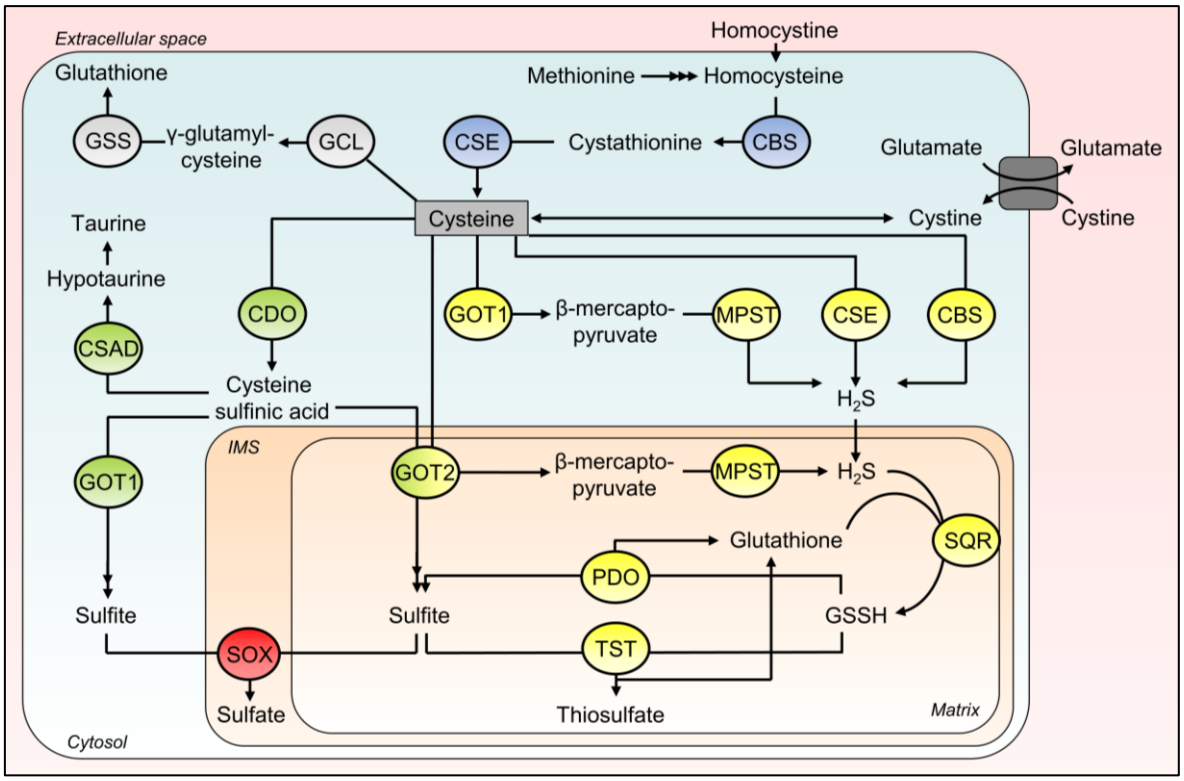

Figure 5: Schematic representation of cysteine catabolism.
Enzymes and metabolites involved in cysteine catabolism. Glutathione biosynthesis is depicted as grey, transsulfuration pathway as blue, oxidative pathway as green and H_2S pathway as yellow. SOX as the final enzyme of both latter pathways is colored in red.

1.5.2 Clinical presentation of SOXD

The metabolic diseases SOXD and MoCD display huge similarities in their clinical presentation with an equally fatal set of symptoms. Similar to MoCD, SOXD presents with feeding difficulties, spasticity, microcephaly, lens dislocation and psychomotor retardation (Johnson & Duran, 2001). As biochemical hallmarks for diagnosis, patients are tested for a vast increase of sulfite and SSC levels in urine accompanied by a decrease of plasma cystine and homocysteine levels (Bindu et al., 2017). While in MoCD additionally uric acid levels in plasma are decreased and urinary xanthine and hypoxanthine are significantly elevated, in SOXD these levels remain unchanged, as they can be attributed to a loss of XOR function upon disturbance of Moco biosynthesis (Endres et al., 1988).

Progression of the disease is dependent on the underlying *SUOX* mutation and the resulting level of residual SOX enzymatic activity. Most patients harbor homozygous mutations, but few heterozygous mutations have been reported earlier (Zhao et al., 2021). While nonsense and frameshift mutations lead to very severe phenotypes, the effect of missense mutations might vary from not impacting the enzyme over leading to impaired, but residual activity to total loss of function, depending on their localization (Claerhout et al., 2018). Recently, a study used machine learning-based random forest classification to

predict the pathology of 303 naturally occurring missense mutations of the *SUOX* gene and found 15 novel pathogenic mutations, while most missense mutations were predicted to not result in manifestation of the disease (Kaczmarek et al., 2021).

Most commonly, SOXD presents as an early onset disease starting hours to days after birth with feeding difficulties, increased irritability and intractable seizures. Infants display rapidly progressing encephalopathy leading to cerebral atrophy and microcephaly, as well as severe developmental retardation and typically die within the first months of life (Bindu et al., 2017; Claerhout et al., 2018). However, several late onset cases have been described in the literature, which typically start between the first six to 18 months of life with developmental delay and impaired neuromotor function. Life expectancy is significantly longer than in case of early onset and can vary between early and late childhood with highly differing individual courses of the disease depending the underlying *SUOX* mutation (Bindu et al., 2017; Claerhout et al., 2018).

Recently, one patient has been described, which developed symptoms one year after birth and was followed up until the age of 9.5 years (Tian et al., 2019). He displayed heterozygous missense mutations in the Mo and dimerization domain, thus supporting the hypothesis of missense mutations leading to a later disease onset. SOX activity was not determined, but residual activity causing an amelioration of the phenotype can be speculated. The patient showed unstable postural control and a borderline level of mental development, but brain lesions observed at an early stage of the disease almost completely recovered over the years and his performance in school was normal. To date, this patient and his two younger siblings, which presented with equally promising development during follow up, are the only patients with a stable clinical course and spontaneous recovery, which have not been treated otherwise (Tian et al., 2019).

1.5.3 Current state of knowledge on the disease mechanism

Although MoCD shows additional symptoms to SOXD due to xanthinuria caused by loss of XOR function, the major disease mechanism, which ultimately results in premature death, can be ascribed to a loss of SOX function. The different aspects of cellular changes due to SOXD are discussed based on the role of the different metabolites being accumulated or depleted in SOXD patients.

Exposure to micromolar concentrations of sulfite in cells has been described to cause a depletion of intracellular ATP, which might be ascribed to a direct inhibition of glutamate dehydrogenase (X. Zhang et al., 2004). Sulfite itself has also been shown to alter the mitochondrial network in fibroblasts from MoCD patients with the result of increased

mitochondrial hyperfusion and presumably decreased mobility as seen in murine *Suox*$^{-/-}$ fibroblasts (Mellis et al., 2021). Additionally, sulfite can attack disulfide bonds in the extracellular space, thus impacting protein folding and stability. As sulfite was also proven to cleave persulfidations, which can function as a protective mechanism for cysteine residues from irreversible oxidation (Dóka et al., 2020), sulfite can also negatively impact protein function. Moreover, sulfite has been hypothesized to react with the aldehyde group of pyridoxal-5'-phosphate (PLP), which in its active form comprises the cofactor of more than 120 enzymes (Footitt et al., 2011). Sulfite has also been found to inhibit the enzyme α-aminoadipic semialdehyde dehydrogenase, which leads to an accumulation of α-aminoadipic semialdehyde and Δ^1-piperideine-6-carboxylate (P6C). P6C can inactivate PLP and represents an alternative mechanism of in PLP depletion in MoCD and SOXD (Mills et al., 2006, 2012). Decreased PLP in cerebrospinal fluid can lead to reduced synthesis of the neurotransmitters dopamine and serotonin, as well as reduced metabolism of glycine and threonine, and can cause an epileptic phenotype (Footitt et al., 2011), thus presumably contributing to the severe neurological phenotype observed in MoCD and SOXD.

In addition to its aforementioned pathological effects, sulfite is also responsible for the formation of SSC, which is seen as an important cause of neurotoxicity. Due to its structural resemblance to glutamate, SSC can cause major N-methyl-D-aspartate receptor (NMDAR)-mediated excitotoxicity ultimately resulting in elevated neurodegeneration (Kumar et al., 2017; Olney et al., 1975). Formation of SSC is seen as a sulfite scavenging mechanism to decrease sulfite accumulation, but additionally causes a depletion of cysteine and cystine in the organism. This in turn can result in decreased levels of GSH, possibly leading to reduced lipid peroxide-detoxifying glutathione peroxidase 4 (GPX4) activity followed by ferroptosis, an iron- and reactive oxygen species (ROS) dependent form of non-apoptotic cell death (Seiler et al., 2008; Yang et al., 2014).

While some aspects of the disease mechanism have been elaborated in greater detail already, others remain broad hypotheses and speculations. MoCD and SOXD present with increased levels of thiosulfate, but might additionally be accompanied by an increased flux of H_2S, a metabolite required for SQR-dependent production of thiosulfate, which in high concentrations is a potent inhibitor of cytochrome *c* oxidase (Dorman et al., 2002; Jackson et al., 2012). Similarly, *Ethe1*$^{-/-}$ mice, which are used as a model for ethylmalonic encephalopathy and lack PDO, display vastly elevated H_2S resulting in death between five to six weeks after birth (Tiranti et al., 2009). Although the exact phenotype of *Suox*$^{-/-}$ mice will be discussed later, they show a remarkably more severe phenotypic expression than *Ethe1*$^{-/-}$ mice. A sole toxicity of H_2S is therefore unlikely to cause the severe phenotypes of

MoCD and SOXD. Most likely, it can be seen as a multi-faceted disease mechanism, thus resulting in such severe progression of the diseases.

1.5.4 Current treatment options for SOXD

In the past, successful treatment of MoCD type A could be achieved by regular administration of cPMP, the product of the first step of Moco biosynthesis (Veldman et al., 2010). Treatment normalized urinary levels of all biochemical hallmarks of the disease within one to two weeks and remained constant over time. Treatment did not restore brain function, but stopped progressive cerebral atrophy from the start of therapy. However, up to date effective long-term treatment strategies are still lacking for MoCD type B and C, as well as for SOXD. So far, therapy is restricted to symptomatic treatment including anti-epileptic medication aiming for a reduction in seizures and spasticity, although the majority of SOXD patients present with pharmacoresistant seizures (Claerhout et al., 2018). Treatment of vomiting, gastroesophageal reflux, and aspiration pneumonia might be included if needed. Additionally, gastrostomy tube placement can be performed to ensure sufficient calorie intake upon feeding difficulties (Bindu et al., 2017).

Search for an effective long-term treatment of SOXD, however, has been subject of research since more than 30 years, with a first therapeutic approach having been tested in 1989 (Tardy et al., 1989). In this case study, a girl presented with facial hypotonia and choreoathetosis, as well as increased urinary excretion of sulfite, SSC and taurine, but without increased blood uric acid concentrations, which combined led to the diagnosis of SOXD. For therapy, D-penicillamine, which previously had been used in cystinuria, Wilson's disease and rheumatological diseases (Halperin et al., 1981; Howard-Lock et al., 1986; Van Caillie-Bertrand et al., 1985), was administered in a single dose of 150 mg with the intention to induce sulfite scavenging under the formation of S-sulfopenicillamine (Tardy et al., 1989). Treatment, however, did not form detectable amounts of urinary S-sulfopenicillamine, thus also having no impact on urinary levels of sulfite and SSC. Still, usage of other sulfite scavengers harboring free thiol groups was suggested to be tested in the future.

Another treatment option involves the dietary restriction of sulfur-containing amino acids to reduce cysteine catabolism and thus sulfite formation. Two patients with mild, late onset forms of SOXD responded well to a dietary treatment approach including low-protein diet supplemented with a synthetic amino acid mixture lacking methionine and cysteine, as it will be discussed in more detail in chapter II (Touati et al., 2000). Dietary restriction of sulfur-containing amino acids achieved a drastic decrease in urinary thiosulfate, taurine and SSC to stable levels within two months. Both patients grew and developed well without signs of further neurological deterioration, thus rendering dietary restriction an effective

treatment for mild cases of SOXD. One of the patients received additional treatment with the sulfite scavenger cysteamine. However, treatment did not show further improvement of the clinical picture and thus was discontinued after nine months (Touati et al., 2000).

Following the success of dietary restriction in late onset patients, in another report from the literature, low-protein diet was tested in a patient with a severe, early onset form of SOXD (Boyer et al., 2019). Eight days after birth, the female infant displayed poor feeding and increased irritability. Neurological examination revealed severe hypertonicity, opisthotonos, as well as status epilepticus, and blood analysis showed signs of metabolic acidosis, lactic acidosis and ketosis. MRI revealed abnormal alteration of white matter hinting towards initial signs of neurodegeneration. In urine, SSC levels were elevated, while xanthine and hypoxanthine levels remained unchanged. Plasma levels of homocysteine and cystine were low or undetectable, while plasma α-aminoadipic semialdehyde and P6C were elevated. In line with those findings, gene analysis found a homozygous single nucleotide duplication resulting in a frameshifting insertion that led to a premature stop codon in the *SUOX* gene. Due to difficulties to adjust to feeding, a low-protein, -methionine and -cystine diet was fed only starting six weeks after birth, when repeated MRI scan already revealed severe loss of brain volume, porencephaly and subdural effusions. Dietary restriction still improved her severe irritability and overall life quality, as well as her biochemical markers, with SSC level reduction of 36%. She continued to display severe developmental retardation with no signs of improvement. At an age of three months the patient was hospitalized again due to pneumonia and feeding intolerance requiring some additional adjustments of the diet. Nevertheless, at four months age she died from sepsis. Observed effects of dietary restriction were not as strong as in mild cases of SOXD, but significant improvements were obtained. As the cause of death was not directly linked to SOXD, a continuous mildly positive effect in the following months of life can be presumed, so low-protein and low-sulfur diets still continue to be a useful approach to stop or decelerate progression of the disease by preventing or lowering accumulation of toxic sulfur metabolites in mild and severe forms of SOXD, respectively.

In another case of severe, early onset SOXD, an alternative treatment strategy was applied (Tan et al., 2005). In addition to low-methionine and low-cysteine diet, administration of thiamine, an important cofactor to different enzymes, was proposed to have a beneficial effect on sulfite toxicity, as sulfites are known to destroy thiamine not only *in vitro*, but also *in vivo* as shown by animal experiments (Buchman et al., 1935; Til et al., 1972). Finally, aiming to counteract excitotoxic mechanisms in the brain, treatment with NMDAR antagonist dextromethorphan aimed to inhibit NMDAR-induced excitotoxicity and resulting neurodegeneration (Tan et al., 2005). Additional administration of phenobarbital

stopped tonic-clonic seizures in the patient after the neonatal period and an EEG revealed the absence of electrographic seizures at three months. As several treatments were applied simultaneously, however, the exact impact of each single treatment cannot be pinpointed. Due to remaining severe developmental retardation and progressive microcephaly, success of the tested therapeutic approach was limited, but might result in more positive findings in mild, late onset cases of SOXD.

In summary, although a few treatment strategies can decelerate progression of the disease, search for an effective long-term treatment targeting the actual disease mechanism still continues to be an important part of ongoing research and was therefore one aim of this thesis. Without doubt, any attempt leading to a reduction of sulfite accumulation would be expected to normalize disease-related biomarkers and improve clinical outcome, especially when applied at early age.

1.5.5 Available mouse models for MoCD and SOXD

1.5.5.1 Mouse model for MoCD type A

In 2002, *Mocs1*$^{-/-}$ mice were published as a mouse model resembling the phenotype of MoCD type A patients (Lee et al., 2002). On a genomic level, exon 3 of the *Mocs1* gene was chosen as a target, as it contains a number of highly conserved residues equally found in human *MOCS1*. The exon was deleted by homologous recombination and substituted by a Neomycin resistance-cassette to completely destroy MOCS1A activity and eventually also influence MOCS1B activity depending on the characteristics of the transcribed mRNA. As MOCS1B is only transcribed as a MOCS1AB fusion protein, instability in the part encoding for MOCS1A was proposed to cause degradation of the entire MOCS1AB transcript.

Homozygous *Mocs1*$^{-/-}$ were born healthy without any visual phenotypic expression, but showed significantly reduced weight gain over the following days and died between one to 11 days after birth with an average life span of 7.5 days. In contrast, heterozygous animals showed no signs of MoCD symptoms and were indistinguishable from wildtype littermates over their entire life span. Northern blot analysis did not detect any *Mocs1* RNA in homozygous mice, hence verifying depletion of both MOCS1A and MOCS1B proteins.

Ataxia and seizures were not observed in *Mocs1*$^{-/-}$ mice, but due to the strong neurological phenotype in human patients, further brain analysis was performed nonetheless. However, in line with phenotypic observations, nuclear staining of neuronal tissues did not show signs of altered cell number or development of the different cell layers. Biochemical analysis further revealed a total absence of MPT in homozygous animals, thus verifying a complete loss of function for all molybdoenzymes. Urinary sulfite, cysteine,

taurine and xanthine levels as well as the signal for an authentic SSC reference compound were markedly increased, while uric acid was not detectable in *Mocs1*$^{-/-}$ mice. As these mice die without any observable neurological phenotype, an increased importance of sulfite toxicity as the major cause of death was hypothesized, including the ability of sulfite to react with disulfide bonds and sulfhydryl groups and a potential sulfite-linked depletion of GSH (Graf et al., 1998; Lee et al., 2002). Presumably, the life span of *Mocs1*$^{-/-}$ mice is too shortened to allow the development of major neurological damage (Lee et al., 2002). Discovery of cPMP as a successful treatment option for these mice as well as for MoCD type A patients, however, still demonstrates the resemblance and thus importance of the mouse model for further understanding of the disease.

1.5.5.2 Mouse model for MoCD type B

In recent years, finally also a mouse model for MoCD type B has been generated (Jakubiczka-Smorag et al., 2016). The *Mocs2* gene was disrupted by insertion of a LacZ gene and a Neomycin resistance cassette after the start codon, which upon homologous recombination caused a deletion between exons 1 and 7, thus affecting almost the entire gene. PCR and western blot analysis of several different tissues confirmed the absence of *MOCS2* RNA and proteins, respectively.

Similar to *Mocs1*$^{-/-}$ mice, *Mocs2*$^{-/-}$ mice were born healthy, but quickly displayed developmental delay and growth retardation, as well as a generally weaker health condition leading to premature death at an average of 4.7 days. As the regulations for animal welfare changed in recent years, termination criteria are reached earlier nowadays, thus explaining the discrepancy between the average survival time of *Mocs1*$^{-/-}$ and *Mocs2*$^{-/-}$ mice. However, homozygous *Mocs2*$^{-/-}$ mice could be divided into two groups, as typically they either died on the first day after birth or survived until day five to ten. They further displayed curly whiskers and a global defect in hair growth accompanied by scaly, wrinkly skin. Serum and urine samples confirmed an increase in xanthine and hypoxanthine levels, while uric acid was undetectable. Additionally, shortly before death, *Mocs2*$^{-/-}$ mice developed urinary retention and, as observed after death, accumulated insoluble xanthine crystals in the bladder, thus confirming loss of XOR function. Direct measurement of SOX activity in liver and kidney revealed a complete loss of SOX function, which resulted in an expected increase of plasma and urinary SSC levels that, contrary to expectations, was not found in any tested tissues from *Mocs2*$^{-/-}$ mice. Stainings of hippocampus, cortex and brainstem sections did not show changes in overall neuron numbers, but revealed an increase in apoptotic neurons, which in more moderate form could also be seen in heterozygous mice. However, even in homozygous mice the changes in the brain were not severe enough to explain the overall

health impairment and shortened life span, so as already hypothesized for the earlier published *Mocs1*$^{-/-}$ mice, presumably other factors cause death in these animals prior to the development of a more severe, lethal cerebral phenotype. In line with findings from previous MoCD mouse models, heterozygous *Mocs2*$^{+/-}$ mice did not show phenotypic changes strong enough to reduce quality of life, hence confirming the sufficiency of 50% residual Moco biosynthesis for a normal development in mice and resembling the situation in human patients.

1.5.5.3 Mouse model for MoCD type C

Gphn$^{-/-}$ mice were generated as the first mouse model for MoCD in 1998 and resemble MoCD type C (G. Feng et al., 1998). Studies in these mice could finally verify the moonlighting function of gephyrin as a scaffold protein for GlyRs and $GABA_A$Rs in inhibitory synapses and a key enzyme in Moco biosynthesis. Full-body knockout (KO) of the *Gphn* gene was achieved by deletion of the promoter region plus exon 1 and successfully caused a complete loss of *Gphn* mRNA and protein as verified via northern and western blot analysis of brain tissue, respectively. *Gphn*$^{-/-}$ mice looked healthy at birth, but in contrast to wildtype and heterozygous litter mates did not show a milk spot and were not able to produce typical neonatal vocalizations. They displayed abnormal response to tactile stimuli by assuming a rigid, hyperextended posture similar to wildtype neonatal mice treated with the GlyR antagonist strychnine. While heterozygous mice developed normally without any impairments, homozygous mice suffered from apnea after 12 hours and died within the first 24 hours of life. Stainings of spinal cord sections revealed a diffuse distribution of GlyRs and $GABA_A$Rs and decreased GABAergic and glycinergic currents in the absence of gephyrin (G. Feng et al., 1998; Kneussel et al., 1999), hence attributing a crucial role in inhibitory synapse formation and function to gephyrin. Moreover, complete loss of SOX and XOR activity verified the second, essential role of gephyrin in Moco biosynthesis (G. Feng et al., 1998).

1.5.5.4 Mouse model for SOXD

While the first mouse models for MoCD have been established more than 20 years ago, for a long time no mouse model for SOXD was available, as only in 2019 the first successful generation of *Suox*$^{-/-}$ mice was described (Kohl, 2019). Via the CRISPR/Cas9 system, a seven base pair deletion in a region of exon 3 encoding for the Mo domain, close to several essential substrate-binding residues, was performed and verified by sequencing. Loss of SOX was confirmed by direct activity measurement in liver extracts and by western blot analysis.

Suox$^{-/-}$ mice presented without visible phenotypic changes at birth, but after the first four days of life started showing developmental delay including reduced weight gain and motor skills as measured in a righting reflex test. This ultimately caused death within the first 12 days of life with an average life span of 9.6 days. As expected, urinary sulfite, thiosulfate and SSC levels were significantly increased, further confirming loss of SOX function. Brain morphology showed differences in brain height and volume, which were believed to result from developmental delay or increased neuronal cell death. Later studies revealed no differences in neuron number similar to the results found in *Mocs1*$^{-/-}$ and *Mocs2*$^{-/-}$ mice (Kohl, Fu et al., in preparation), however more in-depth analyses looking at early stages of neurodegeneration as in *Mocs2*$^{-/-}$ mice have not been performed. Altered brain morphology can therefore be ascribed mainly to a significant developmental delay, while a severe cerebral phenotype would be expected to develop upon an increase of the average life span of *Suox*$^{-/-}$ mice.

Similar to the MoCD mouse models, loss of SOX function led to a decrease in cysteine in plasma and in GSH levels in liver and kidney (Kohl, 2019), which supports the early hypothesis of sulfite-linked depletion of GSH due to a restriction of cysteine in GSH synthesis (Graf et al., 1998). Although *Suox* KO does not affect other molybdoenzymes like XOR, similar to MoCD mouse models, *Suox*$^{-/-}$ mice present with a renal phenotype including proteinuria and increased urinary creatinine (Kohl, 2019). In the past, induction of oxidative stress presenting with increased ROS production and ATP depletion could be observed in several mammalian kidney cell lines upon incubation with micromolar levels of sulfite (Vincent et al., 2004). As SOX has been found to show highest expression and activity in kidney and liver, a loss of SOX function could increase the sensibility of renal cells towards sulfite toxicity (Kohl, 2019). However, although more intensive studies on kidneys from *Suox*$^{-/-}$ mice did confirm a renal phenotype, it is not sufficiently severe to explain the short average life span in those mice and can rather be classified as a secondary effect of yet unknown cause. Overall, further studies will be necessary to fully understand the disease mechanism and the major cause of death in this newly established mouse model of SOXD.

Part B Epidermal skin barrier in health and disease

1.6 Structure and function of the epidermis

The skin is the largest organ of the human body and as such allows protection against exogenic factors, regulates body temperature and hydration and mediates tactile sensation. It comprises three layers named hypodermis, dermis and epidermis.

The hypodermis, also called subcutaneous layer, is the most inner layer. It primarily stores fat and energy, thus functioning as a thermal isolator, and functions as a connection between skin and the underlying bones and muscles. The middle layer dermis adds strength and flexibility to the skin and supports the hypodermis in thermal regulation by producing sweat. It allows hair growth by harboring hair follicles and contains nerve endings enabling tactile sensation. The most outer layer is called epidermis and forms a protective outside-in barrier against exogenic factors like germs, UV radiation and minor mechanical forces, but also provides an inside-out barrier function protecting the body against transepidermal water loss (Monteiro-Riviere, 2005).

For full formation of the epidermal barrier function, several different cell layers are required. The stratum basale (SB) is the deepest layer of the epidermis and is located directly above the dermis, only separated by the basal lamina. The SB contains one single layer of functionally diverse basal cells, which are attached to the basal lamina and also laterally to each other and the following layer via hemidesmosomes and desmosomes, respectively (Monteiro-Riviere, 2005). While some basal cells function as anchoring cells staying attached to the basal lamina, basal keratinocyte stem cells proliferate to form the keratinocytes of the subsequent layers and enable a complete renewal of the epidermis within a 30-day cycle (Lavker & Sun, 1982). Besides keratinocytes, the epidermis contains melanocytes in a ratio varying from 1:4 to 1:11 throughout the body. Melanocytes are neural, crest-derived cells, which produce melanin, thus supporting protection of the skin from UV radiation (Monteiro-Riviere, 2005). Merkel cells are neuronal cells in the basal layer, whose function has not been clearly deciphered yet, but which seem to be involved in the development of hair follicles and in mediating tactile sensation (Abraham & Mathew, 2019; D. K. Kim & Holbrook, 1995).

The second layer of the epidermis - the stratum spinosum (SS) - is also the thickest structure. It is usually made up of five to ten layers of keratinocytes connected via desmosomes and tight junctions and provides the epidermis with flexibility and strength. Additionally, it contains Langerhans cells, which are dendritic cells crucial for protection

against germs, as they function as antigen-presenting cells mediating the immune response of the skin. They are attached to keratinocytes via E-cadherin, which in case of antigen presentation is downregulated to allow migration of the Langerhans cells to the lymph nodes (Barbieri et al., 2014).

The stratum granulosum (SG) is thinner than the SS with only three to five layers of differentiating keratinocytes, which are already flatter in shape and contain two types of granules (Monteiro-Riviere, 2005). Firstly, they harbor dense, basophilic keratohyalin granules filled with proteins contributing to the crosslinking of keratin filaments and the formation of the cell envelope, such as profilaggrin, the precursor of the structural protein filaggrin, and loricrin. They also contain serine proteases and respective inhibitors, which control cleavage of cell adhesion molecules as well as profilaggrin processing, and antimicrobial peptides acting as a primary defense system against exterior pathogens (Fenner & Clark, 2016; Ovaere et al., n.d.; Steven et al., 1990; Yamasaki & Gallo, 2008). Secondly, keratinocytes of the SG secrete lipid-containing lamellar granules into the extracellular space between SG and the most outer layer of the skin, the stratum corneum (SC), to enable the formation of a hydrophobic lipid-enriched lamellar membrane as a protection against loss of water and electrolytes (Feingold, 2007).

Some highly keratinized areas of the skin, such as the palms and the sole of the foot, contain an additional epidermal layer between SG and SC, namely the stratum lucidum (Monteiro-Riviere, 2005). It mainly consists of 2-3 layers of dead, cornified cells filled with phospholipids and a protein called eleidin, which is a transformation product of keratohyalin and similar to keratin (Monteiro-Riviere, 2005; Yousef et al., 2017).

The aforementioned SC is the most outer layer of the epidermis and consists of several layers of dead, flattened, terminally differentiated keratinocytes lacking nucleus and organelles, which are called corneocytes. Among each other they are attached by corneodesmosomes, which desmosomes transform into supported by corneodesmosin, a protein secreted from the lamellar granules of the SG, whose degradation among others is crucial for the desquamation process regularly renewing and replacing the SC by cells migrating from the lower epidermal layers (Simon et al., 1997). Resistance of corneocytes against environmental insults is increased by formation of the cornified cell envelope as an insoluble structure on the inside of the plasma membrane of each cell. This structure is formed by crosslinking of structural proteins such as involucrin, filaggrin and loricrin, with the latter making up for 65-70% of human epidermal cornified cell envelopes (Steven & Steinert, 1994). Crosslinking is mediated by transglutaminases forming Nε-(γ-glutamyl)lysine isopeptide bonds and supported by disulfide bond formation (Abernethy et

al., 1977; Rice & Green, 1977a; Steven & Steinert, 1994). Overall, for the epidermis to be able to provide an essential barrier protecting the organism from exterior insults and preventing dehydration, a highly regulated interplay of a vast number of different factors is required, hence making it a very vulnerable system, whose dysbalance can lead to a number of severe skin disorders.

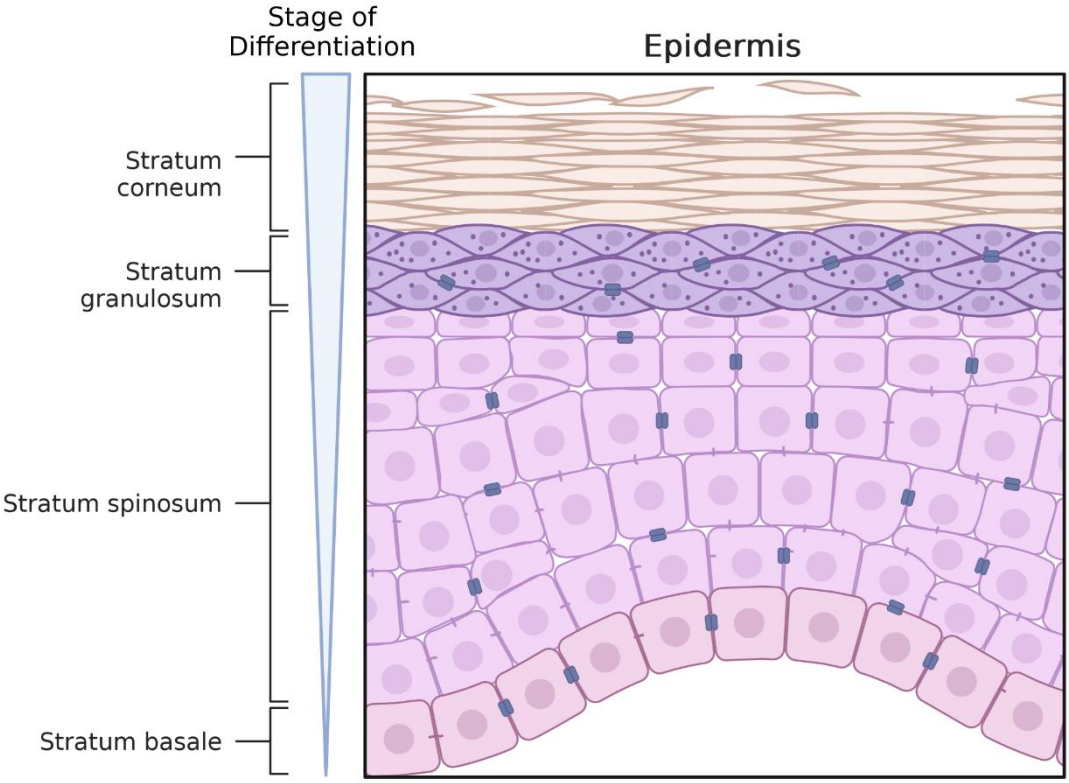

Figure 6: Structure of the epidermis.
The human epidermis typically comprises four distinct layers of highly organized differentiating keratinocytes attached to each other by desmosomes (depicted in blue). Basal cells from the stratum basale start migrating upwards towards the surface undergoing several steps of differentiation in the stratum spinosum and the stratum granulosum, until terminal differentiation and complete cornification are accomplished in the stratum corneum, which among desquamation allows the shedding of dead cells and constant renewal of the epidermis. Figure modified from and with BioRender.

1.7 Epidermal barrier dysfunctions

Epidermal barrier dysfunction can be caused by defects in a variety of different factors, including cornified envelopes, corneocytes, lipids, junctional proteins, proteases, protease inhibitors, antimicrobial peptides and transcription factors. Defects can cause either loss of the outside-in barrier protecting the skin from penetration of exterior insults like germs and chemicals or loss of the inside-out barrier preventing loss of water and electrolytes via the skin, but often affect both simultaneously, as many factors are essential for both barrier functions. Methods to examine barrier function therefore need to investigate both directions independent of each other.

Measurement of transepidermal water loss (TEWL) is the standard method used in humans, as well as in rodent disease models, to study the functionality of the inside-out barrier by quantifying the amount of water evaporating from the skin and shows increased values upon barrier impairment (Fluhr et al., 2006). This method has been used since more than 40 years (Wilson & Maibach, 1980), but is highly sensitive towards environmental factors such as temperature and humidity, so results have to be handled and interpreted with caution (Natsuga, 2014).

Outside-in barrier is typically examined via dye penetration assays, in which dyes like toluidine blue, hematoxylin or X-Gal are used for staining of mouse fetuses or neonates, whose outside-in barrier typically develops at an age of E16.5, with defects resulting in staining of the entire skin (Indra & Leid, 2011).

As problems within an extremely huge number of factors can result in the loss of epidermal barrier function, only a few more common examples will be discussed in the following to understand the complexity and variety of epidermal barrier defects. One part of the epidermis, which can be affected, is the cornified cell envelope, which among others consists of the proteins loricrin, involucrin, filaggrin, periplakin and envoplakin (Mehrel et al., 1990; Rice & Green, 1977b, 1979; Ruhrberg et al., 1996, 1997; Simon et al., 1996).

Loricrin is the most abundant protein of the cornified cell envelope and in humans, mutations in the *LOR* gene cause its accumulation in the nucleus, thus forbidding it to be crosslinked into the cornified cell envelope and resulting in decreased barrier function and increased TEWL (Schmuth et al., 2004). Its KO in mice causes a mild developmental retardation of the epidermal barrier function after birth, which is compensated *in vivo* by an overexpression of other structural proteins of the cornified cell envelope later in life.

Similar to loricrin, a KO of involucrin, periplakin or envoplakin alone does not lead to a visible phenotype (Aho et al., 2004; Djalilian et al., 2006; Määttä et al., 2001), as only a combined triple KO forbids compensatory mechanisms to promote effective barrier formation (Sevilla et al., 2007). Moreover, mutations in the *FLG* gene in humans or its murine orthologue *Flg*, the gene encoding for filaggrin, result in destabilization of the keratin filament organization and alteration of the composition of lamellar granules, which leads to an impairment of the lamellar bilayer and mildly defective barrier function in mice and humans (Gruber et al., 2011; H. Kawasaki et al., 2012).

Another group of genes, whose mutations can cause epidermal barrier defects, includes several distinct genes encoding for keratins, with *KRT1* and *KRT10*, encoding for keratins (K) 1 and 10, respectively, being the most prevalent members. Loss of those

keratins results in a destabilization of keratin filaments and hyperproliferation of suprabasal keratinocytes leading to different skin disorders in humans (Cheng et al., 1992; Porter & Lane, 2003; Rothnagel et al., 1992). In contrast, K10 deficiency in mice does not result in a visible phenotype, as it can be compensated by increased expression of other keratins, while K1 deficiency results in perinatal death (Reichelt et al., 2001; Roth et al., 2012).

Mutations in the *TGM1* gene in humans or its orthologue *Tgm1* in mice, encoding for transglutaminase 1, result in a severe phenotype in mice including severely impaired barrier function as well as neonatal lethality and are also known to cause more severe skin diseases in humans (Huber et al., 1995; Matsuki et al., 1998; Russell et al., 1995). Transglutaminase 1 is an enzyme catalyzing the crosslinking of several structural proteins comprising the cornified cell envelope via formation of Nε-(γ-glutamyl)lysine isopeptide bonds and facilitating the attachment of the lipid layer beneath (Folk & Finlayson, 1977; Richard, 2004).

Defects in the ABC transporter 12, which is crucial for keratinocyte lipid transport, result in an impairment of the intercellular lipid bilayer and can cause several skin disorders in humans, from which the most severe one is imitated in *Abca12* KO mice, which display severe barrier impairment and neonatal lethality (Akiyama, 2011; Akiyama et al., 2005; Lefèvre et al., 2003; Smyth et al., 2008).

Furthermore, mutations in genes encoding for serine proteases can cause epidermal barrier defects. Matriptase and prostatin are both involved in a serine protease cascade, which is presumed to mediate filaggrin monomer formation and is crucial for the terminal differentiation of the epidermis (Netzel-Arnett et al., 2006). Defects can lead to hair and skin abnormalities in humans and mice, but additionally result in postnatal death in mice (Basel-Vanagaite et al., 2007; Leyvraz et al., 2005; List et al., 2002). Interestingly, defects in the human *SPINK5* gene and its murine orthologue *Spink5*, encoding for a serine protease inhibitor named LEKTI also cause skin abnormalities in humans and mice including altered terminal differentiation, impaired keratinization and an overall epidermal barrier defect caused by excessive desmosome cleavage in the SC (Chavanas et al., 2000; Descargues et al., 2005). Hence, maintenance of a tightly regulated balance between serine proteases and serine protease inhibitors is crucial for correct epidermal barrier function.

In addition, several of the factors discussed above may additionally be negatively affected by mutations in specific transcriptions factors. For instance, defects in the transcription factor Grhl3, which controls the expression of the *Tgm1* gene, in mice cause reduced levels of the enzyme transglutaminase 1, thus resulting in severe barrier impairment as discussed above (Ting et al., 2005).

Overall, the epidermis provides an essential barrier protecting the organism from exterior insults and preventing dehydration, hence making defects in epidermal barrier function life-threatening conditions and a fundamental subject of current and ongoing research. However, the examples mentioned above also reveal differences in the effects of genetic defects on human and murine epidermal barrier function as well as overall health condition, thus illustrating certain limitations in the usage of mouse models for human skin disorders.

1.8 Aims of work

MoCD and SOXD are rare genetic disorders resulting in a severe phenotype mostly manifesting in the brain, which inevitably leads to premature death if left untreated, and can be mainly ascribed to a loss of function of the molybdoenzyme SOX. In the three subtypes of MoCD, different steps of Moco biosynthesis are disturbed, whereas SOXD is caused by a direct loss of SOX function due to mutations in the *SUOX* gene. While treatment of MoCD type A has been established almost 15 years ago, MoCD type B and C, as well as SOXD, are still considered incurable diseases. The search for efficient treatments has therefore been an important subject of research since decades and was continued in the present study.

1. Chapter II presents an extensive, summarizing review of the literature on MoCD in humans. The first part focuses on the underlying genetic causes and includes a novel, comprehensive list of published MoCD type B causing mutations of the *MOCS2* and *MOCS3* genes. The second part discusses known and published treatment approaches for MoCD and due to the huge phenotypic resemblance also includes treatments tested in SOXD patients. It further contains proposals for treatment strategies based on new discoveries and hypotheses on the disease mechanism.

2. The recent generation of a new SOXD mouse model for the first time allowed *in vivo* testing of different therapeutic approaches in order to take a step forward towards finding a treatment for SOXD and MoCD types B and C in human patients. Hence, several different therapeutic approaches and their success in the SOXD mouse model are discussed in chapter III. In brief, as the most remarkable feature of SOXD is its neurodegenerative phenotype, different hypothesized rescue mechanisms were primarily investigated using murine primary neurons as a model system. Upon validation of the initial hypotheses, treatments were further tested *in vivo* using *Suox*$^{-/-}$ mice and median average survival times were used as a factor for quantification of the treatment efficiencies.

3. Studies with *Suox*$^{-/-}$ mice accompanying the work presented in Chapter III have proven the cerebral phenotype being significantly milder than reported in patients, thus suggesting a different cause of death leading to the severely shortened life span observed in these mice. In line with this, in the course of this study a dermal phenotype similar to the one already observed in an MoCD type B mouse model became apparent. Hence, in order to examine the utility of *Suox*$^{-/-}$ mice as a model system for SOXD and gain more precise knowledge on the predominant cause of death, studies regarding the characterization of the newly discovered dermal phenotype were performed and summarized in chapter IV.

1.9 References

Abadeh, S., Killacky, J., Benboubetra, M., & Harrison, R. (1992). Purification and partial characterization of xanthine oxidase from human milk. *Biochimica et Biophysica Acta (BBA) - General Subjects*, *1117*(1), 25–32. https://doi.org/10.1016/0304-4165(92)90157-P

Abernethy, J. L., Hill, R. L., & Goldsmith, L. A. (1977). epsilon-(gamma-Glutamyl)lysine cross-links in human stratum corneum. *Journal of Biological Chemistry*, *252*(6), 1837–1839. https://doi.org/10.1016/S0021-9258(18)71831-0

Abraham, J., & Mathew, S. (2019). Merkel Cells: A Collective Review of Current Concepts. *International Journal of Applied and Basic Medical Research*, *9*(1), 9. https://doi.org/10.4103/IJABMR.IJABMR_34_18

Aghanoori, M. R., Shahriary, G. M., Safarpour, M., & Ebrahimi, A. (2016). Screening of a clinically and biochemically diagnosed SOD patient using exome sequencing: A case report with a mutations/variations analysis approach. *Egyptian Journal of Medical Human Genetics*, *17*(1), 131–136. https://doi.org/10.1016/J.EJMHG.2015.06.003

Aho, S., Li, K., Ryoo, Y., McGee, C., Ishida-Yamamoto, A., Uitto, J., & Klement, J. F. (2004). Periplakin gene targeting reveals a constituent of the cornified cell envelope dispensable for normal mouse development. *Molecular and Cellular Biology*, *24*(14), 6410–6418. https://doi.org/10.1128/MCB.24.14.6410-6418.2004

Akiyama, M. (2011). The roles of ABCA12 in keratinocyte differentiation and lipid barrier formation in the epidermis. *Dermato-Endocrinology*, *3*(2), 107–112. https://doi.org/10.4161/DERM.3.2.15136

Akiyama, M., Sugiyama-Nakagiri, Y., Sakai, K., McMillan, J. R., Goto, M., Arita, K., Tsuji-Abe, Y., Tabata, N., Matsuoka, K., Sasaki, R., Sawamura, D., & Shimizu, H. (2005). Mutations in lipid transporter ABCA12 in harlequin ichthyosis and functional recovery by corrective gene transfer. *The Journal of Clinical Investigation*, *115*(7), 1777–1784. https://doi.org/10.1172/JCI24834

Anantharaman, V., & Aravind, L. (2002). MOSC domains: ancient, predicted sulfur-carrier domains, present in diverse metal-sulfur cluster biosynthesis proteins including Molybdenum cofactor sulfurases. *FEMS Microbiology Letters*, *207*(1), 55–61. https://doi.org/10.1111/J.1574-6968.2002.TB11028.X

Arenas, M., Fairbanks, L. D., Vijayakumar, K., Carr, L., Escuredo, E., & Marinaki, A. M. (2009). An unusual genetic variant in the MOCS1 gene leads to complete missplicing of an alternatively spliced exon in a patient with molybdenum cofactor deficiency. *Journal of Inherited Metabolic Disease*, *32*(4), 560–569. https://doi.org/10.1007/S10545-009-1151-7

Arnoux, P., Ruppelt, C., Oudouhou, F., Lavergne, J., Siponen, M. I., Toci, R., Mendel, R. R., Bittner, F., Pignol, D., Magalon, A., & Walburger, A. (2015). Sulphur shuttling across a chaperone during molybdenum cofactor maturation. *Nature Communications*, *6*. https://doi.org/10.1038/NCOMMS7148

Astashkin, A. V., Raitsimring, A. M., Feng, C., Johnson, J. L., Rajagopalan, K. V., & Enemark, J. H. (2002). Pulsed EPR studies of nonexchangeable protons near the Mo(V) center of sulfite oxidase: direct detection of the alpha-proton of the coordinated cysteinyl residue and structural implications for the active site. *Journal of the American Chemical Society*, *124*(21), 6109–6118. https://doi.org/10.1021/JA0115417

Bannai, S. (1986). Exchange of cystine and glutamate across plasma membrane of human fibroblasts. *Journal of Biological Chemistry*, *261*(5), 2256–2263. https://doi.org/10.1016/S0021-9258(17)35926-4

Barbieri, J. S., Wanat, K., & Seykora, J. (2014). Skin: Basic Structure and Function. *Pathobiology of Human Disease: A Dynamic Encyclopedia of Disease Mechanisms*, 1134–1144. https://doi.org/10.1016/B978-0-12-386456-7.03501-2

Basel-Vanagaite, L., Attia, R., Ishida-Yamamoto, A., Rainshtein, L., Ben Amitai, D., Lurie, R., Pasmanik-Chor, M., Indelman, M., Zvulunov, A., Saban, S., Magal, N., Sprecher, E., & Shohat, M. (2007). Autosomal Recessive Ichthyosis with Hypotrichosis Caused by a Mutation in ST14, Encoding Type II Transmembrane Serine Protease Matriptase. *American Journal of Human Genetics*, *80*(3), 467. https://doi.org/10.1086/512487

Bender, D. (2017). *Molecular mechanism of sulfite oxidation and nitrite reduction in vertebrate sulfite oxidase*. University of Cologne.

Bindu, P. S., Nagappa, M., Bharath, R. D., & Taly, A. B. (2017). Isolated Sulfite Oxidase Deficiency. *GeneReviews®*. https://www.ncbi.nlm.nih.gov/books/NBK453433/

Boyer, M., Sowa, M., Wang, R., & Abdenur, J. (2019). Isolated Sulfite Oxidase Deficiency: Response to Dietary Treatment in a Patient with Severe Neonatal Presentation. *Journal of Inborn Errors of Metabolism and Screening*, *7*, e20190001. https://doi.org/10.1590/2326-4594-JIEMS-2019-0001

Buchman, ; E R, Buchman, R. R., Williams, R. R., Ruehle, I. ;) A. E., & Williams, . ; R R. (1935). Studies of Crystalline Vitamin B^1 X. Sulfite Cleavage. III. Chemistry of the Basic Product The action on (II) of nitrous acid and of methyl Oxidation of (II) with nitric acid at 40° gave sulfuric acid and 30% of an acid. *Nachr. Ges. Wiss. Góttingen. Math.~phys. Klasse, III*, *67*(3), 45. https://pubs.acs.org/sharingguidelines

Burgess, B. K., & Lowe, D. J. (1996). Mechanism of molybdenum nitrogenase. *Chemical Reviews*, *96*(7), 2983–3011. https://doi.org/10.1021/CR950055X/ASSET/CR950055X.FP.PNG_V03

Chavanas, S., Bodemer, C., Rochat, A., Hamel-Teillac, D., Ali, M., Irvine, A. D., Bonafé, J. L., Wilkinson, J., Taïeb, A., Barrandon, Y., Harper, J. I., De Prost, Y., & Hovnanian, A. (2000). Mutations in SPINK5, encoding a serine protease inhibitor, cause Netherton syndrome. *Nature Genetics*, *25*(2), 141–142. https://doi.org/10.1038/75977

Cheng, J., Syder, A. J., Yu, Q. C., Letal, A., Paller, A. S., & Fuchs, E. (1992). The genetic basis of epidermolytic hyperkeratosis: a disorder of differentiation-specific epidermal keratin genes. *Cell*, *70*(5), 811–819. https://doi.org/10.1016/0092-8674(92)90314-3

Claerhout, H., Witters, P., Régal, L., Jansen, K., Van Hoestenberghe, M. R., Breckpot, J., & Vermeersch, P. (2018). Isolated sulfite oxidase deficiency. *Journal of Inherited Metabolic Disease*, *41*(1), 101–108. https://doi.org/10.1007/S10545-017-0089-4

Coelho, C., Mahro, M., Trincão, J., P Carvalho, A. T., Joã Ramos, M., Terao, M., Garattini, E., Leimkü hler, S., & Joã Romão, M. (2012). *The First Mammalian Aldehyde Oxidase Crystal Structure*. https://doi.org/10.1074/jbc.M112.390419

Corte, E. D., & Stirpe, F. (1972). The regulation of rat liver xanthine oxidase. Involvement of thiol groups in the conversion of the enzyme activity from dehydrogenase (type D) into oxidase (type O) and purification of the enzyme. *The Biochemical Journal*, *126*(3), 739–745. https://doi.org/10.1042/BJ1260739

Daniels, J. N., Wuebbens, M. M., Rajagopalan, K. V., & Schindelin, H. (2008). Crystal structure of a molybdopterin synthase-precursor Z complex: insight into its sulfur transfer mechanism and its role in molybdenum cofactor deficiency. *Biochemistry*, *47*(2), 615–626. https://doi.org/10.1021/BI701734G

Dejanovic, B., & Schwarz, G. (2014). Neuronal nitric oxide synthase-dependent S-nitrosylation of gephyrin regulates gephyrin clustering at GABAergic synapses. *The Journal of Neuroscience : The Official Journal of the Society for Neuroscience*, *34*(23), 7763–7768. https://doi.org/10.1523/JNEUROSCI.0531-14.2014

Dejanovic, B., Semtner, M., Ebert, S., Lamkemeyer, T., Neuser, F., Lüscher, B., Meier, J. C., & Schwarz, G. (2014). Palmitoylation of Gephyrin Controls Receptor Clustering and Plasticity of GABAergic Synapses. *PLOS Biology*, *12*(7), e1001908. https://doi.org/10.1371/JOURNAL.PBIO.1001908

Demtröder, L., Narberhaus, F., & Masepohl, B. (2019). Coordinated regulation of nitrogen fixation and molybdate transport by molybdenum. *Molecular Microbiology*, *111*(1), 17–30. https://doi.org/10.1111/MMI.14152

Descargues, P., Draison, C., Bonnart, C., Kreft, M., Kishibe, M., Ishida-Yamamoto, A., Elias, P., Barrandon, Y., Zambruno, G., Sonnenberg, A., & Hovnanian, A. (2005). Spink5-deficient mice mimic Netherton syndrome through degradation of desmoglein 1 by epidermal protease hyperactivity. *Nature Genetics*, *37*(1), 56–65. https://doi.org/10.1038/NG1493

Dickinson, M. E., Flenniken, A. M., Ji, X., Teboul, L., Wong, M. D., White, J. K., Meehan, T. F., Weninger, W. J., Westerberg, H., Adissu, H., Baker, C. N., Bower, L., Brown, J. M., Brianna Caddle, L., Chiani, F., Clary, D., Cleak, J., Daly, M. J., Denegre, J. M., … Murakami, A. (2016). High-throughput discovery of novel developmental phenotypes. *Nature 2016 537:7621*, *537*(7621), 508–514. https://doi.org/10.1038/nature19356

Djalilian, A. R., McGaughey, D., Patel, S., Eun, Y. S., Yang, C., Cheng, J., Tomic, M., Sinha, S., Ishida-Yamamoto, A., & Segre, J. A. (2006). Connexin 26 regulates epidermal barrier and wound remodeling and promotes psoriasiform response. *The Journal of Clinical Investigation*, *116*(5), 1243–1253. https://doi.org/10.1172/JCI27186

Dóka, Ida, T., Dagnell, M., Abiko, Y., Luong, N. C., Balog, N., Takata, T., Espinosa, B., Nishimura, A., Cheng, Q., Funato, Y., Miki, H., Fukuto, J. M., Prigge, J. R., Schmidt, E. E., Arnér, E. S. J., Kumagai, Y., Akaike, T., & Nagy, P. (2020). Control of protein function through oxidation and reduction of persulfidated states. *Science Advances*, *6*(1). https://doi.org/10.1126/SCIADV.AAX8358/SUPPL_FILE/AAX8358_SM.PDF

Dorman, D. C., Moulin, F. J. M., McManus, B. E., Mahle, K. C., James, R. A., & Struve, M. F. (2002). Cytochrome Oxidase Inhibition Induced by Acute Hydrogen Sulfide Inhalation:

Correlation with Tissue Sulfide Concentrations in the Rat Brain, Liver, Lung, and Nasal Epithelium. *Toxicological Sciences*, *65*(1), 18–25. https://doi.org/10.1093/TOXSCI/65.1.18

Dos Reis, R., Kornobis, E., Pereira, A., Tores, F., Carrasco, J., Gautier, C., Jahannault-Talignani, C., Nitschké, P., Muchardt, C., Schlosser, A., Maric, H. M., Ango, F., & Allemand, E. (2022). Complex regulation of Gephyrin splicing is a determinant of inhibitory postsynaptic diversity. *Nature Communications 2022 13:1*, *13*(1), 1–17. https://doi.org/10.1038/s41467-022-31264-w

Eh, M., Kaczmarek, A. T., Schwarz, G., & Bender, D. (2022). Molecular mechanism of intramolecular electron transfer in dimeric sulfite oxidase. *Journal of Biological Chemistry*, *298*(3), 101668. https://doi.org/10.1016/j.jbc.2022.101668

Eilers, T., Schwarz, G., Brinkmann, H., Witt, C., Richter, T., Nieder, J., Koch, B., Hille, R., Hansch, R., & Mendel, R. R. (2001). Identification and biochemical characterization of Arabidopsis thaliana sulfite oxidase - A new player in plant sulfur metabolism. *Journal of Biological Chemistry*, *276*(50), 46989–46994. https://doi.org/10.1074/jbc.M108078200

Endres, W., Shin, Y. S., Günther, R., Ibel, H., Duran, M., & Wadman, S. K. (1988). Report on a new patient with combined deficiencies of sulphite oxidase and xanthine dehydrogenase due to molybdenum cofactor deficiency. *European Journal of Pediatrics*, *148*(3), 246–249. https://doi.org/10.1007/BF00441412/METRICS

Feingold, K. R. (2007). The role of epidermal lipids in cutaneous permeability barrier homeostasis. *Journal of Lipid Research*, *48*(12), 2531–2546. https://doi.org/10.1194/JLR.R700013-JLR200

Feng, C., Kedia, R. V., Hazzard, J. T., Hurley, J. K., Tollin, G., & Enemark, J. H. (2002). Effect of solution viscosity on intramolecular electron transfer in sulfite oxidase. *Biochemistry*, *41*(18), 5816–5821. https://doi.org/10.1021/BI016059F

Feng, C., Tollin, G., & Enemark, J. H. (2007). Sulfite oxidizing enzymes. *Biochimica et Biophysica Acta*, *1774*(5), 527. https://doi.org/10.1016/J.BBAPAP.2007.03.006

Feng, G., Tintrup, H., Kirsch, J., Nichol, M. C., Kuhse, J., Betz, H., & Sanes, J. R. (1998). Dual-requirement for gephyrin in glycine receptor clustering and molybdoenzyme activity. *Science*, *282*(5392), 1321–1324. https://doi.org/10.1126/SCIENCE.282.5392.1321/ASSET/4C3C20C8-D9BA-4433-BF2A-399A685BE977/ASSETS/GRAPHIC/SE4787015004.JPEG

Fenner, J., & Clark, R. A. F. (2016). Anatomy, Physiology, Histology, and Immunohistochemistry of Human Skin. *Skin Tissue Engineering and Regenerative Medicine*, 1–17. https://doi.org/10.1016/B978-0-12-801654-1.00001-2

Fluhr, J. W., Feingold, K. R., & Elias, P. M. (2006). Transepidermal water loss reflects permeability barrier status: validation in human and rodent in vivo and ex vivo models. *Experimental Dermatology*, *15*(7), 483–492. https://doi.org/10.1111/J.1600-0625.2006.00437.X

Folk, J. E., & Finlayson, J. S. (1977). The ε-(γ-Glutamyl)Lysine Crosslink and the Catalytic Role of Transglutaminases. *Advances in Protein Chemistry*, *31*(C), 1–133. https://doi.org/10.1016/S0065-3233(08)60217-X

Footitt, E. J., Heales, S. J., Mills, P. B., Allen, G. F. G., Oppenheim, M., & Clayton, P. T. (2011). Pyridoxal 5'-phosphate in cerebrospinal fluid; factors affecting concentration. *Journal of Inherited Metabolic Disease*, *34*(2), 529–538. https://doi.org/10.1007/S10545-011-9279-7

Garattini, E., Fratelli, M., & Terao, M. (2008). Mammalian aldehyde oxidases: Genetics, evolution and biochemistry. In *Cellular and Molecular Life Sciences* (Vol. 65, Issues 7–8, pp. 1019–1048). https://doi.org/10.1007/s00018-007-7398-y

Garattini, E., & Terao, M. (2011). Increasing recognition of the importance of aldehyde oxidase in drug development and discovery. *Drug Metabolism Reviews*, *43*(3), 374–386. https://doi.org/10.3109/03602532.2011.560606

Graf, W. D., Oleinik, O. E., Jack, R. M., Weiss, A. H., & Johnson, J. L. (1998). Ahomocysteinemia in molybdenum cofactor deficiency. *Neurology*, *51*(3), 860–862. https://doi.org/10.1212/WNL.51.3.860

Gray, T. A., & Nicholls, R. D. (2000). Diverse splicing mechanisms fuse the evolutionarily conserved bicistronic MOCS1A and MOCS1B open reading frames. *RNA (New York, N.Y.)*, *6*(7), 928–936. https://doi.org/10.1017/S1355838200000182

Gross-Hardt, S., & Reiss, J. (2002). The bicistronic MOCS1 gene has alternative start codons on two mutually exclusive exons. *Molecular Genetics and Metabolism*, *76*(4), 340–343. https://doi.org/10.1016/S1096-7192(02)00100-2

Gruber, R., Elias, P. M., Crumrine, D., Lin, T. K., Brandner, J. M., Hachem, J. P., Presland, R. B., Fleckman, P., Janecke, A. R., Sandilands, A., McLean, W. H. I., Fritsch, P. O., Mildner, M., Tschachler, E., & Schmuth, M. (2011). Filaggrin Genotype in Ichthyosis Vulgaris Predicts Abnormalities in Epidermal Structure and Function. *The American Journal of Pathology*, *178*(5), 2252. https://doi.org/10.1016/J.AJPATH.2011.01.053

Gruenewald, S., Wahl, B., Bittner, F., Hungeling, H., Kanzow, S., Kotthaus, J., Schwering, U., Mendel, R. R., & Clement, B. (2008). The fourth molybdenum containing enzyme mARC: cloning and involvement in the activation of N-hydroxylated prodrugs. *Journal of Medicinal Chemistry*, *51*(24), 8173–8177. https://doi.org/10.1021/JM8010417

Grunden, A. M., & Shanmugam, K. T. (1997). Molybdate transport and regulation in bacteria. *Archives of Microbiology*, *168*(5), 345–354. https://doi.org/10.1007/S002030050508/METRICS

Hahnewald, R., Leimkühler, S., Vilaseca, A., Acquaviva-Bourdain, C., Lenz, U., & Reiss, J. (2006). A novel MOCS2 mutation reveals coordinated expression of the small and large subunit of molybdopterin synthase. *Molecular Genetics and Metabolism*, *89*(3), 210–213. https://doi.org/10.1016/J.YMGME.2006.04.008

Halperin, E. C., Thier, S. O., & Rosenberg, L. E. (1981). The use of D-penicillamine in cystinuria: efficacy and untoward reactions. *The Yale Journal of Biology and Medicine*, *54*(6), 439. /pmc/articles/PMC2596051/?report=abstract

Hänzelmann, P., Hernández, H. L., Menzel, C., García-Serres, R., Huynh, B. H., Johnson, M. K., Mendel, R. R., & Schindelin, H. (2004). Characterization of MOCS1A, an oxygen-sensitive iron-sulfur protein involved in human molybdenum cofactor biosynthesis. *Journal of Biological Chemistry*, *279*(33), 34721–34732. https://doi.org/10.1074/JBC.M313398200

Harrison, R. (2002). Structure and function of xanthine oxidoreductase: Where are we now? *Free Radical Biology and Medicine*, *33*(6), 774–797. https://doi.org/10.1016/S0891-5849(02)00956-5

Hille, R. (1994). The reaction mechanism of oxomolybdenum enzymes. In *Biochimica et Biophysica Acta* (Vol. 1184).

Hille, R. (2002). Molybdenum enzymes containing the pyranopterin cofactor: an overview. *Metal Ions in Biological Systems*, *39*, 187–226.

Hille, R., & Nishino, T. (1995). Xanthine oxidase and xanthine dehydrogenase. *The FASEB Journal*, *9*(11), 995–1003. https://doi.org/10.1096/FASEBJ.9.11.7649415

Hille, R., Nishino, T., & Bittner, F. (2011). Molybdenum enzymes in higher organisms. *Coordination Chemistry Reviews*. https://doi.org/10.1016/j.ccr.2010.11.034

Hover, B. M., Loksztejn, A., Ribeiro, A. A., & Yokoyama, K. (2013). Identification of a cyclic nucleotide as a cryptic intermediate in molybdenum cofactor biosynthesis. *Journal of the American Chemical Society*, *135*(18), 7019. https://doi.org/10.1021/JA401781T

Howard-Lock, H. E., Lock, C. J. L., Mewa, A., & Kean, W. F. (1986). d-penicillamine: Chemistry and clinical use in rheumatic disease. *Seminars in Arthritis and Rheumatism*, *15*(4), 261–281. https://doi.org/10.1016/0049-0172(86)90022-3

Huber, M., Rettler, I., Bernasconi, K., Frenk, E., Lavrijsen, S. P. M., Ponec, M., Bon, A., Lautenschlager, S., Schorderet, D. F., & Hohl, D. (1995). Mutations of keratinocyte transglutaminase in lamellar ichthyosis. *Science (New York, N.Y.)*, *267*(5197), 525–528. https://doi.org/10.1126/SCIENCE.7824952

Huijmans, J. G. M., Schot, R., de Klerk, J. B. C., Williams, M., de Coo, R. F. M., Duran, M., Verheijen, F. W., van Slegtenhorst, M., & Mancini, G. M. S. (2017). Molybdenum cofactor deficiency: Identification of a patient with homozygote mutation in the MOCS3 gene. *American Journal of Medical Genetics Part A*, *173*(6), 1601–1606. https://doi.org/10.1002/AJMG.A.38240

Indra, A. K., & Leid, M. (2011). Epidermal Permeability Barrier (EPB) measurement in mammalian skin. *Methods in Molecular Biology (Clifton, N.j.)*, *763*, 73. https://doi.org/10.1007/978-1-61779-191-8_4

Jackson, M. R., Melideo, S. L., & Jorns, M. S. (2012). Human sulfide:Quinone oxidoreductase catalyzes the first step in hydrogen sulfide metabolism and produces a sulfane sulfur metabolite. *Biochemistry*, *51*(34), 6804–6815. https://doi.org/10.1021/BI300778T

Jakubiczka-Smorag, J., Santamaria-Araujo, J. A., Metz, I., Kumar, A., Hakroush, S., Brueck, W., Schwarz, G., Burfeind, P., Reiss, J., & Smorag, L. (2016). Mouse model for molybdenum cofactor deficiency type B recapitulates the phenotype observed in molybdenum cofactor deficient patients. *Human Genetics*, *135*(7), 813–826. https://doi.org/10.1007/s00439-016-1676-4

Johnson, J. L., Coyne, K. E., Garrett, R. M., Zabot, M. T., Dorche, C., Kisker, C., & Rajagopalan, K. V. (2002). Isolated sulfite oxidase deficiency: identification of 12 novel SUOX mutations in 10 patients. *Hum Mutat*, *20*(1), 74. https://doi.org/10.1002/humu.9038

Johnson, J. L., & Duran, M. (2001). Molybdenum cofactor deficiency and isolated sulfite oxidase deficiency. In *The Metabolic and Molecular Bases of Inherited Disease* (pp. 3163–3177). Mcgraw-Hill Professional.

Johnson, J. L., & Rajagopalan, K. V. (1979). The oxidation of sulphite in animals systems. *Ciba Foundation Symposium*, *72*, 119–133. https://doi.org/10.1002/9780470720554.CH8

Johnson-Winters, K., Tollin, G., & Enemark, J. H. (2010). Elucidating the Catalytic Mechanism of Sulfite Oxidizing Enzymes using Structural, Spectroscopic and Kinetic Analyses. *Biochemistry*, *49*(34), 7242. https://doi.org/10.1021/BI1008485

Kaczmarek, A. T., Bahlmann, N., Thaqi, B., May, P., & Schwarz, G. (2021). Machine learning-based identification and characterization of 15 novel pathogenic SUOX missense

mutations. *Molecular Genetics and Metabolism*, *134*(1–2), 188–194. https://doi.org/10.1016/J.YMGME.2021.07.011

Kasaragod, V. B., & Schindelin, H. (2016). Structural Framework for Metal Incorporation during Molybdenum Cofactor Biosynthesis. *Structure*, *24*(5), 782–788. https://doi.org/10.1016/J.STR.2016.02.023

Kawasaki, B. T., Hoffman, K. B., Yamamoto, R. S., & Bahr, B. A. (1997). Rapid Communication Variants of the Receptor/Channel Clustering Molecule Gephyrin in Brain: Distinct Distribution Patterns, Developmental Profiles, and Proteolytic Cleavage by Calpain. *J. Neurosci. Res*, *49*, 381–388. https://doi.org/10.1002/(SICI)1097-4547(19970801)49:3<381::AID-JNR13>3.0.CO;2-2

Kawasaki, H., Nagao, K., Kubo, A., Hata, T., Shimizu, A., Mizuno, H., Yamada, T., & Amagai, M. (2012). Altered stratum corneum barrier and enhanced percutaneous immune responses in filaggrin-null mice. *The Journal of Allergy and Clinical Immunology*, *129*(6), 1538-1546.e6. https://doi.org/10.1016/J.JACI.2012.01.068

Kim, D. K., & Holbrook, K. A. (1995). The appearance, density, and distribution of Merkel cells in human embryonic and fetal skin: their relation to sweat gland and hair follicle development. *The Journal of Investigative Dermatology*, *104*(3), 411–416. https://doi.org/10.1111/1523-1747.EP12665903

Kim, J., & Rees, D. C. (1992). Structural Models for the Metal Centers in the Nitrogenase Molybdenum-Iron Protein. *Science*, *257*(5077), 1677–1682. https://doi.org/10.1126/SCIENCE.1529354

Kisker, C., Schindelin, H., Pacheco, A., Wehbi, W. A., Garrett, R. M., Rajagopalan, K. V., Enemark, J. H., & Rees, D. C. (1997). Molecular Basis of Sulfite Oxidase Deficiency from the Structure of Sulfite Oxidase. *Cell*, *91*(7), 973–983. https://doi.org/10.1016/S0092-8674(00)80488-2

Kisker, C., Schindelin, H., & Rees, D. C. (1997). Molybdenum-cofactor-containing enzymes: Structure and mechanism. *Annual Review of Biochemistry*, *66*, 233–267. https://doi.org/10.1146/ANNUREV.BIOCHEM.66.1.233

Kneussel, M., Brandstätter, J. H., Laube, B., Stahl, S., Müller, U., & Betz, H. (1999). Loss of Postsynaptic GABAA Receptor Clustering in Gephyrin-Deficient Mice. *The Journal of Neuroscience*, *19*(21), 9289. https://doi.org/10.1523/JNEUROSCI.19-21-09289.1999

Kohl, J. B. (2019). A Novel Mouse Model of Sulfite Oxidase Deficiency: Pathological Changes in Cysteine and H2S Metabolism. In *Department of Chemistry*.

Kohl, J. B., Mellis, A. T., & Schwarz, G. (2019). Homeostatic impact of sulfite and hydrogen sulfide on cysteine catabolism. *British Journal of Pharmacology*, *176*(4), 554–570. https://doi.org/10.1111/BPH.14464

Koirala, A., & Brözel, V. S. (2021). Phylogeny of nitrogenase structural and assembly components reveals new insights into the origin and distribution of nitrogen fixation across bacteria and archaea. *Microorganisms*, *9*(8), 1662. https://doi.org/10.3390/MICROORGANISMS9081662/S1

Krenitsky, T. A., Neil, S. M., Elion, G. B., & Hitchings, G. H. (1972). A comparison of the specificities of xanthine oxidase and aldehyde oxidase. *Archives of Biochemistry and Biophysics*, *150*(2), 585–599. https://doi.org/10.1016/0003-9861(72)90078-1

Krompholz, N., Krischkowski, C., Reichmann, D., Garbe-Schö, D., Mendel, R.-R., Bittner, F., Clement, B., & Havemeyer, A. (2012). *The Mitochondrial Amidoxime Reducing*

Component (mARC) Is Involved in Detoxification of N-Hydroxylated Base Analogues. https://doi.org/10.1021/tx300298m

Kubitza, C., Bittner, F., Ginsel, C., Havemeyer, A., Clement, B., & Scheidig, A. J. (2018). Crystal structure of human mARC1 reveals its exceptional position among eukaryotic molybdenum enzymes. *Proceedings of the National Academy of Sciences of the United States of America*, *115*(47), 11958–11963. https://doi.org/10.1073/PNAS.1808576115/-/DCSUPPLEMENTAL

Kumar, A., Dejanovic, B., Hetsch, F., Semtner, M., Fusca, D., Arjune, S., Santamaria-Araujo, J. A., Winkelmann, A., Ayton, S., Bush, A. I., Kloppenburg, P., Meier, J. C., Schwarz, G., & Belaidi, A. A. (2017). S-sulfocysteine/NMDA receptor-dependent signaling underlies neurodegeneration in molybdenum cofactor deficiency. *J Clin Invest*, *127*(12), 4365–4378. https://doi.org/10.1172/JCI89885

Kuper, J., Llamas, A., Hecht, H. J., Mendel, R. R., & Schwarz, G. (2004). Structure of the molybdopterin-bound Cnx1G domain links molybdenum and copper metabolism. *Nature*, *430*(7001), 803–806. https://doi.org/10.1038/NATURE02681

Lake, M. W., Temple, C. A., Rajagopalan, K. V., & Schindelin, H. (2000). The crystal structure of the Escherichia coli MobA protein provides insight into molybdopterin guanine dinucleotide biosynthesis. *Journal of Biological Chemistry*, *275*(51), 40211–40217. https://doi.org/10.1074/JBC.M007406200

Lancaster, K. M., Roemelt, M., Ettenhuber, P., Hu, Y., Ribbe, M. W., Neese, F., Bergmann, U., & DeBeer, S. (2011). X-ray emission spectroscopy evidences a central carbon in the nitrogenase iron-molybdenum cofactor. *Science (New York, N.Y.)*, *334*(6058), 974–977. https://doi.org/10.1126/SCIENCE.1206445

Lavker, R. M., & Sun, T. T. (1982). Heterogeneity in epidermal basal keratinocytes: morphological and functional correlations. *Science (New York, N.Y.)*, *215*(4537), 1239–1241. https://doi.org/10.1126/SCIENCE.7058342

Lee, H. J., Adham, I. M., Schwarz, G., Kneussel, M., Sass, J. O., Engel, W., & Reiss, J. (2002). Molybdenum cofactor-deficient mice resemble the phenotype of human patients. *Human Molecular Genetics*, *11*(26), 3309–3317. https://doi.org/10.1093/HMG/11.26.3309

Lefèvre, C., Audebert, S., Jobard, F., Bouadjar, B., Lakhdar, H., Boughdene-Stambouli, O., Blanchet-Bardon, C., Heilig, R., Foglio, M., Weissenbach, J., Lathrop, M., Prud'homme, J. F., & Fischer, J. (2003). Mutations in the transporter ABCA12 are associated with lamellar ichthyosis type 2. *Human Molecular Genetics*, *12*(18), 2369–2378. https://doi.org/10.1093/HMG/DDG235

Leimkühler, S. (2017). Shared function and moonlighting proteins in molybdenum cofactor biosynthesis. In *Biological Chemistry* (Vol. 398, Issue 9, pp. 1009–1026). Walter de Gruyter GmbH. https://doi.org/10.1515/hsz-2017-0110

Leimkühler, S. (2020). The biosynthesis of the molybdenum cofactors in Escherichia coli. *Environmental Microbiology*, *22*(6), 2007–2026. https://doi.org/10.1111/1462-2920.15003

Leimkühler, S., Freuer, A., Araujo, J. A. S., Rajagopalan, K. V., & Mendel, R. R. (2003). Mechanistic studies of human molybdopterin synthase reaction and characterization of mutants identified in group B patients of molybdenum cofactor deficiency. *Journal of Biological Chemistry*, *278*(28), 26127–26134. https://doi.org/10.1074/JBC.M303092200

Leimkühler, S., & Neumann, M. (2011). The role of system-specific molecular chaperones in the maturation of molybdoenzymes in bacteria. *Biochemistry Research International*. https://doi.org/10.1155/2011/850924

Leimkühler, S., & Rajagopalan, K. V. (2001). A Sulfurtransferase Is Required in the Transfer of Cysteine Sulfur in the in Vitro Synthesis of Molybdopterin from Precursor Z in Escherichia coli. *Journal of Biological Chemistry*, *276*(25), 22024–22031. https://doi.org/10.1074/JBC.M102072200

Leyvraz, C., Charles, R. P., Rubera, I., Guitard, M., Rotman, S., Breiden, B., Sandhoff, K., & Hummler, E. (2005). The epidermal barrier function is dependent on the serine protease CAP1/Prss8. *The Journal of Cell Biology*, *170*(3), 487–496. https://doi.org/10.1083/JCB.200501038

List, K., Haudenschild, C. C., Szabo, R., Chen, W. J., Wahl, S. M., Swaim, W., Engelholm, L. H., Behrendt, N., & Bugge, T. H. (2002). Matriptase/MT-SP1 is required for postnatal survival, epidermal barrier function, hair follicle development, and thymic homeostasis. *Oncogene 2002 21:23*, *21*(23), 3765–3779. https://doi.org/10.1038/sj.onc.1205502

Liu, M. T. W., Wuebbens, M. M., Rajagopalan, K. V., & Schindelin, H. (2000). Crystal structure of the gephyrin-related molybdenum cofactor biosynthesis protein MogA from Escherichia coli. *The Journal of Biological Chemistry*, *275*(3), 1814–1822. https://doi.org/10.1074/JBC.275.3.1814

Llamas, A., Otte, T., Multhaup, G., Mendel, R. R., & Schwarz, G. (2006). The Mechanism of Nucleotide-assisted Molybdenum Insertion into Molybdopterin: A NOVEL ROUTE TOWARD METAL COFACTOR ASSEMBLY. *Journal of Biological Chemistry*, *281*(27), 18343–18350. https://doi.org/10.1074/JBC.M601415200

Lu, S. C. (2013). Glutathione synthesis. *Biochimica et Biophysica Acta (BBA) - General Subjects*, *1830*(5), 3143–3153. https://doi.org/10.1016/J.BBAGEN.2012.09.008

Määttä, A., DiColandrea, T., Groot, K., & Watt, F. M. (2001). Gene targeting of envoplakin, a cytoskeletal linker protein and precursor of the epidermal cornified envelope. *Molecular and Cellular Biology*, *21*(20), 7047–7053. https://doi.org/10.1128/MCB.21.20.7047-7053.2001

Mahro, M., Brás, N. F., Cerqueira, N. M. F. S. A., Teutloff, C., Coelho, C., Romão, M. J., & Leimkühler, S. (2013). Identification of Crucial Amino Acids in Mouse Aldehyde Oxidase 3 That Determine Substrate Specificity. *PLOS ONE*, *8*(12), e82285. https://doi.org/10.1371/JOURNAL.PONE.0082285

Maia, L. B., & Moura, J. J. G. (2018). Putting xanthine oxidoreductase and aldehyde oxidase on the NO metabolism map: Nitrite reduction by molybdoenzymes. *Redox Biology*, *19*, 274. https://doi.org/10.1016/J.REDOX.2018.08.020

Maia, L. B., Pereira, V., Mira, L., & Moura, J. J. G. (2015). Nitrite reductase activity of rat and human xanthine oxidase, xanthine dehydrogenase, and aldehyde oxidase: Evaluation of their contribution to NO formation in vivo. *Biochemistry*, *54*(3), 685–710. https://doi.org/10.1021/BI500987W/SUPPL_FILE/BI500987W_SI_001.PDF

Marelja, Z., Mullick Chowdhury, M., Dosche, C., Hille, C., Baumann, O., Löhmannsröben, H. G., & Leimkühler, S. (2013). The L-Cysteine Desulfurase NFS1 Is Localized in the Cytosol where it Provides the Sulfur for Molybdenum Cofactor Biosynthesis in Humans. *PLOS ONE*, *8*(4), e60869. https://doi.org/10.1371/JOURNAL.PONE.0060869

Marelja, Z., Stöcklein, W., Nimtz, M., & Leimkühler, S. (2008). A novel role for human Nfs1 in the cytoplasm: Nfs1 acts as a sulfur donor for MOCS3, a protein involved in molybdenum cofactor biosynthesis. *Journal of Biological Chemistry*, *283*(37), 25178–25185. https://doi.org/10.1074/JBC.M804064200/ATTACHMENT/970E1485-FC62-4792-A0FA-CAE88165B59E/MMC1.PDF

Matsuki, M., Yamashita, F., Ishida-Yamamoto, A., Yamada, K., Kinoshita, C., Fushiki, S., Ueda, E., Morishima, Y., Tabata, K., Yasuno, H., Hashida, M., Iizuka, H., Ikawa, M., Okabe, M., Kondoh, G., Kinoshita, T., Takeda, J., & Yamanishi, K. (1998). Defective stratum corneum and early neonatal death in mice lacking the gene for transglutaminase 1 (keratinocyte transglutaminase). *Proceedings of the National Academy of Sciences of the United States of America*, *95*(3), 1044–1049. https://doi.org/10.1073/PNAS.95.3.1044

Matthies, A., Nimtz, M., & Leimkühler, S. (2005). Molybdenum cofactor biosynthesis in humans: identification of a persulfide group in the rhodanese-like domain of MOCS3 by mass spectrometry. *Biochemistry*, *44*(21), 7912–7920. https://doi.org/10.1021/BI0503448

Matthies, A., Rajagopalan, K. V., Mendel, R. R., & Leimkühler, S. (2004). Evidence for the physiological role of a rhodanese-like protein for the biosynthesis of the molybdenum cofactor in humans. *Proceedings of the National Academy of Sciences of the United States of America*, *101*(16), 5946–5951. https://doi.org/10.1073/PNAS.0308191101

Mayr, S. J., Mendel, R. R., & Schwarz, G. (2021). Molybdenum cofactor biology, evolution and deficiency. *Biochimica et Biophysica Acta (BBA) - Molecular Cell Research*, *1868*(1), 118883. https://doi.org/10.1016/J.BBAMCR.2020.118883

Mayr, S. J., Röper, J., & Schwarz, G. (2020). Alternative splicing of the bicistronic gene molybdenum cofactor synthesis 1 (MOCS1) uncovers a novel mitochondrial protein maturation mechanism. *Journal of Biological Chemistry*, *295*(10), 3029–3039. https://doi.org/10.1074/jbc.RA119.010720

Mehrel, T., Hohl, D., Rothnagel, J. A., Longley, M. A., Bundman, D., Cheng, C., Lichti, U., Bisher, M. E., Steven, A. C., Steinert, P. M., Yuspa, S. H., & Roop, D. R. (1990). Identification of a major keratinocyte cell envelope protein, loricrin. *Cell*, *61*(6), 1103–1112. https://doi.org/10.1016/0092-8674(90)90073-N

Mellis, A. T., Roeper, J., Misko, A. L., Kohl, J., & Schwarz, G. (2021). Sulfite Alters the Mitochondrial Network in Molybdenum Cofactor Deficiency. *Frontiers in Genetics*, *11*, 1672. https://doi.org/10.3389/FGENE.2020.594828/BIBTEX

Mendel, R. R. (2013). The molybdenum cofactor. *The Journal of Biological Chemistry*, *288*(19), 13165–13172. https://doi.org/10.1074/JBC.R113.455311

Mills, P. B., Footitt, E. J., Ceyhan, S., Waters, P. J., Jakobs, C., Clayton, P. T., & Struys, E. A. (2012). Urinary AASA excretion is elevated in patients with molybdenum cofactor deficiency and isolated sulphite oxidase deficiency. *Journal of Inherited Metabolic Disease*, *35*(6), 1031–1036. https://doi.org/10.1007/S10545-012-9466-1

Mills, P. B., Struys, E., Jakobs, C., Plecko, B., Baxter, P., Baumgartner, M., Willemsen, M. A. A. P., Omran, H., Tacke, U., Uhlenberg, B., Weschke, B., & Clayton, P. T. (2006). Mutations in antiquitin in individuals with pyridoxine-dependent seizures. *Nature Medicine*, *12*(3), 307–309. https://doi.org/10.1038/NM1366

Miralles-Robledillo, J. M., Torregrosa-Crespo, J., Martínez-Espinosa, R. M., & Pire, C. (2019). DMSO Reductase Family: Phylogenetics and Applications of Extremophiles. *International Journal of Molecular Sciences*, *20*(13). https://doi.org/10.3390/IJMS20133349

Monteiro-Riviere, N. (2005). Structure and Function of Skin. In *Dermal Absorption Models in Toxicology and Pharmacology* (pp. 1–19). CRC Press. https://doi.org/10.1201/9780203020821.ch1

Natsuga, K. (2014). Epidermal Barriers. *Cold Spring Harbor Perspectives in Medicine*, *4*(4). https://doi.org/10.1101/CSHPERSPECT.A018218

Netzel-Arnett, S., Currie, B. M., Szabo, R., Lin, C. Y., Chen, L. M., Chai, K. X., Antalis, T. M., Bugge, T. H., & List, K. (2006). Evidence for a matriptase-prostasin proteolytic cascade regulating terminal epidermal differentiation. *The Journal of Biological Chemistry*, *281*(44), 32941–32945. https://doi.org/10.1074/JBC.C600208200

Neve, E. P. A., Köfeler, H., Hendriks, D. F. G., Nordling, Å., Gogvadze, V., Mkrtchian, S., Näslund, E., & Ingelman-Sundberg, M. (2015). Expression and Function of mARC: Roles in Lipogenesis and Metabolic Activation of Ximelagatran. *PLoS ONE*, *10*(9). https://doi.org/10.1371/JOURNAL.PONE.0138487

Nishino, T., Nishino, T., Sato, A., Page, T., & Amaya, Y. (2020). XANTHINE DEHYDROGENASE: STRUCTURE AND PROPERTIES. *Flavins and Flavoproteins 1993*, 699–706. https://doi.org/10.1515/9783110885774-118/HTML

Nishino, T., Okamoto, K., Eger, B. T., Pai, E. F., & Nishino, T. (2008). Mammalian xanthine oxidoreductase – mechanism of transition from xanthine dehydrogenase to xanthine oxidase. *The FEBS Journal*, *275*(13), 3278–3289. https://doi.org/10.1111/J.1742-4658.2008.06489.X

Nishino, T., Okamoto, K., Kawaguchi, Y., Matsumura, T., Eger, B. T., Pai, E. F., & Nishino, T. (2015). The C-terminal peptide plays a role in the formation of an intermediate form during the transition between xanthine dehydrogenase and xanthine oxidase. *Wiley Online Library*, *282*(16), 3075–3090. https://doi.org/10.1111/febs.13277

Olney, J. W., Misra, C. H., & de Gubareff, T. (1975). Cysteine-S-sulfate: brain damaging metabolite in sulfite oxidase deficiency. *J Neuropathol Exp Neurol*, *34*(2), 167–177. https://doi.org/10.1097/00005072-197503000-00005

Ono, H., & Ito, A. (1984). Transport of the Precursor for Sulfite Oxidase into Intermembrane Space of Liver Mitochondria: Characterization of Import and Processing Activities. *The Journal of Biochemistry*, *95*(2), 345–352. https://doi.org/10.1093/OXFORDJOURNALS.JBCHEM.A134614

Ott, G., Havemeyer, A., & Clement, B. (2015). The mammalian molybdenum enzymes of mARC. *J Biol Inorg Chem*, *20*, 265–275. https://doi.org/10.1007/s00775-014-1216-4

Ovaere, P., Lippens, S., Vandenabeele, P., & Declercq, W. (n.d.). *The emerging roles of serine protease cascades in the epidermis*. https://doi.org/10.1016/j.tibs.2009.08.001

Palmer, T., Santini, C. L., Iobbi-Nivol, C., Eaves, D. J., Boxer, D. H., & Giordano, G. (1996). Involvement of the narJ and mob gene products in distinct steps in the biosynthesis of the molybdoenzyme nitrate reductase in Escherichia coli. *Molecular Microbiology*, *20*(4), 875–884. https://doi.org/10.1111/J.1365-2958.1996.TB02525.X

Pitterle, D. M., & Rajagopalan, K. V. (1989). Two proteins encoded at the chlA locus constitute the converting factor of Escherichia coli chlA1. *Journal of Bacteriology*, *171*(6), 3373–3378. https://doi.org/10.1128/JB.171.6.3373-3378.1989

Porter, R. M., & Lane, E. B. (2003). Phenotypes, genotypes and their contribution to understanding keratin function. *Trends in Genetics*, *19*(5), 278–285. https://doi.org/10.1016/S0168-9525(03)00071-4

Rajagopalan, K. V. (1980). Sulfite Oxidase (Sulfite: Ferricytochrome C Oxidoreductase)*. In *Molybdenum and Molybdenum-Containing Enzymes* (pp. 241–272). Elsevier. https://doi.org/10.1016/b978-0-08-024398-6.50012-2

Rajagopalan, K. v., & Johnson, J. L. (1992). The pterin molybdenum cofactors. In *Journal of Biological Chemistry* (Vol. 267, Issue 15, pp. 10199–10202). https://doi.org/10.1016/s0021-9258(19)50001-1

Reichelt, J., Büssow, H., Grund, C., & Magin, T. M. (2001). Formation of a normal epidermis supported by increased stability of keratins 5 and 14 in keratin 10 null mice. *Molecular Biology of the Cell*, *12*(6), 1557–1568. https://doi.org/10.1091/MBC.12.6.1557

Reiss, J., Christensen, E., Kurlemann, G., Zabot, M. T., & Dorche, C. (1998). Genomic structure and mutational spectrum of the bicistronic MOCS1 gene defective in molybdenum cofactor deficiency type A. *Human Genetics 1998 103:6*, *103*(6), 639–644. https://doi.org/10.1007/S004390050884

Reiss, J., Cohen, N., Dorche, C., Mandel, H., Mendel, R. R., Stallmeyer, B., Zabot, M.-T., & Dierks, T. (1998). *Mutations in a polycistronic nuclear gene associated with molybdenum cofactor deficiency*. www.ncbi.nlm.

Reiss, J., Gross-Hardt, S., Christensen, E., Schmidt, P., Mendel, R. R., & Schwarz, G. (2001). A mutation in the gene for the neurotransmitter receptor-clustering protein gephyrin causes a novel form of molybdenum cofactor deficiency. *American Journal of Human Genetics*, *68*(1), 208–213. https://doi.org/Doi 10.1086/316941

Reiss, J., & Hahnewald, R. (2011). Molybdenum cofactor deficiency: Mutations in GPHN, MOCS1, and MOCS2. *Human Mutation*, *32*(1), 10–18. https://doi.org/10.1002/HUMU.21390

Reschke, S., Duffus, B. R., Schrapers, P., Mebs, S., Teutloff, C., Dau, H., Haumann, M., & Leimkühler, S. (2019). Identification of YdhV as the First Molybdoenzyme Binding a Bis-Mo-MPT Cofactor in Escherichia coli. *Biochemistry*, *58*(17), 2228–2242. https://doi.org/10.1021/ACS.BIOCHEM.9B00078

Rice, R. H., & Green, H. (1977a). The cornified envelope of terminally differentiated human epidermal keratinocytes consists of cross-linked protein. *Cell*, *11*(2), 417–422. https://doi.org/10.1016/0092-8674(77)90059-9

Rice, R. H., & Green, H. (1977b). The cornified envelope of terminally differentiated human epidermal keratinocytes consists of cross-linked protein. *Cell*, *11*(2), 417–422. https://doi.org/10.1016/0092-8674(77)90059-9

Rice, R. H., & Green, H. (1979). Presence in human epidermal cells of a soluble protein precursor of the cross-linked envelope: activation of the cross-linking by calcium ions. *Cell*, *18*(3), 681–694. https://doi.org/10.1016/0092-8674(79)90123-5

Richard, G. (2004). Molecular genetics of the ichthyoses. *American Journal of Medical Genetics Part C: Seminars in Medical Genetics*, *131C*(1), 32–44. https://doi.org/10.1002/AJMG.C.30032

Rixen, S., Havemeyer, A., Tyl-Bielicka, A., Pysniak, K., Gajewska, M., Kulecka, M., Ostrowski, J., Mikula, M., & Clement, B. (2019). Mitochondrial amidoxime-reducing component 2 (MARC2) has a significant role in N-reductive activity and energy metabolism. *The Journal of Biological Chemistry*, *294*(46), 17593. https://doi.org/10.1074/JBC.RA119.007606

Rothnagel, J. A., Dominey, A. M., Dempsey, L. D., Longley, M. A., Greenhalgh, D. A., Gagne, T. A., Huber, M., Frenk, E., Hohl, D., & Roop, D. R. (1992). Mutations in the rod domains of keratins 1 and 10 in epidermolytic hyperkeratosis. *Science (New York, N.Y.)*, *257*(5073), 1128–1130. https://doi.org/10.1126/SCIENCE.257.5073.1128

Roth, W., Kumar, V., Beer, H. D., Richter, M., Wohlenberg, C., Reuter, U., Thiering, S., Staratschek-Jox, A., Hofmann, A., Kreusch, F., Schultze, J. L., Vogl, T., Roth, J., Reichelt, J., Hausser, I., & Magin, T. M. (2012). Keratin 1 maintains skin integrity and participates in an inflammatory network in skin through interleukin-18. *Journal of Cell Science*, *125*(Pt 22), 5269–5279. https://doi.org/10.1242/JCS.116574

Rudolph, M. J., Wuebbens, M. M., Rajagopalan, K. V, & Schindelin, H. (2001). *Crystal structure of molybdopterin synthase and its evolutionary relationship to ubiquitin activation*. *8*(1). http://structbio.nature.com

Ruhrberg, C., Hajibagheri, M. A. N., Parry, D. A. D., & Watt, F. M. (1997). Periplakin, a novel component of cornified envelopes and desmosomes that belongs to the plakin family and forms complexes with envoplakin. *The Journal of Cell Biology*, *139*(7), 1835–1849. https://doi.org/10.1083/JCB.139.7.1835

Ruhrberg, C., Hajibagheri, M. A. N., Simon, M., Dooley, T. P., & Watt, F. M. (1996). Envoplakin, a novel precursor of the cornified envelope that has homology to desmoplakin. *The Journal of Cell Biology*, *134*(3), 715–729. https://doi.org/10.1083/JCB.134.3.715

Rupar, C. A., Gillett, J., Gordon, B. A., Ramsay, D. A., Johnson, J. L., Garrett, R. M., Rajagopalan, K. V., Jung, J. H., Bacheyie, G. S., & Sellers, A. R. (1996). Isolated sulfite oxidase deficiency. *Neuropediatrics*, *27*(6), 299–304. https://doi.org/10.1055/S-2007-973798/BIB

Russell, L. J., Digiovanna, J. J., Rogers, G. R., Steinert, P. M., Hashem, N., & Compton, J. G. (1995). Mutations in the gene for transglutaminase 1 in autosomal recessive lamellar ichthyosis. *Nature Genetics*, *9*(3), 279–283. https://doi.org/10.1038/NG0395-279

Sbodio, J. I., Snyder, S. H., & Paul, B. D. (2019). Regulators of the transsulfuration pathway. *British Journal of Pharmacology*, *176*(4), 583. https://doi.org/10.1111/BPH.14446

Schmuth, M., Fluhr, J. W., Crumrine, D. C., Uchida, Y., Hachem, J. P., Behne, M., Moskowitz, D. G., Christiano, A. M., Feingold, K. R., & Elias, P. M. (2004). Structural and Functional Consequences of Loricrin Mutations in Human Loricrin Keratoderma (Vohwinkel Syndrome with Ichthyosis). *Journal of Investigative Dermatology*, *122*(4), 909–922. https://doi.org/10.1111/J.0022-202X.2004.22431.X

Schwarz, G. (2005). Molybdenum cofactor biosynthesis and deficiency. *Cell Mol Life Sci*, *62*(23), 2792–2810. https://doi.org/10.1007/s00018-005-5269-y

Schwarz, G., & Mendel, R. R. (2006). Molybdenum cofactor biosynthesis and molybdenum enzymes. *Annual Review of Plant Biology*, *57*, 623–647. https://doi.org/10.1146/ANNUREV.ARPLANT.57.032905.105437

Seiler, A., Schneider, M., Förster, H., Roth, S., Wirth, E. K., Culmsee, C., Plesnila, N., Kremmer, E., Rådmark, O., Wurst, W., Bornkamm, G. W., Schweizer, U., & Conrad, M. (2008). Glutathione peroxidase 4 senses and translates oxidative stress into 12/15-lipoxygenase dependent- and AIF-mediated cell death. *Cell Metabolism*, *8*(3), 237–248. https://doi.org/10.1016/J.CMET.2008.07.005

Sevilla, L. M., Nachat, R., Groot, K. R., Klement, J. F., Uitto, J., Djian, P., Määttä, A., & Watt, F. M. (2007). Mice deficient in involucrin, envoplakin, and periplakin have a defective

epidermal barrier. *The Journal of Cell Biology*, *179*(7), 1599. https://doi.org/10.1083/JCB.200706187

Sharawat, I. K., Saini, L., Singanamala, B., Saini, A. G., Sahu, J. K., Attri, S. V., & Sankhyan, N. (2020). Metabolic crisis after trivial head trauma in late-onset isolated sulfite oxidase deficiency: Report of two new cases and review of published patients. *Brain and Development*, *42*(2), 157–164. https://doi.org/10.1016/J.BRAINDEV.2019.11.003

Simon, M., Haftek, M., Sebbag, M., Montézin, M., Girbal-Neuhauser, E., Schmitt, D., & Serre, G. (1996). Evidence that filaggrin is a component of cornified cell envelopes in human plantar epidermis. *Biochemical Journal*, *317*(Pt 1), 173. https://doi.org/10.1042/BJ3170173

Simon, M., Montézin, M., Guerrin, M., Durieux, J. J., & Serre, G. (1997). Characterization and Purification of Human Corneodesmosin, an Epidermal Basic Glycoprotein Associated with Corneocyte-specific Modified Desmosomes. *Journal of Biological Chemistry*, *272*(50), 31770–31776. https://doi.org/10.1074/JBC.272.50.31770

Smolinsky, B., Eichler, S. A., Buchmeier, S., Meier, J. C., & Schwarz, G. (2008). Splice-specific functions of gephyrin in molybdenum cofactor biosynthesis. *Journal of Biological Chemistry*, *283*(25), 17370–17379. https://doi.org/10.1074/JBC.M800985200

Smyth, I., Hacking, D. F., Hilton, A. A., Mukhamedova, N., Meikle, P. J., Ellis, S., Slattery, K., Collinge, J. E., De Graaf, C. A., Bahlo, M., Sviridov, D., Kile, B. T., & Hilton, D. J. (2008). A mouse model of harlequin ichthyosis delineates a key role for Abca12 in lipid homeostasis. *PLoS Genetics*, *4*(9). https://doi.org/10.1371/JOURNAL.PGEN.1000192

Sola, M., Bavro, V. N., Timmins, J., Franz, T., Ricard-Blum, S., Schoehn, G., Ruigrok, R. W. H., Paarmann, I., Saiyed, T., O'Sullivan, G. A., Schmitt, B., Betz, H., & Weissenhorn, W. (2004). Structural basis of dynamic glycine receptor clustering by gephyrin. *The EMBO Journal*, *23*(13), 2510. https://doi.org/10.1038/SJ.EMBOJ.7600256

Sola, M., Kneussel, M., Heck, I. S., Betz, H., & Weissenhorn, W. (2001). X-ray Crystal Structure of the Trimeric N-terminal Domain of Gephyrin. *Journal of Biological Chemistry*, *276*(27), 25294–25301. https://doi.org/10.1074/jbc.M101923200

Spatzal, T., Aksoyoglu, M., Zhang, L., Andrade, S. L. A., Schleicher, E., Weber, S., Rees, D. C., & Einsle, O. (2011). Evidence for interstitial carbon in nitrogenase FeMo cofactor. *Science (New York, N.Y.)*, *334*(6058), 940. https://doi.org/10.1126/SCIENCE.1214025

Spiegel, R., Schwahn, B. C., Squires, L., & Confer, N. (2022). Molybdenum cofactor deficiency: A natural history. *Journal of Inherited Metabolic Disease*, *45*(3), 456–469. https://doi.org/10.1002/JIMD.12488

Stallmeyer, B., Drugeon, G., Reiss, J., Haenni, A. L., & Mendel, R. R. (1999). Human molybdopterin synthase gene: identification of a bicistronic transcript with overlapping reading frames. *American Journal of Human Genetics*, *64*(3), 698–705. https://doi.org/10.1086/302295

Steven, A. C., Bisher, M. E., Roop, D. R., & Steinert, P. M. (1990). Biosynthetic pathways of filaggrin and loricrin--two major proteins expressed by terminally differentiated epidermal keratinocytes. *Journal of Structural Biology*, *104*(1–3), 150–162. https://doi.org/10.1016/1047-8477(90)90071-J

Steven, A. C., & Steinert, P. M. (1994). *Protein composition of cornified cell envelopes of epidermal keratinocytes*.

Stirpe, F., & Della Corte, E. (1969). The regulation of rat liver xanthine oxidase. Conversion in vitro of the enzyme activity from dehydrogenase (type D) to oxidase (type O). *The Journal of Biological Chemistry*, *244*(14), 3855–3863.

Sullivan, E. P., Hazzard, J. T., Tollin, G., & Enemark, J. H. (1993). Electron Transfer in Sulfite Oxidase: Effects of pH and Anions on Transient Kinetics1". *Biochemistry*, *32*, 12465–12470. https://pubs.acs.org/sharingguidelines

Tan, W. H., Eichler, F. S., Hoda, S., Lee, M. S., Baris, H., Hanley, C. A., Grant, P. E., Krishnamoorthy, K. S., & Shih, V. E. (2005). Isolated sulfite oxidase deficiency: a case report with a novel mutation and review of the literature. *Pediatrics*, *116*(3), 757–766. https://doi.org/10.1542/peds.2004-1897

Tardy, P., Parvy, P., Charpentier, C., Bonnefont, J. P., Saudubray, J. M., & Kamoun, P. (1989). Attempt at therapy in sulphite oxidase deficiency. *Journal of Inherited Metabolic Disease*, *12*(1), 94–95. https://doi.org/10.1007/BF01805537

Tejada-Jiménez, M., Llamas, Á., Sanz-Luque, E., Galván, A., & Fernández, E. (2007). A high-affinity molybdate transporter in eukaryotes. *Proceedings of the National Academy of Sciences of the United States of America*, *104*(50), 20126–20130. https://doi.org/10.1073/PNAS.0704646104/SUPPL_FILE/04646FIG7.PDF

Terao, M., Romão, M. J., Leimkühler, S., Bolis, M., Fratelli, M., Coelho, C., Santos-Silva, T., & Garattini, E. (2016). Structure and function of mammalian aldehyde oxidases. *Archives of Toxicology 2016 90:4*, *90*(4), 753–780. https://doi.org/10.1007/S00204-016-1683-1

Thomé, R., Gust, A., Toci, R., Mendel, R., Bittner, F., Magalon, A., & Walburger, A. (2012). A sulfurtransferase is essential for activity of formate dehydrogenases in Escherichia coli. *Journal of Biological Chemistry*, *287*(7), 4671–4678. https://doi.org/10.1074/JBC.M111.327122

Tian, M., Qu, Y., Huang, L., Su, X., Li, S., Ying, J., Zhao, F., & Mu, D. (2019). Stable clinical course in three siblings with late-onset isolated sulfite oxidase deficiency: a case series and literature review. *BMC Pediatrics 2019 19:1*, *19*(1), 1–8. https://doi.org/10.1186/S12887-019-1889-5

Til, H. P., Feron, V. J., & de Groot, A. P. (1972). The toxicity of sulphite. I. Long-term feeding and multigeneration studies in rats. *Food and Cosmetics Toxicology*, *10*(3), 291–310. https://doi.org/10.1016/S0015-6264(72)80250-5

Ting, S. B., Caddy, J., Wilanowski, T., Auden, A., Cunningham, J. M., Elias, P. M., Holleran, W. M., & Jane, S. M. (2005). The Epidermis of Grhl3-Null Mice Displays Altered Lipid Processing and Cellular Hyperproliferation. *Organogenesis*, *2*(2), 33. https://doi.org/10.4161/ORG.2.2.2167

Tiranti, V., Viscomi, C., Hildebrandt, T., Di Meo, I., Mineri, R., Tiveron, C., D Levitt, M., Prelle, A., Fagiolari, G., Rimoldi, M., & Zeviani, M. (2009). Loss of ETHE1, a mitochondrial dioxygenase, causes fatal sulfide toxicity in ethylmalonic encephalopathy. *Nature Medicine 2009 15:2*, *15*(2), 200–205. https://doi.org/10.1038/nm.1907

Tomatsu, H., Takano, J., Takahashi, H., Watanabe-Takahashi, A., Shibagaki, N., & Fujiwara, T. (2007). An Arabidopsis thaliana high-affinity molybdate transporter required for efficient uptake of molybdate from soil. *Proceedings of the National Academy of Sciences of the United States of America*, *104*(47), 18807–18812. https://doi.org/10.1073/PNAS.0706373104/ASSET/B57FCF00-3657-45C8-98E3-22CEAB8BC8D7/ASSETS/GRAPHIC/ZPQ0450782920005.JPEG

Touati, G., Rusthoven, E., Depondt, E., Dorche, C., Duran, M., Heron, B., Rabier, D., Russo, M., & Saudubray, J. M. (2000). Dietary therapy in two patients with a mild form of sulphite oxidase deficiency. Evidence for clinical and biological improvement. *Journal of Inherited Metabolic Disease*, *23*(1), 45–53. https://doi.org/10.1023/A:1005646813492

Van Caillie-Bertrand, M., Degenhart, H. J., Luijendijk, I., Bouquet, J., & Sinaasappel, M. (1985). Wilson's disease: assessment of D-penicillamine treatment. *Archives of Disease in Childhood*, *60*(7), 652–655. https://doi.org/10.1136/ADC.60.7.652

Veldman, A., Santamaria-Araujo, J. A., Sollazzo, S., Pitt, J., Gianello, R., Yaplito-Lee, J., Wong, F., Ramsden, C. A., Reiss, J., Cook, I., Fairweather, J., & Schwarz, G. (2010). Successful Treatment of Molybdenum Cofactor Deficiency Type A With cPMP. *Pediatrics*, *125*(5), E1249–E1254. https://doi.org/10.1542/peds.2009-2192

Vincent, A. S., Lim, B. G., Tan, J., Whiteman, M., Cheung, N. S., Halliwell, B., & Wong, K. P. (2004). Sulfite-mediated oxidative stress in kidney cells. *Kidney International*, *65*(2), 393–402. https://doi.org/10.1111/J.1523-1755.2004.00391.X

Vorbach, C., Harrison, R., & Capecchi, M. R. (2003). Xanthine oxidoreductase is central to the evolution and function of the innate immune system. *Trends in Immunology*, *24*(9), 512–517. https://doi.org/10.1016/S1471-4906(03)00237-0

Vorbach, C., Scriven, A., & Capecchi, M. R. (2002). The housekeeping gene xanthine oxidoreductase is necessary for milk fat droplet enveloping and secretion: gene sharing in the lactating mammary gland. *Genes & Development*, *16*(24), 3223–3235. https://doi.org/10.1101/GAD.1032702

Wang, J., Krizowski, S., Fischer-Schrader, K., Niks, D., Tejero, J., Sparacino-Watkins, C., Wang, L., Ragireddy, V., Frizzell, S., Kelley, E. E., Zhang, Y., Basu, P., Hille, R., Schwarz, G., & Gladwin, M. T. (2015). Sulfite Oxidase Catalyzes Single-Electron Transfer at Molybdenum Domain to Reduce Nitrite to Nitric Oxide. *Antioxidants & Redox Signaling*, *23*(4), 283. https://doi.org/10.1089/ARS.2013.5397

Wilson, D. R., & Maibach, H. I. (1980). Transepidermal water loss in vivo. Premature and term infants. *Biology of the Neonate*, *37*(3–4), 180–185. https://doi.org/10.1159/000241271

Wu, D., Wang, Y., Yang, G., Zhang, S., Liu, Y., Zhou, S., Guo, H., Liang, S., Cui, Y., Zhang, B., Ma, K., Zhang, C., Liu, Y., Sun, L., Wang, J., & Liu, L. (2020). A novel mitochondrial amidoxime reducing component 2 is a favorable indicator of cancer and suppresses the progression of hepatocellular carcinoma by regulating the expression of p27. *Oncogene 2020 39:38*, *39*(38), 6099–6112. https://doi.org/10.1038/s41388-020-01417-6

Xiang, S., Nichols, J., Rajagopalan, K. V., & Schindelin, H. (2001). The crystal structure of Escherichia coli MoeA and its relationship to the multifunctional protein gephyrin. *Structure*, *9*(4), 299–310. https://doi.org/10.1016/S0969-2126(01)00588-3

Yamasaki, K., & Gallo, R. L. (2008). Antimicrobial peptides in human skin disease. *European Journal of Dermatology : EJD*, *18*(1), 11. https://doi.org/10.1684/EJD.2008.0304

Yang, W. S., Sriramaratnam, R., Welsch, M. E., Shimada, K., Skouta, R., Viswanathan, V. S., Cheah, J. H., Clemons, P. A., Shamji, A. F., Clish, C. B., Brown, L. M., Girotti, A. W., Cornish, V. W., Schreiber, S. L., & Stockwell, B. R. (2014). Regulation of Ferroptotic Cancer Cell Death by GPX4. *Cell*, *156*(0), 317. https://doi.org/10.1016/J.CELL.2013.12.010

Yousef, H., Alhajj, M., & Sharma, S. (2017). Anatomy, Skin (Integument), Epidermis. *StatPearls*. http://europepmc.org/books/NBK470464

Zhang, W., Urban, A., Mihara, H., Leimkühler, S., Kurihara, T., & Esaki, N. (2010). IscS Functions as a Primary Sulfur-donating Enzyme by Interacting Specifically with MoeB and MoaD in the Biosynthesis of Molybdopterin in Escherichia coli. *Journal of Biological Chemistry*, *285*(4), 2302–2308. https://doi.org/10.1074/JBC.M109.082172

Zhang, X., Vincent, A., Halliwell, B., & Wong, K. (2004). A Mechanism of Sulfite Neurotoxicity DIRECT INHIBITION OF GLUTAMATE DEHYDROGENASE*. *Journal of Biological Chemistry*, *279*, 43035–43045. https://doi.org/10.1074/jbc.M402759200

Zhao, J., An, Y., Jiang, H., Wu, H., Che, F., & Yang, Y. (2021). Novel Compound Heterozygous Pathogenic Variants in SUOX Cause Isolated Sulfite Oxidase Deficiency in a Chinese Han Family. *Frontiers in Genetics*, *12*, 607085. https://doi.org/10.3389/FGENE.2021.607085/BIBTEX

II Molybdenum Cofactor Deficiency in Humans

Lena Johannes, Chun-Yu Fu and Günter Schwarz*

Institute of Biochemistry, Department of Chemistry & Center for Molecular Medicine Cologne, University of Cologne, 50674 Cologne, Germany

* Author to whom correspondence should be addressed.

Molecules 2022, 27(20), 6896; https://doi.org/10.3390/molecules27206896

Received: 31 August 2022 / Revised: 23 September 2022 / Accepted: 26 September 2022 / Published: 14 October 2022

Author contributions:

Günter Schwarz conceptualized this review. Lena Johannes, Chun-Yu Fu and Günter Schwarz wrote the manuscript. Lena Johannes wrote the sections on therapies to treat MoCD and contributed to the future perspectives (chapters 2.4.2-2.4.7 and 2.5). Chun-Yu Fu wrote the sections on *MOCS2* mutations, the disease mechanism and the involvement of H_2S to the pathophysiology of MoCD (chapters 2.3.2, 2.4.1 and 2.4.8). Günter Schwarz wrote the introduction, the sections on the clinical presentation of MoCD, and mutations in *MOCS1* and *GPHN*, as well as the section on future perspectives (chapters 2.1, 2.2, 2.3.1, 2.3.3 and 2.5).

Abstract

Molybdenum cofactor (Moco) deficiency (MoCD) is characterized by neonatal-onset myoclonic epileptic encephalopathy and dystonia with cerebral MRI changes similar to hypoxic–ischemic lesions. The molecular cause of the disease is the loss of sulfite oxidase (SOX) activity, one of four Moco-dependent enzymes in men. Accumulating toxic sulfite causes a secondary increase of metabolites such as S-sulfocysteine and thiosulfate as well as a decrease in cysteine and its oxidized form, cystine. Moco is synthesized by a three-step biosynthetic pathway that involves the gene products of *MOCS1, MOCS2, MOCS3,* and *GPHN*. Depending on which synthetic step is impaired, MoCD is classified as type A, B, or C. This distinction is relevant for patient management because the metabolic block in MoCD type A can be circumvented by administering cyclic pyranopterin monophosphate

(cPMP). Substitution therapy with cPMP is highly effective in reducing sulfite toxicity and restoring biochemical homeostasis, while the clinical outcome critically depends on the degree of brain injury prior to the start of treatment. In the absence of a specific treatment for MoCD type B/C and SOX deficiency, we summarize recent progress in our understanding of the underlying metabolic changes in cysteine homeostasis and propose novel therapeutic interventions to circumvent those pathological changes.

2.1 Introduction

Four molybdenum (Mo)-enzymes are known in humans, each catalyzing either catabolic or detoxifying reaction (Schwarz et al., 2009) s. They all share an identical type of molybdenum cofactor (Moco) that is strictly required for the activity of all these enzymes. Sulfite oxidase (SOX) is considered, by far, the most critical enzyme for human health as it catalyzes the terminal step in oxidative cysteine catabolism, the oxidation of sulfite to sulfate. SOX is localized in the intermembrane space of mitochondria and links sulfite oxidation to the reduction of cytochrome *c*. There are two cytosolic Mo-enzymes, xanthine oxidoreductase and aldehyde oxidase, which are closely related Mo–iron–flavin enzymes catalyzing the hydroxylation reactions of purines and various heterocyclic substrates (Schwarz et al., 2009). The mitochondrial amidoxime-reducing component (mARC) has been identified as a fourth vertebrate Mo-enzyme (Havemeyer et al., 2006) and reduces N-hydroxylated prodrugs as well as metabolites such as N-hydroxy-L-arginine.

Patients with isolated deficiencies in SOX or xanthine oxidoreductase are well known in the field (Schwarz, 2016), while deficiencies in aldehyde oxidase and the amidoxime-reducing component have not been reported yet. The largest fraction of patients with deficiencies in those enzymes is represented by defects in the biosynthesis of the molybdenum cofactor, a highly conserved multistep pathway that involves multiple gene products (Mayr et al., 2021). Moco biosynthesis is divided into three major steps based on two intermediates, cyclic pyranopterin monophosphate (cPMP) (Santamaria-Araujo et al., 2004; Wuebbens & Rajagopalan, 1995) and molybdopterin (MPT) (Johnson et al., 1984), that were identified decades ago (Fig. 1).

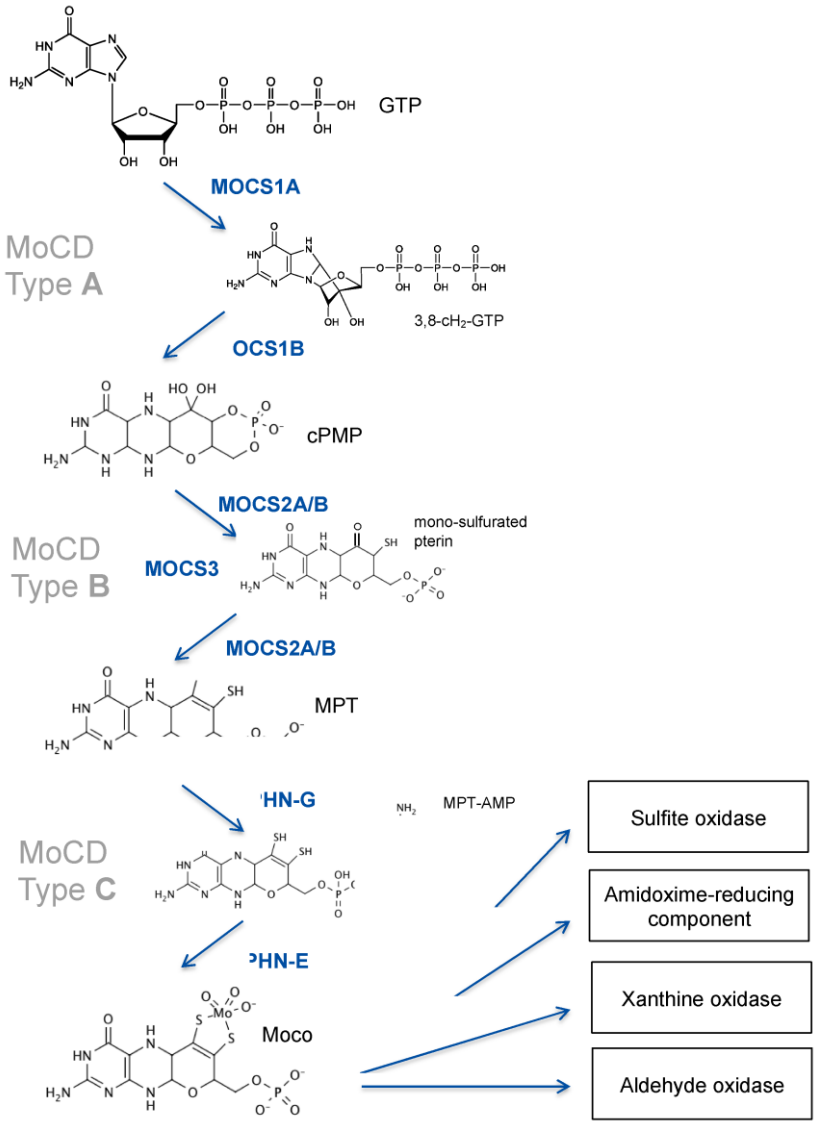

Figure 1: Moco biosynthesis; Mo-enzymes and deficiencies.

Intermediates of Moco synthesis are 3′ 8-cyclo 7,8-dihydro-GTP, cyclic pyranopterin monophosphate (cPMP), mono-sulfurate pterin, metal binding pterin (MPT), and adenylated MPT (MPT-AMP). Proteins and domains (GPHN) involved in Moco synthesis are shown. MOCS3 is involved in both steps of cPMP-to-MPT conversion as it is required for the thiolation of MOCS2A. Deficiencies in MOCS1, MOCS2/3, and GPHN cause MoCD type A, type B, and type C, respectively.

The first step in Moco biosynthesis, the conversion of GTP into cPMP, is catalyzed by two proteins encoded by the *MOCS1* locus (Reiss, Cohen, et al., 1998). *MOCS1* expression undergoes alternative splicing, yielding two different types of transcripts, one bicistronic and one monocistronic mRNA (Gray & Nicholls, 2000). The bicistronic transcript encodes for two open reading frames, MOCS1A and MOCS1B (Reiss, Christensen, et al., 1998), of which only the first is translated into a functional MOCS1A protein. MOCS1A catalyzes the S-adenosyl-methionine and [4Fe-4S] cluster-dependent radical conversion of GTP to 3′ 8-cyclo-7,8 dihydro GTP (Fig. 1). The second monocistronic transcript produces a MOCS1AB fusion protein that is proteolytically cleaved to release a MOCS1B protein (Mayr et al., 2020)

that converts 3′ 8-cyclo-7,8 dihydro GTP to cPMP (Hover, Tonthat, et al., 2015). We have shown that, in addition, alternative splicing will produce protein variants that target either mitochondria or the cytosol (Mayr et al., 2020).

The second step in Moco biosynthesis is catalyzed by MPT synthase, which converts cPMP into molybdopterin (MPT) and is encoded by the bicistronic *MOCS2* gene producing both subunits (MOCS2A and MOCS2B) by a ribosomal leaky scanning mechanism (Stallmeyer, Schwarz, et al., 1999). Heterotetrameric MPT synthase (Gutzke et al., 2001) transfers stepwise two sulfides from the thiocarboxylated C-terminus of MOCS2A to cPMP, thus giving rise to a mono-thiolated pterin intermediate (Wuebbens & Rajagopalan, 2003) (Fig. 1). *MOCS3* encodes for the Moco sulfurase (Matthies et al., 2004), which is required for the ATP-dependent thiolation of MOCS2A.

The third and final step in Moco synthesis involves the synthesis of MPT-AMP and the subsequent molybdate-dependent hydrolysis of MPT-AMP (Belaidi & Schwarz, 2013; Kuper et al., 2004; Llamas et al., 2006) (Fig. 1), releasing Moco. Both reactions are dependent on the *GPHN* gene, which encodes for a multi-domain cytosolic protein named gephyrin, composed of an N-terminal G-domain (GPHN-G), a central domain, and a C-terminal E-domain (GPHN-E). Besides Moco biosynthesis, gephyrin protein functions as a cytosolic membrane-associated receptor-clustering protein, being essential for the formation of inhibitory synapses (Fritschy et al., 2008).

2.2 Clinical Presentation of Molybdenum Cofactor Deficient Patients

Depending on which step in Moco synthesis is impaired, MoCD is classified into three types (A, B, and C), with MoCD type A and B representing the vast majority of cases; MoCD type C is extremely rare due to a very severe presentation (see below).

Biochemically, all three forms of MoCD are indistinguishable and highly similar to isolated SOX deficiency (SOXD). The latter has been reported in more than 50 cases (Claerhout et al., 2018), whereas over 200 cases of MoCD have been described so far (Spiegel et al., 2022), and many more are known to metabolic clinicians. The diagnostic hallmarks of MoCD and SOXD are the accumulation of sulfite, S-sulfocysteine (SSC), thiosulfate, and taurine, accompanied by a reduction in cystine/cysteine as well as homocysteine. Furthermore, a reduction in pyridoxal 5′-phosphate (PLP) has been reported. In addition, as a matter of differential diagnosis, in MoCD patients - but not in SOXD patients - uric acid levels are strongly and progressively declined, while xanthine and hypoxanthine, substrates of another Mo-enzyme, xanthine oxidoreductase, are increased. In addition, urothione, the catabolic end product of Moco, can also be used to differentiate between

MoCD and SOXD patients. Surprisingly, urothione synthesis requires thiopurine methyl transferase, a well-known drug-metabolizing enzyme (Pristup et al., 2022).

Typical newborn MoCD patients present with a broad spectrum of clinical severity, with the vast majority being severely affected from the neonatal age. Most patients initially appear healthy, while some display minor dysmorphic facial features and may have solitary cerebral parenchymal cysts and hypoplastic pons and cerebellums.

The most common presentation of severe, classical MoCD, as first described in 1978 (Duran et al., 1978), is of early myoclonic encephalopathy, often starting within hours to days after birth, with poor feeding, irritability, and a distressed facial expression, and quickly progressing to myoclonic seizures, decreased consciousness, and apnea. The electroencephalogram (EEG) can initially be normal, advancing to a generalized burst suppression pattern. Within the first two weeks, children may regain alertness but show persistent hyperexcitability, frequent myoclonus, tonic spasms and focal seizures with eye deviation, and facial flushing. Seizures are often refractive to anticonvulsants. Infants can display dystonic episodes with prominent limb hypertonia and opisthotonus. A proportion of children develop lens dislocation during infancy and nephrolithiasis has also been reported. Mortality is high due to intercurrent lower respiratory tract infections and seizures, with a reported median survival of 2.4 (Spiegel et al., 2022) or 3 years (Mechler et al., 2015).

Neuroimaging usually demonstrates severe abnormalities. An early stage of generalized edema is quickly followed by features mimicking severe generalized hypoxic–ischemic encephalopathy (Vijayakumar et al., 2011), which evolves within a few weeks to a characteristic appearance, including cortical atrophy and loss of white matter with cyst formation, hypoplastic corpus callosum, abnormal basal ganglia, hydrocephalus ex vacuo, dilated ventricles, cerebellar and brainstem hypoplasia, and mega cisterna magna (Arslanoglu et al., 2001; Bayram et al., 2013; Vijayakumar et al., 2011).

Increasingly, cases with symptom onset later in childhood and attenuated severity have been described. Occasionally, children present merely with dystonia and speech delay (Mayr et al., 2018; Scelsa et al., 2019), and cranial imaging may only show changes to the basal ganglia or even appear normal (Del Rizzo et al., 2013; Spiegel et al., 2022). Attenuated disease probably reflects a slightly higher residual activity of SOX and/or Moco synthesis, and the diagnosis is easily missed if specific diagnostic investigations are not undertaken. Secondary deterioration can occur with intercurrent illness.

2.3 Genetics of Moco Deficiency

2.3.1 *MOCS1* Mutations Lead to cPMP Deficiency

The first and most complex step in Moco biosynthesis is catalyzed by MOCS1A and MOCS1B proteins, which catalyze the stepwise conversion of the purine GTP to cPMP (Fig. 1). Functional aspects of MOCS1 proteins are derived from biochemical studies on their bacterial orthologues, MoaA and MoaC. MOCS1A belongs to the superfamily of radical S-adenosylmethionine (SAM) enzymes (Landgraf et al., 2016), being characterized by a [4Fe-4S] cluster, the radical SAM-cluster, which reductively cleaves SAM, producing an adenosyl radical by oxidizing the [4Fe-4S] cluster from +1 to +2 (Walsby et al., 2002). In addition, MOCS1A represents one of only eight (so far) classified radical SAM enzymes (Landgraf et al., 2016) harboring a second C-terminal auxiliary [4Fe-4S] cluster (Hänzelmann et al., 2004; Morikawa et al., 2001; Ohara-Imaizumi et al., 2010; Reiter et al., 2012). Both [4Fe-4S] clusters are coordinated by three cysteines, resulting in the high oxygen sensitivity of both clusters compared to [4Fe-4S] clusters coordinated by four cysteines. Following the formation of the adenosyl radical, the abstraction of an H-atom from the C3 of the GTP coordinated by the auxiliary [4Fe-4S] cluster of MOCS1A will lead to the cyclization of GTP, thus forming 3′,8-cylodihydro-GTP (3′,8-cH_2-GTP) (Pang et al., 2020; Pang & Yokoyama, 2018). MOCS2B, a trimer of functional dimers, converts 3′,8-cH2-GTP to cPMP with the formation of cyclic phosphate as the thermodynamic driver for pterin ring formation (Hover, Lilla, et al., 2015).

The unique chemical nature of cPMP was first described in 2004, representing a unique geminal diol at the C1′ position and demonstrating the tetrahydropyranopterin nature of this first and rather stable intermediate of the pathway (Santamaria-Araujo et al., 2004). It is important to acknowledge this significant chemical nature of cPMP, given the observed reactivity of cPMP with the downstream MPT synthesis reaction being initiated at the C2′ position (see below).

The *MOCS1* gene consists of ten exons, of which exons 1 to 9 encode for MOCS1A and exon 10 for MOCS1B (Gross-Hardt & Reiss, 2002). Interestingly, alternative splicing in exon 9 produces either monocistronic or bicistronic transcripts that lead to the expression of either MOCS1A or the fusion protein MOCS1AB, respectively. In addition, alternative splicing of exon 1 results in transcripts that lead to MOCS1A proteins targeted to mitochondria, while other variants remain in the cytosol (Mayr et al., 2020). In contrast, all expressed MOCS1AB protein variants are targeted to mitochondria due to an internal targeting motif localized upstream of the MOCS1B domain. Following the translocation of

MOCS1AB to the mitochondrial matrix, proteolytic cleavage at position 432 of MOCS1AB results in the release of a catalytically active MOCS1B protein (Mayr et al., 2020).

Mutations in *MOCS1* lead to MoCD type A, the most prevalent form of MoCD, affecting approximately 50–60% of all known patients to date (Misko et al., 2021; Reiss & Hahnewald, 2011). The last and comprehensive review of all reported MOCS1 variants lists a total of 32 disease-causing variants, out of which 20 mutations represent loss of function variants leading to a complete lack of Moco and, therefore, a full penetrance of the disease. In addition, there are numerous missense variants reported that affect highly/invariant residues involved in iron–sulfur cluster binding or catalysis that are also expected to have a complete loss in activity. A recent review from 2021 by Misko et al. provides an additional reference to the novel and potentially disease-causing MOCS1 variants (Misko et al., 2021) that can be found in the Exome Aggregation Consortium and Genome Aggregation Database. We used a comprehensive bioinformatic approach to investigate the pathogenicity of naturally occurring MOCS1 variants and found multiple novel disease-causing variants that allow a first genetics-based prediction of the incidence of MoCD type A, being in the range of 1:200,000 to 1:500,000, without considering other cofounding factors such as regional consanguinity (Mayr et al. unpublished results). In general, and in agreement with the large number of patients diagnosed at a late stage with severe disease (Mechler et al., 2015), MoCD and MoCD type A, in particular, are considered to be underdiagnosed. However, functional studies have also disclosed a misdiagnosed case (Macaya et al., 2005) carrying a highly frequent c.1064T > C allele, leading to the missense variant I355T, which is fully active (Mayr et al. unpublished results). Reinspection of the original work additionally confirmed a hemizygous condition, excluding MoCD as the underlying cause of the reported encephalopathy.

Amongst other novel *MOCS1* variants reported in recent years (Abe et al., 2021; Kingsmore et al., 2020; Yoshimura et al., 2019)[, there was a recent, only mildly affected patient with a mutation that one would classify as loss of function. The underlying homozygous c.1338delG *MOCS1* mutation causes a frameshift (p.S442fs), with a premature termination of the MOCS1AB translation product at position 477 that suggests the lack of the entire MOCS1B domain. However, a comprehensive biochemical analysis demonstrated an unusual mechanism of translation re-initiation in the *MOCS1* transcript; this resulted in trace amounts of functional MOCS1B protein that were sufficient to partially protect the patient from the most severe symptoms of MoCD. In aggregate, 20 years of genetic studies on *MOCS1* have identified nearly 50 pathogenic variants, with most of them causing a complete loss of function, thus representing the largest group of MoCD patients.

2.3.2 Loss of MPT Synthesis is Caused by Mutations in *MOCS2*

The second step of Moco synthesis involves the stepwise conversion of cPMP to MPT, resulting in the opening of the cyclic phosphate in cPMP and the insertion of the unique dithiolene required to chelate the molybdenum atom. Both sulfur atoms are derived from cysteine and are inserted one after the other, with the formation of a monosulfurated pterin species, as deduced from studies on the bacterial enzyme (Wuebbens & Rajagopalan, 2003). The overall reaction is catalyzed by MPT synthase, which represents a dimer of MOCS2A/B heterodimers, with MOCS2B mediating heterotetramer formation. Two active sites are formed at each MOCS2/B heterodimer, with the C-terminal thiocarboxylated tail of MOCS2A being inserted into MOCS2B, forming the binding site for cPMP. Following thiol transfer, MOCS2A dissociates from the MPT synthase complex and undergoes an ATP- and sulfide-dependent re-thiolation catalyzed by MOCS3 (Rudolph et al., 2003).

The *MOCS2* gene contains seven exons; exons 1–3 encode for 88 residues of the small subunit, MOCS2A, and exons 3–7 encode for the large subunit, MOCS2B. As a very rare situation in higher eukaryotes, the last 77 bps of exon 3 encode in two different open reading frames for two proteins, the C-terminal end of MOCS2A, harboring the catalytically essential double glycine motif, and the N-terminus of MOCS2B. Translation of both overlapping open reading frames is ensured by a ribosomal leaky scanning mechanism (Stallmeyer, Drugeon, et al., 1999).

From the published case reports and review articles so far, we know that about 1/3 of all MoCD patients belong to MoCD type B, with the vast majority of them representing classical early onset patients. Here, we summarized 31 *MOCS2* mutations and 3 *MOCS3* mutations (Table 1). Among all *MOCS2* mutations, 11 of them are located on exon 1 or -2, encoding for MOCS2A; another six mutations reside in exon 3, affecting both MOCS2A and MOCS2B proteins, and another 14 variants were found to impact MOCS2B due to mutations in exons 4–7. Approximate 50% of the *MOCS2* mutations lead to either frameshifting or premature termination, causing a total loss of function of MPT synthase, while the other half represent missense mutations affecting protein complex formation and/or catalysis.

Table 1:List of MoCD Type B Mutations.

Gene	Nucleotide change	Amino acid change/ Predicted effect	Onset	Reference
MOCS2A	c.-9_14del23	Initiation failure	Early	(Hahnewald et al., 2006)
	c.-9G>C	-	Early	(Arican et al., 2019)
	c.1A>G	Initiation failure	-	(Reiss & Hahnewald, 2011)
	c.3G>A	p.M1I (Initiation failure)	Early	(Megahed et al., 2016; Reiss et al., 1999)
	c.16C>T (c.44C>T)	p.Q6X	Early	(Johnson et al., 2001)
	c.19G>T (c.47G>T)	p.V7F*	Early	(Johnson et al., 2001; Tian et al., 2021)
	c.33T>G	p.Y11X	-	(Leimkühler et al., 2005)
	c.45T>A	p.S15R*	-	(Reiss & Johnson, 2003)
	c.88C>T	p.Q30X	-	(Reiss & Johnson, 2003)
	c.106C>T	p.Q36X	-	(Reiss & Johnson, 2003)
	c.130C>T	p.R44X	Early	(Per et al., 2007)
MOCS2A/B	c.218T>C	p.L73P (MOCS2A)	Early	(Yoganathan et al., 2018)
	c.220C>T	p.Q74X (MOCS2A)	Late	(Reiss & Hahnewald, 2011)
	c.226G>A	p.G76R (MOCS2A)	Early	(Vijayakumar et al., 2011)
	c.252insC	Premature termination	Early	(Nagappa et al., 2015)
	c.265T>C	p.X89Q (MOCS2A), silenced p.D26D (MOCS2B)	Late	(Kikuchi et al., 2012)
	c.266A>G	p.X89W (MOCS2A), p.D26G (MOCS2B)	Late	(Kikuchi et al., 2012)

	c.413G>A	p.G76R	Early	(Reiss & Johnson, 2003)
	c.419C>T	p.S140F*	Early	(Edwards et al., 2015)
	c.493 T > C	p.W165R	Late	(E. J. Lee et al., 2021)
	c.501delA	p.K105fs	-	(Reiss & Hahnewald, 2011)
	c.501+2delT	Disruption of splice site	Early	(Edwards et al., 2015)
	c.533_536delGTCA	p.V116fs (Premature termination)	-	(Reiss et al., 1999)
	c.564G>C	p.G126A	-	(Alkufri et al., 2013; Reiss & Johnson, 2003)
MOCS2B	c.564+1G>A	Skipping exon 5	Early	(Reiss & Hahnewald, 2011)
	c.635_637delGCT	p.A150del*	Early	(Reiss & Johnson, 2003)
	c.658_664delTTTAAAAinsG	p.L158_K159del	-	(Reiss & Johnson, 2003)
	c.689G>A	p.E168K*	-	(Reiss & Johnson, 2003)
	c.714_718delGGAAA	p.G178fs (Premature termination)	-	(Reiss & Johnson, 2003)
	c.726_727delAA	p.K180fs (Premature termination)	Late	(Alkufri et al., 2013; Leimkühler et al., 2005; Reiss & Johnson, 2003)
	c.754A>C	p.X189Y	-	(Leimkühler et al., 2005)
	c.325C>G	p.L109V	Early	(Liao et al., 2021)
MOCS3	c.769G>A	p.A257T	Late	(Huijmans et al., 2017)
	c.1375C>T	p.Q459X	Early	(Liao et al., 2021)

MoCD type B patients are usually reported with severe phenotypes due to a large number of severe mutations. However, the relation between the MPT synthase activity and the different missense mutations remains largely unknown. Only six MOCS2 variants have

been characterized in three studies (Edwards et al., 2015; Leimkühler et al., 2003). In the first study, the missense variant MOCS2A-S15R and truncated variant MOCS2B-A150Δ did not yield any stable protein for further analysis. In the size exclusion chromatography, the MOCS2A-V7F variant was impaired in a heterotetramer formation with MOCS2B, yet the MOCS2B-E168K variant formed a complex with MOCS2A, which retained 50% of WT MPT synthase activity, whereas the MOCS2A-V7F/MOCS2B complex showed 10% residual activity. Notably, the patient who carried MOCS2A-V7F was reported as a mild case, while the patient who carried the MOCS2B-E168K variant was reported as a severe case despite the much higher residual activity recorded in vitro (Leimkühler et al., 2003). In the second study, the MOCS2B-S140F variant yielded much lower protein than WT and revealed an alteration in protein folding. The change in the content of helical structures might influence either the oligomerization between MOCS2B protomers or the interaction with MOCS2A subunits; this was further confirmed by binding studies using isothermal titration calorimetry. As a consequence, MOCS2B-S140F was able to form MPT but at a much lower rate than WT MOCS2B (Wuebbens & Rajagopalan, 2003). In the latest study, the variant MOCS2B-L158_K159del was characterized. The structure analysis indicated that residues Leu158 and Lys159 are located at the end of the last helix and are involved in the binding of MPT synthase small subunits. Thus, the heterodimer and active complex formation were impaired in this variant (Jezela-Stanek et al., 2020). In conclusion, these studies demonstrate a link between residual Moco synthesis activity and delayed onset and/or a milder course of the disease.

2.3.3 Patients with *GPHN* Mutations Show a Broad Spectrum of Neurological Disorders

The final step in human Moco biosynthesis is catalyzed by the multi-domain protein gephyrin, also representing a domain fusion of individual enzymatic functions of individual bacterial enzymes. Hereby, the G- and E-domains of gephyrin catalyze the adenylylation of MPT and the insertion of molybdate, suggesting product–substrate channeling as the underlying driving force for domain fusion (Nichols & Rajagopalan, 2002; Stallmeyer, Schwarz, et al., 1999). Crystal structures of both catalytic domains have been determined in the past (Eun et al., 2006; Schwarz et al., 2001), while a full-length structure of the gephyrin is still lacking due to its high conformational flexibility (Sander et al., 2013).

As the name depicts, *GPHN* does not follow the classical *MOCS* gene nomenclature of all other genes involved in Moco synthesis due to its initial identification as a glycine receptor-associated protein (Prior et al., 1992). At that time, the reported binding to microtubules was the main driver of naming the protein according to a proposed bridging function. Today, it is known that, similar to other postsynaptic scaffolding proteins, gephyrin

fulfills a major structural and signaling function at inhibitory synapses in the central nervous system (Fritschy et al., 2008). Gephyrin binds to the large intracellular domains of various subunits of glycine and GABA type A receptors. The high-resolution crystal structure of the dimeric gephyrin E-domain in complex with a peptide derived from the beta-subunit of the glycine receptor discloses two independent, active sites on the E-domain, one involved in Moco synthesis, the other binding the receptor in a key and lock mechanism at the interface of two dimers (Eun et al., 2006).

Vertebrate gephyrin is encoded by the *GPHN* gene, composed of up to 40 exons, with a varying number of exons undergoing alternative splicing (Dos Reis et al., 2022). Although the number of exons and alternative splice products reported in humans is far lower (Rees et al., 2003) than recently reported in mice, it is expected that the highly mosaic gene expression also holds true in humans and reflects the complex regulation of gephyrin function in the central nervous system. In the liver, the majority of gephyrin is encoded by a splice variant harboring the so-called C3-cassette, suggesting that this variant is primarily involved in gephyrin's metabolic function.

In contrast to MoCD types A and B, the number of identified MoCD patients with mutations in *GPHN* is extremely low. To date, only two cases have been reported (Reiss et al., 2001; Reiss & Hahnewald, 2011), with mutations in *GPHN* presenting a very severe disease course. This finding is most likely due to the dual function of gephyrin in Moco synthesis and neuroreceptor clustering and is mirrored by the phenotype of gephyrin-deficient mice that die on the first day of life (Feng et al., 1998), while MOCS1- and MOCS2-deficient mice survive for 8–11 days (Jakubiczka-Smorag et al., 2016; H. J. Lee et al., 2002). Along these lines, numerous studies have identified heterozygous mutations and haploinsufficiency in the *GPHN* gene, causing a variety of neuropsychiatric disorders (Dejanovic et al., 2014; Lionel et al., 2013; MacHa et al., 2022) underlying the fundamental function of gephyrin in the central nervous system.

2.4 Therapies to Treat MoCD

2.4.1 Disease Mechanisms

Most of the symptoms in MoCD patients are mirrored by SOXD, which is caused by mutations in the *SUOX* gene. SOX is one of four Mo-enzymes in mammals, and loss of SOX activity is considered the key enzyme contributing to the pathophysiology of MoCD. The hallmark of SOXD and MoCD is the accumulation of cytotoxic sulfite, which is highly reactive. For example, sulfite is able to reduce disulfide bridges in both small sulfur-containing molecules as well as in proteins. Several molecules were reported as sulfite

scavengers, namely, cystine, oxidized glutathione (GSSG), homocystine, and cystamine; they form S-sulfonated species following their reaction with sulfite. The effects of these S-sulfonated species remain largely unknown except for S-sulfocysteine (SSC). SSC represents a structural analog of glutamate and has been proven to cause excitotoxicity in neurons by activating N-methyl-D-aspartate type glutamate (NMDA) receptors, causing calcium influx and downstream signaling such as calpain activation (Kumar et al., 2017). From many case reports describing SOXD and MoCD patients, it becomes obvious that disease progression is directly related to the severity of neurodegeneration. Consequently, targeting sulfite and its downstream targets (such as SSC) are the main strategies for future treatments (see below).

Although sulfite and SSC are two well-known biomarkers that can be detected in MoCD and SOXD patients very shortly after birth, there are other changes in metabolites that hint at additional mechanisms that might contribute to MoCD and SOXD pathophysiology. First, cystine and cysteine are depleted due to SSC formation and increased renal excretion. Cysteine as the precursor of glutathione (GSH) and low cysteine/cystine levels could lead to reduced cellular GSH levels that could cause ferroptosis, a new form of non-apoptotic cell death (see Section 4.7). Second, MoCD patients were also reported to exhibit lower homocysteine levels that might be caused by the formation and increased excretion of S-sulfohomocysteine and/or reflect a secondary cause of cysteine depletion. Finally, a sulfite-dependent reduction of pyridoxal 5′-phosphate (PLP) in cerebrospinal fluid has been reported in MoCD patients (Footitt et al., 2011). The latter is considered a pro-excitatory effect of sulfite, which could also contribute to neurodegeneration in a similar way to pyridoxine-responsive encephalopathy.

Sulfite is the major downstream intermediate product of cysteine catabolism, which can be divided into two major pathways: Excess cysteine is converted via cysteine sulfinic acid to taurine (Tau) by the subsequent reactions catalyzed by cysteine dioxygenase (CDO) and cysteine sulfinic acid decarboxylase (Fig. 2). Alternatively, aspartate:2-oxoglutarate aminotransferase (AST) converts cysteine sulfinic acid to β-sulfinyl pyruvate, which spontaneously decomposes to pyruvate and sulfite. Recently, we demonstrated that cytosolic AST is the major contributor to sulfite formation (Mellis, Misko, et al., 2021). The second route of cysteine metabolism involves H_2S, which is generated by three alternative routes involving, cystathionine γ-lyase (CSE), cystathionine β-synthase (CBS), and 3-mercaptopyruvate sulfurtransferase (MSPT). The latter enzyme also requires AST; however, here, the mitochondrial isoform of AST has been implicated as a major contributor (Mellis, Misko, et al., 2021).

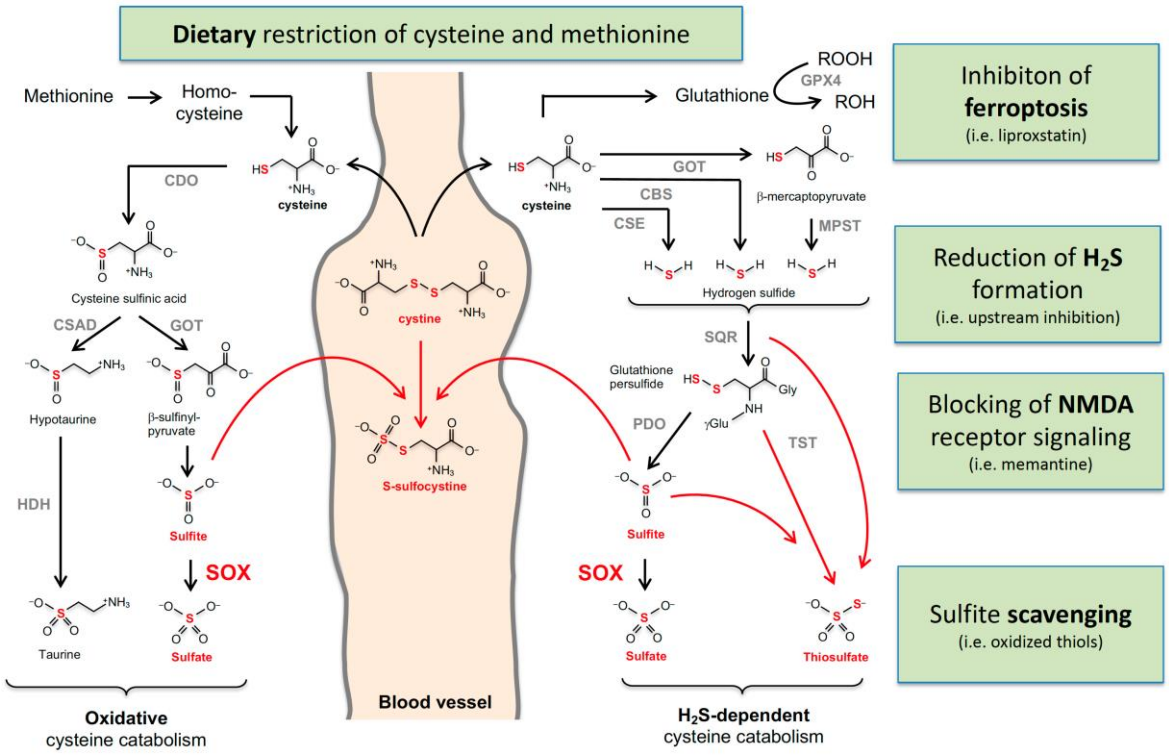

Figure 2: Cysteine catabolism and sulfur-containing metabolites that are altered in MoCD and SOX deficiency.
Oxidative and H_2S-dependent cysteine catabolisms are summarized with the involved enzymes and metabolites. Accumulating metabolites in MoCD and SO deficiency are labeled in red. Cystine and homocysteine were found to be reduced. The arrows from methionine to homocysteine, cysteine, and glutathione represent multiple enzymatic reactions. Enzyme abbreviations are in alphabetical order: GOT, glutamate oxaloacetate transaminase; CBS, cystathionine β-synthase; CSE, cystathionine γ-lyase; CDO, cysteine dioxygenase; CSD; cysteine sulfinate decarboxylase; HDH, hypoxanthine dehydrogenase; MPST, 3-mercaptopyruvate sulfurtransferase; PSD, persulfide dioxygenase; SO, sulfite oxidase; SQR, quinone oxidoreductase; TST, thiosulfate sulfur transferase.

The half-life of H_2S is considered to be short as it rapidly metabolizes in mitochondria to either sulfite or thiosulfate; this involves three enzymes: sulfide quinone oxidoreductase (SQR) catalyzes the H_2S-dependent formation of persulfidate species such as glutathione-persulfide, which is further converted by protein sulfide oxidase (PDO) to sulfite. A third enzyme, thiosulfate sulfur transferase (TST), forms thiosulfate in the presence of sulfite and persulfides.

2.4.2 Treatment of MoCD Type A (MOCS1) Patients with cPMP

To this day, an effective treatment strategy has only been established for MoCD type A. Following successful preclinical studies in a mouse model of MOCS1 deficiency (Schwarz et al., 2004), the first treatment of MoCD in a human patient was reported in 2010 (Veldman et al., 2010). In this patient, daily intravenous administration of purified *E. coli*-derived cPMP, the first intermediate of Moco biosynthesis, was initiated.

Before treatment, the first patient presented with seizures, feeding abnormalities, and cerebral atrophy and displayed abnormally increased urinary levels of SSC, thiosulfate,

xanthine, and sulfite. Gene analysis found a homozygous mutation in exon 10 of the *MOCS1* gene, leading to MoCD type A, in which the first step of Moco biosynthesis is disturbed.

Following the diagnosis of MoCD type and legal approval by the local authorities, treatment of the index case was started with daily intravenous injections of 80 µg/kg cPMP at day 36 of life. After 12 and 35 days of treatment, the dosage was increased to 120 and 160 µg/kg per day, respectively, while after 75 days, the dosage was temporarily increased to 160 µg/kg twice per day. Within a few days after initiating cPMP therapy, urinary levels of SSC, thiosulfate, xanthine, and uric acid decreased drastically until the concentrations were stabilized at control levels and urine sulfite tests became negative. Treatment was tolerated well, without any visible side effects, and when examined by a pediatrician at 18 months, the child was clinically seizure-free and displayed no signs of progressive neurodegeneration.

Since this first success story, more than 20 MoCD patients have benefited from cPMP substitution therapy. In a cohort study from 2015, eleven neonates were treated with intravenous cPMP, beginning between the ages of 0 to 68 days (B. C. Schwahn et al., 2015). Disease biomarker levels were reduced almost back to normal within two days for all of them. Eight of the patients showed a significant improvement in their symptoms, with three of them even displaying near-normal development in the long term. Additionally, the treatment showed no serious adverse events after more than 6000 doses and was considered to be safe (B. C. Schwahn et al., 2015). While in the early years, cPMP was enzymatically synthesized and purified from bacteria (Schwarz et al., 2004), chemical synthesis of cPMP was achieved in 2013 (Clinch et al., 2013), leading to larger quantities and a more cost-effective production of cPMP. Following a clinical phase I safety study with synthetic cPMP, since 2014, patients treated with ‘recombinant’ cPMP were stepwise transferred to the new synthetic cPMP within the frame of a clinical phase II/III study (ORGN001, formerly ALXN1101; https://clinicaltrials.gov (accessed on 15 August 2022)). Finally, in 2021, chemically synthesized cPMP (named ‘Fosdenopterin’) was approved by the FDA and received marketing authorization as a Nulibry product (Farrell et al., 2021). It is administered via daily intravenous injections at a concentration of 400 µg/kg in pre-term infants and 550 µg/kg in term infants until it is increased to 900 µg/kg after the first three months of treatment or directly for children starting the therapy at the age of one year or later (Nulibry prescribing information (B. Schwahn, 2021)).

In MoCD types B and C, the later steps of Moco biosynthesis are affected, and, therefore, cPMP substitution is not applicable to those patients. MPT and Moco, the

products of the second and third step of Moco biosynthesis, however, have a significantly shorter half-life than cPMP and are extremely sensitive to oxidation in aerobic environments (Wuebbens & Rajagopalan, 1995), which, so far, have impeded their usage as a treatment for MoCD types B and C. Therefore, it is crucial to focus on the development of alternative therapeutic approaches that cover all known types of MoCD and SOXD.

2.4.3 Molybdate Treatment

In early studies, before knowing the underlying genetic and biochemical basis of MoCD, molybdate treatment was tested with the aim of increasing Moco formation (Endres et al., 1988). While this was not successful, studies in fibroblasts derived from a *GPHN*-deficient patient demonstrated the possibility of a molybdate-dependent, partial restoration of Moco synthesis (Reiss et al., 2001). However, such an approach could only work in patients with *GPHN* missense mutations that do not affect the receptor-clustering function of gephyrin, as reported for a single case harboring a point mutation affecting the E-domain (Reiss et al., 2011).

Interestingly, the correct mitochondrial maturation of SOX is dependent on Moco (Klein & Schwarz, 2012), while the mitochondrial amidoxime-reducing component mARC1 is targeted to the outer mitochondrial membrane, independent of Moco (Klein et al., 2012). Recently, two SOXD patients with impaired Moco binding have been reported (Bender et al., 2019; Kaczmarek et al., 2021), both of which exhibited an attenuated type of the disease, with milder symptoms. Biochemical characterization of those patients' SOX variants (G362S, R366H) revealed an impairment in Moco coordination within the active site of SOX, resulting in strongly decreased mitochondrial maturation. Following the culture of patient fibroblasts in the presence of molybdate (Bender et al., 2019) or MOCS1 transgene expression (Kaczmarek et al., 2022), significantly increased SOX activity has been observed, thus demonstrating that the increase in Moco availability partially rescues a defect in Moco-dependent SOX maturation. Therefore, the molecular–genetic investigation of SOXD patients may identify future molybdate-responsive patients, opening the path to personalized medicine.

2.4.4 Dietary Restriction

Until today, MoCD types B and C, as well as SOXD, are considered incurable diseases. In order to reduce the accumulation of toxic sulfite, dietary restriction of sulfur-containing amino acids was considered in the past for a number of patients (Abe et al., 2021; Boles et al., 1993; Touati et al., 2000). The best results were obtained in mild cases of SOXD and MoCD type A, with dietary restriction of protein intake leading to significantly decreased urinary SSC and thiosulfate levels; in some cases, patients showed improved development

without further signs of progressive neurodegeneration (Abe et al., 2021; Touati et al., 2000).

In a recent study by Abe et al. (2021), dietary restriction was used in a Japanese MoCD type A patient, as in Japan, cPMP treatment has not yet been officially approved or cPMP could not be obtained at the time of diagnosis. The patient carried a homozygous missense mutation at c.1510C > T (p.504R > W) in exon 10 of the *MOCS1* gene, which has not been reported before. It is located in the N-terminus of the catalytically essential MOCS1B domain, so it is expected to have a strong impact on the catalytic activity of MOCS1B protein. At the age of 16 months, dietary protein was restricted to 1.75 g/kg/day and further reduced in the following month to 1.4 g/kg/day. A further reduction to 1.25 g/kg/day was introduced until 42 months before the diet was finally continued with a protein content of 1.0 g/kg/day. After 4 months of dietary protein restriction, SSC values had decreased by about 50%, and urine sulfite tests became negative. Although the patient remained severely mentally defective, she developed without further regression and remained seizure-free (Abe et al., 2021; Touati et al., 2000).

Two patients with mild forms of SOXD were treated with dietary protein restriction combined with a particular decrease in sulfur-containing amino acids (Touati et al., 2000). The mutations carried by both patients were not mentioned, thus not allowing any speculations on residual SOX activity. The first patient was diagnosed with SOXD late, at the age of 22 months, and, afterwards, began to receive 1.2 g/kg/day supplemented with an amino acid mixture not containing methionine, cystine, and taurine. Methionine intake was limited to 180 mg/day. After seven months, additional taurine (50 mg/kg), magnesium sulfate, and betaine treatment was started, and, two months later, protein intake was increased to 1.3 g/kg/day with 250 mg/day methionine. In this patient, treatment with cysteamine was also tested with the aim of quenching the accumulating sulfite (see below). The treatment, however, did not result in any clinical improvement, so it was stopped after nine months. At the age of 4 years and 5 months, the child presented with age-appropriate development and no signs of severe neurodegeneration. The second patient was diagnosed with a mild form of SOXD at the age of 10 months. At the beginning of treatment, dietary protein intake was severely decreased to 4.0 g/day (approx. 0.5 mg/kg/day), supplemented with an amino acid mixture that was free of methionine, cystine, and taurine. After two weeks, protein intake was adjusted to 1.0 g/kg/day with 125 mg methionine, which was further raised to 200 mg with increasing body weight and supplemented with taurine later on as well. Treatment resulted in very low urinary SSC and thiosulfate levels, which stabilized after the first two months of treatment. Two years and four months after the

beginning of the therapy, the development of the child was progressing steadily, although the child remained timid and showed subnormal psychomotor skills.

The few cases reported above represent mild forms of SOXD and MoCD that benefited from dietary protein restriction. However, this therapeutic approach is not necessarily sufficient to rescue severe phenotypes of both diseases that present with a total loss of SOX activity. In contrast, a patient diagnosed with the classical, rapidly progressing onset of SOXD started a methionine- and cystine-free diet at the age of 12 days (Tan et al., 2005). Additionally, he was treated with thiamine due to an observed sulfite-dependent depletion/reduction of thiamine as well as with dextromethorphan (Tan et al., 2005), a pharmacological blocker of NMDA receptors (see below). However, the patient displayed progressive microcephaly and presented with severe developmental delay, with no significant improvement upon treatment. For another severe case of SOXD, a decline in irritation but no neurological improvement upon methionine and cystine restriction has been reported (H. J. Lee et al., 2002). These experiences suggest that dietary restriction of protein in general and sulfur-containing amino acids in particular may be an effective way of improving the phenotype of mild/attenuated cases of MoCD and SOXD but is not sufficient to prevent severe clinical courses. Moreover, the starting time of dietary restriction is crucial, as disease-related neurological damage is irreversible (Veldman et al., 2010).

2.4.5 Targeting NMDA Receptors

Infant death in MoCD and SOXD patients is usually the result of severe neurodegeneration. As mentioned above, a major contributor to this pathology is SSC, causing an overexcitation of NMDA receptors, a mechanism that was suggested following the first experiments in rats almost 50 years ago (Olney et al., 1975). In a recent study in 2017, SSC has been proven to be the main cause of neuronal cell death in in vitro experiments using primary cortical neurons (Kumar et al., 2017). The NMDA receptor antagonist MK801 was sufficient to rescue neurons from SSC-mediated cell death, strongly supporting the hypothesized mode of action of SSC.

In the same study, an MoCD-like phenotype was induced in adult wild-type mice by treatment with the molybdenum antagonist tungstate (Kumar et al., 2017). Following cellular uptake, tungstate is considered to be incorporated in the same way as molybdenum to molybdopterin, thereby rendering it inactive and causing a loss of function of all Mo-enzymes. Following tungstate treatment, 4-week-old mice displayed a median decrease in SOX activity of 90% and developed a MoCD-like phenotype within three weeks, including weight loss and decreased neuromotor skills, as quantified in the Rotarod performance test (Kumar et al., 2017)). Additionally, in contrast to *Mocs1*$^{-/-}$ (H. J. Lee et al., 2002)

or *Mocs2*$^{-/-}$ (Jakubiczka-Smorag et al., 2016) mice, these animals showed decreased cell density and, thus, signs of neuronal degeneration in the cerebral cortex and the CA1 region of the hippocampus, hence resembling the phenotype of human MoCD and SOXD patients. Body weight and neuromotor skills were successfully rescued by intraperitoneal injection with 5 mg/kg of the NMDA receptor antagonist memantine twice per week; this makes NMDA receptor blockers in general and memantine in particular promising candidates for future therapeutic attempts.

In humans, the approach of applying NMDA receptor antagonists has been studied only sporadically and, in most cases, in patients with severe disease progression. In a three-year-old boy with a mild form of MoCD and accompanying recurrent epilepsy, administration of the NMDA receptor antagonist dextromethorphan (12.5 mg/kg body weight) resulted in the disappearance of seizures, an improved EEG, and no major drug-related “side-effect” (Schuierer et al., 1995). In contrast, in one of the aforementioned dietary approaches, dextromethorphan was administered in combination with a methionine- and cystine-free diet, starting at the age of three weeks (Tan et al., 2005). The treatment, however, did not lead to a significant improvement of the patient’s health condition, which suggests that NMDA receptor blockage is again a convenient therapeutic approach in milder cases of MoCD and SOXD but is not sufficient to improve the phenotype in severely affected patients with manifested neurodegeneration.

2.4.6 Sulfite Scavenging

Given the largely overlapping pathophysiology in MoCD and SOXD, any therapeutic intervention that lowers the accumulation of toxic sulfite is considered to be beneficial for both disorders (Kohl et al., 2019). Therefore, chemical scavenging of excess sulfite to avoid its accumulation and the secondary formation of SSC with the accompanied depletion of cystine needs to be considered. Previous in vitro experiments revealed a 6-to-8-times faster reaction of sulfite with cystamine than with cystine (Jocelyn, 1987), thus proposing cystamine as a potent sulfite scavenger preventing the formation of SSC. Interestingly, cysteamine, the reduced form of amino-thiol, represents an established treatment for nephropathic cystinosis and is used in concentrations of 0.2–0.6 mmol/kg (Smolin et al., 1988). As, in vivo, an equilibrium between the reduced and the oxidized form of any thiol-containing small molecular establishes rapidly, cysteamine and cystamine are expected to have a similar therapeutic effect. However, in vivo, the reduced thiol can not only form disulfide cystamine but also a mixed disulfide with one molecule of cysteine. Thus, it leads to further cysteine depletion, and 50% of the sulfite-derived reaction product will be, again, SSC. Therefore, the oxidized amino-cystamine might be favored for the treatment of sulfite toxicity.

A single case of treatment with cysteamine in combination with dietary restriction (Touati et al., 2000) has been reported in the literature. The treatment had no effect on the patient's overall health condition and was, therefore, stopped after 9 months. However, neither the concentration and frequency of cysteamine treatment nor biomarkers for sulfite intoxication were reported. In addition, it remained unclear to what extent irreversible brain damage might have masked any biochemical improvement. Given the sparse clinical experience and the expected underlying biochemical principles, sulfite scavengers still hold great potential as a possible therapeutic approach to treat sulfite toxicity in MoCD and SOXD.

2.4.7 Ferroptosis Inhibition

Alteration in cysteine homeostasis in MoCD and SOXD hints at a novel form of regulated cell death - ferroptosis - that has been associated with reduced glutathione levels in mammals (Seiler et al., 2008; Yang et al., 2014). Ferroptosis is an iron-dependent form of non-apoptotic cell death that can be triggered by a depletion in cellular cysteine (Fujii et al., 2019). Cysteine is the rate-limiting component in the biogenesis of the antioxidant tripeptide glutathione as the other two required amino acids, glutamate and glycine, are found in significantly higher abundance within the cell (Reed et al., 2008). A reduction in cysteine levels, therefore, causes a decrease in the biogenesis of glutathione, which is an essential cosubstrate in the detoxification of lipid peroxides catalyzed by glutathione peroxidase 4 (GPX4) (Ursini et al., 1982). Reduced levels of glutathione hamper this detoxification process, ultimately leading to increased oxidative stress and cell death.

In 2012, cell death from a glutamate-induced blockade of system x_c^--mediated cystine import in organotypic rat brain slices was first identified as an iron-dependent form of non-apoptotic cell death, which was then termed ferroptosis (Dixon et al., 2012). Since then, ferroptosis has been proposed to play a decisive role in the courses of multiple neurodegenerative diseases, including Alzheimer's, Parkinson's, and Huntington's disease (Mahoney-Sanchez et al., 2021; Mi et al., 2019; Zhang et al., 2021). Cysteine enters the cell in its oxidized form, cystine, which is transported across the plasma membrane by the antiporter system x_c^- in exchange for intracellular glutamate. In MoCD and SOXD, as a consequence of strongly elevated SSC formation derived from the reaction of cystine with sulfite, cysteine levels are strongly decreased (Belaidi et al., 2012; Schwarz & Belaidi, 2013). In addition, due to its structural similarity to glutamate, an increase in extracellular SSC levels may inhibit the x_c^- antiporter, thus further reducing the import of cystine into the cell. So far, there are no data on the glutathione levels in MoCD or SOXD patients available, but previous in vitro studies have shown a rapid decrease in the levels of glutathione disulfide, followed by a slow decrease in glutathione levels in rat hepatocytes upon

treatment with high concentrations of sulfite (Niknahad & O'Brien, 2008). Moreover, glutamate excitotoxicity, which presents as mechanistically similar to SSC-induced toxicity, has also been shown to induce a significant decrease in intracellular glutathione levels in the brain (Pereira & Oliveira, 1997). Based on these findings, it may be hypothesized that ferroptosis contributes to the pathophysiology of MoCD and SOXD, in particular to the rapidly progressing cell death, thus rendering ferroptosis inhibitors a promising treatment strategy to be investigated in the future.

2.4.8 Is H_2S Involved in the Pathophysiology of MoCD?

A hallmark in the diagnosis of MoCD and SOXD is the accumulation and excretion of thiosulfate, a catabolic product of H_2S metabolism. There is only one other disorder known to result in massive thiosulfate accumulation, known as ethylmalonic encephalopathy. Mutations causing a defect in the enzyme ethylmalonic encephalopathy protein 1 (ETHE1), also known as persulfide dioxygenase, result in the accumulation of H_2S and the loss of clearance of small-molecule persulfides such as GSSH. As a consequence, TST-dependent oxidation of persulfides becomes the only path to catabolize H_2S-products, thus leading to elevated levels of thiosulfate. Therefore, thiosulfate accumulation in MoCD and SOXD hints at a re-routing of sulfur flux into the H_2S pathway, leading to increased H_2S turnover. To which extent thiosulfate accumulation will indicate the increased catabolism and/or increased biosynthesis of H_2S requires further investigation.

A hallmark of H_2S-based signaling is the formation of S-persulfidated species in small molecules (cystine-persulfide, glutathione-persulfide, etc.) as well as in protein cysteine side chains. Levels of protein S-persulfidation have been recently associated with cellular stress resistance and longevity in various model systems (Zivanovic et al., 2019). On the other hand, elevated H_2S leads to the inhibition of mitochondrial respiration by blocking cytochrome *c* oxidase (Nicholls & Kim, 1982; Viscomi et al., 2010). In addition, a recent study demonstrated that in H_2S-inhibited mitochondria, accumulating H_2S is further metabolized by SQR, leading to the 'reversal' of the citrate cycle, glutaminolysis, and lipogenesis (Carballal et al., 2021).

In aggregate, accumulating thiosulfate in MoCD and SOXD gives rise to the proposal that alterations in H_2S homeostasis may contribute to a larger extent to mitochondrial dysfunction than initially anticipated, and recent data support this notion (Grings et al., 2019, 2022), being in line with other data showing sulfite-dependent changes in mitochondrial morphology (Mellis, Roeper, et al., 2021).

A recent study in Moco-deficient *Caenorhabditis elegans* demonstrated that the lethal symptoms of MoCD in worms can be suppressed by two principles (Warnhoff & Ruvkun, 2019): (i) On one hand, the uptake of Moco by feeding worms with Moco containing *E. coli* or providing an in vitro source of protein-bound Moco (Warnhoff et al., 2021) was sufficient to protect the worms from sulfite toxicity. This finding suggests that not only cPMP but also Moco may be used to treat MoCD in the future. (ii) Second, a genetic suppressor screen identified CDO and CSE as potential targets for upstream inhibition to reduce cysteine catabolism and cysteine de novo synthesis, respectively. Again, those promising findings need to be verified in more disease-relevant preclinical models.

2.5 Future Perspectives

MoCD and SOXD have been known for nearly five decades, and major progress in understanding the biosynthesis of Moco, the function of individual gene products, and the contribution of Mo-enzymes to the disease pathology has been made. With the first therapy of MoCD type A being recently approved by the FDA, the number of treated patients will grow. Most important will be a timely diagnosis of patients to avoid irreversible brain damage due to sulfite intoxication. Methods such as newborn screening as well as targeted genetic testing will be instrumental in achieving this goal. Further understanding of the underlying disease mechanism, in particular, the role of H_2S, will not only improve therapeutic outcomes but it may also open Moco enzyme research to other fields and challenges in medicine. For example, the benefits of dietary restriction have been recently demonstrated to involve the metabolism of sulfur-containing amino acids. We have recently demonstrated that stress-induced acute kidney injury can be prevented by a reduction of methionine and cysteine in the diet (Koehler et al., 2022).

Therapies for MoCD type B, type C, and SOXD are still lacking; here, we have discussed biochemical principles that require experimental testing in preclinical models of the respective disorders. One additional treatment strategy holding great potential is gene therapy, which, in the past, has already been used for the successful treatment of metabolic disorders such as hemophilia B (Nathwani et al., 2011), lipoprotein lipase deficiency (Stroes et al., 2008), and metachromatic leukodystrophy (Biffi et al., 2013). The most promising and widely used approach involves the usage of virus-mediated gene additions. It aims to rescue the phenotype of genetic diseases by either introducing a novel gene that helps to fight the consequences of a disease or by restoring the function of a defective gene by inserting a healthy copy (McCain, 2005). As MoCD and SOXD are both single-gene disorders, they would be particularly suitable targets for this type of therapy.

2.6 References

Abe, Y., Aihara, Y., Endo, W., Hasegawa, H., Ichida, K., Uematsu, M., & Kure, S. (2021).The effect of dietary protein restriction in a case of molybdenum cofactor deficiency with MOCS1 mutation. *Molecular Genetics and Metabolism Reports*, *26*. https://doi.org/10.1016/J.YMGMR.2021.100716

Alkufri, F., Harrower, T., Rahman, Y., Hughes, E., Mundy, H., Knibb, J. A., Moriarty, J., Connor, S., & Samuel, M. (2013). Molybdenum cofactor deficiency presenting with a Parkinsonism-dystonia syndrome. *Movement Disorders*, *28*(3), 399–401. https://doi.org/10.1002/MDS.25276

Arican, P., Gencpinar, P., Kirbiyik, O., Bozkaya Yilmaz, S., Ersen, A., Oztekin, O., & Olgac Dundar, N. (2019). The Clinical and Molecular Characteristics of Molybdenum Cofactor Deficiency Due to MOCS2 Mutations. *Pediatric Neurology*, *99*, 55–59. https://doi.org/10.1016/j.pediatrneurol.2019.04.021

Arslanoglu, S., Yalaz, M., Gökşen, D., Çoker, M., Tütüncüoğlu, S., Aksu, M., Darcan, Ş., Kultursay, N., Çiriş, M., & Demirtaş, E. (2001). Molybdenum cofactor deficiency associated with Dandy-Walker complex. *Brain and Development*, *23*(8), 815–818. https://doi.org/10.1016/S0387-7604(01)00316-3

Bayram, E., Topcu, Y., Karakaya, P., Yis, U., Cakmakci, H., Ichida, K., & Kurul, S. H. (2013). Molybdenum cofactor deficiency: Review of 12 cases (MoCD and review). *European Journal of Paediatric Neurology*, *17*(1), 1–6. https://doi.org/10.1016/J.EJPN.2012.10.003

Belaidi, A. A., Arjune, S., Santamaria-Araujo, J. A., Sass, J. O., & Schwarz, G. (2012). Molybdenum cofactor deficiency: a new HPLC method for fast quantification of s-sulfocysteine in urine and serum. *JIMD Rep*, *5*, 35–43. https://doi.org/10.1007/8904_2011_89

Belaidi, A. A., & Schwarz, G. (2013). Metal insertion into the molybdenum cofactor: product-substrate channelling demonstrates the functional origin of domain fusion in gephyrin. *Biochemical Journal*, *450*, 149–157. https://doi.org/10.1042/Bj20121078

Bender, D., Kaczmarek, A. T., Santamaria-Araujo, J. A., Stueve, B., Waltz, S., Bartsch, D., Kurian, L., Cirak, S., & Schwarz, G. (2019). Impaired mitochondrial maturation of sulfite oxidase in a patient with severe sulfite oxidase deficiency. *Human Molecular Genetics*, *28*(17), 2885–2899. https://doi.org/10.1093/HMG/DDZ109

Biffi, A., Montini, E., Lorioli, L., Cesani, M., Fumagalli, F., Plati, T., Baldoli, C., Martino, S., Calabria, A., Canale, S., Benedicenti, F., Vallanti, G., Biasco, L., Leo, S., Kabbara, N., Zanetti, G., Rizzo, W. B., Mehta, N. A. L., Cicalese, M. P., … Naldini, L. (2013). Lentiviral hematopoietic stem cell gene therapy benefits metachromatic leukodystrophy. *Science (New York, N.Y.)*, *341*(6148). https://doi.org/10.1126/SCIENCE.1233158

Boles, R. G., Ment, L. R., Meyn, M. S., Horwich, A. L., Kratz, L. E., & Rinaldo, P. (1993). Short-term response to dietary therapy in molybdenum cofactor deficiency. *Annals of Neurology*, *34*(5), 742–744. https://doi.org/10.1002/ANA.410340520

Carballal, S., Vitvitsky, V., Kumar, R., Hanna, D. A., Libiad, M., Gupta, A., Jones, J. W., & Banerjee, R. (2021). Hydrogen sulfide stimulates lipid biogenesis from glutamine that is dependent on the mitochondrial NAD(P)H pool. *Journal of Biological Chemistry*, *297*(2). https://doi.org/10.1016/J.JBC.2021.100950

Claerhout, H., Witters, P., Régal, L., Jansen, K., Van Hoestenberghe, M. R., Breckpot, J., & Vermeersch, P. (2018). Isolated sulfite oxidase deficiency. *Journal of Inherited Metabolic Disease*, *41*(1), 101–108. https://doi.org/10.1007/S10545-017-0089-4

Clinch, K., Watt, D. K., Dixon, R. A., Baars, S. M., Gainsford, G. J., Tiwari, A., Schwarz, G., Saotome, Y., Storek, M., Belaidi, A. A., & Santamaria-Araujo, J. A. (2013). Synthesis of cyclic pyranopterin monophosphate, a biosynthetic intermediate in the molybdenum cofactor pathway. *Journal of Medicinal Chemistry*, *56*(4), 1730–1738. https://doi.org/10.1021/JM301855R

Dejanovic, B., Lal, D., Catarino, C. B., Arjune, S., Belaidi, A. A., Trucks, H., Vollmar, C., Surges, R., Kunz, W. S., Motameny, S., Altmüller, J., Köhler, A., Neubauer, B. A., EPICURE Consortium, Nürnberg, P., Noachtar, S., Schwarz, G., & Sander, T. (2014). Exonic microdeletions of the gephyrin gene impair GABAergic synaptic inhibition in patients with idiopathic generalized epilepsy. *Neurobiology of Disease*, *67*, 88–96. https://doi.org/10.1016/J.NBD.2014.02.001

Del Rizzo, M., Burlina, A. P., Sass, J. O., Beermann, F., Zanco, C., Cazzorla, C., Bordugo, A., Giordano, L., Manara, R., & Burlina, A. B. (2013). Metabolic stroke in a late-onset form of isolated sulfite oxidase deficiency. *Molecular Genetics and Metabolism*, *108*(4), 263–266. https://doi.org/10.1016/J.YMGME.2013.01.011

Dixon, S. J., Lemberg, K. M., Lamprecht, M. R., Skouta, R., Zaitsev, E. M., Gleason, C. E., Patel, D. N., Bauer, A. J., Cantley, A. M., Yang, W. S., Morrison 3rd, B., & Stockwell, B. R. (2012). Ferroptosis: an iron-dependent form of nonapoptotic cell death. *Cell*, *149*(5), 1060–1072. https://doi.org/10.1016/j.cell.2012.03.042

Dos Reis, R., Kornobis, E., Pereira, A., Tores, F., Carrasco, J., Gautier, C., Jahannault-Talignani, C., Nitschké, P., Muchardt, C., Schlosser, A., Maric, H. M., Ango, F., & Allemand, E. (2022). Complex regulation of Gephyrin splicing is a determinant of inhibitory postsynaptic diversity. *Nature Communications*, *13*(1). https://doi.org/10.1038/S41467-022-31264-W

Duran, M., Beemer, F. A., v. d. Heiden, C., Korteland, J., de Bree, P. K., Brink, M., Wadman, S. K., & Lombeck, I. (1978). Combined deficiency of xanthine oxidase and sulphite oxidase: A defect of molybdenum metabolism or transport? *Journal of Inherited Metabolic Disease*, *1*(4), 175–178. https://doi.org/10.1007/BF01805591

Edwards, M., Roeper, J., Allgood, C., Chin, R., Santamaria, J., Schwarz, G., & Whitehall, J. (2015). Investigation of molybdenum cofactor deficiency due to MOCS2 deficiency in a newborn baby. *Metabolic Encephalopathy Meta Gene*, *3*, 43–49. https://doi.org/10.1016/j.mgene.2014.12.003

Endres, W., Shin, Y. S., Günther, R., Ibel, H., Duran, M., & Wadman, S. K. (1988). Report on a new patient with combined deficiencies of sulphite oxidase and xanthine dehydrogenase due to molybdenum cofactor deficiency. *European Journal of Pediatrics*, *148*(3), 246–249. https://doi.org/10.1007/BF00441412

Eun, Y. K., Schrader, N., Smolinsky, B., Bedet, C., Vannier, C., Schwarz, G., & Schindelin, H. (2006). Deciphering the structural framework of glycine receptor anchoring by gephyrin. *EMBO Journal*, *25*(6), 1385–1395. https://doi.org/10.1038/SJ.EMBOJ.7601029

Farrell, S., Karp, J., Hager, R., Wang, Y., Adeniyi, O., Wang, J., Li, L., Ma, L., Peretz, J., Summan, M., Kong, N., White, M., Pacanowski, M., Price, D., Filie, J., Donohue, K., & Joffe, H. (2021). Regulatory news: Nulibry (fosdenopterin) approved to reduce the risk of mortality in patients with molybdenum cofactor deficiency type A: FDA approval summary. *Journal of Inherited Metabolic Disease*, *44*(5), 1085–1087. https://doi.org/10.1002/JIMD.12421

Feng, G., Tintrup, H., Kirsch, J., Nichol, M. C., Kuhse, J., Betz, H., & Sanes, J. R. (1998). Dual requirement for gephyrin in glycine receptor clustering and molybdoenzyme activity. *Science (New York, N.Y.)*, *282*(5392), 1321–1324. https://doi.org/10.1126/SCIENCE.282.5392.1321

Footitt, E. J., Heales, S. J., Mills, P. B., Allen, G. F. G., Oppenheim, M., & Clayton, P. T. (2011). Pyridoxal 5′-phosphate in cerebrospinal fluid; Factors affecting concentration. *Journal of Inherited Metabolic Disease*, *34*(2), 529–538. https://doi.org/10.1007/S10545-011-9279-7

Fritschy, J. M., Harvey, R. J., & Schwarz, G. (2008). Gephyrin: where do we stand, where do we go? *Trends in Neurosciences*, *31*(5), 257–264. https://doi.org/10.1016/j.tins.2008.02.006

Fujii, J., Homma, T., & Kobayashi, S. (2019). Ferroptosis caused by cysteine insufficiency and oxidative insult. *Free Radic Res*, 1–12. https://doi.org/10.1080/10715762.2019.1666983

Gray, T. A., & Nicholls, R. D. (2000). Diverse splicing mechanisms fuse the evolutionarily conserved bicistronic MOCS1A and MOCS1B open reading frames. *RNA*, *6*(7), 928–936. https://doi.org/10.1017/S1355838200000182

Grings, M., Seminotti, B., Karunanidhi, A., Ghaloul-Gonzalez, L., Mohsen, A. W., Wipf, P., Palmfeldt, J., Vockley, J., & Leipnitz, G. (2019). ETHE1 and MOCS1 deficiencies: Disruption of mitochondrial bioenergetics, dynamics, redox homeostasis and endoplasmic reticulum-mitochondria crosstalk in patient fibroblasts. *Scientific Reports 2019 9:1*, *9*(1), 1–13. https://doi.org/10.1038/s41598-019-49014-2

Grings, M., Wajner, M., & Leipnitz, G. (2022). Mitochondrial Dysfunction and Redox Homeostasis Impairment as Pathomechanisms of Brain Damage in Ethylmalonic Encephalopathy: Insights from Animal and Human Studies. *Cellular and Molecular Neurobiology*, *42*(3), 565–575. https://doi.org/10.1007/S10571-020-00976-2

Gross-Hardt, S., & Reiss, J. (2002). The bicistronic MOCS1 gene has alternative start codons on two mutually exclusive exons. *Molecular Genetics and Metabolism*, *76*(4), 340–343. https://doi.org/10.1016/S1096-7192(02)00100-2

Gutzke, G., Fischer, B., Mendel, R. R., & Schwarz, G. (2001). Thiocarboxylation of Molybdopterin Synthase Provides Evidence for the Mechanism of Dithiolene Formation in Metal-binding Pterins. *Journal of Biological Chemistry*, *276*(39), 36268–36274. https://doi.org/10.1074/JBC.M105321200

Hahnewald, R., Leimkühler, S., Vilaseca, A., Acquaviva-Bourdain, C., Lenz, U., & Reiss, J. (2006). A novel MOCS2 mutation reveals coordinated expression of the small and large subunit of molybdopterin synthase. *Molecular Genetics and Metabolism*, *89*(3), 210–213. https://doi.org/10.1016/J.YMGME.2006.04.008

Hänzelmann, P., Hernández, H. L., Menzel, C., García-Serres, R., Huynh, B. H., Johnson, M. K., Mendel, R. R., & Schindelin, H. (2004). Characterization of MOCS1A, an oxygen-sensitive iron-sulfur protein involved in human molybdenum cofactor biosynthesis. *Journal of Biological Chemistry*, *279*(33), 34721–34732. https://doi.org/10.1074/JBC.M313398200

Havemeyer, A., Bittner, F., Wollers, S., Mendel, R., Kunze, T., & Clement, B. (2006). Identification of the missing component in the mitochondrial benzamidoxime prodrug-converting system as a novel molybdenum enzyme. *Journal of Biological Chemistry*, *281*(46), 34796–34802. https://doi.org/10.1074/jbc.M607697200

Hover, B. M., Lilla, E. A., & Yokoyama, K. (2015). Mechanistic Investigation of cPMP Synthase in Molybdenum Cofactor Biosynthesis Using an Uncleavable Substrate Analogue. *Biochemistry*, *54*(49), 7229–7236. https://doi.org/10.1021/ACS.BIOCHEM.5B00857

Hover, B. M., Tonthat, N. K., Schumacher, M. A., & Yokoyama, K. (2015). Mechanism of pyranopterin ring formation in molybdenum cofactor biosynthesis. *Proceedings of the National Academy of Sciences of the United States of America*, *112*(20), 6347–6352. https://doi.org/10.1073/PNAS.1500697112

Huijmans, J. G. M., Schot, R., de Klerk, J. B. C., Williams, M., de Coo, R. F. M., Duran, M., Verheijen, F. W., van Slegtenhorst, M., & Mancini, G. M. S. (2017). Molybdenum cofactor deficiency: Identification of a patient with homozygote mutation in the MOCS3 gene. *American Journal of Medical Genetics, Part A*, *173*(6), 1601–1606. https://doi.org/10.1002/AJMG.A.38240

Jakubiczka-Smorag, J., Santamaria-Araujo, J. A., Metz, I., Kumar, A., Hakroush, S., Brueck, W., Schwarz, G., Burfeind, P., Reiss, J., & Smorag, L. (2016). Mouse model for molybdenum cofactor deficiency type B recapitulates the phenotype observed in molybdenum cofactor deficient patients. *Human Genetics*, *135*(7), 813–826. https://doi.org/10.1007/S00439-016-1676-4

Jezela-Stanek, A., Blaz, W., Gora, A., Bochenska, M., Kusmierska, K., & Sykut-Cegielska, J. (2020). Proteins structure models in the evaluation of novel variant (C.472_477del) in the MOSC2 gene. *Diagnostics*, *10*(10). https://doi.org/10.3390/DIAGNOSTICS10100821

Jocelyn, P. C. (1987). Chemical reduction of disulfides. *Methods Enzymol*, *143*, 246–256. https://doi.org/10.1016/0076-6879(87)43048-6

Johnson, J. L., Coyne, K. E., Rajagopalan, K. V, Van Hove, J. L. K., Mackay, M., Pitt, J., & Boneh, A. (2001). Molybdopterin Synthase Mutations in a Mild Case of Molybdenum Cofactor Defciency. *American Journal of Medical Genetics*, *104*, 169–173. https://doi.org/10.1002/ajmg.1603

Johnson, J. L., Hainline, B. E., Rajagopalan, K. V., & Arison, B. H. (1984). The pterin component of the molybdenum factor. Structural characterization of two fluorescent derivatives. *Journal of Biological Chemistry*, *259*(9), 5414–5422. https://doi.org/10.1016/S0021-9258(18)91027-6

Kaczmarek, A. T., Bahlmann, N., Thaqi, B., May, P., & Schwarz, G. (2021). Machine learning-based identification and characterization of 15 novel pathogenic SUOX missense mutations. *Molecular Genetics and Metabolism*, *134*(1–2), 188–194. https://doi.org/10.1016/J.YMGME.2021.07.011

Kaczmarek, A. T., Bender, D., Gehling, T., Kohl, J. B., Daimagüler, H. S., Santamaria-Araujo, J. A., Liebau, M. C., Koy, A., Cirak, S., & Schwarz, G. (2022). A defect in molybdenum cofactor binding causes an attenuated form of sulfite oxidase deficiency. *Journal of Inherited Metabolic Disease*, *45*(2), 169–182. https://doi.org/10.1002/JIMD.12454

Kikuchi, K., Hamano, S. I., Mochizuki, H., Ichida, K., & Ida, H. (2012). Molybdenum Cofactor Deficiency Mimics Cerebral Palsy: Differentiating Factors for Diagnosis. *Pediatric Neurology*, *47*(2), 147–149. https://doi.org/10.1016/J.PEDIATRNEUROL.2012.04.013

Kingsmore, S. F., Ramchandar, N., James, K., Niemi, A. K., Feigenbaum, A., Ding, Y., Benson, W., Hobbs, C., Nahas, S., Chowdhury, S., & Dimmock, D. (2020). Mortality in a neonate with molybdenum cofactor deficiency illustrates the need for a comprehensive

rapid precision medicine system. *Cold Spring Harbor Molecular Case Studies*, *6*(1). https://doi.org/10.1101/MCS.A004705

Klein, J. M., Busch, J. D., Pottings, C., Baker, M. J., Langers, T., & Schwarz, G. (2012). The mitochondrial amidoxime-reducing component (mARC1) is a novel signal-anchored protein of the outer mitochondrial membrane. *Journal of Biological Chemistry*, *287*(51), 42795–42803. https://doi.org/10.1074/JBC.M112.419424

Klein, J. M., & Schwarz, G. (2012). Cofactor-dependent maturation of mammalian sulfite oxidase links two mitochondrial import pathways. *Journal of Cell Science*, *125*(20), 4876–4855. https://doi.org/10.1242/JCS.110114

Koehler, F. C., Fu, C.-Y., Späth, M. R., Hoyer-Allo, K. J. R., Bohl, K., Göbel, H., Lackmann, J.-W., Grundmann, F., Osterholt, T., Gloistein, C., Steiner, J. D., Antebi, A., Benzing, T., Schermer, B., Schwarz, G., Burst, V., & Müller, R.-U. (2022). A systematic analysis of diet-induced nephroprotection reveals overlapping changes in cysteine catabolism. *Translational Research : The Journal of Laboratory and Clinical Medicine*, *244*, 32–46. https://doi.org/10.1016/J.TRSL.2022.02.003

Kohl, J. B., Mellis, A. T., & Schwarz, G. (2019). Homeostatic impact of sulfite and hydrogen sulfide on cysteine catabolism. *British Journal of Pharmacology*, *176*(4), 554–570. https://doi.org/10.1111/BPH.14464

Kumar, A., Dejanovic, B., Hetsch, F., Semtner, M., Fusca, D., Arjune, S., Santamaria-Araujo, J. A., Winkelmann, A., Ayton, S., Bush, A. I., Kloppenburg, P., Meier, J. C., Schwarz, G., & Belaidi, A. A. (2017). S-sulfocysteine/NMDA receptor-dependent signaling underlies neurodegeneration in molybdenum cofactor deficiency. *J Clin Invest*, *127*(12), 4365–4378. https://doi.org/10.1172/JCI89885

Kuper, J., Llamas, A., Hecht, H. J., Mendel, R. R., & Schwarz, G. (2004). Structure of the molybdopterin-bound Cnx1G domain links molybdenum and copper metabolism. *Nature*, *430*(7001), 803–806. https://doi.org/10.1038/NATURE02681

Landgraf, B. J., McCarthy, E. L., & Booker, S. J. (2016). Radical S-Adenosylmethionine Enzymes in Human Health and Disease. *Annual Review of Biochemistry*, *85*, 485–514. https://doi.org/10.1146/ANNUREV-BIOCHEM-060713-035504

Lee, E. J., Dandamudi, R., Granadillo, J. L., Grange, D. K., & Kakajiwala, A. (2021). Rare cause of xanthinuria: a pediatric case of molybdenum cofactor deficiency B. *CEN Case Reports*, *10*(3), 378–382. https://doi.org/10.1007/S13730-021-00572-3

Lee, H. J., Adham, I. M., Schwarz, G., Kneussel, M., Sass, J. O., Engel, W., & Reiss, J. (2002). Molybdenum cofactor-deficient mice resemble the phenotype of human patients. *Human Molecular Genetics*, *11*(26), 3309–3317. https://doi.org/10.1093/HMG/11.26.3309

Leimkühler, S., Charcosset, M., Latour, P., Dorche, C., Kleppe, S., Scaglia, F., Szymczak, I., Schupp, P., Hahnewald, R., & Reiss, J. (2005). Ten novel mutations in the molybdenum cofactor genes MOCS1 and MOCS2 and in vitro characterization of a MOCS 2 mutation that abolishes the binding ability of molybdopterin synthase. *Human Genetics*, *117*(6), 565–570. https://doi.org/10.1007/S00439-005-1341-9

Leimkühler, S., Freuer, A., Araujo, J. A. S., Rajagopalan, K. V., & Mendel, R. R. (2003). Mechanistic studies of human molybdopterin synthase reaction and characterization of mutants identified in group B patients of molybdenum cofactor deficiency. *Journal of Biological Chemistry*, *278*(28), 26127–26134. https://doi.org/10.1074/JBC.M303092200

Liao, C., Poulter, J. A., Mao, X., Wang, H., Tian, Q., Cao, Y., Shu, L., Chen, Y., Peng, Y., Wang, Y., & Chen, Y. (2021). Case Report: Compound Heterozygous Variants in MOCS3 Identified in a Chinese Infant With Molybdenum Cofactor Deficiency. *Frontiers in Genetics | Www.Frontiersin.Org*, *1*, 651878. https://doi.org/10.3389/fgene.2021.651878

Lionel, A. C., Vaags, A. K., Sato, D., Gazzellone, M. J., Mitchell, E. B., Chen, H. Y., Costain, G., Walker, S., Egger, G., Thiruvahindrapuram, B., Merico, D., Prasad, A., Anagnostou, E., Fombonne, E., Zwaigenbaum, L., Roberts, W., Szatmari, P., Fernandez, B. A., Georgieva, L., … Scherer, S. W. (2013). Rare exonic deletions implicate the synaptic organizer gephyrin (GPHN) in risk for autism, schizophrenia and seizures. *Human Molecular Genetics*, *22*(10), 2055–2066. https://doi.org/10.1093/HMG/DDT056

Llamas, A., Otte, T., Multhaup, G., Mendel, R. R., & Schwarz, G. (2006). The mechanism of nucleotide-assisted molybdenum insertion into molybdopterin - A novel route toward metal cofactor assembly. *Journal of Biological Chemistry*, *281*(27), 18343–18350. https://doi.org/10.1074/jbc.M601415200

Macaya, A., Brunso, L., Fernández-Castillo, N., Arranz, J. A., Ginjaar, H. B., Cuenca-León, E., Corominas, R., Roig, M., & Cormand, B. (2005). Molybdenum cofactor deficiency presenting as neonatal hyperekplexia: A clinical, biochemical and genetic study. *Neuropediatrics*, *36*(6), 389–394. https://doi.org/10.1055/S-2005-872877

MacHa, A., Liebsch, F., Fricke, S., Hetsch, F., Neuser, F., Johannes, L., Kress, V., Djemie, T., Santamaria-Araujo, J. A., Vilain, C., Aeby, A., Van Bogaert, P., Dejanovic, B., Weckhuysen, S., Meier, J. C., & Schwarz, G. (2022). Biallelic gephyrin variants lead to impaired GABAergic inhibition in a patient with developmental and epileptic encephalopathy. *Human Molecular Genetics*, *31*(6), 901–913. https://doi.org/10.1093/HMG/DDAB298

Mahoney-Sanchez, L., Bouchaoui, H., Ayton, S., Devos, D., Duce, J. A., & Devedjian, J. C. (2021). Ferroptosis and its potential role in the physiopathology of Parkinson's Disease. *Prog Neurobiol*, *196*, 101890. https://doi.org/10.1016/j.pneurobio.2020.101890

Matthies, A., Rajagopalan, K. V., Mendel, R. R., & Leimkühler, S. (2004). Evidence for the physiological role of a rhodanese-like protein for the biosynthesis of the molybdenum cofactor in humans. *Proceedings of the National Academy of Sciences of the United States of America*, *101*(16), 5946–5951. https://doi.org/10.1073/PNAS.0308191101

Mayr, S. J., Mendel, R. R., & Schwarz, G. (2021). Molybdenum cofactor biology, evolution and deficiency. *Biochimica et Biophysica Acta - Molecular Cell Research*, *1868*(1). https://doi.org/10.1016/J.BBAMCR.2020.118883

Mayr, S. J., Röper, J., & Schwarz, G. (2020). Alternative splicing of the bicistronic gene molybdenum cofactor synthesis 1 (MOCS1) uncovers a novel mitochondrial protein maturation mechanism. *Journal of Biological Chemistry*, *295*(10), 3029–3039. https://doi.org/10.1074/JBC.RA119.010720

Mayr, S. J., Sass, J. O., Vry, J., Kirschner, J., Mader, I., Hövener, J. B., Reiss, J., Santamaria-Araujo, J. A., Schwarz, G., & Grünert, S. C. (2018). A mild case of molybdenum cofactor deficiency defines an alternative route of MOCS1 protein maturation. *Journal of Inherited Metabolic Disease*, *41*(2), 187–196. https://doi.org/10.1007/S10545-018-0138-7

McCain, J. (2005). The Future of Gene Therapy. *Biotechnology Healthcare*, *2*(3), 52. /pmc/articles/PMC3564347/

Mechler, K., Mountford, W. K., Hoffmann, G. F., & Ries, M. (2015). Ultra-orphan diseases: A quantitative analysis of the natural history of molybdenum cofactor deficiency. *Genetics in Medicine*, *17*(12), 965–970. https://doi.org/10.1038/GIM.2015.12

Megahed, H., Nicouleau, M., Barcia, G., Medina-Cano, D., Siquier-Pernet, K., Bole-Feysot, C., Parisot, M., Masson, C., Nitschké, P., Rio, M., Bahi-Buisson, N., Desguerre, I., Munnich, A., Boddaert, N., Colleaux, L., & Cantagrel, V. (2016). Utility of whole exome sequencing for the early diagnosis of pediatric-onset cerebellar atrophy associated with developmental delay in an inbred population. *Orphanet Journal of Rare Diseases*, *11*(1). https://doi.org/10.1186/S13023-016-0436-9

Mellis, A. T., Misko, A. L., Arjune, S., Liang, Y., Erdélyi, K., Ditrói, T., Kaczmarek, A. T., Nagy, P., & Schwarz, G. (2021). The role of glutamate oxaloacetate transaminases in sulfite biosynthesis and H2S metabolism. *Redox Biology*, *38*. https://doi.org/10.1016/J.REDOX.2020.101800

Mellis, A. T., Roeper, J., Misko, A. L., Kohl, J., & Schwarz, G. (2021). Sulfite Alters the Mitochondrial Network in Molybdenum Cofactor Deficiency. *Frontiers in Genetics*, *11*(January), 1–10. https://doi.org/10.3389/fgene.2020.594828

Misko, A., Mahtani, K., Abbott, J., Schwarz, G., & Atwal, P. (2021). Molybdenum Cofactor Deficiency. *GeneReviews*®. https://pubmed.ncbi.nlm.nih.gov/34870926/

Mi, Y., Gao, X., Xu, H., Cui, Y., Zhang, Y., & Gou, X. (2019). The Emerging Roles of Ferroptosis in Huntington's Disease. *Neuromolecular Med*, *21*(2), 110–119. https://doi.org/10.1007/s12017-018-8518-6

Morikawa, T., Yasuno, R., & Wada, H. (2001). Do mammalian cells synthesize lipoic acid? Identification of a mouse cDNA encoding a lipoic acid synthase located in mitochondria. *FEBS Letters*, *498*(1), 16–21. https://doi.org/10.1016/S0014-5793(01)02469-3

Nagappa, M., Bindu, P. S., Taly, A. B., Sinha, S., & Bharath, R. D. (2015). Child Neurology: Molybdenum cofactor deficiency. *Neurology*, *85*(23), e175–e178. https://doi.org/10.1212/WNL.0000000000002194

Nathwani, A. C., Rosales, C., McIntosh, J., Rastegarlari, G., Nathwani, D., Raj, D., Nawathe, S., Waddington, S. N., Bronson, R., Jackson, S., Donahue, R. E., High, K. A., Mingozzi, F., Ng, C. Y. C., Zhou, J., Spence, Y., McCarville, M. B., Valentine, M., Allay, J., … Davidoff, A. M. (2011). Long-term safety and efficacy following systemic administration of a self-complementary AAV vector encoding human FIX pseudotyped with serotype 5 and 8 capsid proteins. *Molecular Therapy : The Journal of the American Society of Gene Therapy*, *19*(5), 876–885. https://doi.org/10.1038/MT.2010.274

Nicholls, P., & Kim, J. K. (1982). Sulphide as an inhibitor and electron donor for the cytochrome c oxidase system. *Canadian Journal of Biochemistry*, *60*(6), 613–623. https://doi.org/10.1139/O82-076/ASSET/IMAGES/BCB82-076C4.GIF

Nichols, J., & Rajagopalan, K. V. (2002). Escherichia coli MoeA and MogA: Function in metal incorporation step of molybdenum cofactor biosynthesis. *Journal of Biological Chemistry*, *277*(28), 24995–25000. https://doi.org/10.1074/JBC.M203238200

Niknahad, H., & O'Brien, P. J. (2008). Mechanism of sulfite cytotoxicity in isolated rat hepatocytes. *Chem Biol Interact*, *174*(3), 147–154. https://doi.org/10.1016/j.cbi.2008.05.032

Ohara-Imaizumi, M., Yoshida, M., Aoyagi, K., Saito, T., Okamura, T., Takenaka, H., Akimoto, Y., Nakamichi, Y., Takanashi-Yanobu, R., Nishiwaki, C., Kawakami, H., Kato, N.,

Hisanaga, S. I., Kakei, M., & Nagamatsu, S. (2010). Deletion of CDKAL1 affects mitochondrial ATP generation and first-phase insulin exocytosis. *PLoS ONE*, *5*(12). https://doi.org/10.1371/JOURNAL.PONE.0015553

Olney, J. W., Misra, C. H., & Gubareff, T. De. (1975). Cysteine-S-sulfate: brain damaging metabolite in sulfite oxidase deficiency. *Journal of Neuropathology and Experimental Neurology*, *34*(2), 167–177. https://doi.org/10.1097/00005072-197503000-00005

Pang, H., Lilla, E. A., Zhang, P., Zhang, D., Shields, T. P., Scott, L. G., Yang, W., & Yokoyama, K. (2020). Mechanism of Rate Acceleration of Radical C-C Bond Formation Reaction by a Radical SAM GTP 3′,8-Cyclase. *Journal of the American Chemical Society*, *142*(20), 9314–9326. https://doi.org/10.1021/JACS.0C01200

Pang, H., & Yokoyama, K. (2018). Lessons From the Studies of a C–C Bond Forming Radical SAM Enzyme in Molybdenum Cofactor Biosynthesis. *Methods in Enzymology*, *606*, 485–522. https://doi.org/10.1016/BS.MIE.2018.04.014

Pereira, C. M., & Oliveira, C. R. (1997). Glutamate toxicity on a PC12 cell line involves glutathione (GSH) depletion and oxidative stress. *Free Radic Biol Med*, *23*(4), 637–647. https://doi.org/10.1016/s0891-5849(97)00020-8

Per, H., Gümüş, H., Ichida, K., Çağlayan, O., & Kumandaş, S. (2007). Molybdenum cofactor deficiency: Clinical features in a Turkish patient. *Brain and Development*, *29*(6), 365–368. https://doi.org/10.1016/J.BRAINDEV.2006.10.007

Prior, P., Schmitt, B., Grenningloh, G., Pribilla, I., Multhaup, G., Beyreuther, K., Maulet, Y., Werner, P., Langosch, D., Kirsch, J., & Betz, H. (1992). Primary structure and alternative splice variants of gephyrin, a putative glycine receptor-tubulin linker protein. *Neuron*, *8*(6), 1161–1170. https://doi.org/10.1016/0896-6273(92)90136-2

Pristup, J., Schaeffeler, E., Arjune, S., Hofmann, U., Angel Santamaria-Araujo, J., Leuthold, P., Friedrich, N., Nauck, M., Mayr, S., Haag, M., Muerdter, T., Marner, F. J., Relling, M. V., Evans, W. E., Schwarz, G., & Schwab, M. (2022). Molybdenum Cofactor Catabolism Unravels the Physiological Role of the Drug Metabolizing Enzyme Thiopurine S-Methyltransferase. *Clinical Pharmacology and Therapeutics*, *112*(4). https://doi.org/10.1002/CPT.2637

Reed, M. C., Thomas, R. L., Pavisic, J., James, S. J., Ulrich, C. M., & Nijhout, H. F. (2008). A mathematical model of glutathione metabolism. *Theoretical Biology and Medical Modelling*, *5*(1), 1–16. https://doi.org/10.1186/1742-4682-5-8/TABLES/6

Rees, M. I., Harvey, K., Ward, H., White, J. H., Evans, L., Duguid, I. C., Hsu, C. C. H., Coleman, S. L., Miller, J., Baer, K., Waldvogel, H. J., Gibbon, F., Smart, T. G., Owen, M. J., Harvey, R. J., & Snell, R. G. (2003). Isoform Heterogeneity of the Human Gephyrin Gene (GPHN), Binding Domains to the Glycine Receptor, and Mutation Analysis in Hyperekplexia. *Journal of Biological Chemistry*, *278*(27), 24688–24696. https://doi.org/10.1074/JBC.M301070200

Reiss, J., Christensen, E., Kurlemann, G., Zabot, M. T., & Dorche, C. (1998). Genomic structure and mutational spectrum of the bicistronic MOCS1 gene defective in molybdenum cofactor deficiency type A. *Human Genetics*, *103*(6), 639–644. https://doi.org/10.1007/S004390050884

Reiss, J., Cohen, N., Dorche, C., Mandel, H., Mendel, R. R., Stallmeyer, B., Zabot, M. T., & Dierks, T. (1998). Mutations in a polycistronic nuclear gene associated with molybdenum cofactor deficiency. *Nature Genetics*, *20*(1), 51–53. https://doi.org/10.1038/1706

Reiss, J., Dorche, C., Stallmeyer, B., Mendel, R. R., Cohen, N., & Zabot, M. T. (1999). Human molydopterin synthase gene: Genomic structure and mutations in molybdenum cofactor deficiency type B. *American Journal of Human Genetics*, *64*(3), 706–711. https://doi.org/10.1086/302296

Reiss, J., Gross-Hardt, S., Christensen, E., Schmidt, P., Mendel, R. R., & Schwarz, G. (2001). A mutation in the gene for the neurotransmitter receptor-clustering protein gephyrin causes a novel form of molybdenum cofactor deficiency. *American Journal of Human Genetics*, *68*(1), 208–213. https://doi.org/10.1086/316941

Reiss, J., & Hahnewald, R. (2011). Molybdenum cofactor deficiency: Mutations in GPHN, MOCS1, and MOCS2. *Human Mutation*, *32*(1), 10–18. https://doi.org/10.1002/HUMU.21390

Reiss, J., & Johnson, J. L. (2003). Mutations in the molybdenum cofactor biosynthetic genes MOCS1, MOCS2, and GEPH. *Human Mutation*, *21*(6), 569–576. https://doi.org/10.1002/HUMU.10223

Reiss, J., Lenz, U., Aquaviva-Bourdain, C., Joriot-Chekaf, S., Mention-Mulliez, K., & Holder-Espinasse, M. (2011). A GPHN point mutation leading to molybdenum cofactor deficiency. *Clinical Genetics*, *80*(6), 598–599. https://doi.org/10.1111/J.1399-0004.2011.01709.X

Reiter, V., Matschkal, D. M. S., Wagner, M., Globisch, D., Kneuttinger, A. C., Müller, M., & Carell, T. (2012). The CDK5 repressor CDK5RAP1 is a methylthiotransferase acting on nuclear and mitochondrial RNA. *Nucleic Acids Research*, *40*(13), 6235–6240. https://doi.org/10.1093/NAR/GKS240

Rudolph, M. J., Wuebbens, M. M., Turque, O., Rajagopalan, K. V., & Schindelin, H. (2003). Structural studies of molybdopterin synthase provide insights into its catalytic mechanism. *Journal of Biological Chemistry*, *278*(16), 14514–14522. https://doi.org/10.1074/JBC.M300449200

Sander, B., Tria, G., Shkumatov, A. V., Kim, E. Y., Grossmann, J. G., Tessmer, I., Svergun, D. I., & Schindelin, H. (2013). Structural characterization of gephyrin by AFM and SAXS reveals a mixture of compact and extended states. *Acta Crystallographica Section D: Biological Crystallography*, *69*(10), 2050–2060. https://doi.org/10.1107/S0907444913018714

Santamaria-Araujo, J. A., Fischer, B., Otte, T., Nimtz, M., Mendel, R. R., Wray, V., & Schwarz, G. (2004). The Tetrahydropyranopterin Structure of the Sulfur-free and Metal-free Molybdenum Cofactor Precursor. *Journal of Biological Chemistry*, *279*(16), 15994–15999. https://doi.org/10.1074/JBC.M311815200

Scelsa, B., Gasperini, S., Righini, A., Iascone, M., Brazzoduro, V. G., & Veggiotti, P. (2019). Mild phenotype in Molybdenum cofactor deficiency: A new patient and review of the literature. *Molecular Genetics and Genomic Medicine*, *7*(6). https://doi.org/10.1002/MGG3.657

Schuierer, G., Kurlemann, G., Bick, U., & Stephani, U. (1995). Molybdenum-cofactor deficiency: CT and MR findings. *Neuropediatrics*, *26*(1), 51–54. https://doi.org/10.1055/s-2007-979720

Schwahn, B. (2021). Fosdenopterin: a First-in-class Synthetic Cyclic Pyranopterin Monophosphate for the Treatment of Molybdenum Cofactor Deficiency Type A. *Neurology*, *17*(2), 85. https://doi.org/10.17925/USN.2021.17.2.85

Schwahn, B. C., Van Spronsen, F. J., Belaidi, A. A., Bowhay, S., Christodoulou, J., Derks, T. G., Hennermann, J. B., Jameson, E., König, K., McGregor, T. L., Font-Montgomery, E., Santamaria-Araujo, J. A., Santra, S., Vaidya, M., Vierzig, A., Wassmer, E., Weis, I., Wong, F. Y., Veldman, A., & Schwarz, G. (2015). Efficacy and safety of cyclic pyranopterin monophosphate substitution in severe molybdenum cofactor deficiency type A: A prospective cohort study. *The Lancet*, *386*(10007), 1955–1963. https://doi.org/10.1016/S0140-6736(15)00124-5

Schwarz, G. (2016). Molybdenum cofactor and human disease. *Curr Opin Chem Biol*, *31*, 179–187. https://doi.org/10.1016/j.cbpa.2016.03.016

Schwarz, G., & Belaidi, A. A. (2013). Molybdenum in human health and disease. *Met Ions Life Sci*, *13*, 415–450. https://doi.org/10.1007/978-94-007-7500-8_13

Schwarz, G., Mendel, R. R., & Ribbe, M. W. (2009). Molybdenum cofactors, enzymes and pathways. *Nature 2009 460:7257*, *460*(7257), 839–847. https://doi.org/10.1038/nature08302

Schwarz, G., Santamaria-Araujo, J. A., Wolf, S., Lee, H. J., Adham, I. M., Gröne, H. J., Schwegler, H., Sass, J. O., Otte, T., Hänzelmann, P., Mendel, R. R., Engel, W., & Reiss, J. (2004). Rescue of lethal molybdenum cofactor deficiency by a biosynthetic precursor from Escherichia coli. *Human Molecular Genetics*, *13*(12), 1249–1255. https://doi.org/10.1093/HMG/DDH136

Schwarz, G., Schrader, N., Mendel, R. R., Hecht, H. J., & Schindelin, H. (2001). Crystal structures of human gephyrin and plant Cnx1 G domains: Comparative analysis and functional implications. *Journal of Molecular Biology*, *312*(2), 405–418. https://doi.org/10.1006/JMBI.2001.4952

Seiler, A., Schneider, M., Förster, H., Roth, S., Wirth, E. K., Culmsee, C., Plesnila, N., Kremmer, E., Rådmark, O., Wurst, W., Bornkamm, G. W., Schweizer, U., & Conrad, M. (2008). Glutathione peroxidase 4 senses and translates oxidative stress into 12/15-lipoxygenase dependent- and AIF-mediated cell death. *Cell Metabolism*, *8*(3), 237–248. https://doi.org/10.1016/J.CMET.2008.07.005

Smolin, L. A., Clark, K. F., Thoene, J. G., Gahl, W. A., & Schneider, J. A. (1988). A comparison of the effectiveness of cysteamine and phosphocysteamine in elevating plasma cysteamine concentration and decreasing leukocyte free cystine in nephropathic cystinosis. *Pediatr Res*, *23*(6), 616–620. https://doi.org/10.1203/00006450-198806000-00018

Spiegel, R., Schwahn, B. C., Squires, L., & Confer, N. (2022). Molybdenum cofactor deficiency: A natural history. *Journal of Inherited Metabolic Disease*, *45*(3), 456–469. https://doi.org/10.1002/JIMD.12488

Stallmeyer, B., Drugeon, G., Reiss, J., Haenni, A. L., & Mendel, R. R. (1999). Human molybdopterin synthase gene: Identification of a bicistronic transcript with overlapping reading frames. *American Journal of Human Genetics*, *64*(3), 698–705. https://doi.org/10.1086/302295

Stallmeyer, B., Schwarz, G., Schulze, J., Nerlich, A., Reiss, J., Kirsch, J., & Mendel, R. R. (1999). The neurotransmitter receptor-anchoring protein gephyrin reconstitutes molybdenum cofactor biosynthesis in bacteria, plants, and mammalian cells. *Proceedings of the National Academy of Sciences of the United States of America*, *96*(4), 1333–1338. https://doi.org/10.1073/PNAS.96.4.1333

Stroes, E. S., Nierman, M. C., Meulenberg, J. J., Franssen, R., Twisk, J., Henny, C. P., Maas, M. M., Zwinderman, A. H., Ross, C., Aronica, E., High, K. A., Levi, M. M., Hayden,

M. R., Kastelein, J. J., & Kuivenhoven, J. A. (2008). Intramuscular administration of AAV1-lipoprotein lipase S447X lowers triglycerides in lipoprotein lipase-deficient patients. *Arteriosclerosis, Thrombosis, and Vascular Biology*, *28*(12), 2303–2304. https://doi.org/10.1161/ATVBAHA.108.175620

Tan, W. H., Eichler, F. S., Hoda, S., Lee, M. S., Baris, H., Hanley, C. A., Grant, P. E., Krishnamoorthy, K. S., & Shih, V. E. (2005). Isolated sulfite oxidase deficiency: A case report with a novel mutation and review of the literature. *Pediatrics*, *116*(3), 757–766. https://doi.org/10.1542/PEDS.2004-1897

Tian, X. J., Li, X., Fang, F., Liu, Z. M., Wu, W. J., Liu, K., & Sun, S. Z. (2021). [Molybdenum cofactor deficiency type B manifested as Leigh-like syndrome: a case report and literature review]. *Zhonghua Er Ke Za Zhi = Chinese Journal of Pediatrics*, *59*(2), 119–124. https://doi.org/10.3760/CMA.J.CN112140-20200911-00866

Touati, G., Rusthoven, E., Depondt, E., Dorche, C., Duran, M., Heron, B., Rabier, D., Russo, M., & Saudubray, J. M. (2000). Dietary therapy in two patients with a mild form of sulphite oxidase deficiency. Evidence for clinical and biological improvement. *Journal of Inherited Metabolic Disease*, *23*(1), 45–53. https://doi.org/10.1023/A:1005646813492

Ursini, F., Maiorino, M., Valente, M., Ferri, L., & Gregolin, C. (1982). Purification from pig liver of a protein which protects liposomes and biomembranes from peroxidative degradation and exhibits glutathione peroxidase activity on phosphatidylcholine hydroperoxides. *Biochimica et Biophysica Acta (BBA) - Lipids and Lipid Metabolism*, *710*(2), 197–211. https://doi.org/10.1016/0005-2760(82)90150-3

Veldman, A., Santamaria-Araujo, J. A., Sollazzo, S., Pitt, J., Gianello, R., Yaplito-Lee, J., Wong, F., Ramsden, C. A., Reiss, J., Cook, I., Fairweather, J., & Schwarz, G. (2010). Successful treatment of molybdenum cofactor deficiency type a with cPMP. *Pediatrics*, *125*(5). https://doi.org/10.1542/PEDS.2009-2192

Vijayakumar, K., Gunny, R., Grunewald, S., Carr, L., Chong, K. W., Devile, C., Robinson, R., McSweeney, N., & Prabhakar, P. (2011). Clinical neuroimaging features and outcome in molybdenum cofactor deficiency. *Pediatric Neurology*, *45*(4), 246–252. https://doi.org/10.1016/J.PEDIATRNEUROL.2011.06.006

Viscomi, C., Burlina, A. B., Dweikat, I., Savoiardo, M., Lamperti, C., Hildebrandt, T., Tiranti, V., & Zeviani, M. (2010). Combined treatment with oral metronidazole and N-acetylcysteine is effective in ethylmalonic encephalopathy. *Nature Medicine*, *16*(8), 869–871. https://doi.org/10.1038/NM.2188

Walsby, C. J., Hong, W., Broderick, W. E., Cheek, J., Ortillo, D., Broderick, J. B., & Hoffman, B. M. (2002). Electron-nuclear double resonance spectroscopic evidence that S-adenosylmethionine binds in contact with the catalytically active [4Fe-4S]+ cluster of pyruvate formate-lyase activating enzyme. *Journal of the American Chemical Society*, *124*(12), 3143–3151. https://doi.org/10.1021/JA012034S

Warnhoff, K., Hercher, T. W., Mendel, R. R., & Ruvkun, G. (2021). Protein-bound molybdenum cofactor is bioavailable and rescues molybdenum cofactor-deficient C. elegans. *Genes and Development*, *35*(3), 212–217. https://doi.org/10.1101/GAD.345579.120

Warnhoff, K., & Ruvkun, G. (2019). Molybdenum cofactor transfer from bacteria to nematode mediates sulfite detoxification. *Nature Chemical Biology*, *15*(5), 480–488. https://doi.org/10.1038/S41589-019-0249-Y

Wuebbens, M. M., & Rajagopalan, K. V. (1995). Investigation of the early steps of molybdopterin biosynthesis in Escherichia coli through the use of in vivo labeling studies. *Journal of Biological Chemistry*, *270*(3), 1082–1087. https://doi.org/10.1074/JBC.270.3.1082

Wuebbens, M. M., & Rajagopalan, K. V. (2003). Mechanistic and mutational studies of Escherichia coli molybdopterin synthase clarify the final step of molybdopterin biosynthesis. *Journal of Biological Chemistry*, *278*(16), 14523–14532. https://doi.org/10.1074/JBC.M300453200

Yang, W. S., Sriramaratnam, R., Welsch, M. E., Shimada, K., Skouta, R., Viswanathan, V. S., Cheah, J. H., Clemons, P. A., Shamji, A. F., Clish, C. B., Brown, L. M., Girotti, A. W., Cornish, V. W., Schreiber, S. L., & Stockwell, B. R. (2014). Regulation of ferroptotic cancer cell death by GPX4. *Cell*, *156*(1–2), 317–331. https://doi.org/10.1016/J.CELL.2013.12.010

Yoganathan, S., Sudhahakar, V., Sv, S., Thomas, M., Kumar Dutta, K., Danda, A., & Chandran, S. (2018). Novel Imaging Finding and Novel Mutation in an Infant with Molybdenum Cofactor Deficiency, a Mimicker of Hypoxic-Ischaemic Encephalopathy. *Iran J Child Neurol. Spring*, *12*(2), 107–112.

Yoshimura, A., Kibe, T., Hasegawa, H., Ichida, K., Koshimizu, E., Miyatake, S., Matsumoto, N., & Yokochi, K. (2019). The Persistent Generalized Muscle Contraction in Siblings with Molybdenum Cofactor Deficiency Type A. *Neuropediatrics*, *50*(2), 126–129. https://doi.org/10.1055/S-0039-1677869

Zhang, G., Zhang, Y., Shen, Y., Wang, Y., Zhao, M., & Sun, L. (2021). The Potential Role of Ferroptosis in Alzheimer's Disease. *J Alzheimers Dis*, *80*(3), 907–925. https://doi.org/10.3233/JAD-201369

Zivanovic, J., Kouroussis, E., Kohl, J. B., Adhikari, B., Bursac, B., Schott-Roux, S., Petrovic, D., Miljkovic, J. L., Thomas-Lopez, D., Jung, Y., Miler, M., Mitchell, S., Milosevic, V., Gomes, J. E., Benhar, M., Gonzales-Zorn, B., Ivanovic-Burmazovic, I., Torregrossa, R., Mitchell, J. R., … Filipovic, M. R. (2019). Selective Persulfide Detection Reveals Evolutionarily Conserved Antiaging Effects of S-Sulfhydration. *Cell Metabolism*, *30*(6), 1152-1170.e13. https://doi.org/10.1016/j.cmet.2019.10.007

III Investigation of novel treatment approaches for a mouse model of isolated sulfite oxidase deficiency

Abstract

Isolated sulfite oxidase deficiency (SOXD) is a rare metabolic disorder, in which loss of function of sulfite oxidase (SOX), the terminal enzyme of cysteine catabolism, results in an accumulation of toxic sulfite and other formed sulfur metabolites accompanied by a depletion of cysteine. Patients present with feeding difficulties, high irritability and seizures, often starting in the neonatal period, and soon develop a severe neurological phenotype resulting in infant death. Neurodegeneration is mainly caused by the sulfur metabolite S-sulfocysteine, whose structural resemblance to glutamate makes it a potent N-methyl-D-aspartate receptor (NMDAR) agonist. To date, no effective long-term treatment has been established, with treatment strategies being limited to ameliorating disease symptoms, primarily anticonvulsive interventions. The recent generation of a SOXD mouse model finally paved the way for extensive *in vivo* studies on potential treatment options. Hence, the current study investigated several therapeutic approaches aiming to reduce sulfite-induced toxicities by (i) NMDAR blockage to prevent excitotoxic neurodegeneration, (ii) dietary restriction of proteins and sulfur-containing amino acids, (iii) sulfite scavenging, (iv) inhibition of ferroptosis, a non-apoptotic form of regulated cell death triggered by cysteine depletion and (v) an enzyme replacement therapy using a modified version of SOX. Results revealed surprising insights into murine SOXD, which in contrast to SOXD in humans does not involve severe neurodegeneration, but follows a different pathomechanism. Ferroptosis has been ruled out as the major cell death pathway involved, but was actually shown to be prevented upon the loss of SOX function. Lastly, an enzyme replacement therapy provides great potential as a future treatment strategy for *Suox*$^{-/-}$ mice and human SOXD patients.

3.1 Introduction

Molybdenum cofactor deficiency (MoCD) and isolated sulfite oxidase deficiency (SOXD) are rare, recessively inherited metabolic disorders, which present with severe, progressive neurodegeneration, microcephaly, altered facial and head morphology, intractable seizures and major developmental delay inevitably leading to infant death if left untreated (Johnson & Duran, 2001). To date, more than 200 cases of MoCD and approximately 50 cases of SOXD have been reported in the literature (Claerhout et al., 2018; Misko et al., 2020; Sharawat et al., 2020; Tian et al., 2019), but case counts are believed to be significantly higher, as widespread unawareness still results in frequent misdiagnoses exacerbating ongoing research.

MoCD is characterized by defects in molybdenum cofactor (Moco) biosynthesis leading to a loss of function of all Moco-dependent enzymes. Depending on which step of Moco biosynthesis is disturbed, MoCD can be further classified in three different subtypes (Reiss & Hahnewald, 2011). The most prevalent form, MoCD type A, is caused by mutations in the *MOCS1* gene, which encodes for two enzymes catalyzing the first step of Moco biosynthesis (Reiss et al., 1998). MoCD type B patients carry mutations in the *MOCS2* or *MOCS3* gene, which encode for enzymes required for the second step of Moco biosynthesis (Huijmans et al., 2017; Stallmeyer et al., 1999). In MoCD type C, which is the rarest form of MoCD, the final step of Moco biosynthesis is disturbed by mutation of the *GPHN* gene (Reiss et al., 2001).

SOXD is caused by mutations in the *SUOX* gene, which is located on chromosome 12 and encodes for the molybdoenzyme sulfite oxidase (SOX) directly (Johnson et al., 2002). SOX is the final enzyme of cysteine catabolism, where it catalyzes the detoxification of sulfite by oxidation to sulfate (Aghanoori et al., 2016; Johnson et al., 2002). As MoCD and SOXD present with highly similar clinical pictures, symptomatology can be mainly ascribed to a loss of function of SOX.

In the oxidative part of cysteine catabolism, cysteine dioxygenase (CDO) catalyzes formation of the intermediate cysteine sulfinic acid (CSA) from cysteine. On the one hand, CSA is further converted into taurine by the enzyme CSA decarboxylase (CSAD), while on the other hand glutamate oxaloacetate transaminases 1 and 2 (GOT1/2) catalyze its conversion into sulfite (Mellis, Misko, et al., 2021). In contrast, the hydrogen disulfide (H_2S) pathway of cysteine catabolism includes the formation of H_2S by three distinct enzymes, namely cystathionine β-synthase (CBS), cystathionine γ-lyase (CSE) and 3-mercaptopyruvate sulfurtransferase (MPST). H_2S clearance is mediated via several steps starting with sulfide:quinone oxidoreductase (SQR) generating persulfidated glutathione (GSSH), followed by thiosulfate sulfurtransferase (TST) and persulfide dioxygenase (PDO) regenerating glutathione (GSH) under formation of thiosulfate and sulfite, respectively. In both metabolic pathways, SOX is the key enzyme catalyzing clearance of sulfite (Kohl et al., 2019).

Mammalian SOX is located in the intermembrane space (IMS) of mitochondria (Ono & Ito, 1984) and consists of three domains: a central Mo-domain harboring its molybdenum cofactor, which is bridged to an N-terminal heme domain by a flexible linker and a C-terminal dimerization domain enabling homodimer formation (Kisker et al., 1997). Upon oxidation of sulfite, the molybdenum of the central domain accepts two electrons, which are subsequently transferred to the heme domain via two single intramolecular electron transfer

steps. Regeneration of the enzyme is achieved by subsequent transfer of these electrons onto two molecules of cytochrome *c*, which represent the final electron acceptor and contribute to mitochondrial respiration (Hille, 1994). Loss of SOX function causes the accumulation of sulfite and other secondary sulfur metabolites such as thiosulfate, taurine and S-sulfocysteine (SSC), accompanied by a decrease in cysteine and sulfate levels (Rupar et al., 1996).

The majority of symptoms causing the neurological phenotype can partially be ascribed to a neurotoxicity induced by sulfite itself, which may act as a direct inhibitor of glutamate dehydrogenase, thus resulting in ATP depletion and an intracellular energy crisis (Zhang et al., 2004). Moreover, sulfite can alter the mitochondrial network leading to increased hyperfusion and decreased mobility (Mellis, Roeper, et al., 2021). A more general impact of sulfite on protein function includes the attack of disulfide bonds, impacting protein stability and cleavage of persulfidations, which serve as a protective mechanism preventing cysteine residues from irreversible oxidation (Dóka et al., 2020; Zivanovic et al., 2019).

Sulfite can also act as an inhibitor of α-aminoadipic semialdehyde dehydrogenase, hence causing the accumulation of α-aminoadipic semialdehyde and Δ^1-piperideine-6-carboxylate (Mills et al., 2012). The latter, in turn, can inactivate pyridoxal-5'-phosphate (PLP), an essential coenzyme for more than 140 enzymes (Percudani & Peracchi, 2003). A direct attack of sulfite on the aldehyde group of PLP has been proposed to represent another mechanism inducing PLP deficiency (Footitt et al., 2011). Due to its pivotal role as an enzymatic cofactor, decreased levels of PLP in cerebrospinal fluid are known to negatively impact synthesis of the neurotransmitters dopamine and serotonin, as well glycine and threonine metabolism, thus ultimately resulting in a neurological phenotype including epileptic seizures and impaired neuromotor behavior (Footitt et al., 2011; Mills et al., 2005), which aligns with the phenotype observed in SOXD patients.

While sulfite toxicity is a broad, multifactorial phenomenon, the absence of sulfate can be linked more precisely to neuronal dysfunction due to disturbance of neurotransmitter and steroid hormone metabolism (Kříž et al., 2008; Rivett et al., 1982). Depletion of cysteine, on the other hand, is presumed to induce a newly discovered form of non-apoptotic cell death described as ferroptosis, resulting from the accumulation of lipid peroxides (Seiler et al., 2008; Yang et al., 2014). Cysteine is one of three amino acids required for the biosynthesis of the strong antioxidant GSH, which, in turn, is a crucial co-substrate for the enzyme glutathione peroxidase 4 (GPX4) mediating the detoxification of lipid peroxides. Hence, decreased cysteine in SOXD is hypothesized to induce oxidative stress ultimately leading to excessive ferroptotic cell death (Wyse et al., 2018).

One principal and well-studied mechanism of neurotoxicity is mediated by SSC, which is formed in the reaction of sulfite and the disulfide cystine as a physiological mechanism of sulfite scavenging. Due to its structural resemblance to glutamate it can act as an NMDA receptor (NMDAR) agonist causing an overactivation of glutamatergic synapses and increased excitotoxicity (Kumar et al., 2017; Olney et al., 1975). In line with this, in a pharmacologically induced mouse model of SOXD generated by administration of tungstate to render the cofactor and thus the enzyme SOX inactive, a strong impairment of neuromotor skills could be rescued by the NMDAR antagonist memantine (Kumar et al., 2017). In humans, NMDAR blockage has only been described twice as an attempted treatment for SOXD (Kurlemann et al., 1996; Tan et al., 2005). The NMDAR antagonist dextromethorphan was administered in combination with a low-methionine and low-cysteine diet to downregulate cysteine catabolism, the vitamin thiamine, which is reduced upon sulfite toxicity with yet unknown outcome, and phenobarbital to prevent further seizures by GABA-type receptor activation. Treatment success was limited, as seen by continuous developmental retardation and progressive microcephaly, but previously intractable seizures stopped and EEG findings displayed huge improvement. Due to the multifactorial treatment strategy, however, the exact impact of NMDAR blockage on the patient's overall health remained speculative, so further *in vivo* testing would be required to examine its full potential as a therapeutic agent for SOXD.

In the past, reduction of sulfite accumulation was attempted by low-sulfur diets already several times and ranged from having little effect on severe cases to yielding significant health improvement in mild, late onset patients (Boyer et al., 2019; Tan et al., 2005; Touati et al., 2000). However, due to methionine being an essential amino acid and the precursor of cysteine, a complete prevention of sulfite formation from the catabolism of sulfur-containing amino acids is not achievable. An alternative approach therefore implies scavenging of formed sulfite and has been used so far in two cases described in the literature. One patient was given D-penicillamine to induce the formation of S-sulfopenicillamine under scavenging of free sulfite (Tardy et al., 1989). The treatment did not result in an improvement of the patient's health condition, but the absence of detectable levels of S-sulfopenicillamine questioned the potency of the tested compound as an effective sulfite scavenger. Another SOXD patient received cysteamine in addition to a low-sulfur diet, which did not ameliorate symptoms more than the dietary approach alone and was therefore discontinued after nine months (Touati et al., 2000). The disulfide cystamine, formed from two molecules of cysteamine, *in vitro* has been shown to react with sulfite 6-8 times faster than cystine (Jocelyn, 1987), thus holding great potential as sulfite scavenger. As the authors neither stated concentration and frequency of cysteamine

administration, nor examined the level of S-sulfocysteamine formed (Touati et al., 2000), a clear reason for the failure of the treatment could not be determined, so further studies should elaborate the potential of cysteamine as a treatment option for SOXD.

To date, SOXD is still classified as an incurable disease, as no unrestricted, effective long-term treatment strategy could be established so far. While MoCD type A can be treated successfully by administration of the first intermediate of Moco biosynthesis (Schwahn et al., 2010), a therapy for MoCD types B and C has also not been established yet. As the severity of both MoCD and SOXD mainly results from the absence of SOX function, a treatnent for SOXD would presumably show strongly beneficial effects on MoCD patients as well. Recent generation of a *Suox*$^{-/-}$ mouse model (Kohl, 2019) now paved a new way for more extensive *in vivo* testing of potential therapeutic approaches based on the current comprehension and presumption of the disease mechanism.

3.2 Results and Discussion

3.2.1 Effect of tested treatment approaches on median survival time of *Suox*$^{-/-}$ mice

In order to discover an effective long-term treatment for SOXD, several therapeutic approaches were investigated *in vivo* using homozygous *Suox*$^{-/-}$ mice previously generated (Kohl, 2019). Potential therapeutics were either directly administered via i.p. injection or indirectly by manipulation of the chow fed to mothers. The effectiveness of each treatment was mainly quantified via determination of the median time span. For that purpose, animals were kept until attainment of the termination criterion, so collection of body fluids was not feasible, but in the future would be crucial to determine the effect of utilized treatment strategies on biomarker levels.

Differences in average survival times varied between -1.1 to +2.2 days compared to the mock-treated control group (Fig. 1), whose average survival time of 7.6 days shows a reduction of 2.0 days compared to the age of death observed for *Suox*$^{-/-}$ mice in general (Kohl, 2019). Variance might be ascribed to more extensive handling of pups at very young age, which can cause an elevated stress response (Moles et al., 2004) or reduced care by the mother and therefore trigger a slightly earlier onset of the phenotype.

In aggregate, memantine, low-sulfur and low-protein diets, three different tested sulfite scavengers, as well as the ferroptosis inhibitor Liproxstatin-1 did not significantly alter the average life span of *Suox*$^{-/-}$ pups. However, PEGylated mSOX-Mo had a slightly, but significantly beneficial effect on survival (Fig. 1). In the following, reasons for the choice of

each individual treatment and the limited effect observed *in vivo*, as well as their potential as treatments for SOXD will be discussed in detail.

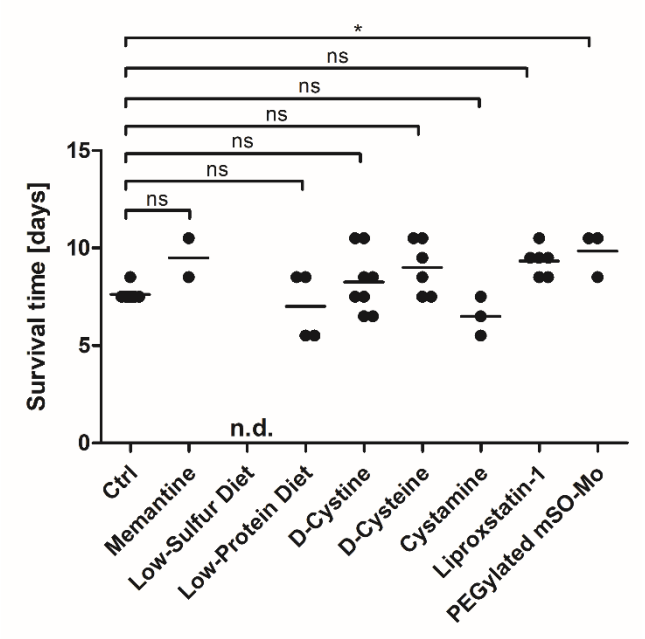

Figure 1: Survival time of *Suox*$^{-/-}$ pups upon application of different treatment methods.
Mice were treated with the respective substances as follows: memantine was fed to expecting mothers from day of confirmed pregnancy at 500 mg/kg bodyweight. Low-sulfur diet contained 10% cystine, 14% methionine and 70% protein and low-protein diet contained 47% cystine, 68% methionine and 45% protein compared to control chow. Sulfite scavengers were administered via daily i.p. injection starting at day of birth. D-cystine, D-cysteine and cystamine were given at concentrations of 3.6, 200 and 100 mg/kg bodyweight, respectively. Liproxstatin-1 was administered at 10 mg/kg bodyweight via daily i.p. injection starting at day of birth. PEGylated mSOX-Mo was administered via a single i.p. injection of 50 pmol enzyme at day P2.5. Mock treatment included daily i.p. injection of PBS (+ 1% DMSO). Data were analyzed with 1-way ANOVA, $F(7,33) = 4.1$, and Dunnett's post-hoc test. *$p<0.05$

3.2.2 Memantine treatment confirms absence of fatal cerebral phenotype in SOXD mouse model

In SOXD patients, accumulation of the sulfur metabolite SSC, which displays high structural resemblance towards glutamate (Fig. 2A+B), results in increased excitotoxicity leading to vast neuronal cell death and overall loss of white matter in several brain areas including the cortex (Dublin et al., 2002; Kumar et al., 2017). In line with this, our *Suox*$^{-/-}$ mouse model displays decreased brain height and volume, as well as highly decreased motor skills (Kohl, 2019). Hence, the first therapeutic approach was supposed to protect neurons from SSC-mediated neurotoxicity by using the non-competitive NMDAR antagonist memantine, whose mode of action is visualized in Fig. 2C. A preliminary experiment performed in this study using primary cortical neurons from wildtype mice examined the cytotoxic effect of SSC and verified a highly protective effect of memantine in a similar manner as described earlier (Kumar et al., 2017). In agreement with previous studies, overnight treatment with SSC resulted in a reduction of cell viability to ~40%, whereas pretreatment with memantine restored cell viability upon SSC treatment entirely (Fig. 2D), thus confirming the strong potential of NMDAR blockage as a treatment target in SOXD.

In vivo, however, memantine treatment resulted in a non-significant increase in average survival time of +1.9 days compared to mock treatment (Fig. 1). Memantine was

administered indirectly as a chow additive, which was fed to mothers starting the day pregnancy was discovered. Earlier studies verified a sufficient transfer from mother to offspring via placenta and breast milk (Victorino et al., 2017), thus allowing an optimal pre- and postnatal treatment. However, data need to be interpreted with caution, as due to this alternative route of administration handling of pups only started at day 4 of life to allow scoring, thus reducing the overall amount of postnatal stress, while daily i.p. injection required handling beginning at P0. Compared to the median survival time of 9.6 ± 1.6 days previously determined for *Suox*$^{-/-}$ mice, memantine treatment with 9.5 ± 1.0 days did not display any improvement in the severity of the phenotype.

Parallel examination of *Suox*$^{-/-}$ brains at P8.5 revealed unchanged cell numbers in several brain layers, thus, against all expectations, not confirming a neurological phenotype (Kohl, Fu et al., in preparation). Decreased brain size and motor abilities can therefore most likely be ascribed to a global developmental delay proportional to the decelerated body weight gain of *Suox*$^{-/-}$ pups. Similar results have been reported in *Mocs1*$^{-/-}$ mice, a mouse model for MoCD type A, which revealed no alterations in overall neuronal cell number or development of different brain cell layers (Lee et al., 2002). In *Mocs2*$^{-/-}$ mice, which resemble the phenotype of MoCD type B patients, changes in neuron numbers were not observed either, however more in-depth analysis revealed an increased number of apoptotic neurons (Jakubiczka-Smorag et al., 2016). One can speculate on a similar increase in apoptotic neurons in *Mocs1*$^{-/-}$ and *Suox*$^{-/-}$ mice due to elevated levels of SSC as observed for all subjects. However, SSC levels were less markedly increased as in human patients, which can be ascribed to the severe depletion of cystine in plasma (Jakubiczka-Smorag et al., 2016; Kohl, 2019; Lee et al., 2002).

It can be hypothesized that *Suox*$^{-/-}$ mice die due to a yet unknown cause of death before the manifestation of a lethal cerebral phenotype due to differences in the developmental stages of human and mouse brains at the time of birth (Semple et al., 2013), thus rendering memantine unsuitable as treatment approach. The generation of a conditional knockout mouse model for SOXD would provide a higher phenotypic resemblance towards human SOXD, but attempts in the past have been unsuccessful (Fu, unpublished data). Alternatively, an amelioration of the observed phenotype in the existing SOXD mouse model might result in an increased median life span allowing the development of a phenotype with higher resemblance to human MoCD and SOXD patients.

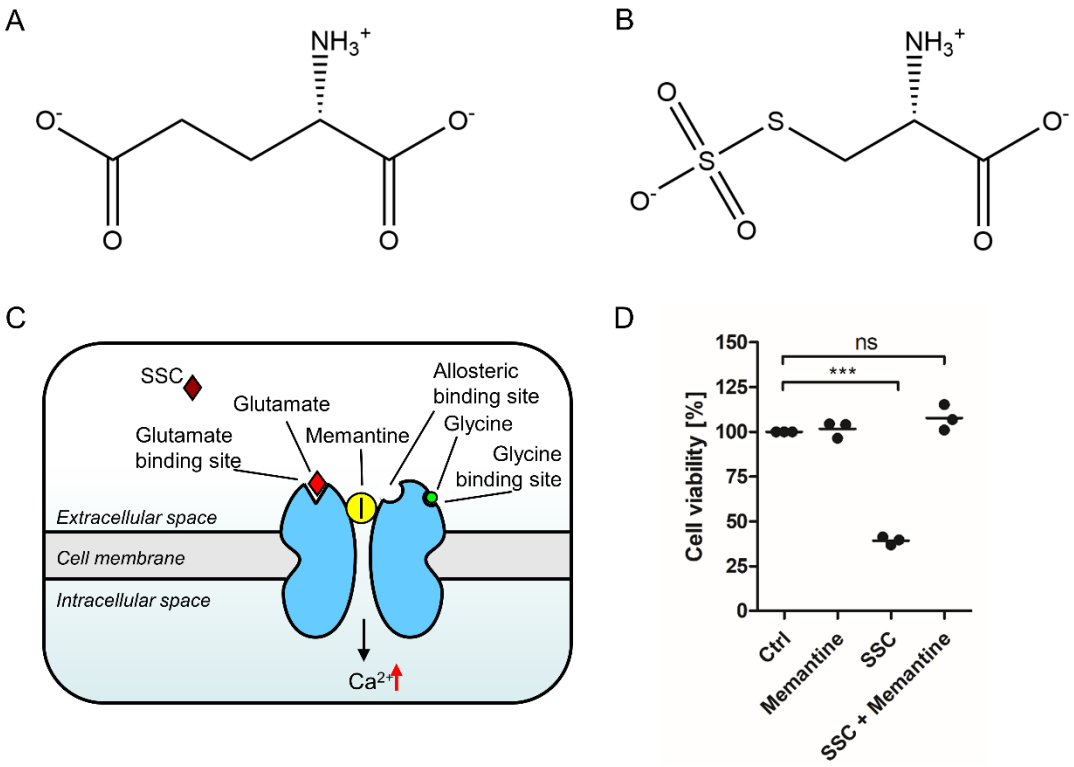

Figure 2: Memantine in SSC-mediated excitotoxicity.
Chemical structures of (A) glutamate and (B) the glutamate analogue SSC. (C) Proposed mode of action of the non-competitive NMDAR antagonist memantine, which upon binding results in an open channel block. (D) Primary cortical neurons DIV8 were treated with 100 µM SSC and/or 10 µM of memantine overnight. Memantine pretreatment was done 30 min prior to SSC treatment. Data were analyzed with 1-way ANOVA, $F(3,8) = 160.8$, and Dunnett's post-hoc test. ***$p<0.0001$, ns $p>0.05$

3.2.3 Low-sulfur and low-protein diet failed to improve the symptomatology of SOXD in mice

A first approach to slow down disease progression in order to allow manifestation of a lethal cerebral phenotype involved the reduction of sulfur-containing amino acids and overall protein content in the diet of heterozygous mothers. Reduction of cysteine intake aimed to downregulate cysteine catabolism, thus producing lower amounts of toxic sulfite (Fig. 3A). Previous studies examined the influence of a low-protein diet on the protein content in milk during lactation and showed a 12% decrease of protein levels in milk after 50% reduction of dietary protein, as yet unknown physiological mechanisms in lactating mothers seem to be able to compensate for decreased protein supply (Derrickson & Lowas, 2007). Decrease in protein levels, however, was sufficient to impact both pre- and postnatal growth of litters negatively. As pups still showed steady weight gain and no observable phenotypic features other than reduced size (Derrickson & Lowas, 2007), a low-protein diet was still considered a suitable approach for *Suox*$^{-/-}$ mice. Low-protein diet used in the current study contained 45% of protein, 47% cystine and 68% methionine as compared to the standard diet. Treatment by administering low-protein diet to mothers resulted in an unaltered average

survival time of 7.0 ± 0.9 days for *Suox*$^{-/-}$ pups (Fig. 1), implying that a reduction of global protein content in milk was not sufficient to lower sulfite-related toxicity in offspring significantly.

Hence, a second approach included a stronger, direct reduction of free methionine and cystine in the mothers‘ diet to further reduce cysteine catabolism. Low-sulfur diet contained 10% cystine and 14% methionine, while protein content was reduced to 70% compared to the standard diet. While litters from mothers fed a low-protein diet only displayed minor pup loss in the first days of life being comparable to the standard numbers of pup mortality in laboratory mice (Weber et al., 2013), dietary restriction of sulfur-containing amino acids resulted in a mortality rate of 80% of pups within the first three days of life (Fig. 3B). The remaining 20% did not contain homozygous *Suox*$^{-/-}$ pups and were thus sacrificed. Considering the trend of the preceding days and the strongly decreased body weight of remaining pups (data not shown), however, a complete extinction of treated litters in the following was anticipated.

Two different mechanisms might have caused the observed high pup mortality following feeding of low-methionine/-cysteine diet to mothers. Firstly, a strong reduction of the essential amino acid methionine has been shown to result in a significant decrease of body weight in the first three weeks of administration, until mice adapt to the change in nutrition and compensate by an increased food intake (Nichenametla et al., 2021). The effect of dietary restriction on gestating mice has not been examined so far, but can be assumed to be even more drastic. In the present study, a switch from normal to low-sulfur diet containing only 10% cystine, 14% methionine and 70% protein compared to the standard diet was executed approximately three days before delivery of the pups, so animals did not have sufficient time to adapt to the dietary restriction. An increased nutrient uptake, however, cannot only be achieved by an increase in food consumption, but temporarily also by augmented infanticide. Alternatively, nutrient in the milk produced by mothers fed low-sulfur diet may have not been sufficient for the pups due to strong dietary restriction, thus leading to premature death accompanied by neonatal cannibalism through the mother. The observed decrease in body weight throughout pups of all genotypes supports the latter hypothesis, however a combination of both cannot be excluded.

In conclusion, the results from the feeding study in mice contrast data from human SOXD patients, in which the effects of dietary restriction of sulfur-containing amino acids and protein reached from having little impact on overall health condition to significantly reducing symptoms in milder forms (Boyer et al., 2019; Tan et al., 2005; Touati et al., 2000). The major difference resides in the route of administration of the diet. While neonates were

fed an artificial, restricted diet, direct feeding of mouse pups was not feasible due to experimental limitations. The indirect administration via the mother thus complicated the right dose-finding. Determination of the nutrient content in the milk of mothers that received dietary restriction in the future could help to further clarify the reasons for failure of this treatment strategy and help experimental optimization. However, as mice are born less developed than humans and showed increased rates of neonatal death upon treatment, dietary restriction might have a more severe negative impact on the development of mice than of humans. Overall, dietary restriction of sulfur-containing amino acids and protein in general seems not suitable for ameliorating the phenotype of SOXD in mice despite the positive results obtained in humans.

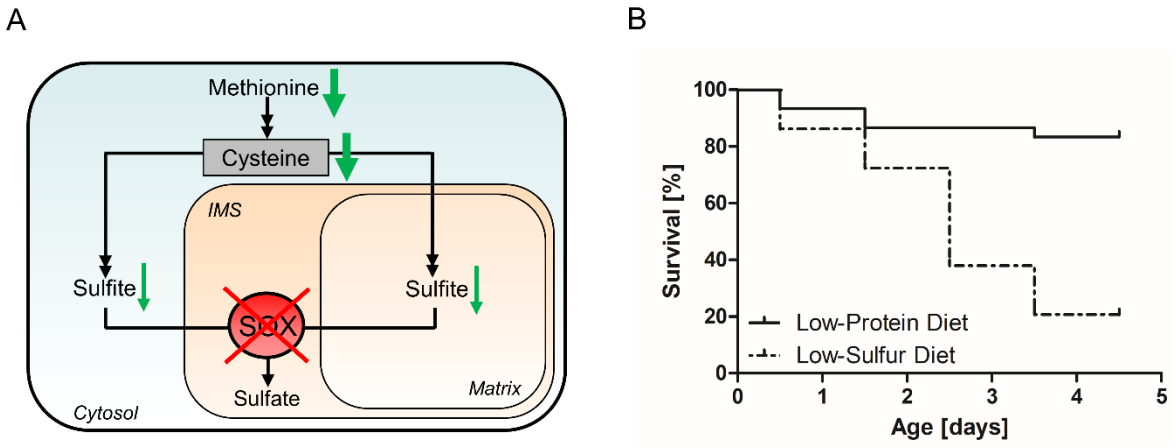

Figure 3: Hypothetical vs. actual effect of protein/ sulfur reduction in mothers' chow on *Suox*$^{-/-}$ pups. (A) Reduction of methionine and cysteine content in mothers' chow is proposed to decrease the rate of sulfite production from cysteine catabolism, hence decelerating disease progression. (B) Survival graph of offspring from mothers fed low-protein/ low-sulfur diet including pups of all genotypes.

3.2.4 Sulfite scavenging was not sufficient to improve the phenotype of *Suox*$^{-/-}$ mice

Dietary restriction failed to mitigate the phenotype of *Suox*$^{-/-}$ mice in order to provoke formation of a more severe cerebral phenotype. Hence, to be able to use the same treatment approach for the *Suox*$^{-/-}$ mouse model and human SOXD patients, the next treatment strategy shifted to more generalized approaches. One highly auspicious approach involved the usage of compounds with sulfite-scavenging properties.

In SOXD patients, usage of a single dose of 150 mg of D-penicillamine to induce formation of S-sulfopenicillamine, as well as administration of cysteamine in unknown concentration and frequency to form S-sulfocysteamine, did not result in any improvement of the patients' phenotypes (Tardy et al., 1989; Touati et al., 2000). D-penicillamine could have functioned in two different ways, as it does not only react with sulfite, but, as shown in mice, also acts as a selective inhibitor of the enzyme CSE (Brancaleone et al., 2016), thus

inhibiting the H_2S pathway of cysteine catabolism and potentially slowing down accumulation of toxic sulfite. The dosage used in the SOXD patient was similar to concentrations successfully inducing CSE inhibition in mice (Brancaleone et al., 2016). Nonetheless, a single dose of D-penicillamine seemed insufficient to influence the course of the disease (Tardy et al., 1989). Furthermore, the expected S-sulfonated compound S-sulfopenicillamine was not detectable in urine of the patient and therefore most likely was formed only in neglectable levels. The kinetics of the reaction of sulfite with D-penicillamine were not reported, but the results hint at a lower reaction rate than for the reaction of sulfite with cystine, hence not allowing scavenging prior to SSC formation. As with the right dosage and upon usage of a compound with higher reaction rate towards sulfite than L-cysteine, sulfite scavenging still remains a promising, straight forward therapeutic approach, in this study alternative sulfite scavengers were tested using the *Suox*$^{-/-}$ mouse model.

In human SOXD patients, an appropriate sulfite scavenger needs to be able to react with sulfite under formation of a non-toxic compound - similar to the formation of SSC from sulfite and cystine - in order to allow prevention of sulfite accumulation and SSC formation in significant amount. As in a previous study cystine levels were undetectable in most *Suox*$^{-/-}$ mice (Kohl, 2019), the major part of cystine was suggested to be present in form of SSC. However, the previous treatment strategy involving the NMDAR antagonist memantine excluded major SSC-induced neurotoxicity in *Suox*$^{-/-}$ mice, which implies a general decrease in cystine levels prior to SSC formation. Hence, the major goal of sulfite scavenging in *Suox*$^{-/-}$ mice is the direct prevention of sulfite accumulation, while lowered SSC formation is considered a secondary effect.

Sulfite is known to be elevated in *Suox*$^{-/-}$ mice at their time of death, however start time and progression of sulfite accumulation remained speculative (Kohl, 2019). Hence, an HPLC-based analysis of sulfite and thiosulfate in urine and plasma of *Suox*$^{-/-}$ mice at different stages of life was conducted to gain further insights into the disease mechanism. Both, sulfite and the secondary sulfur metabolite thiosulfate, which results from elevated sulfite clearance via the H_2S pathway, expectedly showed rather low levels at P0.5 in plasma, as maternal clearance of sulfite in the embryo was already suggested to cause *Mocs1*$^{-/-}$ pups to be born without visible phenotype (Fig. 4A+C) (Reiss et al., 2005). Urinary excretion, however, peaked at P0.5, confirming elevated levels of sulfite and thiosulfate already a few hours after birth (Fig. 4B+D). Creatinine levels showed a continuous increase with age due to urinary retention, thus suggesting impaired kidney function (Fig. 4E), as it was also described for *Mocs2*$^{-/-}$ mice (Jakubiczka-Smorag et al., 2016). Additionally, increasing levels of sulfite and thiosulfate over time render clearance via urinary excretion difficult, thus causing the observed accumulation of both, sulfite and thiosulfate, in plasma.

The data highlight the importance of starting the administration of sulfite scavengers immediately after birth to prevent toxic sulfite accumulation.

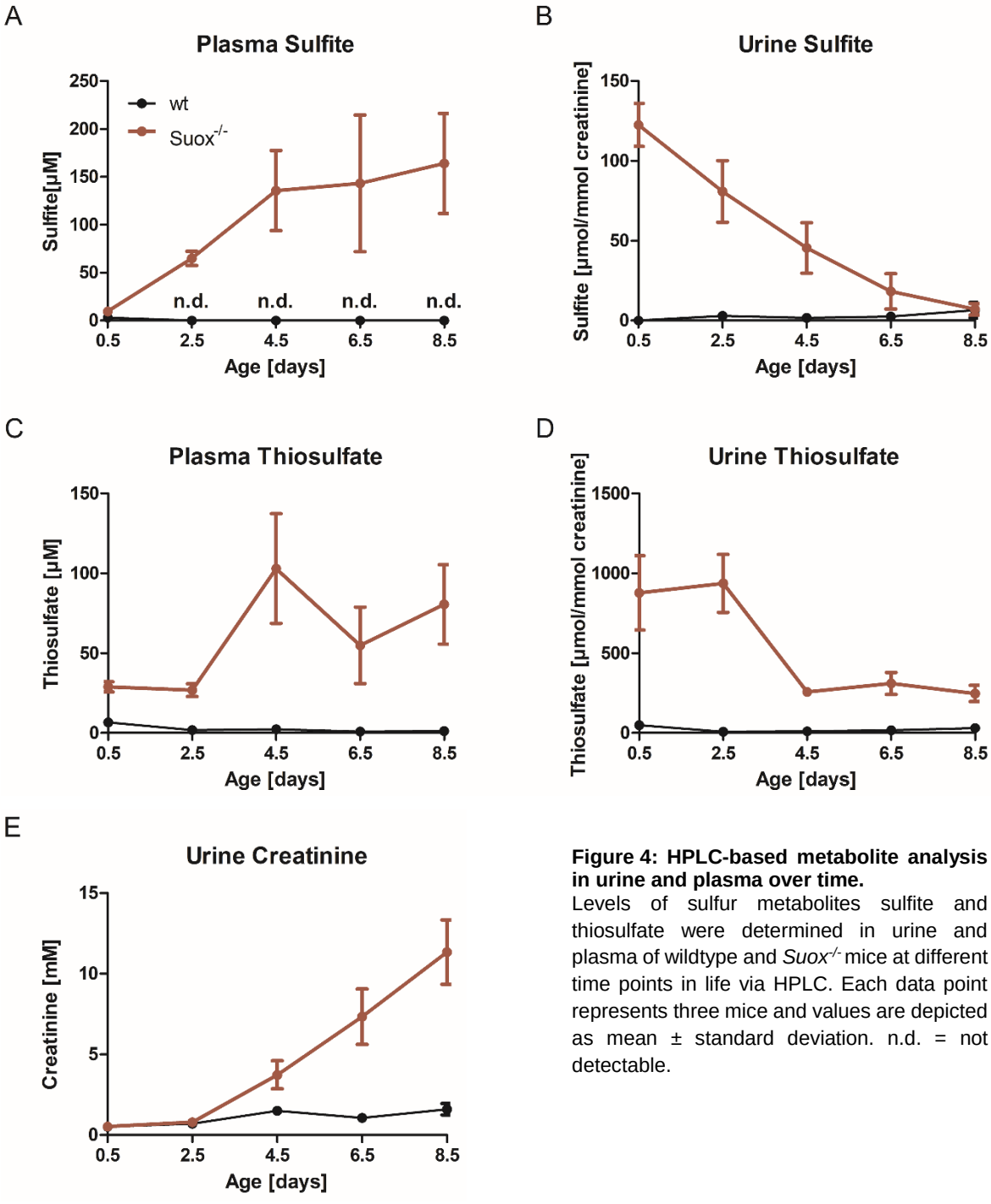

Figure 4: HPLC-based metabolite analysis in urine and plasma over time.
Levels of sulfur metabolites sulfite and thiosulfate were determined in urine and plasma of wildtype and *Suox*$^{-/-}$ mice at different time points in life via HPLC. Each data point represents three mice and values are depicted as mean ± standard deviation. n.d. = not detectable.

Several thiol-reactive compounds were tested as sulfite scavengers in the course of the current study. They aimed to produce non-toxic S-sulfonated compounds from free sulfite to prevent sulfite accumulation and toxic SSC formation (Fig. 5A).

The first sulfite scavenging compound used in this study was D-cystine. Cystine can be transported into the cell via the x_c- antiporter in exchange for glutamate (Bannai, 1986), where an equilibrium between the oxidized and reduced form establishes, with the greater part being present in the reduced form due to the reducing environment of the cytosol. Hence, potential intracellular metabolization of D-cysteine should be considered as well.

In the oxidative part of cysteine catabolism, CDO is the enzyme converting cysteine into CSA, an intermediate further processed by GOT1 and GOT2 to yield sulfite (Kohl et al., 2019). To examine the ability of CDO to metabolize D-cysteine, an *in vitro* activity assay with purified CDO was conducted. The amount of converted cysteine was quantified at different time points and showed a clear preference for L-cysteine over D-cysteine as a substrate (Fig. 5B). While the major part of L-cysteine was converted to CSA within 5 min, after 10 min two third of D-cysteine were still not converted. Therefore, *in vivo* due to higher availability D-cystine is presumed to be preferred in the reaction with sulfite.

Another preliminary experiment examined the toxicity of D-SSC formed from D-cystine on murine primary hippocampal neurons in comparison to classic L-cystine-derived L-SSC. L-SSC showed a reduction of cell viability to 30%, while D-SSC did not alter cell viability, as seen after 16h exposure to 100 µM of sulfite preincubated with equal amounts of D-cystine (Fig. 5C). Furthermore, restoration of cell viability was proportional to an increase in the ratio of D- to L-cystine, confirming the ability of D-cystine to scavenge sulfite even in the presence of L-cystine (Fig. 5D). Therefore, D-cystine was considered a powerful candidate for preventing sulfite accumulation in *Suox*$^{-/-}$ mice. In order to achieve the maximum long-term effect, treatment was performed daily starting at the day of birth rather than limiting it to a single dose as described previously (Tardy et al., 1989). Animals treated with D-cystine displayed an average life span of 8.3 ± 0.6 days, thus not showing a significant improvement compared to the control group (7.6 ± 0.1 days, Fig. 1). Due to the low solubility of D-cystine in aqueous, non-acidic solutions, concentrations of 3.6 mg/ kg bodyweight were used and were most likely insufficient to scavenge significant amounts of sulfite prior to SSC formation.

An alternative approach was the use of reduced D-cysteine, as an oxidation to D-cystine following administration to the animals given the oxidizing extracellular environment can be anticipated. The formation of mixed disulfides from L- and D-cysteine, however, cannot be excluded and would, upon sulfite scavenging, result in the formation of 50% toxic, L-cysteine-derived SSC. Thus, as D-cysteine exhibits a significantly higher solubility in PBS, concentrations were increased to 200 mg/kg bodyweight. Average survival of animals receiving D-cysteine treatment increased to 9.0 ± 0.6 days (Fig. 1). Although

results were not significant, a positive trend was observed upon usage of a higher concentration.

A study on the toxicity of high-dose D-cysteine treatment in adult rats found adverse effects starting at concentrations higher than 1,000 mg/kg/day and estimated the no-observed-adverse-effect-level to be at 500 mg/kg/day (Shibui et al., 2017). Administration, however, was done via oral gavage, which has been demonstrated to generally result in a lower bioavailability than i.p. injection in rats as well as in mice (Al Shoyaib et al., 2019). Hence, no higher concentrations of D-cysteine were tested in newborns due to the limited availability of data on its safety prohibiting approval of such a study by the authorities (LANUV). As animals were kept as long as possible before attainment of the termination criterion, collection of body fluids was not feasible, but in the future would be an important tool to determine the effectiveness of used D-cysteine concentrations in preventing sulfite accumulation.

A third and last potential sulfite scavenger tested in the present study was the disulfide cystamine, which *in vitro* displays a 6-8 times faster reaction with sulfite than cystine (Jocelyn, 1987). The reduced form cysteamine presents an established treatment strategy for patients suffering from nephropathic cystinosis, which receive concentrations between 0.2-0.6 mmol/kg (Smolin et al., 1988). As discussed above, in the past a SOXD patient has already been treated with the reduced form cysteamine, but did not show any signs of symptomatic improvement (Touati et al., 2000). However, authors did not comment on concentration and frequency of administration, thus not allowing any conclusions on the actual effectiveness of the compound as medication. To minimize formation of mixed disulfides from cysteamine and L-cysteine and to maximize the therapeutic effect, in the present study, the oxidized form cystamine was utilized. Formation of the S-sulfonated compound S-sulfocysteamine from the reaction of cystamine with sulfite within 30 min of incubation was verified by HPLC analysis (Fu, unpublished data).

The S-sulfonated compound formed from sulfite and L-cystine, (L-)SSC, is highly neurotoxic, so a potential neurotoxic effect mediated by S-sulfocysteamine was investigated prior to usage in *in vivo* studies. In murine primary hippocampal neurons, neither cystamine itself nor S-sulfocysteamine exhibited significant neurotoxicity (Fig. 5E). Toxicity of daily administration of cystamine in mice was reported for concentrations starting at 400 mg/kg/day, while 100 mg/kg/day were unrestrictedly classified as safe (Dedeoglu et al., 2002), so the latter concentration was used in the present study for daily i.p. injection of *Suox*$^{-/-}$ pups as well. Treatment, again, did not result in an increase of the average survival time, but instead caused a decrease by -1.1 days compared to the control group. As only

two homozygous pups received cystamine treatment and heterozygous as well as wildtype littermates developed normally (data not shown), a toxicity of cystamine for newborns is not assumed. However, a beneficial effect of cystamine treatment on the overall health of *Suox*$^{-/-}$ mice under the conditions applied can be excluded as well. The findings are in line with those received from treatment of the above mentioned SOXD patient, but too low concentration or frequency of administration cannot be ruled out. Hence, for complete elucidation of the effect of cysteamine/cystamine on sulfite and SSC levels, quantitative analysis of biomarkers in urine and plasma of treated individuals are crucial. In case elevated sulfite concentrations remain, search for a compound with stronger sulfite scavenging properties might discover a suitable medication for SOXD. Alternatively, a compound with lower toxicity would allow usage of higher dosages to maximize the therapeutic effect. In case of unaltered phenotypic presentation despite significant reduction of sulfite and SSC levels, an additional pathomechanism involving alternative sulfur compounds elevated in SOXD, including H_2S, thiosulfate and taurine, needs to be considered.

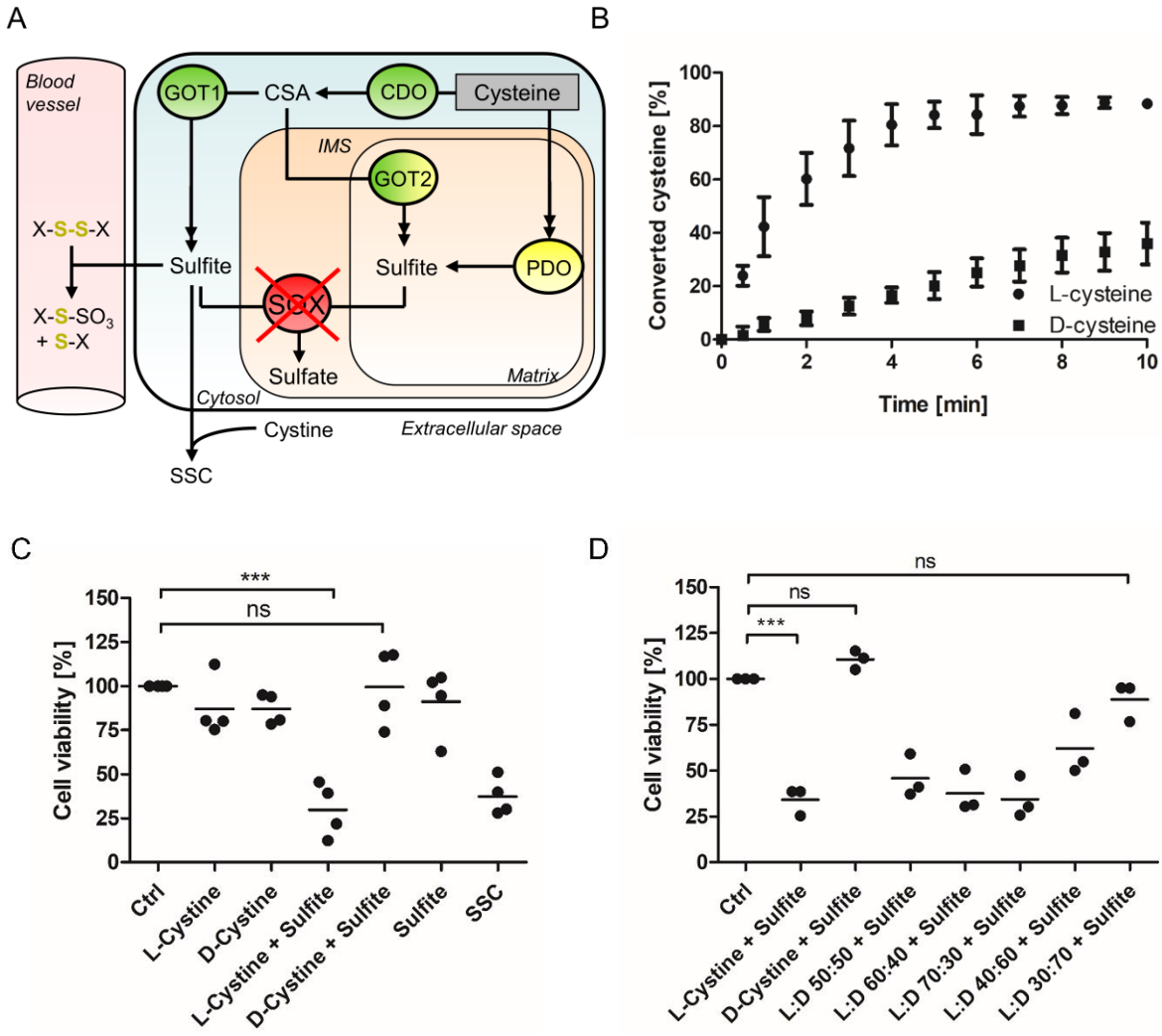

Figure 5: The effect of sulfite scavengers on sulfite- and SSC-mediated toxicity.
(A) Proposed mode of action of sulfite scavengers, which react with sulfite forming different S-sulfonated compounds to prevent reaction of sulfite with cystine under the formation of toxic SSC. Reaction products depicted in Supplementary Fig. 1. (B) *In vitro* CDO activity assay conducted in 100 mM MES buffer pH 6.1 using L-/D-cysteine as substrate. Reaction was stopped at different time points by the addition of DTNB reagent, which reacts with thiol groups under formation of a yellow compound. Quantification was done by measuring the absorption at 412 nm using a Tecan Spark. Measurements were performed as technical and biological triplicates and data are depicted as mean ± standard deviation. (C-E) Primary hippocampal neurons DIV8 were treated with 100 µM of sulfite, SSC , L-/ D-cystine, L- and D-cystine mixtures in varying ratios or cystamine. Scavengers plus sulfite were preincubated for 30 min at RT to allow formation of the respective S-sulfonated compounds. Data were analyzed with 1-way ANOVA, (C) $F(6,21) = 15.8$, (D) $F(7,16) = 27.0$, (E) $F(4,10) = 42.5$ and Dunnett's post-hoc test. ***$p<0.0001$, ns $p>0.05$

3.2.5 Ferroptosis is not caused, but prevented in *Suox*$^{-/-}$ mice

An alternative, hypothesized pathomechanism in SOXD is based on the severe depletion of cystine observed in *Suox*$^{-/-}$ mice, which is believed to be caused by increased SSC formation from its reaction with sulfite and a general depletion of amino acids due to starvation (Kohl, 2019). Depletion of cystine is accompanied by a decrease in intracellular cysteine levels, as cysteine is transported into the cell via its oxidized form cystine (Bannai, 1986). Low levels of cysteine result in a reduction of intracellular GSH, which is an essential co-substrate for GPX4, an enzyme required for the detoxification of lipid peroxides. Hence, depletion of cysteine results in decreased GPX4 activity and increased oxidative stress ultimately leading to ferroptosis, a form of non-apoptotic, regulated cell death (Fig. 6A) (Dixon et al., 2012), which might contribute to the severe phenotype seen in *Suox*$^{-/-}$ mice.

Preliminary studies in murine primary neurons treated with sulfite or SSC showed a protective effect of the ferroptosis inhibitors Ferrostatin-1 and Liproxstatin-1 (Kumar, 2016; Mellis, 2020), which both function as radical-trapping antioxidants (Zilka et al., 2017). However, cell viability was not restored completely, thus pointing towards an interplay of multiple cell death pathways resulting in sulfite- and SSC-mediated cell death. The present study repeated the treatment of primary cortical neurons with Liproxstatin-1 in the presence of 100 µM SSC, however was not able to reproduce the protective effect seen before, as pretreatment did not result in a change of cell viability (Fig. 6B).

A previous study determined GSH levels in brains of *Suox*$^{-/-}$ mice to be unaltered (Kohl, 2019), which is in line with the absence of significant SSC-mediated neurodegeneration, so the importance of Liproxstatin-1-mediated inhibition of ferroptosis in a neuronal context is questionable in *Suox*$^{-/-}$ mice. Nevertheless, a strong decrease of cystine in plasma accompanied by a reduction of GSH in liver and kidney highly suggests ferroptosis as one cell death pathway involved in the disease progression (Kohl, 2019). Thus, a more global, non-neuronal pathomechanism was anticipated and studies were continued *in vivo*.

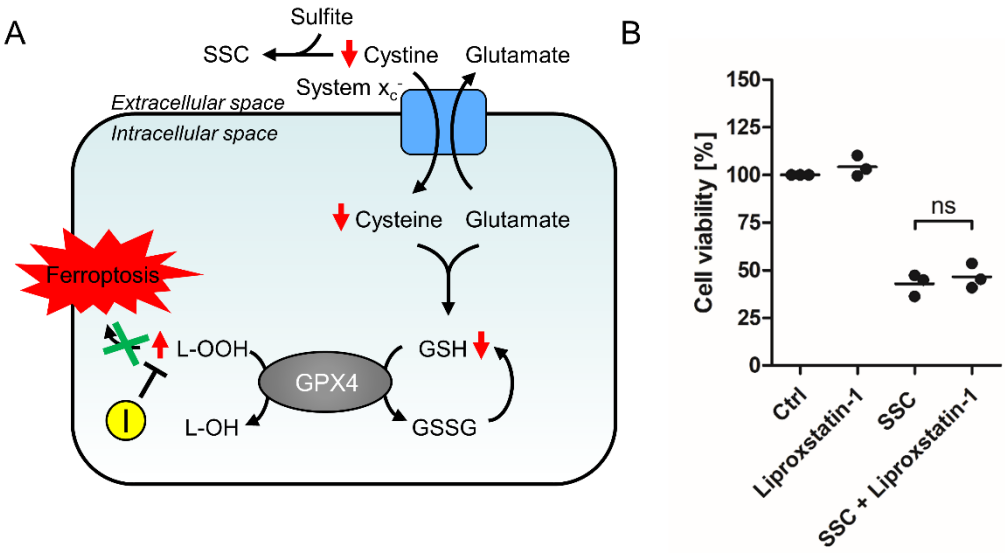

Figure 6: Hypothetical vs. actual effect of ferroptosis inhibitor Liproxstatin-1 on SSC-mediated toxicity. (A) Proposed mode of action of ferroptosis inhibitor Liproxstatin-1 (depicted in yellow), which acts as a radical-trapping antioxidant preventing excess formation of lipid peroxides and thus ferroptotic cell death. Ferroptosis can be caused by a depletion of cysteine leading to a decrease in GSH levels, as it is also proposed to occur in SOXD. (B) Primary cortical neurons DIV8 were treated with 100 µM SSC and/or 1 µM of Liproxstatin-1 overnight. Liproxstatin-1 pretreatment was done 30 min prior to SSC treatment. Data were analyzed with 1-way ANOVA, $F(3,8) = 127.5$, and Dunnett's post-hoc test. ns $p>0.05$

Daily i.p. injection of 10 mg/kg bodyweight Liproxstatin-1 in *Suox*$^{-/-}$ mice resulted in an average survival time of 9.3 ± 0.3 days, thus displaying a non-significant change of +1.7 days compared to the control group (Fig. 1). The concentration was chosen based on previous results from a study using daily i.p. injection of 10 mg/kg bodyweight Liproxstatin-1 as an effective treatment against ferroptosis-induced death in a *Gpx4*$^{-/-}$ mouse model (Friedmann Angeli et al., 2014).

Following the results of Liproxstatin-1 treatment, we asked the question whether there were further evidences that ferroptotic cell death could contribute to the disease pathology in SOXD. Therefore, a lipidomic analysis of lipid peroxides was performed in liver and kidney of *Suox*$^{-/-}$ mice due to the high expression of SOX in both organs (Woo et al., 2003). Contrary to expectations, while liver did not show altered lipid peroxidation, in kidney all quantified peroxidated lipid species were less abundant in SOX-deficient organs than in the wildtype (Fig. 7A+B). As ferroptosis is characterized by a strong increase of lipid peroxides (Dixon et al., 2012), its contribution to the phenotype of *Suox*$^{-/-}$ mice can be rather excluded. In actuality, lipid peroxidation in kidney seems to be inhibited as a consequence of the absence of SOX activity.

This result appears contradictory to earlier findings gained from studies in primary neurons (Kumar, 2016; Mellis, 2020). However, as ferroptosis is known to be inhibited by high levels of vitamin E, which are found in the neurobasal medium commonly used for

culturing of primary neurons, the observation of an actual beneficial effect of Liproxstatin-1 on primary neurons under the given conditions is highly improbable. Therefore, the observed absence of a protective effect of ferroptosis inhibition on SSC-mediated neurotoxicity in the current study is in line with the fact that ferroptotic cell death cannot be triggered under the given experimental conditions.

In vivo, induction of ferroptosis upon cysteine depletion has been shown in various cellular contexts (Badgley et al., 2020; Dixon et al., 2012; Upadhyayula et al., 2023). Nevertheless, *Suox*$^{-/-}$ mice, despite the observed depletion of plasma cystine, display decreased lipid peroxidation, so an alternative mechanism presumably leads to a protection from ferroptosis. One reaction that was anticipated to result in cysteine depletion is the formation of SSC from cystine, the oxidized form of cysteine, and sulfite due to elevated sulfite accumulation. However, similarly to glutamate, SSC was shown to be taken up by the x_c- antiporter in experiments with non-neuronal cells (Mellis, 2020). Subsequent intracellular reduction, presumably by the thioredoxin system, resulted in an increase of cellular cysteine and GSH levels in cell culture and could have been hypothesized to contribute to the resistance of *Suox*$^{-/-}$ mice towards ferroptosis due to increased GPX4 activity (Mellis, 2020; Zivanovic et al., 2019). However, as sulfite levels are highly elevated in *Suox*$^{-/-}$ mice, the low rate of SSC formation strongly suggests a global depletion of cystine and thus cysteine. Hence, the restoration of cysteine and GSH levels from cellular SSC uptake, which was observed in cell culture before, presumably does not occur in our SOXD mouse model. Instead, SSC formation is likely to contribute to the depletion of the intracellular cysteine pool. Undetectable cysteine levels in these mice were accompanied by a global decrease of various amino acids in plasma, which was attributed to a reduction in dietary intake congruent to the decreased rate of weight gain, thus implying starvation as a second mechanism of cysteine reduction (Kohl, 2019). Consistently, as mentioned above, levels of the antioxidant tripeptide GSH were decreased in liver and kidney of *Suox*$^{-/-}$ mice (Kohl, 2019), as cysteine is thought to be the rate-limiting factor for its biosynthesis (Lyons et al., 2000).

Recently, sulfite has been shown to accelerate recovery of GSH levels in wildtype HEK 293 cells after induction of oxidative stress by hydrogen peroxide (H_2O_2) (Mellis, 2020) due to its ability to act as a nucleophile cleaving disulfide bonds upon formation of S-sulfonated compounds (Chan, 1968; Kella & Kinsella, 1985). Similarly, a general increase of GSH levels was observed in *SUOX*$^{-/-}$ HEK 293 cells due to increased sulfite levels (Mellis, 2020). Hence, the author hypothesized a reaction of sulfite with glutathione disulfide (GSSG) resulting in one molecule of S-sulfonated glutathione ($GSSO_3$) and one molecule of reduced GSH adding to the intracellular GSH pool. $GSSO_3$, in turn, is known to be directly

reduced by GSH reductase (GSR) to prevent any cytotoxic effects of the compound, as in cell extracts it functions as an inhibitor of GSH S-transferase, an enzyme detoxifying electrophilic xenobiotics by conjugation to GSH (Booth et al., 1961; Jakoby, 1978). Reduction by the thioredoxin system or other disulfide reductases, as demonstrated generally for S-sulfonated compounds, might act as an additional mechanism of $GSSO_3$ detoxification (Mellis, 2020; Zivanovic et al., 2019). Moreover, consistent with the extensive nucleophilic activity of sulfite towards disulfide bonds in cells, persulfidation levels in *Suox*$^{-/-}$ mice were found to be significantly reduced as well, pointing towards a similar mode of action of sulfite *in vivo* (Kohl, 2019). Therefore, one can propose the same sulfite-mediated cleavage of disulfide bonds on intracellular GSSG, thus increasing the rate of recovery of GSH, the substrate of GPX4, *in vivo* despite the decreased net concentration (Fig. 7C), as was hypothesized in cell culture models previously (Mellis, 2020). The slightly extended average survival time of *Suox*$^{-/-}$ mice upon Liproxstatin-1 treatment is therefore suggested to result from a general protective, radical-trapping antioxidant effect of the compound (Sardesai et al., 1995; Zilka et al., 2017). As ferroptosis was ruled out as the major cell death pathway in *Suox*$^{-/-}$ mice, future studies are required to determine the exact cellular mechanism underlying the severe phenotype of SOXD in humans in order to allow the specific application of cell death inhibitors as promising candidates for an effective long-term therapy.

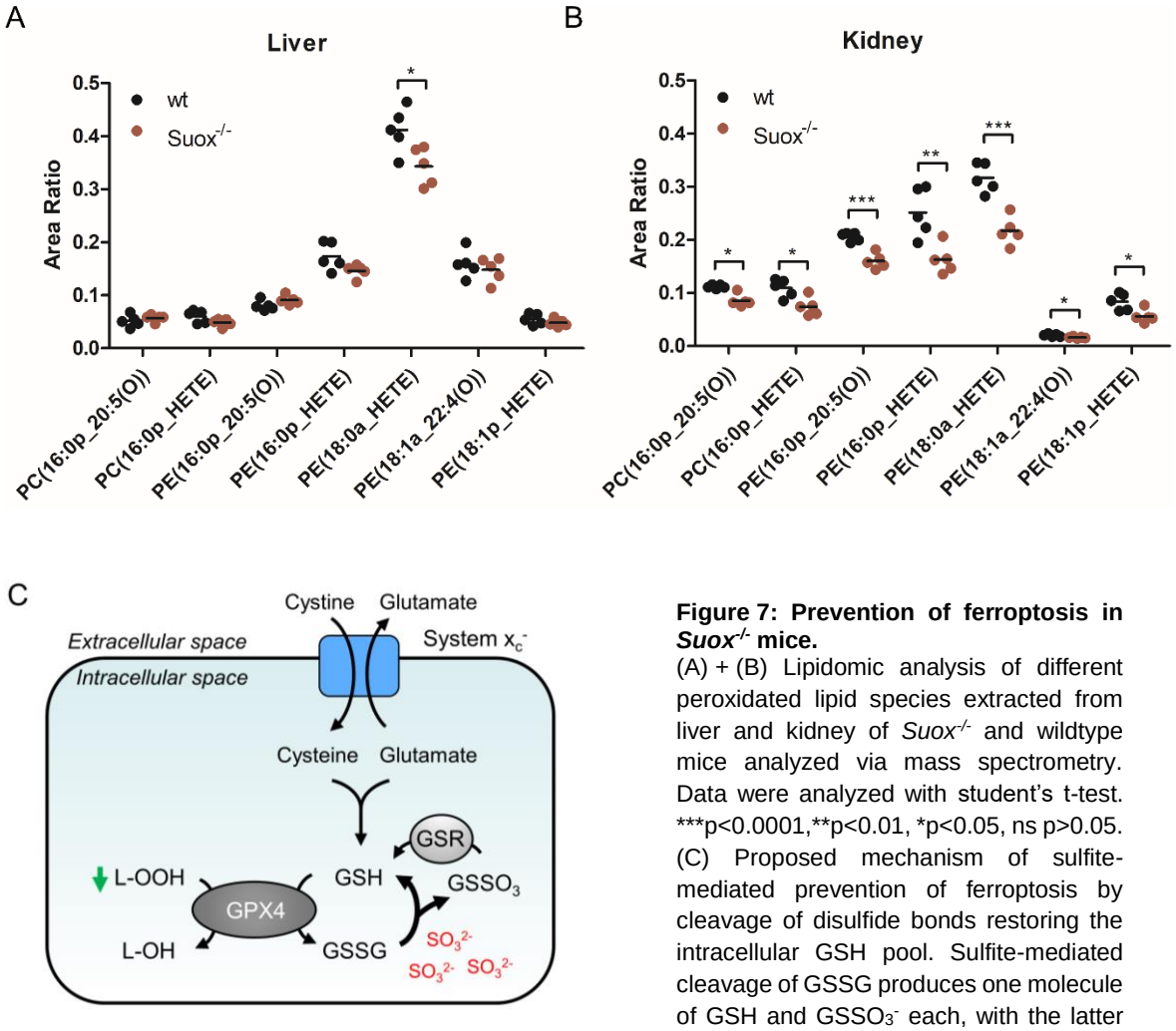

Figure 7: Prevention of ferroptosis in *Suox*$^{-/-}$ mice.
(A) + (B) Lipidomic analysis of different peroxidated lipid species extracted from liver and kidney of *Suox*$^{-/-}$ and wildtype mice analyzed via mass spectrometry. Data were analyzed with student's t-test. ***p<0.0001,**p<0.01, *p<0.05, ns p>0.05. (C) Proposed mechanism of sulfite-mediated prevention of ferroptosis by cleavage of disulfide bonds restoring the intracellular GSH pool. Sulfite-mediated cleavage of GSSG produces one molecule of GSH and $GSSO_3^-$ each, with the latter being further reduced to GSH by GSR.

3.2.6 Enzyme replacement therapy is a promising treatment approach for SOXD in mice

Focus on the inhibition of a specific cell death pathway revealed new insights into the molecular mechanisms occurring in SOXD, but also highlighted again the high complexity of the disease, which will require more additional research to be fully elucidated. Thus, the last treatment approach distanced from targeting single aspects of the pathomechanism and aimed for restoring SOX function by an enzyme replacement therapy.

SOX is located in the IMS of mitochondria, where it uses cytochrome *c* as the final electron acceptor for the oxidation of sulfite to sulfate. Translocation of an exogenous, purified enzyme to the IMS, however, proves difficult, so in the past in order to overcome this problem plant SOX (pSOX) was utilized for an enzyme replacement approach (Belaidi, 2011; Hahnewald, 2009). PSOX lacks the heme domain present in mammalian SOX and thus transfers sulfite-derived electrons directly to the final electron acceptor oxygen,

resulting in H_2O_2 production (Fig. 8A) (Hänsch et al., 2006). Therefore, the enzyme was hypothesized to be able to reduce plasma sulfite levels by transferring electrons onto blood-dissolved oxygen and to not require mitochondrial translocation (Belaidi et al., 2015).

Challenges in the administration of purified enzymes, however, also include development of an adverse immune response and short half-life *in vivo*, both reducing the therapeutic efficiency. A well-established method to lower immunogenicity and to increase the stability of proteins for enzyme replacement therapy is the chemical modification via PEGylation, which has been used successfully since more than 30 years (Nucci et al., 1991). Hence, previously, the potential of PEGylated pSOX as a treatment for MoCD and SOXD was tested in a single pilot study using *Mocs1*$^{-/-}$ mice (Belaidi, 2011; Hahnewald, 2009). Daily i.p. injection of concentrations greater than 50 pmol resulted in a significant prolongation of the average survival time from 7.5 to 16 days with minor variance. Homozygous mice developed normally and stayed indistinguishable from their littermates until the time of death. Animals died without a visible phenotype, but displayed swollen intestines upon postmortem autopsy. This observation suggested gastroenteritis as cause of death, which was hypothesized to be triggered by high levels of H_2O_2 formation as a byproduct from sulfite oxidation. In one of the two reports on the pilot study, H_2O_2 itself was shown to oxidize sulfite from a non-enzymatic reaction as well, however levels were considered to be neglectable *in vivo* (Belaidi, 2011).

Murine SOX lacking the heme domain (mSOX-Mo) was proven to utilize oxygen as the final electron acceptor *in vitro* similar to pSOX however with a lower catalytic efficiency (Belaidi et al., 2015). This resulted in a shift of the equilibrium towards higher non-enzymatic sulfite oxidation via H_2O_2 immediately after its formation and thus was proposed to cause a decrease in H_2O_2 toxicity, as it was observed in an *in vitro* enzyme replacement treatment approach using a cell culture system (Fig. 8B) (Belaidi et al., 2015).

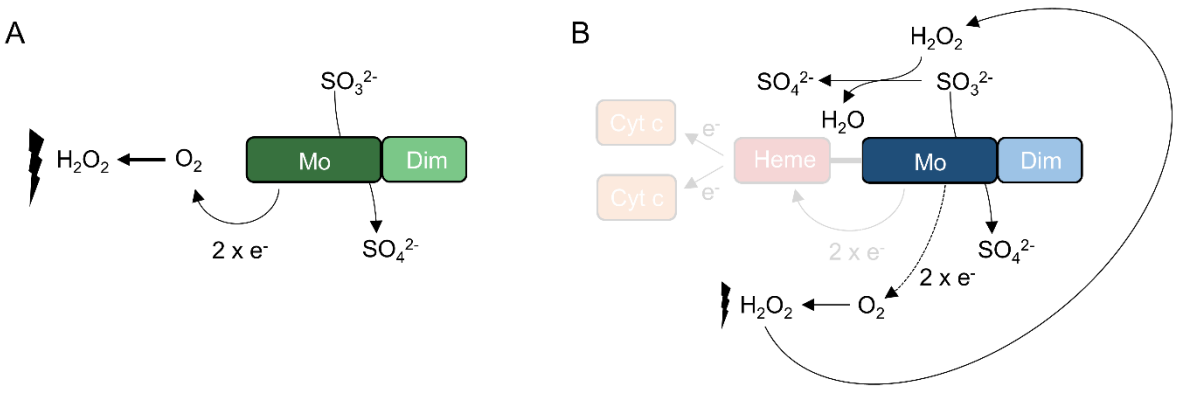

Figure 8: Structure and reaction of pSOX and mSOX-Mo.
Domain structure and schematic reaction of (A) pSOX and (B) mSOX-Mo in contrast to full-length mSOX including the proposed mechanism of H_2O_2 clearance by non-enzymatic oxidation of sulfite.

Based on the promising pilot study with pSOX (Belaidi, 2011; Hahnewald, 2009), the current study attempted to use PEGylated mSOX-Mo as an enzyme replacement therapy. Instead of *Mocs1*$^{-/-}$ mice, *Suox*$^{-/-}$ mice were used as a more direct approach, which were not available at the time of the previous study, but display symptoms exclusively related to the loss of SOX function.

As described before (Belaidi, 2011), mSOX-Mo was purified from *E. coli* via Ni-NTA affinity chromatography resulting in a pure enzyme of 43 kDa without major degradation products (Fig. 9A). The purified enzyme was PEGylated according to the previously applied protocol in a 1:20 enzyme:PEG ratio resulting in an expected shift in molecular weight, which due to the large hydrodynamic radius of the PEG molecule is higher than proportionate to the molecular weight, similar as described for pSOX earlier (Belaidi, 2011). The original source found slightly higher enzymatic activity upon PEGylation of pSOX with high-molecular weight PEG molecules, while mSOX-Mo activity was highest with low molecular weight PEG molecules (Belaidi, 2011). Thus, as a modification compared to the original work, linear PEG with a size of 1.2 kDa instead of 5 kDa was utilized. Also, while excess PEG was originally removed via size exclusion chromatography, to reduce protein loss, removal of excess PEG was performed using a concentrator with a 30 kDa cutoff. An activity assay using the artificial electron acceptor ferricyanide, which is able to take up electrons directly from the Mo domain, verified normal Michaelis-Menten kinetics and full functionality of the enzyme despite the added PEG molecules (Fig. 9B) without loss of activity compared to values for unmodified mSOX-Mo from the literature (Belaidi, 2011).

I.p. injection of 50 pmol of PEGylated mSOX-Mo into *Suox*$^{-/-}$ mice resulted in a significant prolongation of the median life span from 7.6 ± 0.1 to 9.8 ± 0.7 days (Fig. 1), hence implying a sulfite detoxifying effect of mSOX-Mo *in vivo*. Contrary to the *Mocs1*$^{-/-}$ mice in the pilot study, however, *Suox*$^{-/-}$ mice were born healthy, but soon developed classic phenotypic characteristics including growth retardation and impairment of motor function. Notably, the protocol followed for treatment erroneously stated a single i.p. injection at day two after birth instead of continuous injection every second day starting at birth, thus resulting in a significantly lower dosage than required to see the highly beneficial results described before (Belaidi, 2011). *In vitro*, however, 2 pmol of PEGylated mSOX-Mo displayed a V_{max} of 11.2 ± 0.2 µM min^{-1} with a K_m of 50.6 ± 3.3 µM sulfite. As 65 µM of sulfite were detected in plasma of untreated *Suox*$^{-/-}$ mice at age P2.5 and a plateau of 150 µM sulfite was reached at P4.5 (Fig. 4A), 50 pmol of PEGylated mSOX-Mo were expected to result in sufficient sulfite clearance to prevent development of a disease phenotype. Presumably, despite the increased stability of the enzyme due to PEGylation, its half-life was too short to guarantee effective sulfite clearance over multiple days, so at

the time sulfite levels peaked in plasma, enzymatic activity was too low to prevent sulfite accumulation. As a single injection already resulted in a small, but significant increase of the survival time, though, a similarly protective effect of mSOX-Mo on *Suox*$^{-/-}$ pups as observed for pSOX on *Mocs1*$^{-/-}$ pups in the pilot study can be anticipated upon administration of the right dosage. Additionally, the study needs to be repeated with a higher dosage of mSOX-Mo to get more insights into potentially beneficial lowered H_2O_2 levels and thus decreased toxicity upon usage of mSOX-Mo rather than pSOX. In case H_2O_2 levels remain toxically high, simultaneous injection of catalase might be considered as a scavenging mechanism as described in cells earlier (Belaidi, 2011). Overall, enzyme replacement therapy using mSOX-Mo presents a highly promising therapeutic strategy for curing SOXD in mice and as a long-term goal also in human SOXD and MoCD patients.

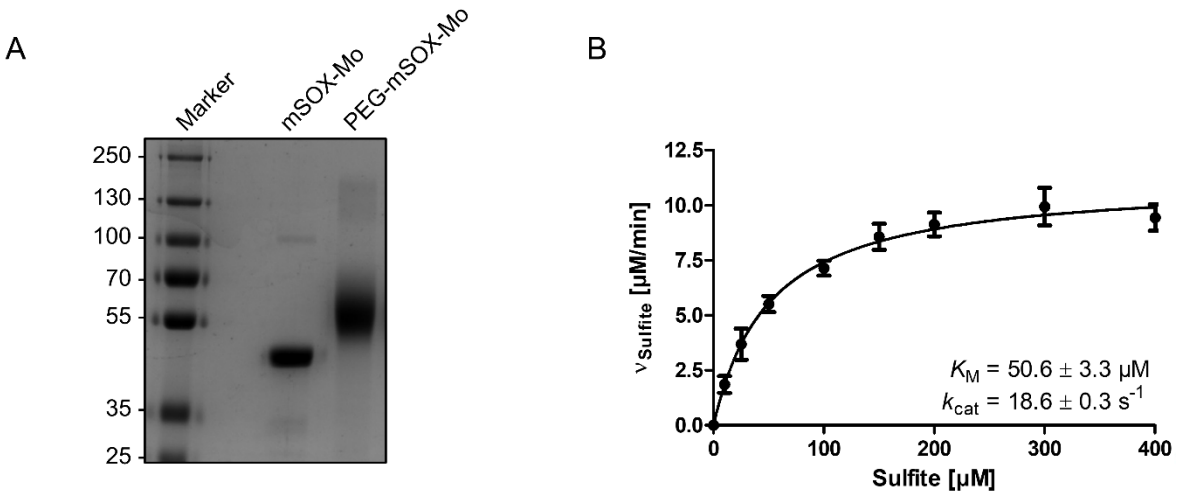

Figure 9: Characterization of PEGylated mSOX-Mo.
(A) SDS-PAGE analysis of mSOX-Mo after purification via Ni-NTA affinity chromatography and after PEGylation with 1.2 kDa linear PEG. (B) Steady-state activity of 10 nM PEGylated mSOX-Mo was measured using the artificial electron acceptor ferricyanide and varying sulfite concentrations in 100 mM Tris/Ac buffer pH 8.0. Measurements were performed as triplicates and data are depicted as mean ± standard deviation.

3.3 Conclusion

The results gained from the treatment strategies investigated in this study provide valuable knowledge needed for the successful establishment of a long-term therapy for SOXD. The most considerable difference in the pathomechanism of human and murine SOXD is the absence of a severe manifestation of the neurological phenotype in mice, which was further confirmed by ineffective memantine treatment. However, it remains to be determined to which extent parental memantine treatment would lead to significant NMDAR inhibition in neonatal mouse pups. This discrepancy between mice and humans complicates the development of a cure effective in both species and limits potential therapeutic strategies to more generalized physiological targets.

Dietary restriction proved difficult in mice, as restriction is only gained indirectly via the mother, which, depending on the level of restriction either resulted in too much stress leading to unproportionately high pup mortality or was not strong enough to show any improvement of the health condition of pups.

Sulfite scavenging also did not act beneficial on the phenotype of *Suox*$^{-/-}$ mice, which is in line with treatment attempts in humans (Tardy et al., 1989; Touati et al., 2000). Lack of data from biomarker analysis, however, limits the interpretation of this approach as it remains unclear to which extent the applied sulfite scavenging compounds were able to reduce sulfite levels in the mice.

The current study foreclosed ferroptosis as a major cell death pathway involved in the disease mechanism. In fact, prevention of ferroptosis during SOXD represents a novel, beneficial cellular mechanism resulting from loss of SOX function. Search for a cell death pathway accounting for the severe phenotype of SOXD represents an alternative treatment approach, which could be pursued in the future, but might be challenging due to the growing evidence of intimate links between different forms of regulated cell death (Cui et al., 2021).

Currently, the most feasible approach of SOXD treatment appears to be an enzyme replacement therapy using mSOX-Mo, which resulted in an improvement of the phenotype of *Suox*$^{-/-}$ mice following treatment with very low concentrations of enzyme in a first attempt. Therefore, optimization of the treatment protocol regarding concentration, route of administration and prevention of a potential H_2O_2 toxicity so far represents the most promising strategy in establishing a cure for SOXD in mice and humans.

3.4 Material and Methods

3.4.1 Material

3.4.1.1 Bacterial strains

Table 1: Utilized bacterial strains.

Strain	Genotype	Application	Reference
DH5α Turbo	*F' proA+B+ lacIq ΔlacZM15 / fhuA2 Δ(lac-proAB) glnV galK16 galE15 R(zgb-210::Tn10)TetS endA1 thi-1 Δ(hsdS-mcrB)5*	Plasmid amplification	New England Biolabs
TP1004	*ΔlacU169, araD139, rpsL150, relA1, flbB, deoC1, ptsF, rbsR, non-9, gyrA219, (ΔmobAB)*	Protein expression	Palmer et al., 1996

3.4.1.2 Eukaryotic cell lines

Table 2: Utilized eukaryotic cell lines.

Strain	Source	Description	Application
Primary hippocampal neurons	Mouse *(Mus musculus)*	Primary embryonic hippocampus-derived neurons	Toxicity studies
Primary cortical neurons	Mouse *(Mus musculus)*	Primary embryonic cortex-derived neurons	Toxicity studies

3.4.1.3 Plasmids

Table 3: Utilized plasmids.

Plasmid	Promotor	Resistance	Affinity tag	Source
pQE80L	T5	Ampicillin	N-terminal fusion of 6xHis-Tag	QIAGEN

3.4.1.4 Constructs

Table 4: Utilized constructs.

Construct	Vector	Purpose	Source
Mouse SOX Mo-domain	pQE80L	Protein expression	Abdel Belaidi, University of Cologne

3.4.1.5 Enzymes and chemicals

Enzymes and chemicals used during this study were purchased from Applichem (Darmstadt, Germany), Biozol (Eching, Germany), Carl-Roth (Karlsruhe, Germany),

Cayman Chemicals (Michigan, USA), Fermentas (St. Leon-Rot, Germany), GE Healthcare (Munich, Germany), Merck (Darmstadt, Germany), New England Biolabs (Frankfurt am Main, Germany), Roche (Mannheim, Germany), Sarstedt (Nürnbrecht, Germany), Sigma-Aldrich (Munich, Germany), ThermoFisher Scientific (Karlsruhe, Germany) and VWR (Darmstadt, Germany).

3.4.1.6 Mouse strains

C57BL/6N mice were obtained from breedings in the Institute of Genetics, University of Cologne, or purchased from Charles River Laboratories. Animals were kept in sterile conditions at 22°C and 12/12 h light/dark cycles. All breedings and experiments were performed in accordance with the German animal welfare act under surveillance of the local ethics committee (Landesamt für Natur, Umwelt und Verbraucherschutz (LANUV)). In compliance with the 3R principle, the number of mouse experiments (replacement), utilized animals (reduction) and their stress level (refinement) were reduced to a minimum. Euthanasia was performed by decapitation for pups and by cervical dislocation for older animals.

3.4.2 Cultivation of primary neurons

Primary hippocampal and cortical neurons were prepared from murine embryonic hippocampi and cortices (embryonic day 17.5) and cultured in poly-L-lysine coated 96-well plates with a density of 35,000 cells per well for hippocampus and 30,000 cells per well for cortex. Neurons were cultured in neurobasal medium supplemented with B-27, N-2 and glutamine (NB+/+).

3.4.3 MTT-based cell viability assay

Cell viability was analyzed in a colorimetric assay using the yellow dye 3-(4,5-dimethylthiazol-2-yl)-2,5-diphenyltetrazolium bromide (MTT), which in living cells is metabolized to insoluble purple-colored formazan. Primary neurons were grown as described above for 7-9 days *in vitro*, before overnight treatment with different metabolites and inhibitors was started. After 16h of incubation at 37°C, cells were treated with 10 µl of a 12 mM stock solution of MTT prepared in PBS followed by another incubation of 4h at 37°C. Subsequently, medium was exchanged to 100% DMSO and plates were again incubated for 15-20 mins at 37°C to resolve formed formazan. Cell viability was determined by measuring the absorption at 570 nm (reference 630 nm) using a well plate reader (Tecan Spark).

3.4.4 Treatment strategies

Administration of various potential therapeutic via intraperitoneal injection of 10 µl/ g bodyweight was performed using a Hamilton syringe (100 µl, point style 4, angle 12°, length 30 mm, VWR). In animals younger than P4.5, injection was done in the left side of the body below the liver at an angle of 90°. For older animals, injection was performed at a 45° angle into the lower right quadrant of the abdomen. Diets low in protein or sulfur-containing amino acids were purchased from Altromin as standard deficient diets C1003 and C1007, respectively. Memantine-supplemented chow was produced by Altromin as a customized diet.

3.4.5 Recombinant protein expression and purification of mSOX-Mo

Recombinant protein expression of His-tagged mouse SOX Mo-domain using the PQE80L vector was performed in the *E. coli* strain TP1004 (Palmer et al., 1996) in 2l LB-medium supplemented with 1 mM sodium molybdate in 5l Erlenmeyer flasks. IPTG-induced expression was performed for 72 h at 18°C and 80 rpm. Cells were harvested by centrifugation at 5000 rpm for 5 min. Cells were lysed in 30 ml lysis buffer (50 mM Tris/Ac pH 8.0, 300 mM NaCl, 10 mM Imidazole) per liter culture supplemented with protease inhibitor and 11 mg lysozyme (Sigma) per liter culture for 30 min while stirring at RT. Pellet suspensions were sonicated 3x30 sec with 15 sec pause at an amplitude of 40% and then disrupted utilizing an Emulsiflex C-5 cell disruptor (Avestin) at a pressure of 15,000-17,000 bar. After two runs, samples were centrifuged at 20,000 rpm and 4°C for 45 min to separate proteins from cell debris.

Purification via Ni-NTA affinity chromatography using 2.5 ml of HIS-Select® Nickel Affinity Gel (Sigma-Aldrich) per initial liter of culture. Prior to use, matrix was washed with 5 column volume (CV) water and was equilibrated by 5 CV lysis buffer. All following steps were performed at 4°C. Crude extracts were applied to the column and flow-through was discarded. The column was washed with lysis buffer, until the flow-through reached an OD_{280} < 0.15. Proteins bound to the Ni-NTA matrix were eluted with 3 CV elution buffer (50 mM Tris/Ac pH 8.0, 300 mM NaCl, 250 mM Imidazole). Eluted proteins were concentrated by centrifugation at 4°C and 4000 rpm in 5 min step using a concentrator with 30,000 Da cut-off (Sigma). Buffer exchange into protein storage buffer (20 mM Tris/Ac pH 8.0, 50 mM NaCl) was performed utilizing PD-10 desalting columns (GE Healthcare) and proteins were stored at -80°C until further use. Protein concentrations were determined using Coomassie Brilliant Blue G-250 (Roti®-Quant) according to (MM, 1976).

3.4.6 HPLC-based quantification of Moco

The amount of Moco-saturated protein was determined by oxidation and dephosphorylation of Moco to Form A and quantification via HPLC. In brief, 100 pmol of protein were diluted in 100 mM Tris/HCl pH 7.2 to a final volume of 140 µl. After addition of 17.5 µl acidic oxidation mix (17.5 µl 1.5/2.0% I_2/KI solution + 1.7 µl conc. HCl) samples were incubated overnight at RT in the dark. The next day, after samples were centrifuged at 15,000 rpm for 5 min, dephosphorylation was done by the addition of 20 µl freshly prepared 1% ascorbic acid. PH was adjusted to 8.3 by adding 70 µl 1 M Tris unbuffered. After the addition of 5 µl 1 M $MgCl_2$ and 0.5 µl alkaline phosphatase, samples were again incubated for 30 min at RT in the dark. Samples were centrifuged at 15,000 rpm for 10 min and then diluted 1:10 and 1:100 in ddH_2O to a final volume of 500 µl. Measurements were performed utilizing a high-performance liquid chromatography with a Reversed Phase Column (250 x 4,6 mm 5 µm C18, Dr. Maisch GmbH) and Form A HPLC buffers A (10 mM KH_2PO_4, pH 3.0) and B (100% methanol). Quantification of dephospho Form A was measuring the fluorescence of eluted compounds and comparison to a standard (excitation 370 nm, emission 450 nm).

3.4.7 SDS gel electrophoresis

A discontinuous sodium dodecyl sulfate polyacrylamide gel electrophoresis (SDS-PAGE) (Laemmli, 1970) was performed. Separation was done using a separation gel containing 8% or 12% acrylamide and a stacking gel containing 3.5% acrylamide. Prior to loading, samples were denatured and reduced by the addition of 5x SDS loading buffer (50% glycerol, 3.5% SDS, 15% β-mercaptoethanol, 0.02% bromophenol blue) and an incubation at 95°C for 5 min. Electrophoresis was done for 1-1.5 h at 35 mA per gel and 200 V in SDS running buffer (25 mM Tris, 192 mM glycine, 0.1% SDS, pH 8.3). Further analysis of the SDS gels was done by coomassie staining via incubation in Coomassie staining solution (40% methanol, 10% acetic acid, 0.2% Coomassie Brilliant Blue R-250) for 30 min. Gels were destained with destaining solution (40% methanol, 10% acetic acid) until bands were visible properly.

3.4.8 Enzyme PEGylation

PEGylation as a strategy to increase enzyme stability was performed as described earlier (Belaidi, 2011). In brief, a stock solution of linear PEG size 1.2 kDa was added to purified mSOX-Mo in PBS pH 8.0 in a 20:1 ratio followed by incubation under anaerobic conditions for 30 min. Removal of excess PEG was performed using a concentrator with a 30 kDa cutoff.

3.4.9 Sulfite:ferricyanide activity assay

To determine enzymatic activity of mouse SOX Mo-domain, steady-state kinetics of purified enzyme were measured in a well plate-based activity assay utilizing the artificial electron acceptor ferricyanide (FeCN). In brief, activity of final protein concentrations of 10 nM was measured in 100 mM Tris/Ac pH 8.0 using varying sodium sulfite concentrations from 0-300 µM. Reactions were started by the addition of sulfite up to a final volume of 200 µl. The change in absorption at 412 nm resulting from FeCN reduction was recorded in a well plate reader (BioTek ELx808^{TM}). Activity was calculated as the initial velocities using the Lambert-Beer Law with ε_{412nm} = 1040 $M^{-1}cm^{-1}$ and d = 0.857 cm. Results were plotted and fitted as Michaelis-Menten kinetics. Measurements were done in triplicates and depicted as means ± standard deviation.

3.4.10 Well plate-based CDO activity assay

Metabolization of D-cysteine was investigated in a well plate-based CDO activity assay using DTNB, a substance that is cleaved by sulfhydryl groups under the formation of a yellow compound. In brief, activity of 3 µM final CDO was measured in the presence of 0.3 mM ammonium iron(II) sulfate in 100 mM MES buffer pH 6.1. Reactions were started by the addition of 0.2 mM final L- or D-cysteine and stopped at various time points over 10 min by the addition of DTNB reagent mixture (0.1 mM DTNB in 100 mM Tris/HCl pH 8.0 final). The change in absorption resulting from residual cysteine was measured at 412 nm in a well plate reader (Tecan Spark®).

3.4.11 Lipid peroxidation analysis

Liver and kidney samples from wildtype and *Suox*$^{-/-}$ mice were taken at P8.5 after decapitation and immediately frozen in liquid nitrogen. Quantitative analysis of oxidized glycerophospholipids was performed by the CECAD Lipidomics Core Facility by mass spectrometric detection of endogenous lipids and comparison to an internal standard added to each sample prior to measurement.

3.5 References

Aghanoori, M. R., Shahriary, G. M., Safarpour, M., & Ebrahimi, A. (2016). Screening of a clinically and biochemically diagnosed SOD patient using exome sequencing: A case report with a mutations/variations analysis approach. *Egyptian Journal of Medical Human Genetics*, *17*(1), 131–136. https://doi.org/10.1016/J.EJMHG.2015.06.003

Al Shoyaib, A., Archie, S. R., & Karamyan, V. T. (2019). Intraperitoneal Route of Drug Administration: Should it Be Used in Experimental Animal Studies? *Pharmaceutical Research*, *37*(1), 12. https://doi.org/10.1007/S11095-019-2745-X

Badgley, M. A., Kremer, D. M., Carlo Maurer, H., DelGiorno, K. E., Lee, H. J., Purohit, V., Sagalovskiy, I. R., Ma, A., Kapilian, J., Firl, C. E. M., Decker, A. R., Sastra, S. A., Palermo,

C. F., Andrade, L. R., Sajjakulnukit, P., Zhang, L., Tolstyka, Z. P., Hirschhorn, T., Lamb, C., … Olive, K. P. (2020). Cysteine depletion induces pancreatic tumor ferroptosis in mice. *Science (New York, N.Y.)*, *368*(6486). https://doi.org/10.1126/SCIENCE.AAW9872

Bannai, S. (1986). Exchange of cystine and glutamate across plasma membrane of human fibroblasts. *Journal of Biological Chemistry*, *261*(5), 2256–2263. https://doi.org/10.1016/S0021-9258(17)35926-4

Belaidi, A. A. (2011). *Human Molybdenum Cofactor Biosynthesis and Deficiency: Novel Functions and Therapies*.

Belaidi, A. A., Roper, J., Arjune, S., Krizowski, S., Trifunovic, A., & Schwarz, G. (2015). Oxygen reactivity of mammalian sulfite oxidase provides a concept for the treatment of sulfite oxidase deficiency. *Biochemical Journal*, *469*, 211–221. https://doi.org/10.1042/Bj20140768

Booth, J., Boyland, E., & Sims, P. (1961). An enzyme from rat liver catalysing conjugations with glutathione. *Biochemical Journal*, *79*(3), 516. https://doi.org/10.1042/BJ0790516

Boyer, M., Sowa, M., Wang, R., & Abdenur, J. (2019). Isolated Sulfite Oxidase Deficiency: Response to Dietary Treatment in a Patient with Severe Neonatal Presentation. *Journal of Inborn Errors of Metabolism and Screening*, *7*, e20190001. https://doi.org/10.1590/2326-4594-JIEMS-2019-0001

Brancaleone, V., Esposito, I., Gargiulo, A., Vellecco, V., Asimakopoulou, A., Citi, V., Calderone, V., Gobbetti, T., Perretti, M., Papapetropoulos, A., Bucci, M., & Cirino, G. (2016). d-Penicillamine modulates hydrogen sulfide (H2S) pathway through selective inhibition of cystathionine-γ-lyase. *British Journal of Pharmacology*, *173*(9), 1556–1565. https://doi.org/10.1111/BPH.13459

Chan, W. W. C. (1968). A Method for the Complete S Sulfonation of Cysteine Residues in Proteins. *Biochemistry*, *7*(12), 4247–4254. https://doi.org/10.1021/BI00852A016

Claerhout, H., Witters, P., Régal, L., Jansen, K., Van Hoestenberghe, M. R., Breckpot, J., & Vermeersch, P. (2018). Isolated sulfite oxidase deficiency. *Journal of Inherited Metabolic Disease*, *41*(1), 101–108. https://doi.org/10.1007/S10545-017-0089-4

Cui, J., Zhao, S., Li, Y., Zhang, D., Wang, B., Xie, J., & Wang, J. (2021). Regulated cell death: discovery, features and implications for neurodegenerative diseases. *Cell Communication and Signaling*, *19*(1), 1–29. https://doi.org/10.1186/S12964-021-00799-8/TABLES/1

Dedeoglu, A., Kubilus, J. K., Jeitner, T. M., Matson, S. A., Bogdanov, M., Kowall, N. W., Matson, W. R., Cooper, A. J., Ratan, R. R., Beal, M. F., Hersch, S. M., & Ferrante, R. J. (2002). Therapeutic effects of cystamine in a murine model of Huntington's disease. *J Neurosci*, *22*(20), 8942–8950. https://www.ncbi.nlm.nih.gov/pubmed/12388601

Derrickson, E. M., & Lowas, S. R. (2007). The effects of dietary protein levels on milk protein levels and postnatal growth in laboratory mice (Mus musculus). *Journal of Mammalogy*, *88*(6), 1475–1481. https://doi.org/10.1644/06-MAMM-A-253R2.1/2/JMAMMAL-88-6-1475-FIG4.JPEG

Dixon, S. J., Lemberg, K. M., Lamprecht, M. R., Skouta, R., Zaitsev, E. M., Gleason, C. E., Patel, D. N., Bauer, A. J., Cantley, A. M., Yang, W. S., Morrison 3rd, B., & Stockwell, B. R. (2012). Ferroptosis: an iron-dependent form of nonapoptotic cell death. *Cell*, *149*(5), 1060–1072. https://doi.org/10.1016/j.cell.2012.03.042

Dóka, Ida, T., Dagnell, M., Abiko, Y., Luong, N. C., Balog, N., Takata, T., Espinosa, B., Nishimura, A., Cheng, Q., Funato, Y., Miki, H., Fukuto, J. M., Prigge, J. R., Schmidt, E. E., Arnér, E. S. J., Kumagai, Y., Akaike, T., & Nagy, P. (2020). Control of protein function through oxidation and reduction of persulfidated states. *Science Advances*, *6*(1). https://doi.org/10.1126/SCIADV.AAX8358/SUPPL_FILE/AAX8358_SM.PDF

Dublin, A. B., Hald, J. K., & Wootton-Gorges, S. L. (2002). Isolated Sulfite Oxidase Deficiency: MR Imaging Features. *AJNR: American Journal of Neuroradiology*, *23*(3), 484. /pmc/articles/PMC7975306/

Footitt, E. J., Heales, S. J., Mills, P. B., Allen, G. F. G., Oppenheim, M., & Clayton, P. T. (2011). Pyridoxal 5'-phosphate in cerebrospinal fluid; factors affecting concentration. *Journal of Inherited Metabolic Disease*, *34*(2), 529–538. https://doi.org/10.1007/S10545-011-9279-7

Friedmann Angeli, J. P., Schneider, M., Proneth, B., Tyurina, Y. Y., Tyurin, V. A., Hammond, V. J., Herbach, N., Aichler, M., Walch, A., Eggenhofer, E., Basavarajappa, D., Radmark, O., Kobayashi, S., Seibt, T., Beck, H., Neff, F., Esposito, I., Wanke, R., Forster, H., … Conrad, M. (2014). Inactivation of the ferroptosis regulator Gpx4 triggers acute renal failure in mice. *Nat Cell Biol*, *16*(12), 1180–1191. https://doi.org/10.1038/ncb3064

Hahnewald, R. (2009). Tiermodelle der Molybdän-Cofaktor-Defizienz und ihre Therapie.

Hänsch, R., Lang, C., Riebeseel, E., Lindigkeit, R., Gessler, A., Rennenberg, H., & Mendel, R. R. (2006). Plant Sulfite Oxidase as Novel Producer of H2O2. *Journal of Biological Chemistry*, *281*(10), 6884–6888. https://doi.org/10.1074/jbc.m513054200

Hille, R. (1994). The reaction mechanism of oxomolybdenum enzymes. *Biochimica et Biophysica Acta (BBA) - Bioenergetics*, *1184*(2–3), 143–169. https://doi.org/10.1016/0005-2728(94)90220-8

Huijmans, J. G. M., Schot, R., de Klerk, J. B. C., Williams, M., de Coo, R. F. M., Duran, M., Verheijen, F. W., van Slegtenhorst, M., & Mancini, G. M. S. (2017). Molybdenum cofactor deficiency: Identification of a patient with homozygote mutation in the MOCS3 gene. *American Journal of Medical Genetics Part A*, *173*(6), 1601–1606. https://doi.org/10.1002/AJMG.A.38240

Jakoby, W. B. (1978). The glutathione S-transferases: a group of multifunctional detoxification proteins. *Advances in Enzymology and Related Areas of Molecular Biology*, *46*, 383–414. https://doi.org/10.1002/9780470122914.CH6

Jakubiczka-Smorag, J., Santamaria-Araujo, J. A., Metz, I., Kumar, A., Hakroush, S., Brueck, W., Schwarz, G., Burfeind, P., Reiss, J., & Smorag, L. (2016). Mouse model for molybdenum cofactor deficiency type B recapitulates the phenotype observed in molybdenum cofactor deficient patients. *Human Genetics*, *135*(7), 813–826. https://doi.org/10.1007/s00439-016-1676-4

Jocelyn, P. C. (1987). Chemical reduction of disulfides. *Methods Enzymol*, *143*, 246–256. https://doi.org/10.1016/0076-6879(87)43048-6

Johnson, J. L., Coyne, K. E., Garrett, R. M., Zabot, M. T., Dorche, C., Kisker, C., & Rajagopalan, K. V. (2002). Isolated sulfite oxidase deficiency: identification of 12 novel SUOX mutations in 10 patients. *Hum Mutat*, *20*(1), 74. https://doi.org/10.1002/humu.9038

Johnson, J. L., & Duran, M. (2001). Molybdenum cofactor deficiency and isolated sulfite oxidase deficiency. In *The Metabolic and Molecular Bases of Inherited Disease* (pp. 3163–3177). Mcgraw-Hill Professional.

Kella, N. K. D., & Kinsella, J. E. (1985). A method for the controlled cleavage of disulfide bonds in proteins in the absence of denaturants. *Journal of Biochemical and Biophysical Methods*, *11*(4–5), 251–263. https://doi.org/10.1016/0165-022X(85)90007-7

Kisker, C., Schindelin, H., Pacheco, A., Wehbi, W. A., Garrett, R. M., Rajagopalan, K. V., Enemark, J. H., & Rees, D. C. (1997). Molecular Basis of Sulfite Oxidase Deficiency from the Structure of Sulfite Oxidase. *Cell*, *91*(7), 973–983. https://doi.org/10.1016/S0092-8674(00)80488-2

Kohl, J. B. (2019). A Novel Mouse Model of Sulfite Oxidase Deficiency: Pathological Changes in Cysteine and H2S Metabolism. In *Department of Chemistry*.

Kohl, J. B., Mellis, A. T., & Schwarz, G. (2019). Homeostatic impact of sulfite and hydrogen sulfide on cysteine catabolism. *British Journal of Pharmacology*, *176*(4), 554–570. https://doi.org/10.1111/BPH.14464

Kříž, L., Bičíková, M., & Hampl, R. (2008). Roles of steroid sulfatase in brain and other tissues. *Physiological Research*, *57*(5), 657–668. https://doi.org/10.33549/PHYSIOLRES.931207

Kumar, A. (2016). Molecular Mechanism of Neurodegeneration in Molybdenum Cofactor Deficency:

Kumar, A., Dejanovic, B., Hetsch, F., Semtner, M., Fusca, D., Arjune, S., Santamaria-Araujo, J. A., Winkelmann, A., Ayton, S., Bush, A. I., Kloppenburg, P., Meier, J. C., Schwarz, G., & Belaidi, A. A. (2017). S-sulfocysteine/NMDA receptor-dependent signaling underlies neurodegeneration in molybdenum cofactor deficiency. *J Clin Invest*, *127*(12), 4365–4378. https://doi.org/10.1172/JCI89885

Kurlemann, G., Debus, O., & Schuierer, G. (1996). Dextrometorphan in molybdenum cofactor deficiency [3]. *European Journal of Pediatrics*, *155*(5), 422–423. https://doi.org/10.1007/BF01955280/METRICS

Laemmli, U. K. (1970). Cleavage of structural proteins during the assembly of the head of bacteriophage T4. *Nature*, *227*(5259), 680–685. https://doi.org/10.1038/227680A0

Lee, H. J., Adham, I. M., Schwarz, G., Kneussel, M., Sass, J. O., Engel, W., & Reiss, J. (2002). Molybdenum cofactor-deficient mice resemble the phenotype of human patients. *Human Molecular Genetics*, *11*(26), 3309–3317. https://doi.org/10.1093/HMG/11.26.3309

Lyons, J., Rauh-Pfeiffer, A., Yu, Y. M., Lu, X. M., Zurakowski, D., Tompkins, R. G., Ajami, A. M., Young, V. R., & Castillo, L. (2000). Blood glutathione synthesis rates in healthy adults receiving a sulfur amino acid-free diet. *Proceedings of the National Academy of Sciences of the United States of America*, *97*(10), 5071–5076. https://doi.org/10.1073/PNAS.090083297/ASSET/E70EDE2E-255C-4C9C-A006-E37D22C896CC/ASSETS/GRAPHIC/PQ0900832002.JPEG

Mellis, A. T. (2020). *Sulfite Metabolism in Health and Disease: Biogenesis, Biochemical Changes and Mitochondrial Morphology*.

Mellis, A. T., Misko, A. L., Arjune, S., Liang, Y., Erdelyi, K., Ditroi, T., Kaczmarek, A. T., Nagy, P., & Schwarz, G. (2021). The role of glutamate oxaloacetate transaminases in sulfite biosynthesis and H2S metabolism. *Redox Biol*, *38*, 101800. https://doi.org/10.1016/j.redox.2020.101800

Mellis, A. T., Roeper, J., Misko, A. L., Kohl, J., & Schwarz, G. (2021). Sulfite Alters the Mitochondrial Network in Molybdenum Cofactor Deficiency. *Frontiers in Genetics*, *11*, 1672. https://doi.org/10.3389/FGENE.2020.594828/BIBTEX

Mills, P. B., Footitt, E. J., Ceyhan, S., Waters, P. J., Jakobs, C., Clayton, P. T., & Struys, E. A. (2012). Urinary AASA excretion is elevated in patients with molybdenum cofactor deficiency and isolated sulphite oxidase deficiency. *Journal of Inherited Metabolic Disease*, *35*(6), 1031–1036. https://doi.org/10.1007/S10545-012-9466-1

Mills, P. B., Surtees, R. A. H., Champion, M. P., Beesley, C. E., Dalton, N., Scamber, P. J., Heales, S. J. R., Briddon, A., Scheimberg, I., Hoffmann, G. F., Zschocke, J., & Clayton, P. T. (2005). Neonatal epileptic encephalopathy caused by mutations in the PNPO gene encoding pyridox(am)ine 5′-phosphate oxidase. *Human Molecular Genetics*, *14*(8), 1077–1086. https://doi.org/10.1093/HMG/DDI120

Misko, A. L., Liang, Y., Kohl, J. B., & Eichler, F. (2020). Delineating the phenotypic spectrum of sulfite oxidase and molybdenum cofactor deficiency. *Neurology: Genetics*, *6*(4). https://doi.org/10.1212/NXG.0000000000000486

MM, B. (1976). A rapid and sensitive method for the quantitation of microgram quantities of protein utilizing the principle of protein-dye binding. *Analytical Biochemistry*, *72*(1–2), 248–254. https://doi.org/10.1006/ABIO.1976.9999

Moles, A., Rizzi, R., & D'Amato, F. R. (2004). Postnatal Stress in Mice: Does "Stressing" the Mother Have the Same Effect as "Stressing" the Pups? *Developmental Psychobiology*, *44*(4), 230–237. https://doi.org/10.1002/DEV.20008

Nichenametla, S. N., Mattocks, D. A. L., Midya, V., & Shneyder, J. (2021). Differential Effects of Sulfur Amino Acid-Restricted and Low-Calorie Diets on Gut Microbiome Profile and Bile Acid Composition in Male C57BL6/J Mice. *The Journals of Gerontology Series A: Biological Sciences and Medical Sciences*, *76*(11), 1922. https://doi.org/10.1093/GERONA/GLAA270

Nucci, M. L., Shorr, R., & Abuchowski, A. (1991). The therapeutic value of poly(ethylene glycol)-modified proteins. *Advanced Drug Delivery Reviews*, *6*(2), 133–151. https://doi.org/10.1016/0169-409X(91)90037-D

Olney, J. W., Misra, C. H., & de Gubareff, T. (1975). Cysteine-S-sulfate: brain damaging metabolite in sulfite oxidase deficiency. *J Neuropathol Exp Neurol*, *34*(2), 167–177. https://doi.org/10.1097/00005072-197503000-00005

Ono, H., & Ito, A. (1984). Transport of the Precursor for Sulfite Oxidase into Intermembrane Space of Liver Mitochondria: Characterization of Import and Processing Activities. *The Journal of Biochemistry*, *95*(2), 345–352. https://doi.org/10.1093/OXFORDJOURNALS.JBCHEM.A134614

Palmer, T., Santini, C. L., Iobbi-Nivol, C., Eaves, D. J., Boxer, D. H., & Giordano, G. (1996). Involvement of the narJ and mob gene products in distinct steps in the biosynthesis of the molybdoenzyme nitrate reductase in Escherichia coli. *Molecular Microbiology*, *20*(4), 875–884. https://doi.org/10.1111/J.1365-2958.1996.TB02525.X

Percudani, R., & Peracchi, A. (2003). A genomic overview of pyridoxal-phosphate-dependent enzymes. *EMBO Reports*, *4*(9), 850. https://doi.org/10.1038/SJ.EMBOR.EMBOR914

Reiss, J., Bonin, M., Schwegler, H., Sass, J. O., Garattini, E., Wagner, S., Lee, H. J., Engel, W., Riess, O., & Schwarz, G. (2005). The pathogenesis of molybdenum cofactor deficiency, its delay by maternal clearance, and its expression pattern in microarray analysis. *Molecular Genetics and Metabolism*, *85*(1), 12–20. https://doi.org/DOI 10.1016/j.ymgme.2005.01.008

Reiss, J., Christensen, E., Kurlemann, G., Zabot, M. T., & Dorche, C. (1998). Genomic structure and mutational spectrum of the bicistronic MOCS1 gene defective in molybdenum cofactor deficiency type A. *Human Genetics 1998 103:6*, *103*(6), 639–644. https://doi.org/10.1007/S004390050884

Reiss, J., Gross-Hardt, S., Christensen, E., Schmidt, P., Mendel, R. R., & Schwarz, G. (2001). A mutation in the gene for the neurotransmitter receptor-clustering protein gephyrin causes a novel form of molybdenum cofactor deficiency. *American Journal of Human Genetics*, *68*(1), 208–213. https://doi.org/Doi 10.1086/316941

Reiss, J., & Hahnewald, R. (2011). Molybdenum cofactor deficiency: Mutations in GPHN, MOCS1, and MOCS2. *Human Mutation*, *32*(1), 10–18. https://doi.org/10.1002/HUMU.21390

Rivett, A. J., Eddy, B. J., & Roth, J. A. (1982). Contribution of sulfate conjugation, deamination, and O-methylation to metabolism of dopamine and norepinephrine in human brain. *Journal of Neurochemistry*, *39*(4), 1009–1016. https://doi.org/10.1111/J.1471-4159.1982.TB11490.X

Rupar, C. A., Gillett, J., Gordon, B. A., Ramsay, D. A., Johnson, J. L., Garrett, R. M., Rajagopalan, K. V., Jung, J. H., Bacheyie, G. S., & Sellers, A. R. (1996). Isolated sulfite oxidase deficiency. *Neuropediatrics*, *27*(6), 299–304. https://doi.org/10.1055/S-2007-973798/BIB

Sardesai, V. M., Requests, R., Sardesai, : V M, & Sardesai, V. M. (1995). Role of Antioxidants in Health Maintenance. *Nutrition in Clinical Practice*, *10*(1), 19–25. https://doi.org/10.1177/011542659501000119

Schwahn, B. C., Galloway, P. G., Bowhay, S., Veldman, A., Santamaria, J. A., Schwarz, G., & Belaidi, A. A. (2010). Successful Treatment of Two Neonates with Molybdenum Cofactor Deficiency (Mocd) Type a, Using Cyclic Pyranopterine Monophosphate (Cpmp). *Journal of Inherited Metabolic Disease*, *33*, S29–S29. <Go to ISI>://WOS:000281735000038

Seiler, A., Schneider, M., Förster, H., Roth, S., Wirth, E. K., Culmsee, C., Plesnila, N., Kremmer, E., Rådmark, O., Wurst, W., Bornkamm, G. W., Schweizer, U., & Conrad, M. (2008). Glutathione peroxidase 4 senses and translates oxidative stress into 12/15-lipoxygenase dependent- and AIF-mediated cell death. *Cell Metabolism*, *8*(3), 237–248. https://doi.org/10.1016/J.CMET.2008.07.005

Semple, B. D., Blomgren, K., Gimlin, K., Ferriero, D. M., & Noble-Haeusslein, L. J. (2013). Brain development in rodents and humans: Identifying benchmarks of maturation and vulnerability to injury across species. *Progress in Neurobiology*, *0*, 1. https://doi.org/10.1016/J.PNEUROBIO.2013.04.001

Sharawat, I. K., Saini, L., Singanamala, B., Saini, A. G., Sahu, J. K., Attri, S. V., & Sankhyan, N. (2020). Metabolic crisis after trivial head trauma in late-onset isolated sulfite oxidase deficiency: Report of two new cases and review of published patients. *Brain and Development*, *42*(2), 157–164. https://doi.org/10.1016/J.BRAINDEV.2019.11.003

Shibui, Y., Sakai, R., Manabe, Y., & Masuyama, T. (2017). Comparisons of l-cysteine and d-cysteine toxicity in 4-week repeated-dose toxicity studies of rats receiving daily oral administration. *Journal of Toxicologic Pathology*, *30*(3), 217. https://doi.org/10.1293/TOX.2017-0002

Smolin, L. A., Clark, K. F., Thoene, J. G., Gahl, W. A., & Schneider, J. A. (1988). A comparison of the effectiveness of cysteamine and phosphocysteamine in elevating plasma

cysteamine concentration and decreasing leukocyte free cystine in nephropathic cystinosis. *Pediatr Res*, *23*(6), 616–620. https://doi.org/10.1203/00006450-198806000-00018

Stallmeyer, B., Drugeon, G., Reiss, J., Haenni, A. L., & Mendel, R. R. (1999). Human molybdopterin synthase gene: identification of a bicistronic transcript with overlapping reading frames. *American Journal of Human Genetics*, *64*(3), 698–705. https://doi.org/10.1086/302295

Tan, W. H., Eichler, F. S., Hoda, S., Lee, M. S., Baris, H., Hanley, C. A., Grant, P. E., Krishnamoorthy, K. S., & Shih, V. E. (2005). Isolated sulfite oxidase deficiency: a case report with a novel mutation and review of the literature. *Pediatrics*, *116*(3), 757–766. https://doi.org/10.1542/peds.2004-1897

Tardy, P., Parvy, P., Charpentier, C., Bonnefont, J. P., Saudubray, J. M., & Kamoun, P. (1989). Attempt at therapy in sulphite oxidase deficiency. *Journal of Inherited Metabolic Disease*, *12*(1), 94–95. https://doi.org/10.1007/BF01805537

Tian, M., Qu, Y., Huang, L., Su, X., Li, S., Ying, J., Zhao, F., & Mu, D. (2019). Stable clinical course in three siblings with late-onset isolated sulfite oxidase deficiency: a case series and literature review. *BMC Pediatrics 2019 19:1*, *19*(1), 1–8. https://doi.org/10.1186/S12887-019-1889-5

Touati, G., Rusthoven, E., Depondt, E., Dorche, C., Duran, M., Heron, B., Rabier, D., Russo, M., & Saudubray, J. M. (2000). Dietary therapy in two patients with a mild form of sulphite oxidase deficiency. Evidence for clinical and biological improvement. *Journal of Inherited Metabolic Disease*, *23*(1), 45–53. https://doi.org/10.1023/A:1005646813492

Upadhyayula, P. S., Higgins, D. M., Mela, A., Banu, M., Dovas, A., Zandkarimi, F., Patel, P., Mahajan, A., Humala, N., Nguyen, T. T. T., Chaudhary, K. R., Liao, L., Argenziano, M., Sudhakar, T., Sperring, C. P., Shapiro, B. L., Ahmed, E. R., Kinslow, C., Ye, L. F., … Canoll, P. (2023). Dietary restriction of cysteine and methionine sensitizes gliomas to ferroptosis and induces alterations in energetic metabolism. *Nature Communications*, *14*(1). https://doi.org/10.1038/S41467-023-36630-W

Victorino, D. B., Bederman, I. R., & Costa, A. C. S. (2017). Pharmacokinetic Properties of Memantine after a Single Intraperitoneal Administration and Multiple Oral Doses in Euploid Mice and in the Ts65Dn Mouse Model of Down's Syndrome. *Basic Clin Pharmacol Toxicol*, *121*(5), 382–389. https://doi.org/10.1111/bcpt.12816

Weber, E. M., Algers, B., Hultgren, J., & Olsson, I. A. S. (2013). Pup mortality in laboratory mice--infanticide or not? *Acta Veterinaria Scandinavica*, *55*(1), 83. https://doi.org/10.1186/1751-0147-55-83/FIGURES/5

Woo, W. H., Yang, H., Wong, K. P., & Halliwell, B. (2003). Sulphite oxidase gene expression in human brain and in other human and rat tissues. *Biochemical and Biophysical Research Communications*, *305*(3), 619–623. https://doi.org/10.1016/S0006-291X(03)00833-7

Wyse, A. T. S., Grings, M., Wajner, M., & Leipnitz, G. (2018). The Role of Oxidative Stress and Bioenergetic Dysfunction in Sulfite Oxidase Deficiency: Insights from Animal Models. *Neurotoxicity Research 2018 35:2*, *35*(2), 484–494. https://doi.org/10.1007/S12640-018-9986-Z

Yang, W. S., Sriramaratnam, R., Welsch, M. E., Shimada, K., Skouta, R., Viswanathan, V. S., Cheah, J. H., Clemons, P. A., Shamji, A. F., Clish, C. B., Brown, L. M., Girotti, A. W., Cornish, V. W., Schreiber, S. L., & Stockwell, B. R. (2014). Regulation of Ferroptotic Cancer Cell Death by GPX4. *Cell*, *156*(0), 317. https://doi.org/10.1016/J.CELL.2013.12.010

Zhang, X., Vincent, A., Halliwell, B., & Wong, K. (2004). A Mechanism of Sulfite Neurotoxicity DIRECT INHIBITION OF GLUTAMATE DEHYDROGENASE*. *Journal of Biological Chemistry*, *279*, 43035–43045. https://doi.org/10.1074/jbc.M402759200

Zilka, O., Shah, R., Li, B., Friedmann Angeli, J. P., Griesser, M., Conrad, M., & Pratt, D. A. (2017). On the Mechanism of Cytoprotection by Ferrostatin-1 and Liproxstatin-1 and the Role of Lipid Peroxidation in Ferroptotic Cell Death. *ACS Central Science*, *3*(3), 232–243. https://doi.org/10.1021/ACSCENTSCI.7B00028/ASSET/IMAGES/LARGE/OC-2017-000286_0007.JPEG

Zivanovic, J., Kouroussis, E., Kohl, J., Adhikari, B., Bursac, B., Schott-Roux, S., Petrovic, D., Miljkovic, J., Thomas-Lopez, D., Jung, Y., Miler, M., Mitchell, S., Milosevic, V., Gomes, J., Benhar, M., Gonzales-Zorn, B., Ivanovic-Burmazovic, I., Torregrossa, R., Mitchell, J., … Filipovic, M. (2019). Selective Persulfide Detection Reveals Evolutionarily Conserved Antiaging Effects of S-Sulfhydration. *Cell Metabolism*, *30*(6), 1152-1170.e13. https://doi.org/10.1016/J.CMET.2019.10.007

3.6 Supplementary Information

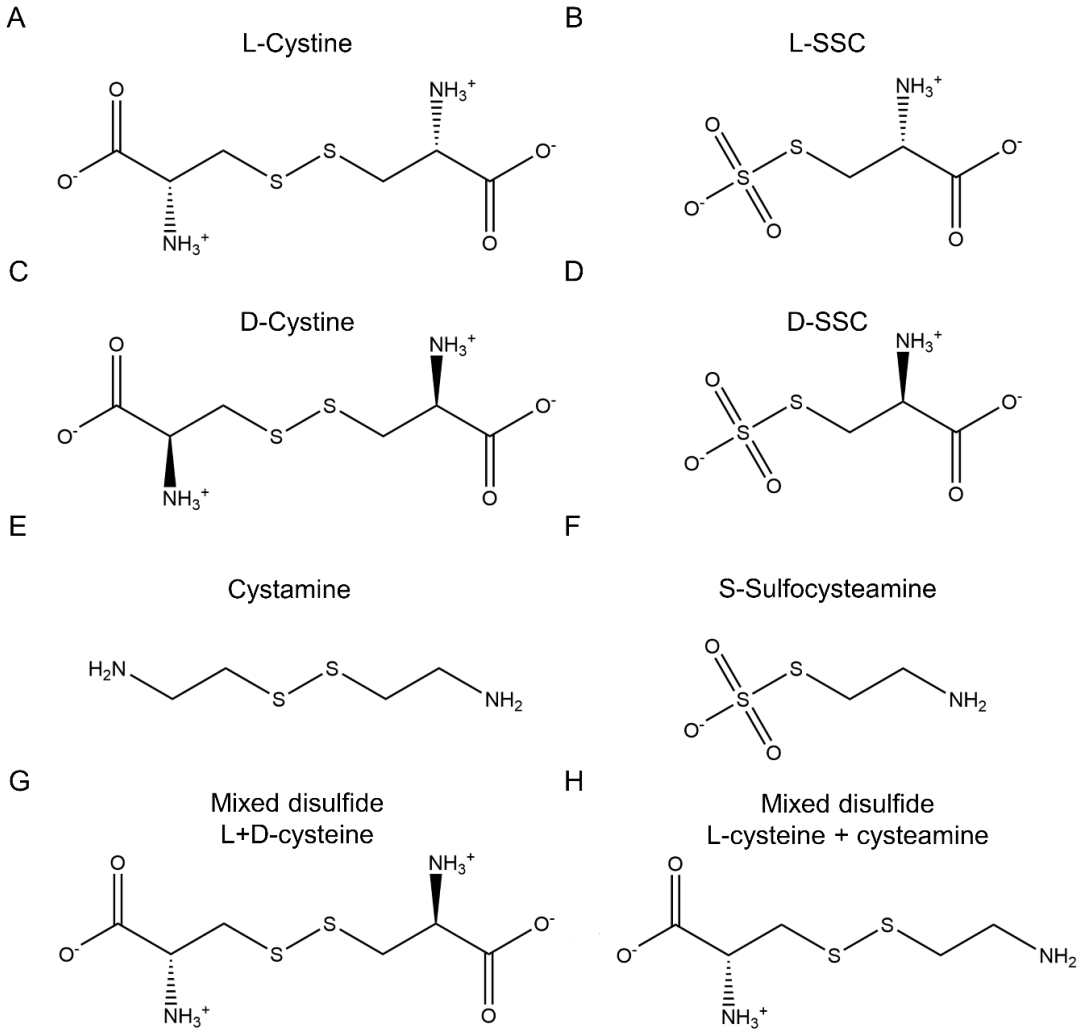

Supplementary Figure 1: Chemical structures of sulfite scavengers and formed reaction products.
(A,C,E) Disulfides used as sulfite scavengers. (B,D,F) Reaction products formed from reaction of chemical sulfite scavengers in reaction with sulfite. (G+H) Mixed disulfides formed from one molecule L-cysteine and one molecule (G) D-cysteine and (H) cysteamine. Reaction with sulfite thus results in 50% toxic L-SSC and 50% scavenged sulfite.

IV Novel, postnatal manifestation of an epidermal barrier defect in a mouse model of isolated sulfite oxidase deficiency

Lena Johannes[1], Julia Löhr[2], Matthias Rübsam[2], Xiaolei Ding[3], Sabine Eming[3], Carien Niessen[2], Günter Schwarz[1]

[1]Institute for Biochemistry, Department of Chemistry, University of Cologne, Cologne, Germany, [2]CECAD Research Center, University of Cologne, Cologne, Germany, [3]Department of Dermatology, University Hospital Cologne, Cologne, Germany

In preparation

Author contributions:
Lena Johannes, Günter Schwarz, Carien Niessen and Sabine Eming conceptualized this study. The manuscript was written by Lena Johannes and reviewed by Günter Schwarz and Carien Niessen. Mouse work, data analysis and figure preparation were performed by Lena Johannes. Sample preparation was done by Lena Johannes and Julia Löhr. Stainings and microscopy pictures were done by Julia Löhr, Matthias Rübsam and Lena Johannes. QPCR analysis was performed by Xiaolei Ding.

4.1 To the Editor

Isolated sulfite oxidase deficiency (SOXD) is a rare metabolic disorder typically presenting with postnatal intractable seizures and progressive neurodegeneration, resulting in infant death if left untreated (Johnson & Duran, 2001). It is caused by a loss of function of the enzyme sulfite oxidase (SOX), which catalyzes the clearance of sulfite via oxidation to sulfate as the final step of cysteine catabolism (Irreverre et al., 1967). A loss in SOX activity results in an accumulation of toxic sulfite and elevated levels of the sulfur metabolites taurine, thiosulfate and S-sulfocysteine. Due to its structural resemblance to glutamate, S-sulfocysteine acts as an NMDA receptor agonist, thus causing vast excitotoxicity and manifestation of a progressive neurological phenotype (Kumar et al., 2017).

Recently, a mouse model for SOXD has been successfully established through inactivation of the *Suox* gene (Kohl, 2019). Heterozygous animals develop wildtype-like without visible phenotype. Homozygous *Suox*$^{-/-}$ mice are born healthy as well, presumably due to maternal clearance of excess sulfur metabolites, but starting around postnatal day 4 display growth retardation and decreased neuromotor abilities, and die between P6 and P12 with an average survival time of 9.6 days. However, brain morphological analysis shortly before death did not reveal significant abnormalities, thus excluding neurodegeneration as major cause of death, indicating different pathomechanisms and

causes of death for *Suox*$^{-/-}$ mice and human SOXD patients (Kohl, Fu et al., in preparation). Here we report the postnatal development of dry and scaly skin in *Suox*$^{-/-}$ mice, which suggested the manifestation of an underlying epidermal phenotype.

Initially, newborn *Suox*$^{-/-}$ mice displayed normal epidermal morphology in H&E stained histological sections of back skin at P0 with no change in localization of keratin (K) 14, marking the proliferating basal layer, and K10, an early differentiation marker that marks all suprabasal layers (Fuchs & Green, 1980). Moreover, staining for Ki67 demonstrated similar proliferation between control and *Suox*$^{-/-}$ newborn mice. Together, these data indicate that the skin epidermis develops normally *in utero* upon loss of SOX, similar to the brain.

At P5, H&E histochemical analysis revealed a significant increase in epidermal thickness in homozygous *Suox*$^{-/-}$ animals. Upon closer examination, cells in the stratum basale (SB) displayed an increased size and distance towards each other, while the stratum spinosum (SS) showed an overall increased thickness. The stratum granulosum (SG) appeared thinner, containing less cell layers, while cells in the stratum corneum (SC) showed decreased structural organization and parakeratosis. Expression of basal cell marker K14 was highly increased, as it was stained not only in the SB, but also in suprabasal cell layers. In contrast, intensity of K10, which promotes terminal differentiation of keratinocytes, was reduced. Mice showing altered expression of K14 and K10 also revealed an increased number of cells positive for proliferation marker Ki67, thus pointing towards hyperproliferation in combination with a defect in differentiation.

To further elucidate the possibility of altered terminal differentiation, late stage differentiation markers involucrin, filaggrin and loricrin were examined. Involucrin displayed wildtype-like expression in all tested samples. In contrast, filaggrin showed an abnormal expression pattern only starting in SC and residual SG and thus very late in differentiation, while loricrin intensity was severely reduced overall, hence verifying impaired terminal differentiation. This was accompanied by an increase in the expression of hyperproliferation-associated stress keratin K6a, whose expression is typically induced in stressed keratinocytes at the suprabasal layers of the epidermis upon wounding or inflammation (Zhang, 2018).

Quantitative PCR analysis revealed no significant alteration in the expression of most inflammatory genes, however, *Il1b* RNA levels were significantly elevated. Previously, IL-1β was shown to induce the expression of K6a (Komine et al., 2001), while additionally activating transcription factor NF-κB, which causes the downregulation of filaggrin and loricrin expression (Michaelidou et al., 2023). Moreover, RNA levels of *Tslp* were vastly

elevated. In humans, cytokine TSLP was found to impair epidermal barrier integrity by upregulating the expression of nuclear cytokine IL-33, which in turn is involved in the downregulation of loricrin, filaggrin and K10 expression (Dai et al., 2021, 2022). Thus, the observed overexpression of IL-1β and TSLP presumably contributes to the altered expression patterns of respective marker proteins in our *Suox*$^{-/-}$ mouse model as well.

A significant increase of almost all tested stress response genes further verified the impairment of epidermal barrier integrity. Interestingly, expression of Sprr2d, a member of the small proline-rich protein (Sprr) family, which includes multiple proteins acting as loricrin crosslinkers, in a lower magnitude was also found to be upregulated in *Lor*$^{-/-}$ mice as a compensation mechanism for loss of loricrin (Koch et al., 2000). Upregulation of several Sprrs in the current study might equally function as a protective mechanism aiming to prevent the formation of a more severe epidermal phenotype.

SOX shows moderate expression in the skin (Uhlén et al., 2015), but has not been ascribed a role in skin homeostasis yet. However, sulfite, which accumulates upon SOX deficiency, can act as a nucleophile cleaving disulfide bonds (Kella & Kinsella, 1985), which are crucial for epidermal barrier integrity, as they are involved in the cross-linkage of keratin filaments and other structural proteins such as loricrin, the major component of the cornified cell envelope (Hohl et al., 1991; Suns & Green, 1978). In addition, in a knock-in mouse model expressing K14 with a single cysteine-to-alanine mutation, loss of disulfide bond formation resulted in the inhibition of a signaling cascade altering transcription, which led to increased epidermal thickness, basal and suprabasal distribution of K14, as well as decreased K10, filaggrin and loricrin intensity (Guo et al., 2020).

Overall, the results indicate late onset differentiation and hyperproliferation as a mechanism to counteract a potential epidermal barrier dysfunction in *Suox*$^{-/-}$ mice. Notably, data revealed a broad distribution, ranging from control-like to severely altered epidermal morphology. As the life span of *Suox*$^{-/-}$ mice typically lies between six to twelve days, the phenotypic variation can be ascribed to a difference in the age of onset and thus expected survival time. In line with this, normal epidermal morphology at birth revealed healthy epidermal barrier formation *in utero* and fully postnatal manifestation of the observed phenotype proportional to the severity of the overall disease progression. We therefore propose a progressive, postnatal loss of epidermal barrier integrity due to excessive accumulation of sulfite. Further studies will be required to understand the contribution of cysteine modifications and unravel the exact pathomechanism.

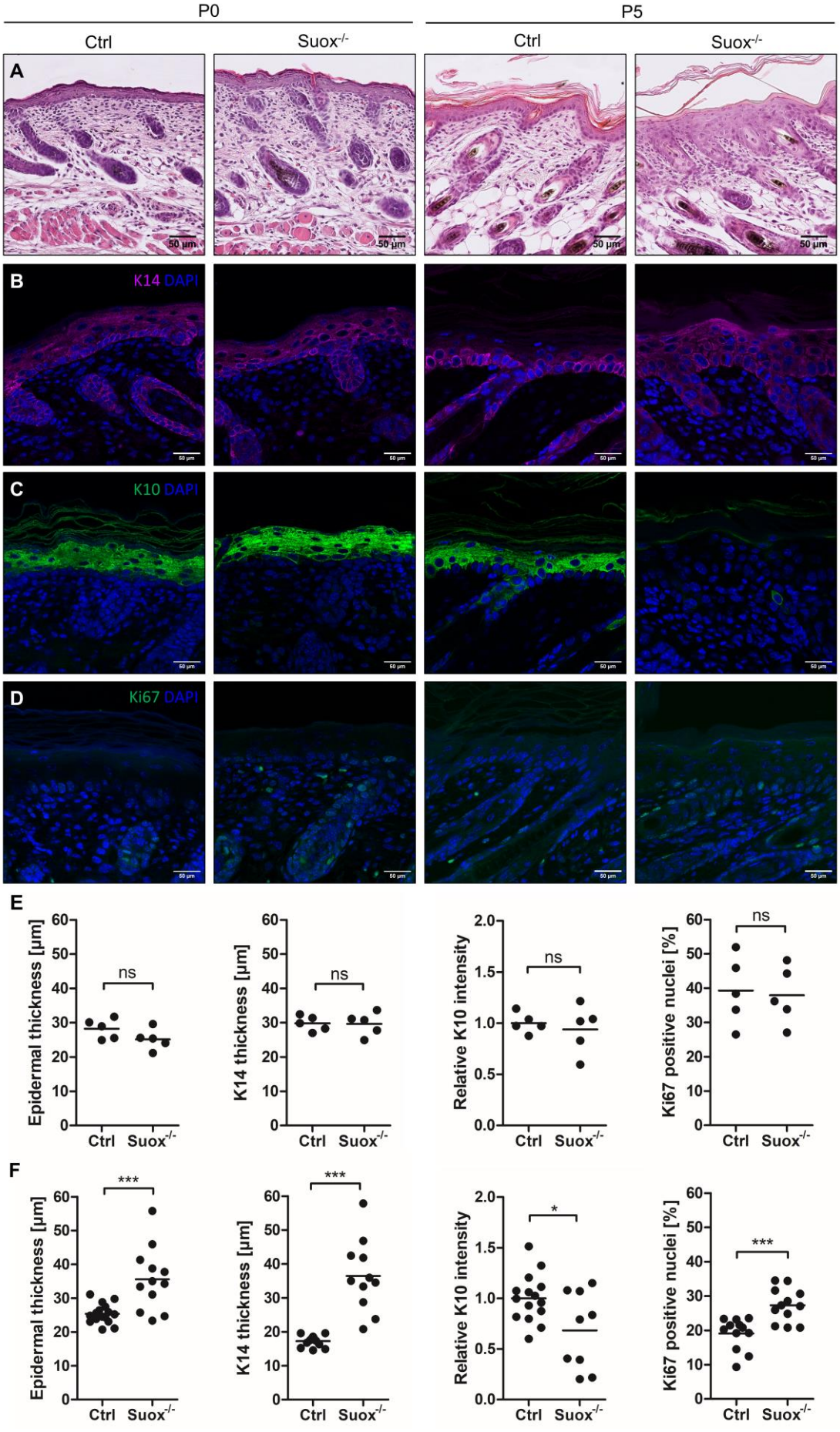
P0
P5
Ctrl
Suox-/-
Ctrl
Suox-/-
A
B
K14 DAPI
C
K10 DAPI
D
Ki67 DAPI
50 µm
E
Epidermal thickness [µm]
K14 thickness [µm]
Relative K10 intensity
Ki67 positive nuclei [%]
ns
F
***
*
***
Ctrl
Suox-/-

Figure 1 (previous page): *Suox*$^{-/-}$ mice develop altered epidermal morphology and dysregulated early keratinocyte differentiation within the first days of life. (A) H&E stainings of back skin sections of *Suox*$^{-/-}$ pups from P0 (left) and P5 (right). (B-D) Immunofluorescent stainings of paraffin-embedded back skin sections for (B) basal cell marker K14, (C) early differentiation marker K10 and (D) proliferation marker Ki67, each at P0 (left) and P5 (right). (E+F) From left to right quantification of epidermal thickness (excluding SC), K14 thickness, K10 intensity and Ki67-positive cells for (E) P0 and (F) P5, respectively. Each data point represents one animal, per animal ten microscopic pictures were analyzed.

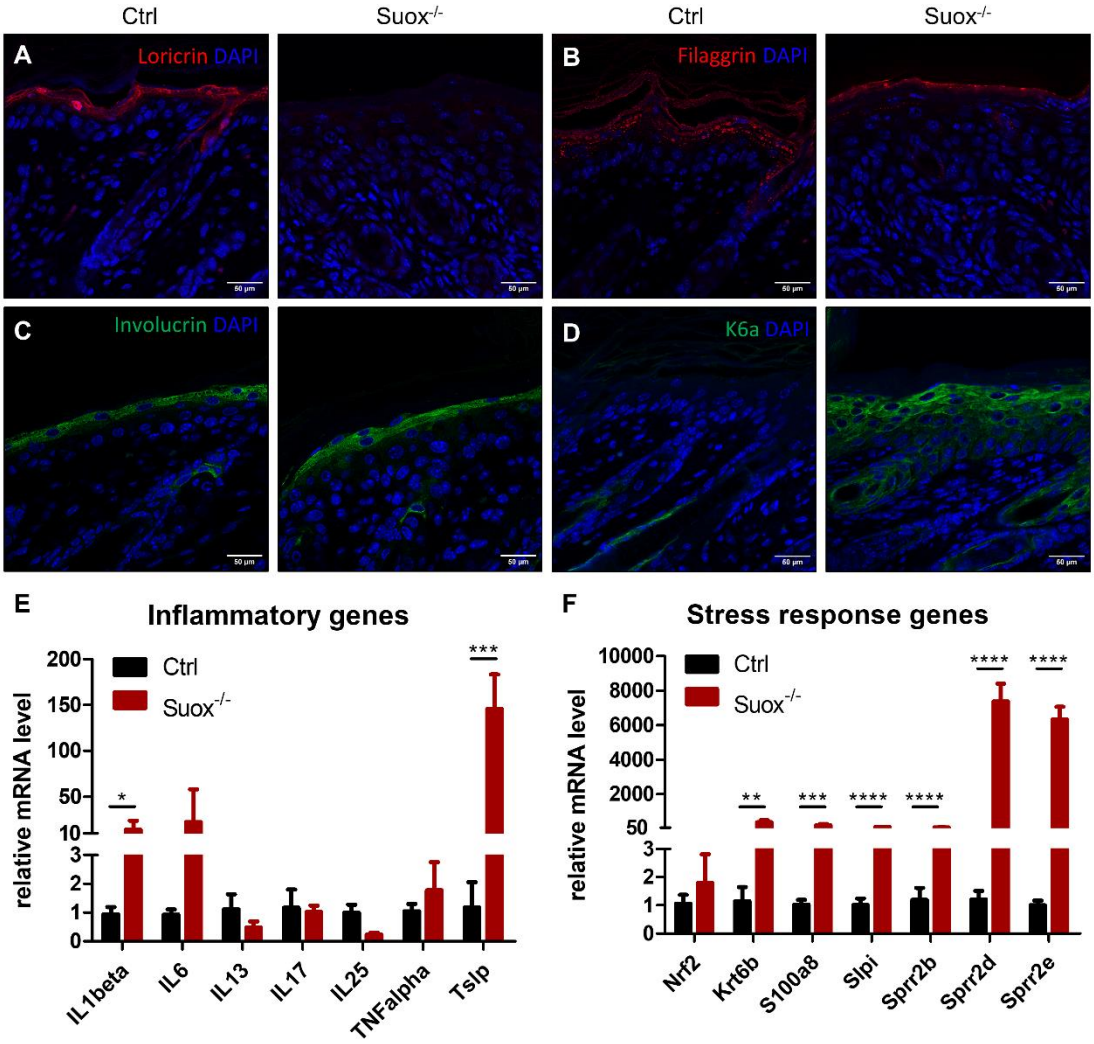

Figure 2: *Suox*$^{-/-}$ mice develop dysregulated late keratinocyte differentiation and increased stress response within the first days of life. (A-D) Immunofluorescent stainings of paraffin-embedded back skin sections of *Suox*$^{-/-}$ pups P5 for structural proteins and late differentiation markers (A) Loricrin, (B) Filaggrin, (C) Involucrin and (D) hyperproliferation-associated stress keratin K6a. (E+F) qRT-PCR analysis of (E) inflammatory and (F) stress response genes in back skin sections from *Suox*$^{-/-}$ pups P5 displaying a severe phenotype.

4.2 Material and Methods

4.2.1 Mouse strains

C57BL/6N mice were obtained from breedings in the Institute of Genetics, University of Cologne, or purchased from Charles River Laboratories. Animals were kept in sterile conditions at 22°C and 12/12 h light/dark cycles. All breedings and experiments were performed in accordance with the German animal welfare act under surveillance of the local ethics committee (Landesamt für Natur, Umwelt und Verbraucherschutz (LANUV)). In compliance with the 3R principle, the number of mouse experiments (replacement), utilized animals (reduction) and their stress level (refinement) were reduced to a minimum. Euthanasia was performed by decapitation for pups and by cervical dislocation for older animals.

4.2.2 Preparation of paraffin sections

For histological analysis of *Suox*$^{-/-}$ back skin, samples of the lower back skin of animals P5.5 were taken. One piece was fixed in cold 4% PFA for 1 h and then preserved in 70% ethanol until processing. Dehydration as well as paraffin embedding was performed by an automatic tissue processing machine (Leica ASP200S). Paraffin blocks were stored at RT until further processing. Sections of 5 µm were cut using a microtome and then placed on microscope slides.

Table 1: Protocol for tissue infiltration for skin samples

Step	Time
70% ethanol	2 h
80% ethanol	2 h
96% ethanol	2 h
100% ethanol	2 h
100% ethanol	2 h
100% ethanol	2 h
Xylene	2 h
Xylene	2 h
Paraffin	1 h (62°C)
Paraffin	1 h (62°C)
Paraffin	2 h (62°C)

4.2.3 Hematoxylin and eosin staining of skin sections

H&E staining of paraffin-embedded back skin sections was performed according to the following protocol:

Table 2: Protocol for Deparaffinization

Step	Time
Xylol I	5 min
Xylol II	5 min
Isopropanol	5 min
96% ethanol	5 min
75% ethanol	5 min
50% ethanol	5 min
ddH_2O	5 min or longer

Table 3: Protocol for H&E staining

Step	Time
Hematoxylin	45-90 s
ddH_2O	1 min
HCl alcohol (30 ml HCl alcohol + 150 ml ddH_2O)	30 s
ddH_2O	30 s
Tap water	1-2 min
Eosin	5-10 s
50% ethanol	10 s
75% ethanol	10 s
96% ethanol	10s
Isopropanol	20 s
Xylol I	30 s
Xylol II	30 s or longer

4.2.4 Immunofluorescence staining of skin sections

For visualizing epidermal markers via immunofluorescence stainings, paraffin sections were deparaffinized as described above. Antigen demasking was done for 20 min in antigen retrieval buffer (appropriate to the particular primary antibody). Sections were blocked in 10% normal goat serum, 1% bovine serum albumin and 0.2% fish skin gelatine for 1 h at RT and incubated for 1 at RT or overnight at 4°C with primary antibodies against different epidermal markers (diluted in antibody diluent solution from DAKO). The next day, sections were washed 3x5 min with PBS. Sections were incubated for 1h at RT with Alexa Fluor secondary antibodies and nuclei counterstain (DAPI 1:500). Sections were mounted with Mowiol and stored in the dark at 4°C.

4.2.5 Microscopy analysis

Confocal images were obtained with a Leica TCS SP8, equipped gateable hybrid detectors. Objectives used with this microscope: PlanApo ×63, 1.4 NA. Epifluorescence images were obtained with a Leica DMI6000. Objectives used with this microscope: PlanApo ×63, 1.4 NA; PlanApo ×20, 0.75 NA.

4.2.6 Image processing

Image processing and analysis of immunofluorescence stainings was done with ImageJ, counting of Ki67 and surviving positive nuclei was done with the StarDist plugin. Per sample, ten microscope pictures were taken and analyzed and the average was displayed as one data point per animal.

4.2.7 Quantitative RT-PCR analysis

Quantitative RT-PCR analysis was performed by AG Eming from the Department of Dermatology, University Hospital Cologne as described previously (Ding et al., 2020).

4.3 References

Dai, X., Muto, J., Shiraishi, K., Utsunomiya, R., Mori, H., Murakami, M., & Sayama, K. (2022). TSLP Impairs Epidermal Barrier Integrity by Stimulating the Formation of Nuclear IL-33/Phosphorylated STAT3 Complex in Human Keratinocytes. *Journal of Investigative Dermatology*, *142*(8), 2100-2108.e5. https://doi.org/10.1016/J.JID.2022.01.005

Dai, X., Utsunomiya, R., Shiraishi, K., Mori, H., Muto, J., Murakami, M., & Sayama, K. (2021). Nuclear IL-33 Plays an Important Role in the Suppression of FLG, LOR, Keratin 1, and Keratin 10 by IL-4 and IL-13 in Human Keratinocytes. *Journal of Investigative Dermatology*, *141*(11), 2646-2655.e6. https://doi.org/10.1016/J.JID.2021.04.002

Ding, X., Willenborg, S., Bloch, W., Wickström, S. A., Wagle, P., Brodesser, S., Roers, A., Jais, A., Brüning, J. C., Hall, M. N., Rüegg, M. A., & Eming, S. A. (2020). Epidermal mammalian target of rapamycin complex 2 controls lipid synthesis and filaggrin processing in epidermal barrier formation. *The Journal of Allergy and Clinical Immunology*, *145*(1), 283-300.e8. https://doi.org/10.1016/J.JACI.2019.07.033

Fuchs, E., & Green, H. (1980). Changes in keratin gene expression during terminal differentiation of the keratinocyte. *Cell*, *19*(4), 1033–1042. https://doi.org/10.1016/0092-8674(80)90094-X

Guo, Y., Redmond, C. J., Leacock, K. A., Brovkina, M. V, Ji, S., Jaskula-Ranga, V., & Coulombe, P. A. (2020). *Keratin 14-dependent disulfides regulate epidermal homeostasis and barrier function via 14-3-3s and YAP1*. https://doi.org/10.7554/eLife.53165

Hohl, D., Mehrel, T., Lichti, U., Turner, M. L., Roop, D. R., & Steinert, P. M. (1991). Characterization of human loricrin. Structure and function of a new class of epidermal cell envelope proteins. *Journal of Biological Chemistry*, *266*(10), 6626–6636. https://doi.org/10.1016/S0021-9258(18)38163-8

Irreverre, F., Mudd, S. H., Heizer, W. D., & Laster, L. (1967). Sulfite oxidase deficiency: Studies of a patient with mental retardation, dislocated ocular lenses, and abnormal urinary

excretion of S-sulfo-l-cysteine, sulfite, and thiosulfate. *Biochemical Medicine*, *1*(2), 187–217. https://doi.org/10.1016/0006-2944(67)90007-5

Johnson, J. L., & Duran, M. (2001). Molybdenum cofactor deficiency and isolated sulfite oxidase deficiency. In *The Metabolic and Molecular Bases of Inherited Disease* (pp. 3163–3177). Mcgraw-Hill Professional.

Kella, N. K. D., & Kinsella, J. E. (1985). A method for the controlled cleavage of disulfide bonds in proteins in the absence of denaturants. *Journal of Biochemical and Biophysical Methods*, *11*(4–5), 251–263. https://doi.org/10.1016/0165-022X(85)90007-7

Koch, P. J., De Viragh, P. A., Scharer, E., Bundman, D., Longley, M. A., Bickenbach, J., Kawachi, Y., Suga, Y., Zhou, Z., Huber, M., Hohl, D., Kartasova, T., Jarnik, M., Steven, A. C., & Roop, D. R. (2000). Lessons from Loricrin-Deficient Mice: Compensatory Mechanisms Maintaining Skin Barrier Function in the Absence of a Major Cornified Envelope Protein. *The Journal of Cell Biology*, *151*(2), 389. https://doi.org/10.1083/JCB.151.2.389

Kohl, J. B. (2019). A Novel Mouse Model of Sulfite Oxidase Deficiency: Pathological Changes in Cysteine and H2S Metabolism. In *Department of Chemistry*.

Komine, M., Rao, L. S., Freedberg, I. M., Simon, M., Milisavljevic, V., & Blumenberg, M. (2001). Interleukin-1 induces transcription of keratin K6 in human epidermal keratinocytes. *Journal of Investigative Dermatology*, *116*(2), 330–338. https://doi.org/10.1046/j.1523-1747.2001.01249.x

Kumar, A., Dejanovic, B., Hetsch, F., Semtner, M., Fusca, D., Arjune, S., Santamaria-Araujo, J. A., Winkelmann, A., Ayton, S., Bush, A. I., Kloppenburg, P., Meier, J. C., Schwarz, G., & Belaidi, A. A. (2017). S-sulfocysteine/NMDA receptor-dependent signaling underlies neurodegeneration in molybdenum cofactor deficiency. *J Clin Invest*, *127*(12), 4365–4378. https://doi.org/10.1172/JCI89885

Michaelidou, M., Redhu, D., Kumari, V., Babina, M., & Worm, M. (2023). IL-1α/β and IL-18 profiles and their impact on claudin-1, loricrin and filaggrin expression in patients with atopic dermatitis. *Journal of the European Academy of Dermatology and Venereology*. https://doi.org/10.1111/jdv.19153

Suns, T., & Green, H. (1978). *Keratin filaments of cultured human epidermal cells. Formation of intermolecular disulfide bonds during terminal differentiation. 253*(6), 2053–2060. https://doi.org/10.1016/S0021-9258(19)62353-7

Uhlén, M., Fagerberg, L., Hallström, B. M., Lindskog, C., Oksvold, P., Mardinoglu, A., Sivertsson, Å., Kampf, C., Sjöstedt, E., Asplund, A., Olsson, I. M., Edlund, K., Lundberg, E., Navani, S., Szigyarto, C. A. K., Odeberg, J., Djureinovic, D., Takanen, J. O., Hober, S., … Pontén, F. (2015). Tissue-based map of the human proteome. *Science*, *347*(6220). https://doi.org/10.1126/SCIENCE.1260419/SUPPL_FILE/1260419_UHLEN.SM.PDF

Zhang, L. (2018). Keratins in Skin Epidermal Development and Diseases. *Keratin*. https://doi.org/10.5772/INTECHOPEN.79050

V General Discussion

Molybdenum cofactor deficiency (MoCD) and isolated sulfite oxidase deficiency (SOXD) are rare, recessively inherited metabolic disorders, in which sulfur metabolism is disturbed due to a loss of function of sulfite oxidase (SOX), the terminal enzyme of cysteine catabolism (Johnson & Duran, 2001). In MoCD, disturbance of Moco biosynthesis results in the loss of function of all molybdoenzymes including SOX. Depending on which step is affected, the disease is further classified into MoCD types A, B or C. SOXD is caused by mutation of the *SUOX* gene, which encodes for SOX, but results in a similar phenotype as MoCD. Therefore, this severe phenotype is the result of the sole loss of SOX function in both diseases (Johnson et al., 2002; Reiss & Johnson, 2003). Resulting accumulation of sulfite and other toxic sulfur metabolites including S-sulfocysteine (SSC), the product formed during the reaction of sulfite and cystine, accompanied by a depletion of cysteine in both defects causes rapid neurodegeneration and inevitably leads to premature death if left untreated. Neurodegeneration is majorly triggered by SSC, whose structural resemblance to glutamate renders it a potent N-methyl-D-aspartate receptor (NMDAR) agonist, thus causing highly elevated excitotoxic neuronal cell death (Kumar et al., 2017; Olney et al., 1975).

Despite decades of research, reaching back to the 1960s, MoCD types B and C, as well as SOXD, are still classified as incurable diseases (Gerschenfeld et al., 1967). For MoCD type A, an effective treatment strategy is the regular administration of cPMP, the product of the first step of Moco biosynthesis, which was established in 2010 (Veldman et al., 2010). In contrast, to date therapeutic strategies for MoCD type B and C, as well as SOXD, are limited to symptomatic treatment, which primarily includes anticonvulsive interventions, and attempted deceleration of the disease progression. The latter is mainly done by dietary restriction of cysteine to prevent sulfite accumulation, but only leads to clinical improvement in late onset patients (Abe et al., 2021; Bindu et al., 2017).

Recently, the generation of a *Suox*$^{-/-}$ mouse line provided a new model system and thus new possibilities in the search for an effective long-term treatment for both MoCD and SOXD. Hence, the current work tested several different treatment strategies including NMDAR blockage to prevent excitotoxic neurodegeneration, reduction of sulfite accumulation by sulfite scavenging and dietary restriction of proteins and sulfur-containing amino acids, inhibition of ferroptosis, a non-apoptotic regulated cell death triggered by cysteine depletion, and an enzyme replacement therapy using a modified variant of SOX (see chapter III). However, further characterization of the phenotypic expression revealed

significant differences between SOXD in mice and humans and suggested differing underlying pathomechanisms, thus complicating the establishment of a therapeutic approach that is equally efficient in murine and human SOXD.

5.1 Cerebral phenotype differs in human and murine SOXD

SOXD patients typically present with feeding difficulties, increased irritability and intractable seizures within the first hours to days of life and soon develop altered facial and head morphology, lens dislocation, severe, progressive neurodegeneration, microcephaly and major developmental delay (Johnson & Duran, 2001), mainly ascribed to the formation of neurotoxic SSC from excess sulfite and cystine (Olney et al., 1975). Presumably, the absence of a prenatal phenotype is the result of maternal-placental clearance of sulfite at least until late pregnancy protecting the fetus *in utero*, while rapid clinical deterioration can be observed as soon as the neonate's metabolism is uncoupled from the mother, as it was described in MoCD as well (Veldman et al., 2011). Depending on the level of residual SOX activity resulting from the underlying *SUOX* mutation, a minor number of patients display a late onset form of the disease with symptoms manifesting only at the age of six to 18 months and a life expectancy of several years (Bindu et al., 2017). In both cases, biomarker analysis at the age of onset reveals an increase of urinary and plasma sulfite, thiosulfate and SSC, accompanied by low levels of homocysteine and free cystine in plasma (Bindu et al., 2017; Kožich et al., 2022).

In our SOXD mouse model, disruption of the *Suox*$^{-/-}$ gene by a 7-base pair deletion results in complete loss of SOX function, thus hypothetically resembling the phenotype of early onset patients. *Suox*$^{-/-}$ mice are born healthy and indistinguishable from their wildtype and heterozygous littermates, but similar to humans start developing symptoms within the first days of life, most likely due to a similar protection by maternal clearance of sulfite *in utero*. Homozygous knockout mice soon display growth retardation and decreased motor function, as observed in a righting reflex test, which was ascribed to an increased neurodegeneration as observed in human patients (Kohl, 2019). However, recent morphological analysis of *Suox*$^{-/-}$ mouse brains at P8.5 revealed unaltered cell numbers in several tested brain layers, thus excluding a major cerebral phenotype shortly before death (Kohl, Fu et al., in preparation). As plasma SSC levels of 8 µM are detected both in humans and mice with SOXD, but humans show 125 µM of urinary SSC, while *Suox*$^{-/-}$ mice show significantly lower levels of 30 µM (Kohl, 2019; Kožich et al., 2022), overall lower SSC toxicity and thus lower neurotoxicity can be anticipated. This difference can be explained by the levels of cysteine in each species. Healthy humans show cysteine levels of 250 µM in plasma, which are decreased to 50 µM in SOXD (Kožich et al., 2022). In contrast, plasma

levels in control mice show significantly lower cysteine levels of 8 µM, while levels in *Suox*$^{-/-}$ mice are below detection limit (Kohl, Fu et al., in preparation). This suggests complete conversion of cysteine into SSC and forbids the formation of equally high SSC levels in mice as detected in humans.

Furthermore, at birth brains of rodents are significantly less developed than human brains. While in humans the peak brain growth spurt and gliogenesis, as well as an increase in axonal and dendritic density, occur between 36 to 40 weeks of gestation, in rodents the same brain development is only reached 7-10 days after birth (Semple et al., 2013). Therefore, a similar excitotoxic neuronal cell death as observed in humans would be questionable even at equally elevated SSC levels. *Mocs2*$^{-/-}$ mice, a mouse model of MoCD, did not present with changes in neuron numbers as well, but revealed an increased number of apoptotic neurons, as well as neurons expressing apoptosis marker caspase 3 (Jakubiczka-Smorag et al., 2016). Hence, manifestation of a neurological phenotype later on in disease progression, which is only prevented by the early death due to a yet unknown cause, can be presumed for *Suox*$^{-/-}$ mice as well. In line with this, induction of MoCD in adult wildtype mice by administration of tungstate, which competes for molybdenum insertion into the Moco and results in a loss of function of all molybdoenzymes, led to the development of a severe neurological phenotype curable by the NMDAR antagonist memantine (Kumar et al., 2017).

Taken together, the cumulative data suggest less distinctive SSC toxicity in our *Suox*$^{-/-}$ mouse model due to lower overall SSC levels caused by altered cysteine/cystine homeostasis and an increased tolerance, presumably due to delayed brain development. Hence, administration of an NMDAR antagonist to *Suox*$^{-/-}$ mice in order to counteract SSC-mediated neurodegeneration is an unsuitable treatment method, which agrees with the results obtained in the current work. For future studies, an inducible mouse model of SOXD, in which gene knockout should be induced not before 7-10 days of age, would increase the comparability of the mouse model and the human phenotype. However, generation of a conditional *Suox*$^{-/-}$ knockout in the past proved difficult due to an unfavorable gene structure including comparably short introns (Fu, unpublished data). Instead, a conditional *Mocs2*$^{-/-}$ mouse model is currently being generated in our working group and will present a valuable tool for more in-depth investigation of SOXD and MoCD (Fu et al., unpublished data).

5.2 The potential of therapeutic sulfite scavenging strategies in SOXD

Full body knockout of SOX did not result in the expected neurological phenotype, which is the main cause of death in human SOXD patients. However, mice do show a severe phenotype, including reduced weight gain and motor abilities, as well as a significantly

shortened survival time, which is presumably linked to the observed higher accumulation of sulfite than seen in human patients, as well as markedly elevated levels of secondary sulfur metabolites such as thiosulfate and hydrogen sulfide (H_2S). To date, no effective long-term treatment for human SOXD has been established, but due to the prominent neurological phenotype seen in human patients, treatment attempts have mainly targeted SSC-mediated neuronal cell death and its associated symptoms. The simultaneous accumulation of other sulfur metabolites, however, makes full recovery upon sole inhibition of SSC-mediated neurodegeneration questionable. A more severe manifestation of sulfite and potentially H_2S-driven toxicity can therefore be hypothesized in case of significant prolongation of life. Hence, successful treatment of SOXD in mice can further add to the understanding of SSC-unrelated lethality of loss of SOX function.

Thus, to better understand the cause of the severe phenotype of *Suox*$^{-/-}$ mice, the potential toxicity mediated by alternative sulfur metabolites needs to be analyzed in more detail. In *Suox*$^{-/-}$ mice, sulfite plasma levels at birth resemble those of wildtype littermates, but soon increase vastly until they reach a plateau of 150 µM at P4.5, while urinary sulfite levels already reveal increased postnatal excretion of 120 µmol/mmol creatinine (see chapter III). A decrease in excretion with increasing age can be ascribed to urinary retention, which leads to a significant increase of creatinine over time, but no net decrease in sulfite levels. In contrast, humans show plasma sulfite levels of 27 µM and urinary sulfite of 100 µmol/mmol creatinine in urine (Kožich et al., 2022). Hence, sulfite shows a 5.5-fold increase in plasma of mice compared to humans and renders *Suox*$^{-/-}$ mice a suitable model for the study of sulfite toxicity, whose exact pathomechanism is still elusive.

Therefore, administration of various chemical sulfite scavengers aimed for a direct reduction of sulfite accumulation accompanied by an indirect reduction of related sulfur metabolite levels. This approach, however, using D-cystine, D-cysteine or cystamine as scavengers, did not result in a significant prolongation of the average survival time of *Suox*$^{-/-}$ mice (see chapter III). Unfortunately, as animals were kept until reaching the termination criterion, collection of body fluids was not possible. Thus, the absence of a beneficial effect could either be ascribed to a low efficiency of the used sulfite scavengers and therefore unchanged sulfite accumulation or to a lower overall toxicity of sulfite than anticipated.

Several different thiol-reactive compounds were tested as potential sulfite scavengers in *Suox*$^{-/-}$ mice. D-cysteine and D-cystine both aimed to prevent toxic L-SSC formation under formation of nontoxic D-SSC, as proven in primary neurons in the current study. While the absence of a beneficial effect of D-cystine most likely could be attributed to the usage of too low concentrations due to the very low solubility of the compound,

D-cysteine administered in higher concentrations was expected to significantly improve symptomatology. *In vitro*, D-cysteine can undergo spontaneous racemization to form L-cysteine yielding a D/L ratio of 0.33 in two days, thus having the fastest turnover rate among all amino acids (Roychaudhuri et al., 2022), while still being slow enough to allow a reaction with sulfite to take place sufficiently, as sulfite reacts with cysteine within minutes (Fu, unpublished data).

In vivo, cysteine is metabolized by cysteine dioxygenase (CDO) yielding cysteine sulfinic acid (CSA), but the current work demonstrated a clear preference of the enzyme towards the L- over D-form, thus implying little to no contribution of D-cysteine to the formation of sulfite from the oxidative catabolism of cysteine. Degradation of D-amino acids *in vivo* is catalyzed by the enzyme diamine oxidase (DAO), which in humans shows highest catalytic efficiency towards D-cysteine (Roychaudhuri et al., 2022). DAO metabolizes D-cysteine to 3-mercaptopyruvate, which is further converted to H_2S catalyzed by 3-mercaptopyruvate sulfurtransferase (MPST). Hence, although not contributing to the oxidative pathway of cysteine catabolism, administration of D-cysteine presumably leads to an elevation of H_2S levels and ultimately sulfite accumulation from sulfide:quinone oxidoreductase (SQR) and persulfide dioxygenase (PDO)-mediated H_2S clearance. A potential reduction in sulfite levels due to the compound's sulfite scavenging properties might therefore be compromised by an increase in H_2S levels and resulting sulfite formation.

The third tested sulfite scavenger cystamine was chosen due to the 6-8 times higher reaction rate of sulfite with cystamine than with cystine *in vitro* (Jocelyn, 1987), resulting in the formation of the alternative compound S-sulfocysteamine (Fu, unpublished data). This makes it a promising sulfite scavenger preventing the formation of toxic SSC and depleting free sulfite. Moreover, the reduced form cysteamine has already been used as a therapy for cystinosis, a disease caused by lysosomal accumulation of cystine due to a loss of function of the cystine transporter cystinosin (Kalatzis et al., 2001). Cysteamine efficiently converts cystine into cysteine and a cysteine-cysteamine disulfide, which are cleared by the cysteine transporter and the lysine/arginine (PQLC2) transporter, respectively, thus decreasing lysosomal cystine accumulation (Jeźégou et al., 2012; Pisoni et al., 1985). Due to the reducing environment of the cytosol, cystamine is expected to be present as its reduced form cysteamine intracellularly, while in plasma the oxidized form would react with sulfite directly, thus presumably clearing sulfite before the occurrence of sulfite-mediated toxicity. However, patients suffering from cystinosis have to follow a strict medication plan including the administration of cysteamine every six hours due to its short half-life of 1.75 hours in plasma of humans (Cherqui, 2012; Tennezé et al., 1999). Hence, i.p. injection of cystamine once per day might not result in sufficient sulfite clearance in our *Suox*$^{-/-}$ mice

over time. Future studies using a modified treatment protocol including a higher administration frequency will reveal the efficiency of cysteamine as a therapeutic measure against SOXD in mice and possibly humans.

5.3 Reduction of sulfite production is not sufficient to treat murine SOXD

While the first attempt to treat SOXD in mice was still based on the assumption of a distinct cerebral phenotype, continuous studies aimed on a more global reduction in all sulfur metabolites elevated upon loss of SOX function with a primary focus on sulfite. One strategy involved chemical sulfite scavenging, but under the tested conditions did not result in significant improvement of the disease phenotype. A more conservative approach to reduce sulfite accumulation involved dietary restriction of protein in general or cystine and methionine in particular, both aiming to reduce net amounts of sulfur-containing amino acids entering cysteine catabolism. Deceleration of the disease progression aimed to increase the average survival time and allow possible manifestation of a cerebral phenotype in *Suox*$^{-/-}$ pups, hence resulting in a higher phenotypic resemblance towards human SOXD patients.

In late onset cases of human SOXD and MoCD, dietary restriction indeed successfully normalized biomarker levels and slowed down disease progression (Abe et al., 2021; Boles et al., 1993; Tan et al., 2005). However, in *Suox*$^{-/-}$ as well as in wildtype mice reduction of cystine and methionine was too restrictive and resulted in decreased weight gain, leading to increased neonatal pup loss among all genotypes. In contrast, a second approach including a diet with decreased protein content was not compromising the overall health condition, but restriction was probably too mild to improve symptoms and prolong the average survival time of homozygous mice (see chapter III). As the experimental challenges of direct pup feeding were too difficult, manipulation of the mothers' chow to alter composition of the milk fed to pups was the only option feasible. However, this indirect approach complicated the right dosage finding and possibly limited the potential of this therapeutic strategy, thus making it unsuitable as an approach to slow down disease progression of SOXD in mice despite the success in human patients. In general, this treatment strategy might be more suitable in a future conditional *Mocs2*$^{-/-}$ mouse model, in which induction of the disease at an older age would allow direct control over the dietary intake.

Previously, an alternative attempt to reduce sulfite production in *Suox*$^{-/-}$ mice was the simultaneous knockout of CDO, which catalyzes the conversion of cysteine into CSA as the first step of the oxidative part of cysteine catabolism (Fu et al., in preparation). In cells, glutamate oxaloacetate transaminase 1 (GOT1) was found to be the main producer of sulfite from CSA, as sulfite accumulation in *SUOX*$^{-/-}$ HEK 293 cells was reduced to wildtype

levels via a simultaneous knockout of GOT1 (Mellis, 2020). Knockout of the upstream enzyme CDO, hence, aimed to inhibit major sulfite accumulation. In fact, *Suox*$^{-/-}$/*Cdo*$^{-/-}$ double knockout mice showed a significant reduction in sulfite levels, although levels remained above wildtype (Fu et al., in preparation). At the same time, the average survival time was further decreased in these animals, thus questioning the role of sulfite as the main and sole mediator of toxicity. Nonetheless, due to its ability to cleave disulfide bonds, sulfite can globally affect protein stability (Leggett et al., 1959), thus potentially interfering in various metabolic pathways and making it a risk factor for every organ, potentially even at less drastically elevated concentrations.

5.4 The potential of therapeutic reduction of H_2S production in SOXD

While *Suox*$^{-/-}$/*Cdo*$^{-/-}$ mice showed the expected reduction in sulfite levels, H_2S and thiosulfate levels were markedly increased compared to *Suox*$^{-/-}$ mice, implying a shift of balance in cysteine catabolism towards the H_2S pathway (Fu et al., in preparation). H_2S is a gaseous signaling molecule in the cardiovascular and nervous system and has been attributed a cytoprotective effect in sub-micromolar concentrations, possibly due to its ability to neutralize several different reactive oxygen species (ROS) and upregulate endogenous antioxidant systems, as well as anti-inflammatory and cytoprotective genes (Szabõ, 2007). However, high micromolar to millimolar concentrations of H_2S mediate cytotoxicity by the formation of free radicals and oxidants, glutathione (GSH) depletion, intracellular iron release and the induction of mitochondrial cell death pathways as a strong inhibitor of complex IV (Petersen, 1977; Szabõ, 2007). H_2S is produced by cystathionine γ-lyase (CSE), cystathionine β-synthase (CBS) and 3-mercaptopyruvate sulfurtransferase (MPST), while its clearance is mediated via several steps starting with sulfide:quinone oxidoreductase (SQR), which generates persulfidated GSH (GSSH), followed by thiosulfate sulfurtransferase (TST) and persulfide dioxygenase (PDO) regenerating GSH under formation of thiosulfate and sulfite, respectively (Kohl et al., 2019).

Knockout of the *Ethe1* gene, which encodes for PDO, in mice results in a severe phenotype ascribed to H_2S toxicity (Tiranti et al., 2009). *Ethe1*$^{-/-}$ mice show growth arrest and decreased motor function as examined in an activity cage test, thus displaying symptoms similar to *Suox*$^{-/-}$ mice. They display a significant increase in tissue H_2S levels, as well as elevated urinary thiosulfate accompanied by undetectable sulfite levels, which is hypothesized to be caused by increased H_2S fixation via sulfite and thus increased conversion of the latter into thiosulfate as the final step of the H_2S pathway of cysteine catabolism (Tiranti et al., 2009). Increased H_2S levels in *Ethe1*$^{-/-}$ mice result in the inhibition of short-chain acyl CoA dehydrogenase, an enzyme involved in the fatty acid oxidation

pathway (Hildebrandt et al., 2013). This, in turn, results in increased levels of the substrate ethylmalonic acid (EMA), which in the past was shown to impair brain mitochondrial succinate and malate transport and reduce mitochondrial membrane potential, thus inhibiting mitochondrial respiration (Amaral et al., 2012). In addition, increased H_2S levels inhibit cytochrome *c* oxidase, which functions as complex IV in the mitochondrial respiratory chain, in various tested organs (Tiranti et al., 2009). In line with this, *Ethe1*$^{-/-}$ mice display elevated levels of the glycolytic enzymes fructose biphosphate aldolase and pyruvate kinase, which points towards a shift from mitochondrial respiration to glycolysis, presumably to prevent an energy crisis caused by the dysfunction of mitochondrial metabolism (Sahebekhtiari et al., 2016). Their overall survival time of five to six weeks is significantly higher than in *Suox*$^{-/-}$ mice (Tiranti et al., 2009), so H_2S toxicity as the only cause of death in *Suox*$^{-/-}$ mice can be excluded, but mitochondrial dysfunction can be anticipated to contribute to the severe phenotype, as shown previously in MoCD patient-derived fibroblasts (Mellis, 2020).

A shutdown of the oxidative pathway of cysteine catabolism did not result in an improvement of the phenotype of *Suox*$^{-/-}$ mice, so the inhibition of the H_2S pathway of cysteine catabolism should be considered as an alternative approach to reduce overall sulfite levels and, equally important, H_2S production in the first place. While the generation of double knockout mice is an inefficient and costly procedure, as breedings yield the correct phenotype at a chance of only 6.25%, chemical inhibition presents an easier and more straight forward approach additionally allowing precisely timed shutdown of enzymatic function. Aminooxyacetic acid (AOAA) is a commonly used inhibitor of transaminases, which inhibits CSE and CBS with an IC_{50} of 1 µM and 8.5 µM, respectively (Asimakopoulou et al., 2013). Inhibition of those enzymes disrupts cysteine catabolism and results in an increase in homocysteine levels, as seen in CBS deficiency (Sacharow et al., 2017), which could counteract the homocysteine depletion observed in SOXD (Bindu et al., 2017). Moreover, in case the increased elevation of H_2S levels in *Suox*$^{-/-}$*/Cdo*$^{-/-}$ mice is a major contributor to the worsening of the phenotype in comparison to *Suox*$^{-/-}$ mice, a reduction of the elevated H_2S production in *Suox*$^{-/-}$ mice should already result in a significant phenotypic improvement. However, AOAA is known to react with a variety of pyridoxal-5'-phosphate-dependent enzymes, which does not only include CSE and CBS, but also GOT1 and GOT2, which catalyze the conversion of CSA into sulfite in the oxidative catabolism of cysteine (Mellis et al., 2021). Due to its moderate potency and an IC_{50} value of 100 µM (Antti & Sellstedt, 2018), usage of low doses is crucial, but should be sufficient to prevent shut down of both the oxidative and the H_2S pathway of cysteine catabolism. Overall, chemical

inhibition of the H_2S pathway presents a promising tool for future studies on the contribution of H_2S-mediated toxicity to the severe phenotype of SOXD.

5.5 The contribution of regulated cell death to SOXD

Alternative to the reduction of sulfur metabolite-mediated toxicity, another therapeutic approach aimed to unravel the cell death pathways triggered by the molecular consequences of SOXD. The severe depletion of cysteine in *Suox*$^{-/-}$ mice suggested the involvement of ferroptotic cell death in the course of the disease, as ferroptosis is a form of regulated, non-apoptotic cell death, which is triggered by cysteine depletion and a resulting decrease in intracellular GSH (Dixon et al., 2012). The latter is an essential co-substrate for the enzyme glutathione peroxidase 4 (GPX4), which is required for the detoxification process of lipid peroxides (Dixon et al., 2012).

In contrast to the biochemical assumption, administration of the ferroptosis inhibitor Liproxstatin-1 in the current study did not result in an increase of the median survival time in *Suox*$^{-/-}$ mice (see chapter III). Following analysis of lipid peroxide levels revealed a significant decrease in kidneys of untreated, homozygous pups compared to wildtype littermates. This finding excluded ferroptosis as the major cell death pathway triggered in SOXD, although cysteine depletion in *Suox*$^{-/-}$ mice is accompanied by a decrease of the antioxidant tripeptide GSH liver and kidney (Kohl, 2019), which suggested a simultaneous decrease in GPX4 activity. Instead, altered levels of at least one of the sulfur metabolites affected in SOXD appears to exhibit an anti-ferroptotic effect resulting in decreased formation of lipid peroxides. Sulfite has been shown to act as a strong nucleophile with the ability to cleave disulfide bonds, which in cells led to increased GSH recovery after hydrogen peroxide (H_2O_2)-induced oxidative stress (Mellis, 2020). Hence, a similar mechanism for the increased regeneration of GSH from glutathione disulfide (GSSG) was proposed to result in elevated resistance towards ferroptosis in *Suox*$^{-/-}$ mice. As the current study excluded the contribution of ferroptosis to the severe phenotype of SOXD, a potential induction of other cell death pathways should be considered.

Intrinsic apoptosis is a common form of regulated cell death, which is characterized by intracellular stress factors resulting in irreversible mitochondrial outer membrane permeabilization (MOMP), a process controlled by pro-apoptotic and anti-apoptotic members of the BCL2 protein family. Pro-apoptotic proteins like BOK, BAX and BAK are able to form pores across the mitochondrial outer membrane, thus promoting MOMP and apoptotic cell death. Anti-apoptotic proteins such as BCL2 itself, BCL2L1 or MCL1 mainly inhibit apoptosis by binding the pro-apoptotic members of the BCL2 family, thus preventing their oligomerization and pore-forming activity. MOMP results in the release of apoptogenic

factors into the cytosol, which activates a cascade resulting in the activation of excessive protein cleavage by caspases 3 and 7, the major executors of apoptotic cell death (Galluzzi et al., 2018).

Extrinsic apoptosis is a form of apoptosis triggered by extracellular stress factors, which are sensed by death receptors via binding of specific ligands. Upon activation, death receptors initiate the formation of the “death-inducing signaling complex” (DISC), which results in the recruitment and activation of caspase 8. Caspase 8, in turn, initiates a signaling cascade resulting in the activation of effector caspases 3 and 7, as seen in intrinsic apoptosis. This pathway, however, cannot be inhibited by overexpression of the anti-apoptotic BCL2 protein or the inactivation of anti-apoptotic proteins. Instead, the anti-apoptotic factor c-FLIP can interact with the DISC and inhibit caspase 8 function (Galluzzi et al., 2018).

Previously, SSC-mediated activation of caspase 3 has been shown in primary hippocampal neurons, peaking at 12 h after SSC treatment. Pretreatment with the pan-caspase inhibitor Z-VAD-FMK partially, but not completely prevented SSC-mediated neuronal cell death, thus verifying the contribution of intrinsic or extrinsic apoptosis in SSC-mediated cell death, but also implying the involvement of other, non-apoptotic cell death pathways (Kumar, 2016). *Suox*$^{-/-}$ mice show a relatively mild, but significant elevation in SSC levels, which is hypothesized to result in a similar activation of apoptotic cell death. Therefore, overexpression of the anti-apoptotic proteins BCL2 or c-FLIP in *Suox*$^{-/-}$ mice could prevent either intrinsic or extrinsic apoptosis, respectively, while continuous treatment with a pan-caspase inhibitor would shut down both pathways simultaneously. In the past, the latter strategy has been used successfully in mouse models for various diseases, while for liver disease, epilepsy and arthritis it even reached a phase II clinical trial, thus holding great potential as therapeutics both in mice and humans (Dhani et al., 2021). These experimental approaches, hence, will give new insights into the role of apoptosis in SOXD and potentially result in an enhancement of the phenotype by preventing major apoptotic cell death.

However, caspase 3 activation so far has only been verified to contribute partially to SSC-mediated neuronal cell death, as its inhibition resulted in incomplete restoration of cell viability, thus implying the involvement of at least one other cell death pathway (Kumar, 2016). Moreover, although *Mocs2*$^{-/-}$ brains showed elevated caspase 3 activation (Jakubiczka-Smorag et al., 2016), the major symptoms in murine MoCD and SOXD result from the damage of non-neuronal cells, which has not been linked to apoptosis yet, but is

presumed to be mediated by the toxicity of one or more sulfur metabolites elevated due to the loss of SOX function.

In the past, sulfite toxicity has been examined in various, non-neuronal cell types. However, all of these studies were performed in wildtype cells expressing functional SOX. In hepatocytes, sulfite-mediated cell death has been ascribed to apoptosis and the non-regulated form of cell death necrosis in two different publications (Bai et al., 2013; Han et al., 2020). In gastric mucosal cells, sulfite leads to necrotic cell death caused by the induction of oxidative stress and in mast cells sulfite causes pyroptosis, a common form of inflammatory, regulated cell death, which is caused by pore formation in the plasma membrane mediated by members of the gasdermin protein family (Galluzzi et al., 2018; Liu et al., 2021; Oshimo et al., 2021).

H_2S in low concentrations has been demonstrated to protect cells from different forms of cell death, including apoptosis in pancreatic beta-cells, inflammation and apoptosis in neuronal cells following cerebral ischemia-reperfusion injury and pyroptosis and necroptosis as a prevention for diabetic cardiomyopathy (Deng et al., 2023; Gong et al., 2022; Kar et al., 2019; Okamoto et al., 2015). Recently, H_2S was also shown to exhibit an indirect anti-ferroptotic effect, as it led to increased SQR-catalyzed formation of hydrogen persulfides, which exhibit potent radical scavenging activity (Barayeu et al., 2023). In high concentrations, however, its effect shifts to major cytotoxicity, as seen in its induction of necrosis in hepatocytes, of apoptosis in human aorta smooth muscle cells and of tracheal pyroptosis in broiler (Song et al., 2021; Truong et al., 2008; Yang et al., 2004).

Overall, the molecular mechanisms of sulfite and H_2S-mediated cell death are highly diverse, so in the future analysis of marker molecules relevant for different cell death pathways will be crucial to clarify their overall importance in the disease progression of SOXD and MoCD. In the long term, inhibitors of majorly involved cell death pathways might therefore provide a promising therapeutic strategy for SOXD in humans.

5.6 Reconstitution of SOX activity provides a promising treatment strategy for murine and potentially human SOXD

Following the targeting of different aspects of the pathomechanism, the last therapeutic approach for SOXD aimed to function as an overall treatment ameliorating every aspect discussed before by restoring SOX function via an enzyme replacement therapy. Due to promising results from a single pilot study using *Mocs1*$^{-/-}$ mice and plant SOX (pSOX) (Belaidi, 2011; Hahnewald, 2009), this study used a comparable approach in *Suox*$^{-/-}$ mice anticipating a similarly beneficial outcome.

Instead of pSOX, a murine, heme-deficient SOX variant (mSOX-Mo) was used for treatment as a more physiological relevant SOX variant and resulted in a mild, but significant increase in the average survival time of *Suox*$^{-/-}$ mice (see chapter III). Mice still developed the classic SOXD phenotype, as the treatment protocol erroneously stated a single i.p. injection at day two after birth instead of continuous injection every second day starting at birth (Belaidi, 2011). Hence, a similar treatment success of mSOX-Mo in *Suox*$^{-/-}$ pups as observed for pSOX in *Mocs1*$^{-/-}$ pups in the pilot study can be anticipated upon usage of the same treatment frequency.

In the past, mSOX-Mo had been shown to be able to use oxygen as the final electron acceptor for sulfite oxidation in a similar manner as pSOX and thus was anticipated to be able to use blood-dissolved oxygen, which makes up 2% of total oxygen in blood (Pittman, 2011), *in vivo* as well (Belaidi, 2011). Preliminary *in vitro* experiments in the pilot study displayed lower levels of H_2O_2 formation for mSOX-Mo than for pSOX, while still achieving complete sulfite clearance. Due to the lower catalytic activity observed for mSOX-Mo, the author hypothesized a higher non-enzymatic, H_2O_2-mediated sulfite reduction, thus scavenging a part of the produced H_2O_2 under formation of H_2O, while maintaining similar sulfite detoxification efficiency (Belaidi, 2011). A similar reaction had been proposed for pSOX previously, however only at high sulfite concentrations (Hänsch et al., 2006). This finding presents a major advantage of using mSOX-Mo instead of pSOX as a therapeutic agent in order to reduce toxic H_2O_2 formation and prevent development of gastroenteritis caused by elevated levels of ROS. Alternatively, the simultaneous injection of catalase was proposed to achieve H_2O_2 detoxification in case mSOX-Mo-induced H_2O_2 formation still reaches critical levels (Belaidi, 2011). Catalase was shown to be inhibited by sulfite at high concentrations, however half-maximal inhibition was reached at 260 µM sulfite (Hänsch et al., 2006), so a maximum of 150 µM in the plasma of *Suox*$^{-/-}$ mice should not result in problematic levels of catalase inhibition. Alternatively, usage of salen-manganese complexes, which are a class of synthetic compounds with superoxide dismutase and catalase function, might overcome potential sulfite-mediated inhibition and could additionally prevent general ROS production (Baker et al., 1998; McCord, 2008), potentially resulting in a slight increase of the average survival time of *Suox*$^{-/-}$ mice.

An alternative therapeutic approach to fully restore SOX function in *Suox*$^{-/-}$ mice is the usage of gene therapy, which compared to enzyme replacement therapeutic approaches has several major advantages. Introduction of an expression cassette for SOX would allow better control on the localization of the enzyme than injection, enabling its subcellular localization to the mitochondrial intermembrane space. Hence, usage of mSOX-Mo to allow utilization of oxygen as an alternative electron acceptor would not be required.

Instead, expression of full-length protein would result in reconstitution of its biological function, thus simultaneously preventing toxicity caused by H_2O_2 formation. As gene expression guarantees the continuous physiological production of novel enzyme, chemical modifications like PEGylation are not needed to enhance stability and half-life of the enzyme. Furthermore, while enzyme replacement therapy is a life-long treatment and thus involves high time investment and high dependency on the availability of the medication, effective gene therapy aims to have a long-lasting effect that does not require high frequency treatment.

There are two main approaches for gene therapy, which are germline and somatic gene therapy. Germline therapy, however, is ethically forbidden in humans and thus no considerable option. In somatic gene therapy, three different types are known and used so far, which all include gene delivery either by non-viral vectors requiring chemical or physical methods of DNA delivery or by viral gene transduction (Nayerossadat et al., 2012). *Ex vivo* delivery includes the *in vitro* genetic manipulation of cells taken from the target organ or tissue followed by transplantation to reduce immune responses, but is limited due to the small percentage of cells in the organism that ultimately end up genetically modified. *In situ* delivery includes the direct administration of the gene product to the target tissue, but still displays low efficiency. In contrast, in *in vivo* gene therapy vectors are usually administered by injection into the bloodstream, but are designed in such a way that allows their allocation to one specific site or tissue depending the type of vector used (Nayerossadat et al., 2012).

In the past, a viral gene therapeutic approach involving adeno-associated virus (AAV)-mediated gene transfer of an expression cassette containing the Reiss variant of human *MOCS1* has been used as an attempt to cure the phenotype of *Mocs1*$^{-/-}$ mice (Hahnewald, 2009). As the expression of SOX in a healthy organism is highest in the liver (Woo et al., 2003), a chimeric AAV1/2, which was shown to result in a high tropism for liver and muscle tissue, was used to maximize the therapeutic effect. The first cohort of *Mocs1*$^{-/-}$ mice was treated by intrahepatic injection at P1 and P4, which resulted in a liver SOX activity of 5% at an age of ~70 days and an average survival time of 302 days (Hahnewald, 2009). Mice developed indistinguishable from their wildtype littermates, however were unable to produce viable offspring. A second cohort of *Mocs1*$^{-/-}$ mice was pretreated with cPMP to allow survival until adult age before injection of AAV-*MOCS1* at P40. Later treatment resulted in an average survival time of 356 days and a liver SOX activity of 75% compared to the wildtype, which rendered mice fertile and able to produce viable offspring displaying the phenotype of untreated *Mocs1*$^{-/-}$ mice. Simultaneously, this confirmed the absence of AAV-mediated genetic alterations in produced offspring and is thus in agreement with the prohibition of germline therapy in humans. The discrepancy in SOX activity between

different injection timepoints can be ascribed to a dilution effect due to increased cell division in the liver of neonatal compared to adult mice and highlights the importance of finding a treatment against SOXD that allows survival at least until young adult age. A combination of enzyme replacement therapy at an early age followed by subsequent gene therapy might be considered to achieve an optimal therapeutic effect.

The downside of gene therapy is the development of malignant tumors that were reported in 16% of treated mice depending on the site of integration in the genome (Hahnewald, 2009). Further modification, as for example altering transduction efficiency by site directed mutagenesis to allow usage of lower virus concentrations (Ran et al., 2020) or considering the usage of an *ex vivo* approach to allow selection of cells without random and thus potentially carcinogenic vector integration (Schultz & Chamberlain, 2008), will be required in the future to make this therapeutic strategy safe for the treatment of human SOXD and MoCD patients.

5.7 Concluding remarks on potential treatment strategies for SOXD

The current study evaluated the potential of several different treatment strategies, including NMDAR blockage as a prevention of excitotoxic neurodegeneration, sulfite scavenging as a direct way to reduce sulfite levels, dietary restriction of proteins and sulfur-containing amino acids to prevent sulfite accumulation, inhibition of ferroptosis, a non-apoptotic regulated cell death triggered by cysteine depletion, and an enzyme replacement therapy for the reconstitution of SOX activity. In conclusion, none of the tested strategies resulted in a sufficiently distinct improvement of the overall health condition of *Suox*$^{-/-}$ mice.

Due to the absence of a major cerebral phenotype in *Suox*$^{-/-}$ mice, NMDAR blockage can be considered an unsuitable treatment approach, so studies aiming on the prevention of SSC-mediated neurotoxicity for the moment can be discontinued. However, in case of successful generation of a conditional *Mocs2*$^{-/-}$ mouse model, a later induction of the disease most likely will allow the development of the classic, human-like SOXD phenotype majorly impacting the brain. For this mouse model, treatment with the NMDAR antagonist memantine might be reconsidered as a treatment strategy.

SSC-mediated toxicity was shown to be a minor contributor to the phenotype of *Suox*$^{-/-}$ mice, while the 5.5-fold higher accumulation of sulfite compared to human patients was considered to result in major sulfite-mediated toxicity in our mouse model. Usage of thiol-reactive compounds as sulfite scavengers was so far unsuccessful, but as an easy, straightforward treatment approach still holds great potential for future studies. Adjustment

of dosage and frequency of administration, as well as the search for a more effective compound, will be ways to optimize this treatment strategy.

Dietary restriction proved unsuitable in neonates due to the experimental impracticality of a direct manipulation of the pups' diet. Usage of this technique might be considered as an additive approach in a conditional knockout mouse model with induction of the disease at an adult age, which allows better control of the dietary intake.

Besides sulfite toxicity, our current knowledge also strongly suggests a major contribution of H_2S-mediated toxicity to the development of the severe phenotype of SOXD in mice. Hence, inhibition of the H_2S pathway of cysteine catabolism via the CBS and CSE inhibitor AOAA in the future will be tested as an attempt to reduce H_2S and sulfite accumulation and thus improve symptomatology in *Suox*$^{-/-}$ mice.

Ferroptosis inhibition in the current study did not result in an amelioration of the phenotype of *Suox*$^{-/-}$ mice, as ferroptosis was proven to not be caused, but rather inhibited due to loss of SOX function. In the future, search for the cell death pathway(s) majorly found in SOXD will allow usage of the right cell death inhibitor as a therapeutic agent.

Lastly, reconstitution of SOX activity presents a powerful treatment strategy aiming for the amelioration of all aspects of SOXD symptomatology. The enzyme replacement therapy using mSOX-Mo, which was tested in the course of the current study, will require minor adjustment of the dosage and a potential co-administration of catalase as an H_2O_2-detoxifying enzyme, but overall is a promising candidate as a therapeutic for SOXD and MoCD. Alternatively, advancement of a gene therapeutic approach, which had been tested as a cure for *Mocs1*$^{-/-}$ mice in the past, might also lead to the discovery of a potent therapy for SOXD and MoCD in mice and humans.

Overall, several potential treatment strategies remain to be elucidated in upcoming studies (Fig. 1). Hence, presumably in the near future a suitable therapy for SOXD in mice will be established, which will provide a foundation for the development of a treatment strategy for SOXD in humans.

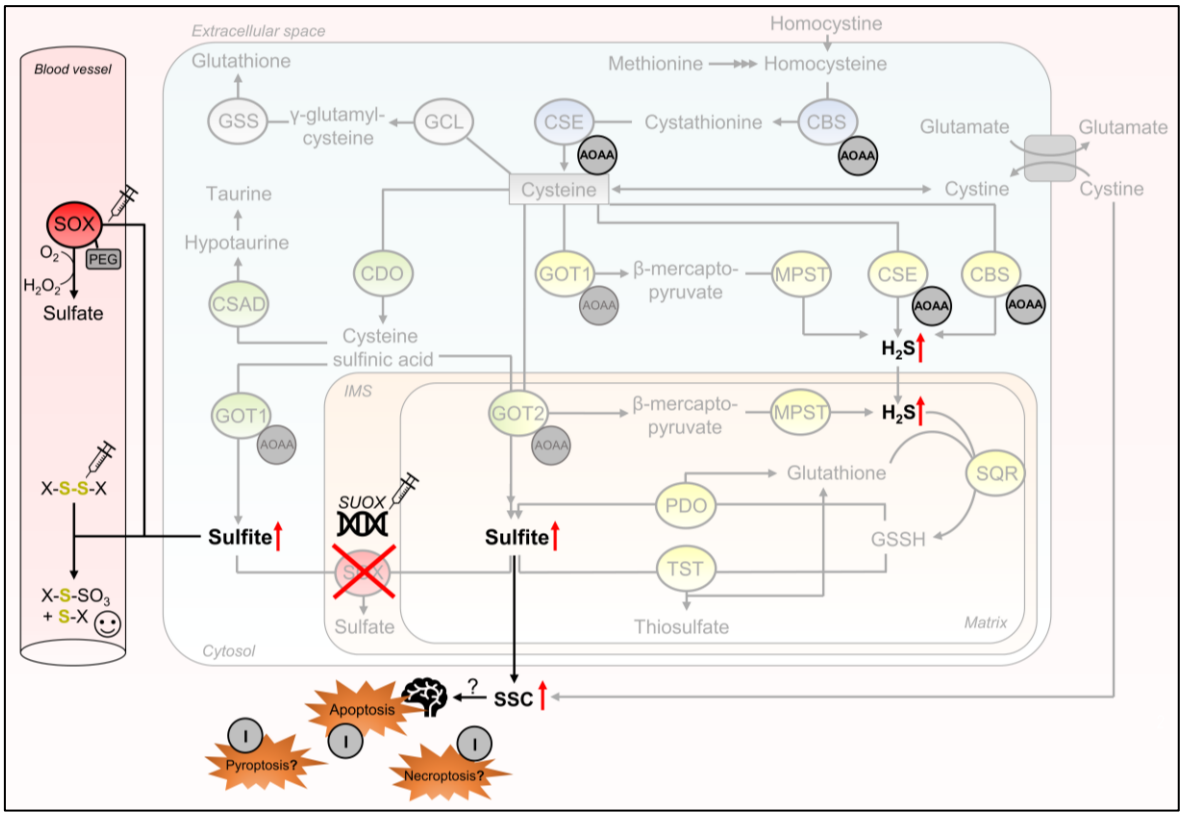

Figure 1: Overview of potential treatment approaches to cure SOXD in mice.
In the current study, chemical sulfite scavenging and enzyme replacement therapy did not exhibit a sufficiently beneficial effect on the average survival time of *Suox*$^{-/-}$ mice, but remain promising treatment strategies upon adjustment of the utilized experimental protocols. In addition, inhibition of the H_2S pathway of cysteine catabolism via AOAA (strong inhibition shown in black, weak inhibition shown in grey) to reduce H_2S and sulfite accumulation, inhibition of different regulated cell death pathways potentially triggered by sulfite and H_2S accumulation, as well as gene therapy to reconstitute SOX activity, present promising strategies in the search for a curation of murine SOXD.

5.8 Human vs murine epidermal development

Mouse models have been used to study human skin diseases since decades, however often are unable to fully reproduce human symptomatology due to evident structural differences in murine and human skin physiology. In general, in both species the skin is comprised of three layers starting with the innermost hypodermic layer, followed by the dermis and the epidermis (Gerber et al., 2014). The epidermis as the outmost layer provides a robust, protective outside-in barrier against exogenic factors such as germs, UV radiation and minor mechanical forces, while simultaneously providing an inside-out barrier function protecting the organism against dehydration from transepidermal water loss (TEWL) (Monteiro-Riviere, 2005). Epidermal development in humans starts at the end of embryonic week 4 with the formation of the ectoderm, which presents the precursor of the epidermal basal layer, the stratum basale (SB). After initiation of the stratification process after 5 weeks of embryonic development, formation of the periderm yields a single layer of cells that covers the skin until the differentiation process is completed under formation of the epidermis. After

three months, basal cells start proliferating and forming multiple layers named stratum intermedium, which after six months has developed into stratum spinosum (SS), stratum granulosum (SG) and stratum corneum (SC) (Zingkou et al., 2022). Mouse epidermal development follows a similar pattern, but proceeds significantly faster, with the stratification process starting at E10.5 and a functional epidermal barrier being formed at E18.5 (Du et al., 2018).

Despite the similarities in the structural layers, there are several differences between human and murine skin. The first crucial difference residues in the thickness of the formed epidermis, with 100 µM in humans and 25 µM in mice (Khavari, 2006). While human epidermis consists of five to ten layers of keratinocytes, mice only show two to three layers accompanied by faster epidermal turnover, looser skin attachment and lower barrier function (Berking, 2002; Menon, 2002; Salgado et al., 2017). Furthermore, mice show distinct fur growth resulting in a higher number of densely distributed hair follicles, which undergo synchronous cycles of hair growth, while humans show significantly lower hair growth in asynchronous growth cycles (van der Veen et al., 1999). Moreover, mice harbor an additional thin, subcutaneous muscle layer named panniculus carnosus, which humans only show in the platysma muscle of the neck (Wong et al., 2011). This results in differences in wound healing, as human skin heals by granulation tissue formation and re-epithelization, while mouse skin mainly heals via contraction (Wong et al., 2011). In comparison to humans, mice also express a significantly altered set of skin-related genes. A previous study determined 666 skin-associated genes in humans and 873 in mice (Gerber et al., 2014). A comparison between both lists revealed 201 shared genes between humans and mice, thus only making up 30.2% of identity. For example, mice showed a group of genes associated with the panniculus carnosus, while humans express more genes associated with keratinocytes, being consistent with the increased thickness of human epidermis. In contrast, mice show an increased number of extracellular matrix and carbohydrate-binding components, which implies a decreased relative level of interstitial matrix to keratinocytes, thus being in line with a lowered epidermal barrier function (Gerber et al., 2014). Overall, these significant differences highlight the complexity and challenges of using mouse models for human skin diseases.

5.9 Potentially sulfite-related epidermal phenotype in *Suox*$^{-/-}$ mice

The unexpected absence of a prominent neurological phenotype in *Suox*$^{-/-}$ mice raised the question of the cause underlying the severely shortened life span of this mouse model and required the examination of different organs regardless of an absence of other prominent organ failures in human SOXD. Histologic analysis of different *Suox*$^{-/-}$ organs so far showed

impairment of several somatic functions. The first study on *Suox*$^{-/-}$ mice found elevated levels of urinary proteins in general and albuminuria in particular, which indicates decreased glomerular function and represents a hallmark for multiple kidney diseases (Kohl, 2019; Larkins et al., 2019). In a follow-up study, enlarged alveolar airspaces in the lung, which imply a severe pulmonary phenotype, as well as increased levels of β-hydroxybutyrate, a potential signaling metabolite in starvation response, were found (Fu et al., in preparation) (Rojas-Morales et al., 2016). Thus, defining one major cause of death in these mice remains challenging. Most likely, accumulation of sulfite and accompanying sulfur metabolites in the entire organism ultimately results in multi-organ damage, so analysis of more organs is required to understand the complete symptomatology and pathomechanism of human SOXD.

The current study for the first time characterized a dermal phenotype observed in *Suox*$^{-/-}$ mice (see chapter IV), which had already been reported but not further examined in a mouse model of MoCD type B that presented with flaky and wrinkly skin (Jakubiczka-Smorag et al., 2016). Similarly, *Suox*$^{-/-}$ mice presented with dry, flaky skin patches, which suggested a decreased barrier function resulting in increased TEWL. However, as mice are born without a visual phenotype and classic mouse models with barrier dysfunctions die within the first 24 hours of life due to vast dehydration, a postnatal manifestation of the phenotype was hypothesized. To examine this hypothesis, skin samples were taken at P0 and, in another cohort, at P5, as *Suox*$^{-/-}$ mice usually die between six to twelve days and major pup loss prior to sample collection was aimed to be avoided.

A first analysis of H&E-stained histological samples indeed revealed proper structural organization and no distinct differences between homozygous *Suox*$^{-/-}$ mice and healthy control littermates at P0. In line with this finding, basal cell marker keratin (K) 14 and early differentiation marker K10 were expressed and distributed normally, and staining for Ki67 demonstrated similar proliferation between control and *Suox*$^{-/-}$ newborn mice, thus verifying healthy epidermal development *in utero* despite loss of SOX function.

In contrast, histological analyses of samples taken at P5 revealed major differences in epidermal architecture, as the majority of *Suox*$^{-/-}$ mice displayed an increase in epidermal thickness and structural differences in every epidermal layer. Importantly, skin samples of *Suox*$^{-/-}$ mice displayed a high variation in their phenotypic representation, which appears to be proportional to the expected individual survival time of each animal. The manifestation of a similar phenotype can be anticipated as a distinct symptom of all *Suox*$^{-/-}$ mice at an advanced stage of the disease, hence highlighting the importance of understanding the

mechanism underlying this epidermal phenotype. The discussion will therefore focus on results obtained from animals already presenting with a distinct phenotype at P5.

In *Suox*$^{-/-}$ mice at P5, cells in the SB were increased in size and showed a decreased structural organization, the SS showed an overall increase in thickness in opposition to the SG, which presented thinner with a lower number of cell layers, and the SC displayed parakeratosis, thus suggesting impaired terminal differentiation. Basal cell marker K14 was widely distributed throughout the SB, but also present in the SS, while early differentiation marker K10 displayed a significant decrease in expression. Combined with the observed parakeratosis in the SC, one can hypothesize a strongly defective, very late onset differentiation, which uses hyperproliferation as a compensatory mechanism.

Subsequently, the structural proteins filaggrin, involucrin and loricrin were analyzed as late stage differentiation markers. Involucrin did not show any phenotypic alterations between *Suox*$^{-/-}$ and wildtype mice. In contrast, staining for loricrin, the major structural protein of the cornified cell envelope, showed a severe decrease in intensity, while filaggrin expression was mildly reduced and started only in residual SG and SC, thus relatively late in differentiation, consequently pointing towards a loss of structural integrity in later epidermal layers. Moreover, increased expression of stress keratin K6a and proliferation marker Ki67 gave additional evidence for hyperproliferation as an attempt to restore structural integrity.

Quantitative PCR analysis of *Suox*$^{-/-}$ mice with a severe phenotype showed no major alterations in most inflammatory genes, but revealed a significant increase in interleukin *IL-1β* and a vast increase in cytokine *Tslp* mRNA levels. In human atopic dermatitis, a chronic inflammatory skin disease characterized by severe itch, recurrent eczema and skin lesions (Weidinger et al., 2018), upregulated expression of IL-1β results in the activation of NF-κB, a rapid-acting transcription factor, which in turn causes the downregulation of filaggrin and loricrin expression (Michaelidou et al., 2023). Additionally, IL-1β has been demonstrated to induce the expression of stress keratin K6a (Komine et al., 2001), thus agreeing with the results obtained in the current study. Cytokine TSLP in human keratinocytes is known to interrupt epidermal barrier integrity by upregulating the expression of IL-33, a molecule that acts as a cytokine and a nuclear factor, and stimulating the formation of a nuclear complex from IL-33 and phosphorylated STAT3, which acts as a direct transcription factor downregulating the gene expressing filaggrin (Dai et al., 2022). Additionally, nuclear IL-33 reduces expression of the transcription factor RUNX1, which results in a downregulation of loricrin and K10 expression (Dai et al., 2021).

While only specific inflammatory genes were upregulated in *Suox*$^{-/-}$ mice, a vast increase in the mRNA levels of the majority of tested stress response genes could be observed, including genes encoding for proteins involved in peptide-crosslinking, such as small-proline rich proteins (Sprrs) Sprr2b, Sprr2d and Sprr2e, which were upregulated 50-, 6150- and 6330-fold, respectively (Steinert et al., 1998). Genes encoding for proteins involved in wound healing, such as S100a8 and Slpi, displayed a 191- and 94-fold increase, respectively (Su et al., 2022; Wingens et al., 1998). Notably, two members of the Sprr protein family, namely Sprr2d and Sprr2h, also showed five-fold upregulation in *Lor*$^{-/-}$ mouse embryos, where this acts as a compensatory mechanism for the loss of loricrin to allow delayed, but functional epidermal barrier formation (Koch et al., 2000). Hence, a severe upregulation of genes expressing proteins involved in peptide-crosslinking and wound healing in *Suox*$^{-/-}$ mice presumably aims to counteract the loss of epidermal integrity.

Progressive loss of epidermal integrity is accompanied by an impairment of epidermal barrier function. Integrity of the epidermal outside-in barrier is typically examined in a dye penetration assay, in which loss of barrier function results in staining of the entire skin (Indra & Leid, 2011). A toluidine blue staining assay was performed in the course of the current study as well, but did not reveal increased staining of *Suox*$^{-/-}$ skin compared to controls at P5 (Supplementary Fig. 1A). However, dye penetration assays are usually performed in mouse fetuses or neonates, as loss of epidermal barrier function is mostly found to be caused by defective epidermal development *in utero*, which results in neonatal death (Ding et al., 2016; Maass et al., 2004; Matsuki et al., 1998). The toluidine blue assay in particular has been developed as a measure to analyze epidermal barrier formation starting at embryonic day E16 (Hardman et al., 1998). Hence, the thickness of murine skin at P5 may prohibit the detection of outside-in barrier defects in a toluidine blue dye penetration assay.

In contrast, analysis of the inside-out barrier function by measuring TEWL is a standard experiment performed on mice of all ages (Indra & Leid, 2011). In the course of the current study, TEWL measurement was performed on mice at P5, but due to technical issues with the Tewameter®, a device used for measuring TEWL, did not yield reliable data. Results obtained showed no significant increase of TEWL in *Suox*$^{-/-}$ mice compared to healthy littermates (Supplementary Fig. 1B), but could not be verified in a sufficiently high animal number and therefore need to be treated with caution. The severe epidermal phenotype that develops during progression of murine SOXD can be assumed to result in excess TEWL shortly before death, however might not be elevated significantly several days in advance. A repetition of the measurement will be crucial to understand the impact of the observed morphological changes on the inside-out barrier function of *Suox*$^{-/-}$ skin.

In a study assessing the effects of dehydration caused by water deprivation, mice showed decreased activity up to lethargy, weight loss, as well as decreased food intake, a phenomenon described as dehydration anorexia (Watts, 1998). Dehydrated mice presented with altered blood parameters including increased plasma osmolality and sodium as well as hematocrit values implying fluid loss in intracellular as well as extracellular compartments (Bekkevold et al., 2013). Furthermore, they displayed renal distal tubular dilatation pointing towards an impairment of kidney integrity, while brain, lung, heart and liver morphology were unaltered. Although the cited study was conducted on adult mice, several parallels can be drawn to our *Suox*$^{-/-}$ mouse model, in which dehydration might cause the observed renal phenotype, as well as a decrease in mobility, weight and potentially food intake, as stomach content typically contains lower amounts of milk in *Suox*$^{-/-}$ mice. Notably, as mice at P5 are still nursed, a decreased food intake simultaneously results in further dehydration, thus presumably deteriorating dehydration shortly before death.

Overall, our data strongly suggest a loss of epidermal barrier integrity as a cause of SOX deficiency. Although SOX is moderately expressed in the skin (Uhlén et al., 2015), it has not yet been shown to contribute to skin homeostasis. Therefore, the observed phenotype can more likely be ascribed to the increased accumulation of sulfur metabolites in general and sulfite in particular in SOXD, rather than to a direct loss of enzymatic function.

Sulfite is a strong nucleophile that has been shown to cleave disulfide bridges (Kella & Kinsella, 1985), which are crucial structural elements in epidermal barrier formation due to their ability to crosslink keratin filaments and structural proteins in terminal differentiation (Hohl et al., 1991; Suns & Green, 1978). Previously, the disulfide bond-forming cysteine residue C373 in the basal cell marker K14 has been proven crucial for intact epidermal homeostasis and barrier function (Guo et al., 2020). Loss of this particular disulfide bridge in K14 due to a cysteine to alanine substitution resulted in increased cell proliferation and impaired terminal differentiation characterized by an increase in the area of K14 staining accompanied by a decrease in staining of early differentiation marker K10 and late differentiation markers filaggrin and loricrin (Guo et al., 2020). The study demonstrated the essential role of this disulfide bond for the interaction between K14 and 14-3-3σ, which enables the latter to inhibit the function of YAP1, a transcriptional co-activator that promotes cell proliferation and suppresses terminal differentiation in epidermal keratinocytes by modulating its cellular localization (Sambandam et al., 2015; Zhang et al., 2011). Notably, this effect was only verified in skin taken from ear and tail, as back skin was shown to contain a lower level of disulfide-bridged K14 (Guo et al., 2020). However, the study utilized adult mice and differences in the distribution and amount of disulfide bridges during early postnatal development can be speculated. Hence, a similar loss of disulfide-bonded K14 is

proposed to result in the loss of epidermal integrity observed in *Suox*$^{-/-}$ skin. Immunofluorescent staining for 14-3-3σ and YAP1, as well as western blot analysis of disulfide-bonded K14 in *Suox*$^{-/-}$ skin in the future will allow verification of this hypothesis.

Moreover, extensive disulfide bond-mediated cross-linkage of the structural protein loricrin, which is the major component of the cornified cell envelope, promotes stabilization of the SC (Ishitsuka & Roop, 2020). In contrast, the structural protein involucrin is a major substrate to transglutaminase-mediated Nε-(γ-glutamyl)lysine cross-linkage (Simon & Green, 1985). As cross-linkage of glutamine and lysine is anticipated to be unaffected by sulfite, this provides an explanation for the unaltered levels of involucrin accompanied by a severe loss of loricrin, which presumably results in a destabilization of the SC in *Suox*$^{-/-}$ mice. A quantification of sulfite in lysates of *Suox*$^{-/-}$ skin in the future will be important to confirm the presence of sulfite levels elevated to a degree enabling extensive sulfite-mediated disulfide bond cleavage.

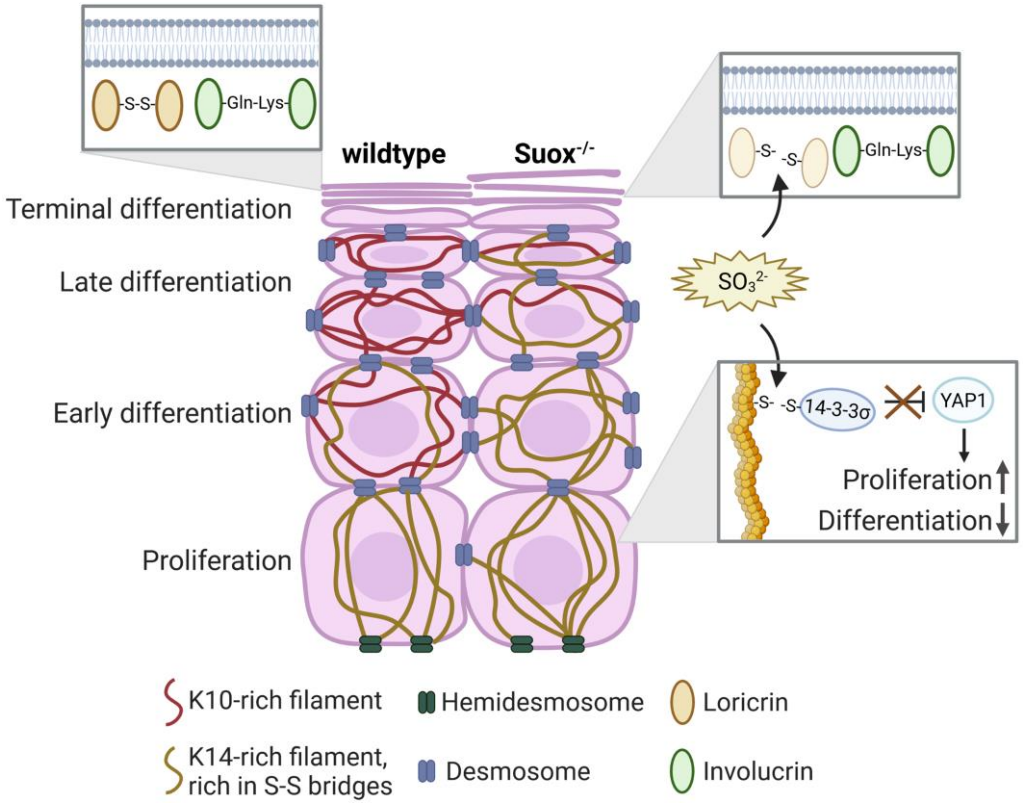

Figure 2: Proposed mechanism of sulfite-mediated destabilization of the epidermal barrier in Suox$^{-/-}$ mice.
Sulfite is hypothesized to attack disulfide bonds formed by K14, which are crucial for its interaction with 14-3-3σ. Loss of this interaction results in a loss of the inhibitory effect of 14-3-3σ on transcription factor YAP1, which when active promotes cell proliferation and suppresses terminal differentiation. In addition, sulfite is proposed to cleave disulfide bond-mediated cross-linkage of the structural protein loricrin resulting in its degradation and a potential destabilization of the SC, while Nε-(γ-glutamyl)lysine cross-linkage of involucrin remains unaffected by sulfite. K14-rich filaments are depicted in yellow, K10- rich filaments in red. Desmosomes are depicted in blue, hemidesmosomes in dark green. Loricrin is shown in yellow and involucrin in light green. Figure created with BioRender.

In summary, discovery of a novel, epidermal phenotype in *Suox*$^{-/-}$ mice for the first time attributed a role in epidermal homeostasis to SOX, which had not been linked to the skin before. Nevertheless, the absence of a defective inside-out barrier at P5 despite an already apparent lowered body weight and motor function in *Suox*$^{-/-}$ mice implies the contribution of additional factors to the severity of the observed phenotype and excludes loss of epidermal barrier function as the sole, major cause of death in these animals. Instead, a complex interplay between different, presumably mainly sulfite- and H_2S-driven mechanisms is anticipated to result in multi-organ failure. In the future, morphologic analysis of additional organs such as liver, heart, intestine and the lymphatic system will be required to further elucidate the exact pathomechanism underlying murine SOXD.

In contrast to mice, the symptomatology of human SOXD patients does not include the development of skin alterations in the progress of the disease. One major difference between murine and human skin is the epidermal thickness, which is four times greater in humans than in mice (Khavari, 2006). In addition, the *in utero* formation of the epidermis in humans is completed after six months, thus after two third of gestation, while the murine epidermal barrier is only formed at E18.5, thus shortly before birth (Du et al., 2018; Zingkou et al., 2022). Therefore, development of the skin until birth is presumably more advanced in humans than in mice, with the latter being born with thin, almost transparent skin. This implies the existence of a more robust epidermal barrier in humans at birth and consequently the lack of an epidermal phenotype.

Taken together, overall human skin in all probability is less susceptible to sulfite-induced disruption of epidermal barrier integrity. However, studies on the pathomechanism of human SOXD mainly focus on the neurological impairments caused by brain morphological alterations. Hence, as discussed above, an increase in the life expectancy of SOXD patients due to curation of the cerebral phenotype might result in an increased manifestation of non-cerebral impairments including the skin, assuming a different pace for the development of symptoms in humans and mice due to their physiological varieties. Therefore, investigation of the skin phenotype in mice could provide valuable insights into any possible skin symptoms in human patients.

5.10 Conclusion

In summary, the findings of the current study emphasize the great complexity of murine SOXD and strongly suggest the co-existence of not only a single, but multiple underlying sulfite- and H_2S-mediated pathomechanisms causing the severe phenotype that develops within the first days of life. In addition, this work proved the manifestation of a postnatal epidermal phenotype in *Suox*$^{-/-}$ mice, which is characterized by hyperproliferation and

defective terminal differentiation presumably resulting in epidermal barrier disruption during further disease progression. Hence, in agreement with the preliminary results obtained in this study, a treatment strategy focusing on reconstitution of SOX activity to allow reduction of all sulfur metabolites accumulating in SOXD, thus preventing multi-organ damage, will be the most promising candidate for future studies. As this general approach does not focus on single aspects of the disease mechanism, studies will provide valuable insights for the subsequent development of a treatment strategy applicable for human SOXD and presumably also MoCD patients.

5.11 References

Abe, Y., Aihara, Y., Endo, W., Hasegawa, H., Ichida, K., Uematsu, M., & Kure, S. (2021). The effect of dietary protein restriction in a case of molybdenum cofactor deficiency with MOCS1 mutation. *Molecular Genetics and Metabolism Reports*, *26*, 100716. https://doi.org/10.1016/J.YMGMR.2021.100716

Amaral, A. U., Cecatto, C., Busanello, E. N. B., Ribeiro, C. A. J., Melo, D. R., Leipnitz, G., Castilho, R. F., & Wajner, M. (2012). Ethylmalonic acid impairs brain mitochondrial succinate and malate transport. *Molecular Genetics and Metabolism*, *105*(1), 84–90. https://doi.org/10.1016/J.YMGME.2011.10.006

Antti, H., & Sellstedt, M. (2018). Metabolic effects of an aspartate aminotransferase-inhibitor on two T-cell lines. *PLoS ONE*, *13*(12). https://doi.org/10.1371/JOURNAL.PONE.0208025

Asimakopoulou, A., Panopoulos, P., Chasapis, C. T., Coletta, C., Zhou, Z., Cirino, G., Giannis, A., Szabo, C., Spyroulias, G. A., & Papapetropoulos, A. (2013). Selectivity of commonly used pharmacological inhibitors for cystathionine β synthase (CBS) and cystathionine γ lyase (CSE). *British Journal of Pharmacology*, *169*(4), 922. https://doi.org/10.1111/BPH.12171

Bai, J., Lei, P., Zhang, J., Zhao, C., & Liang, R. (2013). Sulfite exposure-induced hepatocyte death is not associated with alterations in p53 protein expression. *Toxicology*, *312*(1), 142–148. https://doi.org/10.1016/J.TOX.2013.08.004

Baker, K., Marcus, C. B., Huffman, K., Kruk, H., Malfroy, B., & Doctrow, S. R. (1998). *Synthetic Combined Superoxide Dismutase/Catalase Mimetics Are Protective as a Delayed Treatment in a Rat Stroke Model: A Key Role for Reactive Oxygen Species in Ischemic Brain Injury*. http://www.jpet.org

Barayeu, U., Schilling, D., Eid, M., Xavier da Silva, T. N., Schlicker, L., Mitreska, N., Zapp, C., Gräter, F., Miller, A. K., Kappl, R., Schulze, A., Friedmann Angeli, J. P., & Dick, T. P. (2023). Hydropersulfides inhibit lipid peroxidation and ferroptosis by scavenging radicals. *Nature Chemical Biology*, *19*(1), 28–37. https://doi.org/10.1038/S41589-022-01145-W

Bekkevold, C. M., Robertson, K. L., Reinhard, M. K., Battles, A. H., & Rowland, N. E. (2013). Dehydration Parameters and Standards for Laboratory Mice. *Journal of the American Association for Laboratory Animal Science : JAALAS*, *52*(3), 233. /pmc/articles/PMC3690443/

Belaidi, A. A. (2011). *Human Molybdenum Cofactor Biosynthesis and Deficiency: Novel Functions and Therapies*.

Berking, C. (2002). Photocarcinogenesis in human adult skin grafts. *Carcinogenesis*, *23*(1), 181–187. https://doi.org/10.1093/carcin/23.1.181

Bindu, P. S., Nagappa, M., Bharath, R. D., & Taly, A. B. (2017). Isolated Sulfite Oxidase Deficiency. *GeneReviews*®. https://www.ncbi.nlm.nih.gov/books/NBK453433/

Boles, R. G., Ment, L. R., Meyn, M. S., Horwich, A. L., Kratz, L. E., & Rinaldo, P. (1993). Short-term response to dietary therapy in molybdenum cofactor deficiency. *Annals of Neurology*, *34*(5), 742–744. https://doi.org/10.1002/ANA.410340520

Cherqui, S. (2012). Cysteamine therapy: a treatment for cystinosis, not a cure. *Kidney International*, *81*(2), 127. https://doi.org/10.1038/KI.2011.301

Dai, X., Muto, J., Shiraishi, K., Utsunomiya, R., Mori, H., Murakami, M., & Sayama, K. (2022). TSLP Impairs Epidermal Barrier Integrity by Stimulating the Formation of Nuclear IL-33/Phosphorylated STAT3 Complex in Human Keratinocytes. *Journal of Investigative Dermatology*, *142*(8), 2100-2108.e5. https://doi.org/10.1016/J.JID.2022.01.005

Dai, X., Utsunomiya, R., Shiraishi, K., Mori, H., Muto, J., Murakami, M., & Sayama, K. (2021). Nuclear IL-33 Plays an Important Role in the Suppression of FLG, LOR, Keratin 1, and Keratin 10 by IL-4 and IL-13 in Human Keratinocytes. *Journal of Investigative Dermatology*, *141*(11), 2646-2655.e6. https://doi.org/10.1016/J.JID.2021.04.002

Deng, G., Muqadas, M., Adlat, S., Zheng, H., Li, G., Zhu, P., & Nasser, M. I. (2023). Protective Effect of Hydrogen Sulfide on Cerebral Ischemia–Reperfusion Injury. *Cellular and Molecular Neurobiology*, *43*(1), 15–25. https://doi.org/10.1007/S10571-021-01166-4/FIGURES/2

Dhani, S., Zhao, Y., & Zhivotovsky, B. (2021). A long way to go: caspase inhibitors in clinical use. *Cell Death & Disease*, *12*(10), 949. https://doi.org/10.1038/s41419-021-04240-3

Ding, X., Bloch, W., Iden, S., Rüegg, M. A., Hall, M. N., Leptin, M., Partridge, L., & Eming, S. A. (2016). mTORC1 and mTORC2 regulate skin morphogenesis and epidermal barrier formation. *Nature Communications*, *7*, 13226. https://doi.org/10.1038/NCOMMS13226

Dixon, S. J., Lemberg, K. M., Lamprecht, M. R., Skouta, R., Zaitsev, E. M., Gleason, C. E., Patel, D. N., Bauer, A. J., Cantley, A. M., Yang, W. S., Morrison 3rd, B., & Stockwell, B. R. (2012). Ferroptosis: an iron-dependent form of nonapoptotic cell death. *Cell*, *149*(5), 1060–1072. https://doi.org/10.1016/j.cell.2012.03.042

Du, H., Wang, Y., Haensel, D., Lee, B., Dai, X., & Nie, Q. (2018). Multiscale modeling of layer formation in epidermis. *PLOS Computational Biology*, *14*(2), e1006006. https://doi.org/10.1371/journal.pcbi.1006006

Galluzzi, L., Vitale, I., Aaronson, S. A., Abrams, J. M., Adam, D., Agostinis, P., Alnemri, E. S., Altucci, L., Amelio, I., Andrews, D. W., Annicchiarico-Petruzzelli, M., Antonov, A. V., Arama, E., Baehrecke, E. H., Barlev, N. A., Bazan, N. G., Bernassola, F., Bertrand, M. J. M., Bianchi, K., … Kroemer, G. (2018). Molecular mechanisms of cell death: recommendations of the Nomenclature Committee on Cell Death 2018. *Cell Death & Differentiation 2018 25:3*, *25*(3), 486–541. https://doi.org/10.1038/s41418-017-0012-4

Gerber, P. A., Buhren, B. A., Schrumpf, H., Homey, B., Zlotnik, A., & Hevezi, P. (2014). The top skin-associated genes: A comparative analysis of human and mouse skin transcriptomes. *Biological Chemistry*, *395*(6), 577–591. https://doi.org/10.1515/HSZ-2013-0279

Gerschenfeld, . H M, Ascher, P., Tauic, L., Frank, ; K, Tauc, L., Oomura, ; Y, Ooyama, H., & Sawada, M. (1967). Sulfite oxidase deficiency in man: Demonstration of the enzymatic defect. *Science*, *156*(3782), 1599–1602. https://doi.org/10.1126/SCIENCE.156.3782.1599

Gong, W., Zhang, S., Chen, Y., Shen, J., Zheng, Y., Liu, X., Zhu, M., & Meng, G. (2022). Protective role of hydrogen sulfide against diabetic cardiomyopathy via alleviating necroptosis. *Free Radical Biology and Medicine*, *181*, 29–42. https://doi.org/10.1016/J.FREERADBIOMED.2022.01.028

Guo, Y., Redmond, C. J., Leacock, K. A., Brovkina, M. V, Ji, S., Jaskula-Ranga, V., & Coulombe, P. A. (2020). *Keratin 14-dependent disulfides regulate epidermal homeostasis and barrier function via 14-3-3s and YAP1*. https://doi.org/10.7554/eLife.53165

Hahnewald, R. (2009). Tiermodelle der Molybdän-Cofaktor-Defizienz und ihre Therapie.

Hänsch, R., Lang, C., Riebeseel, E., Lindigkeit, R., Gessler, A., Rennenberg, H., & Mendel, R. R. (2006). Plant Sulfite Oxidase as Novel Producer of H2O2: COMBINATION OF ENZYME CATALYSIS WITH A SUBSEQUENT NON-ENZYMATIC REACTION STEP. *Journal of Biological Chemistry*, *281*(10), 6884–6888. https://doi.org/10.1074/JBC.M513054200

Han, X., Zhu, F., Chen, L., Wu, H., Wang, T., & Chen, K. (2020). Mechanism analysis of toxicity of sodium sulfite to human hepatocytes L02. *Molecular and Cellular Biochemistry*, *473*(1–2), 25–37. https://doi.org/10.1007/S11010-020-03805-8/TABLES/2

Hardman, M. J., Sisi, P., Banbury, D. N., & Byrne, C. (1998). Patterned acquisition of skin barrier function during development. *Development*, *125*(8), 1541–1552. https://doi.org/10.1242/DEV.125.8.1541

Hildebrandt, T. M., Di Meo, I., Zeviani, M., Viscomi, C., & Braun, H. P. (2013). Proteome adaptations in Ethe1-deficient mice indicate a role in lipid catabolism and cytoskeleton organization via post-translational protein modifications. *Bioscience Reports*, *33*(4), 575–584. https://doi.org/10.1042/BSR20130051

Hohl, D., Mehrel, T., Lichti, U., Turner, M. L., Roop, D. R., & Steinert, P. M. (1991). Characterization of human loricrin. Structure and function of a new class of epidermal cell envelope proteins. *Journal of Biological Chemistry*, *266*(10), 6626–6636. https://doi.org/10.1016/S0021-9258(18)38163-8

Indra, A. K., & Leid, M. (2011). Epidermal Permeability Barrier (EPB) measurement in mammalian skin. *Methods in Molecular Biology (Clifton, N.j.)*, *763*, 73. https://doi.org/10.1007/978-1-61779-191-8_4

Ishitsuka, Y., & Roop, D. R. (2020). Loricrin: Past, Present, and Future. *International Journal of Molecular Sciences 2020, Vol. 21, Page 2271*, *21*(7), 2271. https://doi.org/10.3390/IJMS21072271

Jakubiczka-Smorag, J., Santamaria-Araujo, J. A., Metz, I., Kumar, A., Hakroush, S., Brueck, W., Schwarz, G., Burfeind, P., Reiss, J., & Smorag, L. (2016). Mouse model for molybdenum cofactor deficiency type B recapitulates the phenotype observed in molybdenum cofactor deficient patients. *Human Genetics*, *135*(7), 813–826. https://doi.org/10.1007/s00439-016-1676-4

Jeżégou, A., Llinares, E., Anne, C., Kieffer-Jaquinod, S., O'Regan, S., Aupetit, J., Chabli, A., Sagné, C., Debacker, C., Chadefaux-Vekemans, B., Journet, A., Andreć, B., & Gasnier, B. (2012). Heptahelical protein PQLC2 is a lysosomal cationic amino acid exporter underlying the action of cysteamine in cystinosis therapy. *Proceedings of the National*

Academy of Sciences of the United States of America, *109*(50). https://doi.org/10.1073/PNAS.1211198109

Jocelyn, P. C. (1987). Chemical reduction of disulfides. *Methods Enzymol*, *143*, 246–256. https://doi.org/10.1016/0076-6879(87)43048-6

Johnson, J. L., Coyne, K. E., Garrett, R. M., Zabot, M. T., Dorche, C., Kisker, C., & Rajagopalan, K. V. (2002). Isolated sulfite oxidase deficiency: identification of 12 novel SUOX mutations in 10 patients. *Hum Mutat*, *20*(1), 74. https://doi.org/10.1002/humu.9038

Johnson, J. L., & Duran, M. (2001). Molybdenum cofactor deficiency and isolated sulfite oxidase deficiency. In *The Metabolic and Molecular Bases of Inherited Disease* (pp. 3163–3177). Mcgraw-Hill Professional.

Kalatzis, V., Cherqui, S., Antignac, C., & Gasnier, B. (2001). Cystinosin, the protein defective in cystinosis, is a H+-driven lysosomal cystine transporter. *The EMBO Journal*, *20*(21), 5940. https://doi.org/10.1093/EMBOJ/20.21.5940

Kar, S., Shahshahan, H. R., Hackfort, B. T., Yadav, S. K., Yadav, R., Kambis, T. N., Lefer, D. J., & Mishra, P. K. (2019). Exercise Training Promotes Cardiac Hydrogen Sulfide Biosynthesis and Mitigates Pyroptosis to Prevent High-Fat Diet-Induced Diabetic Cardiomyopathy. *Antioxidants 2019, Vol. 8, Page 638*, *8*(12), 638. https://doi.org/10.3390/ANTIOX8120638

Kella, N. K. D., & Kinsella, J. E. (1985). A method for the controlled cleavage of disulfide bonds in proteins in the absence of denaturants. *Journal of Biochemical and Biophysical Methods*, *11*(4–5), 251–263. https://doi.org/10.1016/0165-022X(85)90007-7

Khavari, P. A. (2006). Modelling cancer in human skin tissue. *Nature Reviews Cancer 2006 6:4*, *6*(4), 270–280. https://doi.org/10.1038/nrc1838

Koch, P. J., De Viragh, P. A., Scharer, E., Bundman, D., Longley, M. A., Bickenbach, J., Kawachi, Y., Suga, Y., Zhou, Z., Huber, M., Hohl, D., Kartasova, T., Jarnik, M., Steven, A. C., & Roop, D. R. (2000). Lessons from Loricrin-Deficient Mice: Compensatory Mechanisms Maintaining Skin Barrier Function in the Absence of a Major Cornified Envelope Protein. *The Journal of Cell Biology*, *151*(2), 389. https://doi.org/10.1083/JCB.151.2.389

Kohl, J. B. (2019). A Novel Mouse Model of Sulfite Oxidase Deficiency: Pathological Changes in Cysteine and H2S Metabolism. In *Department of Chemistry*.

Kohl, J. B., Mellis, A. T., & Schwarz, G. (2019). Homeostatic impact of sulfite and hydrogen sulfide on cysteine catabolism. *British Journal of Pharmacology*, *176*(4), 554–570. https://doi.org/10.1111/BPH.14464

Komine, M., Rao, L. S., Freedberg, I. M., Simon, M., Milisavljevic, V., & Blumenberg, M. (2001). Interleukin-1 induces transcription of keratin K6 in human epidermal keratinocytes. *Journal of Investigative Dermatology*, *116*(2), 330–338. https://doi.org/10.1046/j.1523-1747.2001.01249.x

Kožich, V., Schwahn, B. C., Sokolová, J., Křížková, M., Ditroi, T., Krijt, J., Khalil, Y., Křížek, T., Vaculíková-Fantlová, T., Stibůrková, B., Mills, P., Clayton, P., Barvíková, K., Blessing, H., Sykut-Cegielska, J., Dionisi-Vici, C., Gasperini, S., García-Cazorla, Á., Haack, T. B., … Nagy, P. (2022). Human ultrarare genetic disorders of sulfur metabolism demonstrate redundancies in H2S homeostasis. *Redox Biology*, *58*, 102517. https://doi.org/10.1016/J.REDOX.2022.102517

Kumar, A. (2016). Molecular Mechanism of Neurodegeneration in Molybdenum Cofactor Deficency:

Kumar, A., Dejanovic, B., Hetsch, F., Semtner, M., Fusca, D., Arjune, S., Santamaria-Araujo, J. A., Winkelmann, A., Ayton, S., Bush, A. I., Kloppenburg, P., Meier, J. C., Schwarz, G., & Belaidi, A. A. (2017). S-sulfocysteine/NMDA receptor-dependent signaling underlies neurodegeneration in molybdenum cofactor deficiency. *J Clin Invest*, *127*(12), 4365–4378. https://doi.org/10.1172/JCI89885

Larkins, N. G., Teixeira-Pinto, A., & Craig, J. C. (2019). A narrative review of proteinuria and albuminuria as clinical biomarkers in children. *Journal of Paediatrics and Child Health*, *55*(2), 136–142. https://doi.org/10.1111/jpc.14293

Leggett, J., And, B., & Colei, R. D. (1959). Studies on the Reaction of Sulfite with Proteins*. *THE JOURNAL OF Bro~o~rca~ CHE~.USTRY*, *234*(7). https://doi.org/10.1016/S0021-9258(18)69917-X

Liu, M., Lu, J., Chen, Y., Shi, X., Li, Y., Yang, S., Yu, J., & Guan, S. (2021). Sodium Sulfite-Induced Mast Cell Pyroptosis and Degranulation. *Journal of Agricultural and Food Chemistry*, *69*(27), 7755–7764. https://doi.org/10.1021/ACS.JAFC.1C02436

Maass, K., Ghanem, A., Kim, J. S., Saathoff, M., Urschel, S., Kirfel, G., Grümmer, R., Kretz, M., Lewalter, T., Tiemann, K., Winterhager, E., Herzog, V., & Willecke, K. (2004). Defective Epidermal Barrier in Neonatal Mice Lacking the C-Terminal Region of Connexin43. *Molecular Biology of the Cell*, *15*(10), 4597. https://doi.org/10.1091/MBC.E04-04-0324

Matsuki, M., Yamashita, F., Ishida-Yamamoto, A., Yamada, K., Kinoshita, C., Fushiki, S., Ueda, E., Morishima, Y., Tabata, K., Yasuno, H., Hashida, M., Iizuka, H., Ikawa, M., Okabe, M., Kondoh, G., Kinoshita, T., Takeda, J., & Yamanishi, K. (1998). Defective stratum corneum and early neonatal death in mice lacking the gene for transglutaminase 1 (keratinocyte transglutaminase). *Proceedings of the National Academy of Sciences of the United States of America*, *95*(3), 1044–1049. https://doi.org/10.1073/PNAS.95.3.1044/ASSET/834EA3D5-9ADD-4C3B-AEF9-C608474FAB31/ASSETS/GRAPHIC/PQ0383437005.JPEG

McCord, J. M. (2008). Superoxide Dismutase, Lipid Peroxidation, and Bell-Shaped Dose Response Curves. *Dose-Response*, *6*(3), 223. https://doi.org/10.2203/DOSE-RESPONSE.08-012.MCCORD

Mellis, A. T. (2020). *Sulfite Metabolism in Health and Disease: Biogenesis, Biochemical Changes and Mitochondrial Morphology*.

Mellis, A. T., Misko, A. L., Arjune, S., Liang, Y., Erdelyi, K., Ditroi, T., Kaczmarek, A. T., Nagy, P., & Schwarz, G. (2021). The role of glutamate oxaloacetate transaminases in sulfite biosynthesis and H2S metabolism. *Redox Biol*, *38*, 101800. https://doi.org/10.1016/j.redox.2020.101800

Menon, G. K. (2002). New insights into skin structure: scratching the surface. *Advanced Drug Delivery Reviews*, *54*, S3–S17. https://doi.org/10.1016/S0169-409X(02)00121-7

Michaelidou, M., Redhu, D., Kumari, V., Babina, M., & Worm, M. (2023). IL-1α/β and IL-18 profiles and their impact on claudin-1, loricrin and filaggrin expression in patients with atopic dermatitis. *Journal of the European Academy of Dermatology and Venereology*. https://doi.org/10.1111/jdv.19153

Monteiro-Riviere, N. (2005). Structure and Function of Skin. In *Dermal Absorption Models in Toxicology and Pharmacology* (pp. 1–19). CRC Press. https://doi.org/10.1201/9780203020821.ch1

Nayerossadat, N., Maedeh, T., & Ali, P. A. (2012). Viral and nonviral delivery systems for gene delivery. *Advanced Biomedical Research*, *1*(1), 27. https://doi.org/10.4103/2277-9175.98152

Okamoto, M., Ishizaki, T., & Kimura, T. (2015). Protective effect of hydrogen sulfide on pancreatic beta-cells. *Nitric Oxide*, *46*, 32–36. https://doi.org/10.1016/J.NIOX.2014.11.007

Olney, J. W., Misra, C. H., & de Gubareff, T. (1975). Cysteine-S-sulfate: brain damaging metabolite in sulfite oxidase deficiency. *J Neuropathol Exp Neurol*, *34*(2), 167–177. https://doi.org/10.1097/00005072-197503000-00005

Oshimo, M., Nakashima, F., Kai, K., Matsui, H., Shibata, T., & Akagawa, M. (2021). Sodium sulfite causes gastric mucosal cell death by inducing oxidative stress. *Free Radical Research*, *55*(6), 731–743. https://doi.org/10.1080/10715762.2021.1937620

Petersen, L. C. (1977). The effect of inhibitors on the oxygen kinetics of cytochrome c oxidase. *Biochimica et Biophysica Acta*, *460*(2), 299–307. https://doi.org/10.1016/0005-2728(77)90216-X

Pisoni, R. L., Thoene, J. G., & Christensen, H. N. (1985). Detection and characterization of carrier-mediated cationic amino acid transport in lysosomes of normal and cystinotic human fibroblasts. Role in therapeutic cystine removal? *Journal of Biological Chemistry*, *260*(8), 4791–4798. https://doi.org/10.1016/S0021-9258(18)89141-4

Pittman, R. N. (2011). *Oxygen Transport*. https://www.ncbi.nlm.nih.gov/books/NBK54103/

Ran, G., Chen, X., Xie, Y., Zheng, Q., Xie, J., Yu, C., Pittman, N., Qi, S., Yu, F.-X., Agbandje-Mckenna, M., Srivastava, A., & Ling, C. (2020). *Site-Directed Mutagenesis Improves the Transduction Efficiency of Capsid Library-Derived Recombinant AAV Vectors*. https://doi.org/10.1016/j.omtm.2020.03.007

Reiss, J., & Johnson, J. L. (2003). Mutations in the molybdenum cofactor biosynthetic genes MOCS1, MOCS2, and GEPH. *Hum Mutat*, *21*(6), 569–576. https://doi.org/10.1002/humu.10223

Rojas-Morales, P., Tapia, E., & Pedraza-Chaverri, J. (2016). β-Hydroxybutyrate: A signaling metabolite in starvation response? *Cellular Signalling*, *28*(8), 917–923. https://doi.org/10.1016/J.CELLSIG.2016.04.005

Roychaudhuri, R., Snyder, S. H., & Robin Roychaudhuri, C. (2022). Mammalian D-cysteine: A novel regulator of neural progenitor cell proliferation. *BioEssays*, *44*(7), 2200002. https://doi.org/10.1002/BIES.202200002

Sacharow, S. J., Picker, J. D., & Levy, H. L. (2017). Homocystinuria Caused by Cystathionine Beta-Synthase Deficiency. *GeneReviews®*. https://www.ncbi.nlm.nih.gov/books/NBK1524/

Sahebekhtiari, N., Thomsen, M. M., Sloth, J. J., Stenbroen, V., Zeviani, M., Gregersen, N., Viscomi, C., & Palmfeldt, J. (2016). Quantitative proteomics suggests metabolic reprogramming during ETHE1 deficiency. *PROTEOMICS*, *16*(7), 1166–1176. https://doi.org/10.1002/PMIC.201500336

Salgado, G., Ng, Y. Z., Koh, L. F., Goh, C. S. M., & Common, J. E. (2017). Human reconstructed skin xenografts on mice to model skin physiology. *Differentiation*, *98*, 14–24. https://doi.org/10.1016/j.diff.2017.09.004

Sambandam, S. A. T., Kasetti, R. B., Xue, L., Dean, D. C., Lu, Q., & Li, Q. (2015). 14-3-3σ regulates keratinocyte proliferation and differentiation by modulating Yap1 cellular

localization. *The Journal of Investigative Dermatology*, *135*(6), 1621. https://doi.org/10.1038/JID.2015.42

Schultz, B. R., & Chamberlain, J. S. (2008). Recombinant Adeno-associated Virus Transduction and Integration. *Molecular Therapy : The Journal of the American Society of Gene Therapy*, *16*(7), 1189. https://doi.org/10.1038/MT.2008.103

Semple, B. D., Blomgren, K., Gimlin, K., Ferriero, D. M., & Noble-Haeusslein, L. J. (2013). Brain development in rodents and humans: Identifying benchmarks of maturation and vulnerability to injury across species. *Progress in Neurobiology*, *0*, 1. https://doi.org/10.1016/J.PNEUROBIO.2013.04.001

Simon, M., & Green, H. (1985). Enzymatic cross-linking of involucrin and other proteins by keratinocyte particulates in vitro. *Cell*, *40*(3), 677–683. https://doi.org/10.1016/0092-8674(85)90216-8

Song, N., Li, X., Cui, Y., Zhang, T., Xu, S., & Li, S. (2021). Hydrogen sulfide exposure induces pyroptosis in the trachea of broilers via the regulatory effect of circRNA-17828/miR-6631-5p/DUSP6 crosstalk on ROS production. *Journal of Hazardous Materials*, *418*, 126172. https://doi.org/10.1016/J.JHAZMAT.2021.126172

Steinert, P. M., Candi, E., Kartasova, T., & Marekov, L. (1998). Small Proline-Rich Proteins Are Cross-Bridging Proteins in the Cornified Cell Envelopes of Stratified Squamous Epithelia. *Journal of Structural Biology*, *122*(1–2), 76–85. https://doi.org/10.1006/jsbi.1998.3957

Suns, T., & Green, H. (1978). *Keratin filaments of cultured human epidermal cells. Formation of intermolecular disulfide bonds during terminal differentiation. 253*(6), 2053–2060. https://doi.org/10.1016/S0021-9258(19)62353-7

Su, W., Wang, P., Dong, Q., Li, S., & Hu, S. (2022). S100A8 accelerates wound healing by promoting adipose stem cell proliferation and suppressing inflammation. *Regenerative Therapy*, *21*, 166–174. https://doi.org/10.1016/j.reth.2022.06.010

Szabõ, C. (2007). Hydrogen sulphide and its therapeutic potential. *Nature Reviews Drug Discovery 2007 6:11*, *6*(11), 917–935. https://doi.org/10.1038/nrd2425

Tan, W. H., Eichler, F. S., Hoda, S., Lee, M. S., Baris, H., Hanley, C. A., Grant, P. E., Krishnamoorthy, K. S., & Shih, V. E. (2005). Isolated sulfite oxidase deficiency: a case report with a novel mutation and review of the literature. *Pediatrics*, *116*(3), 757–766. https://doi.org/10.1542/peds.2004-1897

Tennezé, L., Daurat, V., Tibi, A., Chaumet-Riffaud, P., & Funck-Brentano, C. (1999). A study of the relative bioavailability of cysteamine hydrochloride, cysteamine bitartrate and phosphocysteamine in healthy adult male volunteers. *British Journal of Clinical Pharmacology*, *47*(1), 49. https://doi.org/10.1046/J.1365-2125.1999.00844.X

Tiranti, V., Viscomi, C., Hildebrandt, T., Di Meo, I., Mineri, R., Tiveron, C., D Levitt, M., Prelle, A., Fagiolari, G., Rimoldi, M., & Zeviani, M. (2009). Loss of ETHE1, a mitochondrial dioxygenase, causes fatal sulfide toxicity in ethylmalonic encephalopathy. *Nature Medicine 2009 15:2*, *15*(2), 200–205. https://doi.org/10.1038/nm.1907

Truong, D. H., Eghbal, M. A., Hindmarsh, W., Roth, S. H., & O'Brien, P. J. (2008). Molecular Mechanisms of Hydrogen Sulfide Toxicity. *Http://Dx.Doi.Org/10.1080/03602530600959607*, *38*(4), 733–744. https://doi.org/10.1080/03602530600959607

Uhlén, M., Fagerberg, L., Hallström, B. M., Lindskog, C., Oksvold, P., Mardinoglu, A., Sivertsson, Å., Kampf, C., Sjöstedt, E., Asplund, A., Olsson, I. M., Edlund, K., Lundberg, E., Navani, S., Szigyarto, C. A. K., Odeberg, J., Djureinovic, D., Takanen, J. O., Hober, S., … Pontén, F. (2015). Tissue-based map of the human proteome. *Science*, *347*(6220). https://doi.org/10.1126/SCIENCE.1260419/SUPPL_FILE/1260419_UHLEN.SM.PDF

van der Veen, C., Handjiski, B., Paus, R., Müller-Röver, S., Maurer, M., Eichmüller, S., Ling, G., Hofmann, U., Foitzik, K., & Mecklenburg, L. (1999). A Comprehensive Guide for the Recognition and Classification of Distinct Stages of Hair Follicle Morphogenesis. *Journal of Investigative Dermatology*, *113*(4), 523–532. https://doi.org/10.1046/j.1523-1747.1999.00740.x

Veldman, A., Hennermann, J. B., Schwarz, G., Van Spronsen, F., Weis, I., Wong, F. Y., & Schwahn, B. C. (2011). Timing of cerebral developmental disruption in molybdenum cofactor deficiency. *Journal of Child Neurology*, *26*(8), 1059–1060. https://doi.org/10.1177/0883073811415851

Veldman, A., Santamaria-Araujo, J. A., Sollazzo, S., Pitt, J., Gianello, R., Yaplito-Lee, J., Wong, F., Ramsden, C. A., Reiss, J., Cook, I., Fairweather, J., & Schwarz, G. (2010). Successful Treatment of Molybdenum Cofactor Deficiency Type A With cPMP. *Pediatrics*, *125*(5), E1249–E1254. https://doi.org/10.1542/peds.2009-2192

Watts, A. G. (1998). Dehydration-Associated Anorexia: Development and Rapid Reversal. *Physiology & Behavior*, *65*(4–5), 871–878. https://doi.org/10.1016/S0031-9384(98)00244-3

Weidinger, S., Beck, L. A., Bieber, T., Kabashima, K., & Irvine, A. D. (2018). Atopic dermatitis. *Nature Reviews Disease Primers*, *4*(1), 1. https://doi.org/10.1038/s41572-018-0001-z

Wingens, M., van Bergen, B. H., van Vlijmen-Willems, I. M. J. J., Zeeuwen, P. L. J. M., van Ruissen, F., Schalkwijk, J., Hiemstra, P. S., Meis, J. F. G. M., Mulder, J., & Kramps, H. A. (1998). Induction of SLPI (ALP/HUSI-I) in Epidermal Keratinocytes. *Journal of Investigative Dermatology*, *111*(6), 996–1002. https://doi.org/10.1046/j.1523-1747.1998.00425.x

Wong, V. W., Sorkin, M., Glotzbach, J. P., Longaker, M. T., & Gurtner, G. C. (2011). Surgical Approaches to Create Murine Models of Human Wound Healing. *Journal of Biomedicine and Biotechnology*, *2011*, 1–8. https://doi.org/10.1155/2011/969618

Woo, W. H., Yang, H., Wong, K. P., & Halliwell, B. (2003). Sulphite oxidase gene expression in human brain and in other human and rat tissues. *Biochemical and Biophysical Research Communications*, *305*(3), 619–623. https://doi.org/10.1016/S0006-291X(03)00833-7

Yang, G., Sun, X., & Wang, R. (2004). Hydrogen sulfide-induced apoptosis of human aorta smooth muscle cells via the activation of mitogen-activated protein kinases and caspase-3. *The FASEB Journal*, *18*(14), 1782–1784. https://doi.org/10.1096/FJ.04-2279FJE

Zhang, H., Pasolli, H. A., & Fuchs, E. (2011). Yes-associated protein (YAP) transcriptional coactivator functions in balancing growth and differentiation in skin. *Proceedings of the National Academy of Sciences of the United States of America*, *108*(6), 2270–2275. https://doi.org/10.1073/PNAS.1019603108/-/DCSUPPLEMENTAL

Zingkou, E., Pampalakis, G., & Sotiropoulou, G. (2022). Keratinocyte differentiation and proteolytic pathways in skin (patho) physiology. *The International Journal of Developmental Biology*, *66*(1-2–3), 269–275. https://doi.org/10.1387/ijdb.210161gs

5.12 Supplementary Information

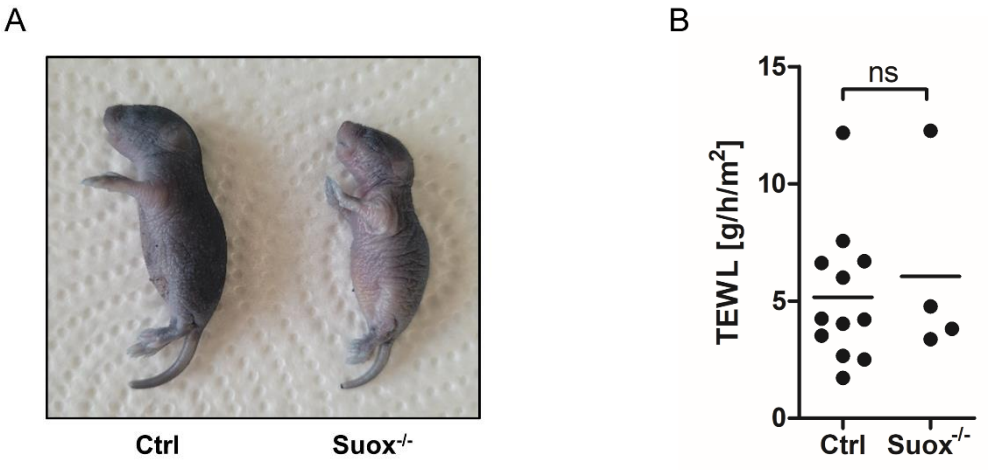

Supplementary Figure 1: Experimental analysis of epidermal outside-in and inside-out barrier function in *Suox*$^{-/-}$ mice.
(A) Toluidine blue staining assay of *Suox*$^{-/-}$ and control mice at P5.5 to assess epidermal outside-in barrier function was performed as described earlier (Ding et al., 2016). (B) TEWL was measured using a Tewameter® at P5.5 to assess epidermal inside-out barrier function. Each data point represents the average TEWL of one mouse in 60 s.